Modulation of Stimulus Driven Neuronal Oscillations by the Emotional and Motivational Significance of Visual Stimuli

Dissertation zur Erlangung des akademischen Grades des Doktors der Naturwissenschaften

an der Universität Konstanz

Fachbereich Psychologie

vorgelegt von

Stephan Moratti

Tag der mündlichen Prüfung: 16. 06. 2005

1. Referent: Dr. Andreas Keil
2. Referent: Prof. Dr. Thomas Elbert

DANKSAGUNG

Ohne die Hilfe und Betreuung meines Betreuers Dr. Andreas Keil wäre die vorliegende Arbeit nie zustande gekommen. Andreas hat mich an die faszinierende Welt oszillatorischer Prozesse herangeführt und mich nicht nur methodisch, sondern auch inhaltlich bereichert. Aber auch Frau Professor Dr. Brigitte Rockstroh und Herrn Professor Dr. Thomas Elbert gebührt Dank für ihre unermüdliche Unterstützung und die Schaffung optimaler Arbeitsbedingungen. Ich kann mir gut vorstellen, dass sie auch mal auf das Experimentieren und Analysieren neidisch waren, als sie mal wieder über Anträge brüten mussten, um das Labor am Laufen zu halten.

Aber auch an unsere technischen Assistentinnen Ursula Lommen, Barbar Awiszus und Christiane Wolf, die bei den Messungen und den Vorbereitungen der Versuchspersonen halfen, möchte ich meinen Dank richten. Unsere wissenschaftliche Hilfskraft Leonie Koban möchte ich besonders hervorheben, die ebenfalls bei den meisten Messungen geholfen und die Versuchspersonen organisiert hat sowie auch mal an einem Samstag für eine Messung bereit war. Vielen Dank euch allen.

Die vorliegende Arbeit entstand in einem Projekt, welches von der DFG gefördert war. Deshalb gebührt auch der DFG Dank, die dieses Forschungsvorhaben finanziell unterstützte.

Den größten Dank allerdings gilt nach wie vor meinen Eltern, die mir das Studium als Voraussetzung für die Promotion ermöglichten. Sie selbst hatten nicht die Möglichkeit eine Universität zu besuchen. Ohne ihre Ratschläge im Speziellen oder Allgemeinen wäre diese Arbeit sicherlich unmöglich gewesen. Vielen Dank euch beiden.

Konstanz, März 2005,
Stephan Moratti

CONTENTS

PREFACE

The present thesis investigates cortical responses to visual affective stimuli in humans. In the last decade many neuroimaging studies mapping the brain during affective picture viewing have been published trying to identify brain mechanism underlying emotional reactions. The main findings of these studies will be reviewed in the chapters describing the experiments. Various methodologies have been used such as functional magnetic resonance tomography (fMRI), positron emission tomography (PET) and electroencephalography (EEG). Whereas fMRI and PET techniques have the advantages of a better spatial resolution and depth sensitivity enabling the researcher to map deep structures like the amygdala, a core candidate for emotional reactions, EEG recordings provide better temporal resolution. All experiments but one of the present studies employed the magnetoencephalogram (MEG), a technique similar to EEG, having the same temporal precision. The MEG measures small magnetic fields induced by the electrical activity of the brain. The EEG records electrical potential differences that are sensitive to volume conductor effects present because of currents being distorted by the various tissues of the brain and scalp. Conversely, magnetic fields are not distorted by tissue and hence provide a better spatial resolution at least when using simple volume conductor models in order to determine the sources of cortical activity.

The aim of the present thesis is to track cortical activation during the presentation of affective stimuli over a presentation time of various seconds. Thereby, the MEG was recorded in all but one of the reported experiments using a steady state visual evoked field (SSVEF) paradigm. The SSVEF is the counterpart of the steady state visual evoked potential (SSVEP) that can be recorded with EEG. The steady state technique will be described in chapter 1 illustrating the results of an EEG experiment that was part of a schizophrenia study in order to investigate aberrant brain dynamics. Here, only the results of the healthy controls are reported in order to familiarize the reader with the SSVEP/ SSVEF technique.

As not only neuroimaging techniques have undergone changes during the last decades, but also statistical analyzing methods have profited from increasing available computing power of our days, the second chapter introduces the concept of linear mixed models, random effects and the utilization of serial correlation structures in order to meet the requirements that interdepended measures such as time series data pose. The method of linear mixed models will be demonstrated by model comparisons using heart rate data of one of the experiments described in later chapters.

Chapter 3 reports an MEG study presenting affective picture material using the SSVEF technique in order to track neuromagnetic cortical responses over picture presentation

time. The pictures were taken from the International Affective Picture System (CSEA, 1999) developed by the Lang group in Florida, USA at the Center for the Study of Emotion and Attention. In that chapter, a minimum norm estimation technique is presented and described in detail that serves for source localization and will be used in the following chapters. Enhanced processing in sensory and above all in fronto-parietal cortical attention networks of emotionally high arousing stimuli will be discussed in the framework of the concept of motivated attention in emotion. As this study was the first one, traditional statistical analysis methods were employed.

However, in chapter 4 and 5 the linear mixed models approach described in chapter 2 is extensively applied. Both chapters report results of discriminative Pavlovian fear conditioning experiments. To date, these are the first studies that incorporate the SSVEF technique into a conditioning experiment rising the possibility to observe sensory processing differences between an aversively reinforced and nonreinforced visual cue over stimulus presentation time with a high temporal and spatial resolution. The motivation to use simple visual conditioned stimuli such as gratings arose from the difficulties that emerge using complex affective pictures taken from the IAPS. It is easier to match simple one colored gratings with respect to luminance and complexity than is the case with IAPS pictures. Second, we wanted to investigate how the acquisition of an association between a previously neutral stimulus and an aversive event is reflected in sensory processing in the brain.

The experimental designs in chapter 4 and 5 are identical except that the instructions were manipulated. In the experiment of chapter 4, subjects were not informed about the contingencies between the conditioned and unconditioned stimulus, leading to the circumstance that only a small fraction of subjects were aware of that association. In the experiment of chapter 5, participants were told the contingency in order to induce full awareness of the conditioning procedure. Similarities and differences between the results of the two experiments will be discussed.

Many theories about emotions exist today. In the general introduction I will focus just on two emotion theories that are of special relevance for the experiments of the current thesis. The first theory that is the most influential regarding the undertaken experiments is the ‘bioinformational theory’ of Peter J. Lang (Lang, Bradley, & Cuthbert, 1997) emphasizing motivational aspects of emotional behavior. The second theory that will be outlined briefly is a model proposed by Rolls (Rolls, 1990) that highlights the importance of learning theory and processes of classical conditioning for emotional reactions. In general, in order to avoid conflict with the concepts of emotions used in daily language and not to confuse entities like

moods or feelings, a short working definition of emotions is given as widely accepted in psychophysiological research. *Emotions, in the context of the present thesis, are considered as phasic reactions of motivational systems to distinct biologically significant stimuli in the environment of an individual preparing it for action*. That means, that I will not infer from brain data what kind of feelings, thoughts or moods subjects had during affective stimulus depiction. I will mainly describe behavioral, autonomic and cortical reactions that are associated with the motivational relevance of the stimuli.

GENERAL INTRODUCTION

Bioinformational theory

The 'bioinformational theory" of emotion proposed by Peter J. Lang (Lang, Bradley, & Cuthbert, 1998) will be outlined here in more detail because especially the motivational and attentional aspects of emotion discussed by this theory will be one of the most important theoretical groundings of the experiments described in chapters 3 to 5. One of the advantages of the bioinformational approach is that it comprises motivational, physiological/ behavioral and cognitive components embedded in the tradition of evolutionary theories of defensive and approach systems. This offers the possibility to investigate emotional responses in humans and bridging the gap between findings in human studies and the knowledge obtained by animal research. In particular, because of great advances in neuroimaging methods, more detailed insights in human brain functioning are possible now. As human beings cannot be pulled out of the line of evolution, the above-mentioned approach seems to offer a vast repertoire of hypothesis linking human brain functioning and findings of animal research.

Two dimensional affective space

The Lang model assumes that emotion is fundamentally organized around two motivational systems. An appetitive and a defensive motive system evolved during evolution in order to deal with situations that promote or threaten the survival of the individual (Lang et al., 1997). The appetitive system is activated when approach related behavior is appropriate, e. g. in situations of food intake or procreation. The defensive motivational system comes into play when withdrawal ensures the survival or prevents harm and promotes behaviors such as escape. The two motivational systems are located in neuronal brain circuits that are also responsible for somatic and autonomic reactions linked to attention and action (Lang et al.,

1997). In general, the Lang model states that any emotional behavior is the product of the output of the appetitive or/ and defensive system. What kind of system is predominately triggered by a stimulus can be inferred by its hedonic valence such as pleasure and unpleasantness (appetitive and defensive, respectively). The amount of activation of the two motivational systems can be inferred by the amount of arousal elicited by a stimulus (Bradley, Codispoti, Cuthbert, & Lang, 2001). From a neuroanatomical point of view, the approach of describing emotions by a two dimensional affective space (valence and arousal) seems to be justified. The appetitive system mainly consists of the dopaminergic mesolimbic system with the ventral tegmental area projecting via the nucleus accumbens to the frontal cortex. This system is also well known as the reward system. Contrary, the amygdala is considered as a core structure of the defensive motive system (LeDoux, 1994; Shi & Davis, 2001) and mediates via projections to the brainstem and hypothalamus defensive behaviors like freezing and autonomic responses. The role of the amygdala in the context of fear expression and conditioning has been well established in animal research (Klüver & Bucy, 1937; LeDoux, 1990; Shi & Davis, 2001; Weiskrantz, 1956). In chapters 4 and 5 the amygdala will be discussed intensively in the context of Pavlovian fear conditioning. The arousal dimension is not explicitly associated with a neuronal circuit in the Lang model and simply represents the activation level within the two motive systems.

Multivariate analysis of affective language has shown that not only animal behavior is organized around hedonic valence and arousal, but also emotional meaning expressed in the human language can be reduced to two factors, namely pleasure and arousal (Osgood, Suci, & Tannenbaum, 1957). This led Lang and his collaborators to the idea that emotions triggered by visual stimuli such as pictures displaying various emotional contents can be evaluated adequately by the two dimensions of pleasure and arousal. Using a self assessment scale (self-assessment manikin, (SAM, CSEA, 1999), subjects had to rate affective picture material according to arousal and valence. In that way, Lang et al. (CSEA, 1999) obtained normative ratings of a picture set (International Affective Picture System, IAPS) that triggered many studies in different laboratories contributing to greater comparability. When the mean responses of the subjects are plotted in a Cartesian coordinate system with arousal as the x- and valence as the y-axis (spanning the affective space), a boomerang shaped scatter plot emerges (see figure 1.)

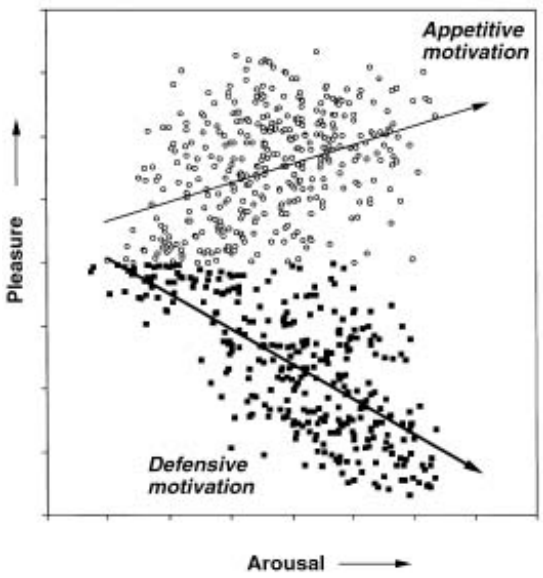

Figure 1: Mean arousal and valence ratings of pictures taken from the international affective picture system. Every dot corresponds to a certain picture. Arousal and valence ratings were performed on a 9 point scale (SAM, see text). Taken from Bradley et al. (2001).

The upper arm of the boomerang represents appetitive and the lower arm indexes defensive motivation. Most importantly, subjective evaluations of valence and arousal co-vary with activity in the autonomic and central nervous system associated with activity in the appetitive and defensive motivational systems (Bradley et al., 2001) further illustrating the validity of the two dimensional affective space and its mapping using the SAM.

Cognitive component

Although modern versions of the bioinformational theory heavily incorporate neuroanatomic insights regarding the defensive and appetitive motivational systems and therefore 'locate' emotional responding to activity in certain neuroanatomical structures (see above), the theory is still a network framework. The resolution of this putative contradiction emerges when asking how these motivational systems become activated.

In their earlier work Lang et al. (Lang, Melamed, & Hart, 1970) observed that high autonomic arousal and reported distress during systematic desensitization of anxiety patients corresponded with good treatment outcome. This observation was explained by assuming that cognitive representations of stimuli associated with fear can trigger fear responses. Therefore semantic propositions embedded in a fear network possibly extended by generalization can trigger activity in motivational systems (see figure 2).

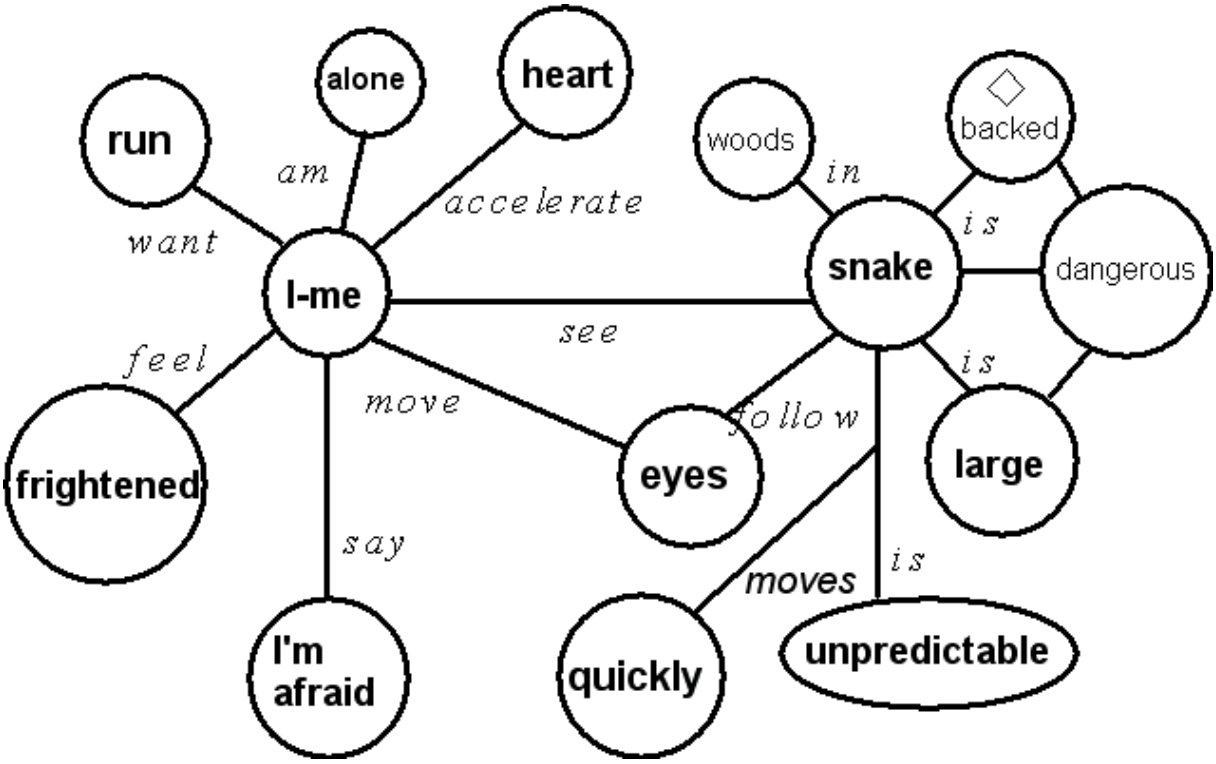

Figure 2: Example of a propositional network representing a fear network.

The network itself can be activated by enabling one of its elements. During the therapeutic intervention pathological misrepresentations in that network can be corrected but only when it is activated, explaining the correlation between high autonomic arousal and treatment success (Foa & Kozak, 1998).

The cognitive component represented in the network aspect of the bioinformational theory is very important with regard to assumptions about how the brain, especially the neocortex is involved in the processing of emotional stimuli. Although the propositional networks presented in the model are semantic in nature, it is evident that also simple stimulus features can be embedded in such a network. Therefore, the model would predict that there is no 'emotion center' in the brain, but that a cortical network representing the stimulus features will be activated during emotional stimulus processing interacting with subcortical motive systems.

As attention is an important mechanism for feature integration in the processing of stimuli (Treisman & Kanwisher, 1998), cortical attention systems should also come into play when analyzing emotional stimuli that are important for the organism in order to facilitate perception. Lang (Lang et al., 1997; Lang, Greenwald, Bradley, & Hamm, 1993) argued that high arousing pictures should automatically draw the subjects' attention representing a further aspect of motivated attention in emotion. Indeed, autonomic responses associated with attention such as elevated skin conductance and heart rate bradycardia can be elicited by high

arousing negative stimuli (Lang & Hnatiow, 1962). Researchers in the field of selective attention have argued that there might exist a 'sensory gain' mechanism (Hillyard & Anllo-Vento, 1998) facilitating processing of the 'to-be-attended' stimulus in sensory cortex. EEG studies have consistently shown that to-be-attended stimuli elicit greater electrocortical responses (Morgan, Hansen, & Hillyard, 1996; Muller & Hubner, 2002). As will be discussed intensively in the subsequent chapters, motivationally significant stimuli can elicit greater activations in sensory cortex (Ito, Larsen, Smith, & Cacioppo, 1998; Junghöfer, Bradley, Elbert, & Lang, 2001; Keil et al., 2002; Mini, Palomba, Angrilli, & Bravi, 1996; Palomba, Angrilli, & Mini, 1997; Schupp et al., 2000; Schupp, Junghöfer, Weike, & Hamm, 2002) where the stimuli are represented paralleling the results of attention research (see above). Significant stimuli also may activate a general fronto-parietal cortical attention system as described by Fernandez-Duque et al. (Fernandez-Duque & Posner, 2001) that facilitates feature integration. Thus, the originally cognitive network component of the Lang model makes important assumption about the cortical processing of affective stimuli.

Behavioral/ physiological components

Very early, Lang (1968) proposed that fear and emotions per se express themselves in three systems: physiological, verbal and behavioral. Because of contextual requirements it is not always adaptive for the organism to overtly perform an action that has been prepared by the activity of the motivational systems. Therefore, emotions are considered as action dispositions (Lang, 1995). Thus, it is possible that physiological, verbal and behavioral measures of emotional reactions are not synchronous.

Further, within a response level (e. g. psychophysiology), asynchronous response patterns are possible. The activation of opposing motivational systems (approach and defensive) can trigger parallel or diverging autonomic reactions. For example whereas skin conductance rises during viewing of both high arousing unpleasant and pleasant pictures, startle potentiation has been observed only for the former and startle inhibition has been reported for the latter (Cuthbert, Bradley, & Lang, 1996). Therefore, the common approach of the studies presented in the current work is multivariate in nature and tries to complete the findings with respect to neuromagnetic responses reflecting cortical processing of emotional stimuli by adding behavioral and autonomic measures.

Learning theory and neuroanatomical considerations

The basic concept of Rolls (1990) about emotions is that states of the organism produced by reinforcement are the building blocks of emotional responding. Primary (or unlearned) reinforcers that elicit emotional reactions are e.g. pain or taste of food while other previously biologically insignificant stimuli become reeinforcers by learning. This type of learning occurs according to Rolls via the process of classical conditioning. Rolls (1995) argues that by analyzing the various aspects of the history of the emergence of an association between an unconditioned (US) and conditioned stimulus (CS) a wide range of human emotions can be described beyond the concepts of positive and negative affect. Some of these factors comprise e.g (i) the reinforcement contingency, (ii) the intensity of the reinforcer, (iii) the conflict of associations (one stimulus is associated with reward and punishment), (iv) the quality of the unconditioned stimulus, (v) the quality of the conditioned stimulus and (vi) the possibility of active or passive responses during the learning situation (Rolls, 1990, 1995). For example, the inability to react actively in an aversive learning setting has been linked to negative affect and depressive symptoms such as sadness and hopelessness (Miller & Seligman, 1975; Seligman, 1972). Therefore, investigating processes of classical conditioning could have the power to elucidate some basic building blocks of emotional responding, one further motivation for the studies presented in chapters 4 and 5.

Theories about classical conditioning (Mackintosh, 2003) have stressed the importance of the salience of the CS and hence the involvement of attention during processes of association formation. This is in line with Rolls (1990) position based on classical concepts of hierarchical sensory processing that a fine grained analysis of the CS has to be done in order to gain predictive value (Rolls, 1999). According to this perspective visual stimuli have to be processed completely in all stages of the ventral pathway in the temporal lobe before afferents from the TE regions project information to the amygdala (Amaral, Price, Pitkaenen, & Carmichael, 1992) where affective evaluation (Adolphs, Tranel, Damasio, & Damasio, 1995; Calder et al., 1996) and processes of plastic changes in association cortex (McGaugh, Cahill, & Roozendaal, 1996) are mediated. The amygdala itself receives afferents from many sensory systems located in the neocortex and has many back projections to these structures (Amaral, 1986). Thus, the amygdala is neuroanatomically well placed to integrate e.g. visual (temporal lobe) and visceral (insula) information. As the amygdala also projects to the hypothalamus and various brainstem nuclei, this structure has been believed to mediate behavioral, endocrine and autonomic reactions such as heart rate bradycardia in aversive conditioning (Kuniecki, Coenen, & Kaiser, 2002). Efferents from the amygdala to the ventral striatum

including the nucleus accumbens may be the neural substrate of learning by reward (Cador, Robbins, & Everitt, 1989). Thus, the amygdala seems to be a core structure for emotional responding and learning associations between neutral stimuli and primary reeinforcers (see above).

Besides the amygdala (see above), the orbitofrontal cortex (i) and the basal forebrain (ii) comprising the hypothalamus (Rolls, 1995) are considered as parts of an interacting network accomplishing the various mechanisms for association formation. Whereas the amygdala is considered as the core structure to form associations between a previous neutral stimulus and an biologically significant event, the orbitofrontal cortex has been associated with emotion regulation in general (Davidson, Putnam, & Larson, 2000) and with reversal learning in particular that has been characterized as changing emotional behavior after contingency changes between stimuli (Rolls, 1999; Rolls, Hornak, Wade, & McGrath, 1994). Further, Rolls observed in a series of studies (Burton, Mora, & Rolls, 1975; Burton, Rolls, & Mora, 1976; Rolls, Burton, & Mora, 1976, 1980) that neurons in the hypothalamus responded to visual stimuli associated with reward (food) and other neurons that showed enhanced discharges to visual cues reinforced with punishment (Rolls, Sanghera, & Roper-Hall, 1979). Rolls has speculated that the hypothalamus receives highly processed information from the inferior temporal lobe via the amygdala (Rolls, 1990).

In contrast to the theory of Rolls (1990) that implicates a late differentiation of emotional stimuli, work from the LeDoux group (J. LeDoux, 1992; J. E. LeDoux, 1992; LeDoux, 1993; LeDoux, 2000) and Micheal Davis (Shi & Davis, 2001) have shown that thalamo-amygdalafugal pathways enable the amygdala to perform a fast evaluation of noxious stimuli without complex computations in the neocortex. Studies in humans have shown that conditioned masked stimuli can evoke conditioned responses such as elevated skin conductance (Esteves, Parra, Dimberg, & Ohman, 1994) and also activate the amygdala via the colliculi and pulvinar (Morris, Ohman, & Dolan, 1999). Further, Hamm et al. (Hamm et al., 2003) have demonstrated that a cortically blind patient can acquire a conditioned response to visual stimuli although no visual evoked potentials could be recorded in that patient contradicting Rolls point of view. Further, many electrophysiologcal studies have shown early discrimination of emotional stimuli in time windows about 100-200ms (Junghöfer et al., 2001; Keil et al., 2002; Pizzagalli, Regard, & Lehmann, 1999). Aversive picture material elicited enhanced gamma band activity in the EEG even in earlier time windows around 80ms (Keil et al., 2001). In a recent conditioning study using evoked potentials Stolarova et al. (in preparation) could demonstrate a very early (about 60-80ms) facilitation of conditioned

stimuli reflected by an enhancement of the C1 component originating in primary visual cortex. As no detailed visual analysis in the ventral temporal stream could have taken place before, it is likely that amygdalafugal projections from the amygdala, which itself received visual information from the thalamus, tuned the primary visual cortex. This result adds further powerful evidence that a fast evaluation route in addition to a slow one exists.

So far, two emotion theories have been introduced that are related to the experiments reported in chapters 3 to 5. In the introduction sections of the corresponding chapters theoretical backgrounds will be presented in more detail. Further, specific hypothesis will be formulated regarding the experiments in question. However, one main hypothesis within the current work will be that visual stimuli of high motivational relevance whether inherently (IAPS pictures chapter 3) or acquired (conditioning studies chapters 4 and 5) will facilitate sensory processing and engage attention systems in the brain. This main hypothesis is derived from Lang's motivational approach that has relied on autonomic measures of attention and Rolls neuroanatomical model incorporating learning theory.

REFERENCES

Adolphs, R., Tranel, D., Damasio, H., & Damasio, A. R. (1995). Fear and the human amygdala. *J Neurosci, 15*(9), 5879-5891.

Amaral, D. G. (1986). Amygdalohippocampal and amygdalocortical projections in the primate brain. *Adv Exp Med Biol, 203*, 3-17.

Amaral, D. G., Price, J. L., Pitkaenen, A., & Carmichael, S. T. (1992). Anatomical organization of the primate amygdaloid complex. In J. P. Aggleton (Ed.), *The amygdala: Neurobiological aspects of emotion, memory, and mental dysfunction.* (pp. 1-66). New York: Wiley-Liss.

Bradley, M. M., Codispoti, M., Cuthbert, B. N., & Lang, P. J. (2001). Emotion and Motivation I: Defensive and Appetitive Reactions in Picture Processing. *Emotion, 1*(3), 276-298.

Burton, M. J., Mora, F., & Rolls, E. T. (1975). Proceedings: Visual and taste neurones in the lateral hypothalamus and substantia innominata: modulation of responsiveness by hunger. *J Physiol, 252*(2), 50P-51P.

Burton, M. J., Rolls, E. T., & Mora, F. (1976). Effects of hunger on the responses of neurons in the lateral hypothalamus to the sight and taste of food. *Exp Neurol, 51*(3), 668-677.

Cador, M., Robbins, T. W., & Everitt, B. J. (1989). Involvement of the amygdala in stimulus-reward associations: interaction with the ventral striatum. *Neuroscience, 30*(1), 77-86.

Calder, A. J., Young, A. W., Rowland, D., Perrett, D. I., Hodges, J. R., & Etcoff, N. L. (1996). Facial emotion recognition after bilateral amygdala damage: Differentially severe impairment of fear. *Cognitive Neuropsychology, 13*, 699-745.

CSEA. (1999). *International affective picture system (IAPS): Technical manual and affective ratings.* Gainesville, FL: NIMH-Center for the study of emotion and attention, University of Florida.

Cuthbert, B. N., Bradley, M. M., & Lang, P. J. (1996). Probing picture perception: activation and emotion. *Psychophysiology, 33*(2), 103-111.

Davidson, R. J., Putnam, K. M., & Larson, C. L. (2000). Dysfunction in the neural circuitry of emotion regulation--a possible prelude to violence. *Science, 289*(5479), 591-594.

Esteves, F., Parra, C., Dimberg, U., & Ohman, A. (1994). Nonconscious associative learning: Pavlovian conditioning of skin conductance responses to masked fear-relevant facial stimuli. *Psychophysiology, 31*(4), 375-385.

Fernandez-Duque, D., & Posner, M. I. (2001). Brain imaging of attentional networks in normal and pathological states. *J Clin Exp Neuropsychol, 23*(1), 74-93.

Foa, E. B., & Kozak, M. J. (1998). Clinical Applications of Bioinformational Theory: Understanding Anxiety and Its Treatment. *Behavior Therapy, 29*, 675-690.

Hamm, A. O., Weike, A. I., Schupp, H. T., Treig, T., Dressel, A., & Kessler, C. (2003). Affective blindsight: intact fear conditioning to a visual cue in a cortically blind patient. *Brain, 126*(Pt 2), 267-275.

Hillyard, S. A., & Anllo-Vento, L. (1998). Event-related brain potentials in the study of visual selective attention. *Proc Natl Acad Sci U S A, 95*(3), 781-787.

Ito, T. A., Larsen, J. T., Smith, N. K., & Cacioppo, J. T. (1998). Negative information weighs more heavily on the brain: the negativity bias in evaluative categorizations. *J Pers Soc Psychol, 75*(4), 887-900.

Junghöfer, M., Bradley, M. M., Elbert, T. R., & Lan, P. J. (2001). Fleeting images: a new look at early emotion discrimination. *Psychophysiology, 38*(2), 175-178.

Keil, A., Bradley, M. M., Hauk, O., Rockstroh, B., Elbert, T., & Lang, P. J. (2002). Large-scale neural correlates of affective picture processing. *Psychophysiology, 39*(5), 641-649.

Keil, A., Muller, M. M., Gruber, T., Wienbruch, C., Stolarova, M., & Elbert, T. (2001). Effects of emotional arousal in the cerebral hemispheres: a study of oscillatory brain activity and event-related potentials. *Clin Neurophysiol, 112*(11), 2057-2068.

Klüver, H., & Bucy, J. P. (1937). Psychich blindness and other symptoms following bilateral temporal lobectomy in rhesus monkeys. *Am Jn Physiol, 119*, 352-353.

Kuniecki, M., Coenen, A. M., & Kaiser, J. (2002). Correlation between long latency evoked potentials from amygdala and evoked cardiac response to fear conditioned stimulus in rats. *Acta Neurobiol Exp (Wars), 62*(2), 85-92.

Lang, P. J. (1968). Fear reduction and fear behavior: Problems in treating a construct, *Research in psychotherapy III*. Washington: American Psychiatric Association.

Lang, P. J. (1995). The emotion probe: Studies of motivation and attention. 102nd Annual Convention of the American Psychological Association Distinguished Scientific

Contributions Award Address (1994, Los Angeles, California). *American Psychologist, 50*(5), 372-385.

Lang, P. J., Bradley, M. M., & Cuthbert, B. N. (1997). Motivated Attention: Affect, Activation, and Action. In P. J. Lang & R. F. Simons & M. T. Balaban (Eds.), *Attention and Orienting: Sensory and Motivational Processes* (pp. 97-135). Hillsdale, N.J.: Lawrence Erlbaum Associates.

Lang, P. J., Bradley, M. M., & Cuthbert, B. N. (1998). Emotion, motivation, and anxiety: brain mechanisms and psychophysiology. *Biol Psychiatry, 44*(12), 1248-1263.

Lang, P. J., Greenwald, M. K., Bradley, M. M., & Hamm, A. O. (1993). Looking at pictures: affective, facial, visceral, and behavioral reactions. *Psychophysiology, 30*(3), 261-273.

Lang, P. J., & Hnatiow, M. (1962). Stimulus repetition and the heart rate response. *Journal of Comparative and Physiological Psychology, 55*, 781-785.

Lang, P. J., Melamed, B. G., & Hart, J. (1970). A psychophysiological analysis of fear modification using an automated desensitization procedure. *J Abnorm Psychol, 76*(2), 220-234.

LeDoux, J. (1992). Emotional memories in the brain. In e. nd (Ed.), *Neuropsychology of memory* (pp. 463-469): Guilford Press, New York, NY, US.

LeDoux, J. E. (1990). Fear pathways in the brain: Implications for a theory of the emotional brain. In P. F. Brain & S. Parmigiani & R. J. Blanchard & D. Mainardi (Eds.), *Fear and defence. Ettore Majorana international life sciences series, Vol. 8.* (pp. 163-177): Harwood Academic Publishers, London, England.

LeDoux, J. E. (1992). Emotion and the amygdala. In P. A. John (Ed.), *The amygdala: Neurobiological aspects of emotion, memory, and mental dysfunction.* (pp. 339-351): Wiley-Liss, New York, NY, US.

LeDoux, J. E. (1993). Emotional networks in the brain. In J. M. H. Michael Lewis (Ed.), *Handbook of emotions.* (pp. 109-118): Guilford Press, New York, NY, US.

LeDoux, J. E. (1994). Emotion, memory and the brain. *Sci Am, 270*(6), 50-57.

LeDoux, J. E. (2000). Emotion circuits in the brain. *Annu Rev Neurosci, 23*, 155-184.

Mackintosh, N. J. (2003). Pavlov and associationism. *Span J Psychol, 6*(2), 177-184.

McGaugh, J. L., Cahill, L., & Roozendaal, B. (1996). Involvement of the amygdala in memory storage: interaction with other brain systems. *Proc Natl Acad Sci U S A, 93*(24), 13508-13514.

Miller, W. R., & Seligman, M. E. (1975). Depression and learned helplessness in man. *J Abnorm Psychol, 84*(3), 228-238.

Mini, A., Palomba, D., Angrilli, A., & Bravi, S. (1996). Emotional information processing and visual evoked brain potentials. *Percept Mot Skills, 83*(1), 143-152.

Morgan, S. T., Hansen, J. C., & Hillyard, S. A. (1996). Selective attention to stimulus location modulates the steady-state visual evoked potential. *Proc Natl Acad Sci U S A, 93*(10), 4770-4774.

Morris, J. S., Ohman, A., & Dolan, R. J. (1999). A subcortical pathway to the right amygdala mediating "unseen" fear. *Proc Natl Acad Sci U S A, 96*(4), 1680-1685.

Muller, M. M., & Hubner, R. (2002). Can the spotlight of attention be shaped like a doughnut? Evidence from steady-state visual evoked potentials. *Psychol Sci, 13*(2), 119-124.

Osgood, C., Suci, G., & Tannenbaum, P. (1957). *The measurement of meaning*: Urbana, Univeristy of Illinois.

Palomba, D., Angrilli, A., & Mini, A. (1997). Visual evoked potentials, heart rate responses and memory to emotional pictorial stimuli. *Int J Psychophysiol, 27*(1), 55-67.

Pizzagalli, D., Regard, M., & Lehmann, D. (1999). Rapid emotional face processing in the human right and left brain hemispheres: an ERP study. *Neuroreport, 10*(13), 2691-2698.

Rolls, E. T. (1990). A theory of emotion, and its application to understanding the neural basis of emotion. *Cognition and Emotion, 4*, 161-190.

Rolls, E. T. (1995). A theory of emotion and consciousness, and its application to understanding the neural basis of emotion. In M. S. Gazzaniga (Ed.), *The cognitive neurosciences.* (pp. 1091-1106). Cambridge, MA, US: MIT Press.

Rolls, E. T. (1999). *The Brain and Emotion*. Oxford: Oxford University Press.

Rolls, E. T., Burton, M. J., & Mora, F. (1976). Hypothalamic neuronal responses associated with the sight of food. *Brain Res, 111*(1), 53-66.

Rolls, E. T., Burton, M. J., & Mora, F. (1980). Neurophysiological analysis of brain-stimulation reward in the monkey. *Brain Res, 194*(2), 339-357.

Rolls, E. T., Hornak, J., Wade, D., & McGrath, J. (1994). Emotion-related learning in patients with social and emotional changes associated with frontal lobe damage. *J Neurol Neurosurg Psychiatry, 57*(12), 1518-1524.

Rolls, E. T., Sanghera, M. K., & Roper-Hall, A. (1979). The latency of activation of neurones in the lateral hypothalamus and substantia innominata during feeding in the monkey. *Brain Res, 164*, 121-135.

Schupp, H. T., Cuthbert, B. N., Bradley, M. M., Cacioppo, J. T., Ito, T., & Lang, P. J. (2000). Affective picture processing: the late positive potential is modulated by motivational relevance. *Psychophysiology, 37*(2), 257-261.

Schupp, H. T., Junghöfer, M., Weike, A. I., & Hamm, A. O. (2002). Emotional facilitation of sensory processing in the visual cortex. *Psychological Science*, in press.

Seligman, M. E. (1972). Learned helplessness. *Annu Rev Med, 23*, 407-412.

Shi, C., & Davis, M. (2001). Visual pathways involved in fear conditioning measured with fear-potentiated startle: behavioral and anatomic studies. *J Neurosci, 21*(24), 9844-9855.

Treisman, A. M., & Kanwisher, N. G. (1998). Perceiving visually presented objects: recognition, awareness, and modularity. *Curr Opin Neurobiol, 8*(2), 218-226.

Weiskrantz, L. (1956). Behavioral changes associated with ablation of the amygdaloid complex in monkeys. *Journal of Comparative and Physiological Psychology, 49*, 381-391.

Chapter 1

Steady State Visual evoked Potentials/ Fields and Transient Stimulation

INTRODUCTION

The main technique used in all experiments of the present thesis will be the steady state visual evoked field (SSVEF) paradigm. Therefore, this procedure will be introduced in this chapter. The data comes from a study investigating brain dynamics in schizophrenic patients and healthy controls. Here, only the data of the healthy subjects will be reported and the influence of oscillatory brain responses on evoked potentials during transient stimulation will be demonstrated. However, the study consisted of electroencephalography (EEG) data and therefore all data and techniques presented here relate to SSVEPs. The methods for analyzing SSVEFs are not different from the ones explained in this section.

Steady state visual evoked fields are the neuromagnetic equivalent of steady state visual evoked potentials (SSVEP) measured using EEG. The SSVEP is elicited by luminance-modulated visual stimuli such as flickering pictures or patterns, which are presented over a longer time period (i.e. typically > 2 s). The SSVEP has the same fundamental frequency as the driving visual stimulus often including higher harmonics (Regan, 1989; Silberstein, Ciorciari, & Pipingas, 1995) and produces scalp potentials originating in visual sensory cortex (Herrmann, 2001). Using magnetencephalography (MEG), Müller et al. (Müller, Teder, & Hillyard, 1997) demonstrated that the neuromagnetic SSVEF can be explained by equivalent current dipoles located in visual cortex. Therefore, the SSVEP/ SSVEF technique allows the researcher to tag neural responses in sensory cortex by manipulating the frequency of the driving stimulus used in the experiment. A further advantage is that during a short period of time many stimulations are done and that the power of the SSVEP/ SSVEF is concentrated into a few discrete frequency bands resulting in a high signal to noise ratio (Regan, 1989).

The SSVEP/ SSVEF technique is not only used to tag stimulus driven neural activity in visual sensory cortex, but also in other sensory modalities such as auditory and somatosensory domains (Diesch, Preissl, Haerle, Schaller, & Birbaumer, 2001; Weisz, Keil, Wienbruch, Hoffmeister, & Elbert, 2004). Further, it has been shown that the oscillatory

activity driven by repetitive stimulus presentation can be modulated by tonic changes of the organism such as sleep, anesthesia, or vigilance (Picton, Vajsar, Rodriguez, & Campbell, 1987; Plourde & Picton, 1990; Silberstein et al., 1990). The SSVEP technique also has been used to investigate selective spatial attention whereas it has been demonstrated that attended stimuli generated a greater SSVEP response than unattended stimuli (Morgan, Hansen, & Hillyard, 1996; Müller & Hillyard, 2000; Muller & Hubner, 2002; Müller et al., 1998). Finally, SSVEPs have not been used solely to investigate stimulus driven neural activity in sensory cortex but also to tag electromagnetic brain responses at higher stages of stimulus processing such as working memory (Perlstein et al., 2003; Silberstein, Nunez, Pipingas, Harris, & Danieli, 2001) or interaction of spatial attention and motive systems during viewing of emotional pictures (Keil, Moratti, Sabatinelli, Bradley, & Lang, 2004).

There are several techniques for analyzing SSVEPs/ SSVEFs that will be described in this chapter. First, data of a single subject of the sample of the present study will be reported in order to demonstrate analyzing techniques such as Fast Fourier Transformation and complex demodulation in order to show that repetitive visual stimulation is reflected in high power in a narrow frequency band around stimulation frequency and in a stable phase of the elicited signal. These two characteristics have been considered as important features of an SSVEP (Regan, 1989). Second, an earlier study by Clementz et al. (Clementz, Keil, & Kissler, 2004) demonstrated that after offset of repetitive stimulation the oscillating activity reflected in the SSVEP still goes on for a while. Schizophrenic patients showed a prolonged decay of the SSVEP response compared to healthy subjects (Clementz et al., 2004). Consequently, the research question arose how the P1, N1, P2 and P3 complex evoked by a transient visual stimulus presented during and after steady state offset will be affected. Therefore, we presented a visual transient stimulus during and at increasing time distances from offset of the repetitive stimulation (240 ms before-, 240 ms, 480 ms and 720 ms after offset).

METHODS

Participants

12 paid native English speaking volunteers (6 females, 6 males, 10 right handed, 2 left handed; Oldfield, 1971) recruited from the University of Athens, Georgia, USA and the community gave written consent to participate in the study. Their mean age was 44.3 years (range: 24 to 55 years). They had normal or corrected-to-normal vision and no family history of photic epilepsy.

Stimuli and procedure

Steady state stimuli were pairs of red 8x8 checkerboards (4 red boxes, and 4 boxes of background color in alternating sequence) presented bilaterally to the left and right visual hemi-fields and synchronously luminance modulated at a fixed rate of 12.5 Hz. They were presented on a 19-in computer monitor positioned at 80 cm distance from the subject. The inner border of the checker board subtended an angle of 13.4° versus 26.7° for the outer boarder relative to the subject's nasion. The checkerboards were 9.6 cm x 9.6 cm in size, each check having a width and height of 1.2 cm. The refresh rate of the monitor was 100 Hz. The luminance modulation was done by presenting the checkerboards for 30 ms followed by 30 ms black screen. Synchronization with the 10 ms retrace time of the monitor added further 10 ms to the presentation times resulting in a 80 ms on/ off cycle (12.5 Hz). The flashing checkerboards were presented for 2000 ms by depicting 25 of the 80 ms on/ off cycles.

Transient stimuli were boxes of the same color as the checkerboards presented in the middle of the screen for a time period of 240 ms subtending a visual angle of 6.9° (they were equally sized as the checkerboards). Transient stimuli were presented during depiction of the flashing checkerboards at 240 ms before offset of the steady state stimuli (corresponding to the last four 80 ms on/ off cycles) and 240 ms, 480 ms and 720 ms after offset of steady state stimulation. This resulted in four conditions (-240 ms, 240 ms, 480 ms and 720 ms conditions). Each condition consisted of 66 trials whereas 6 trials within each condition were target trials whereby pink boxes were centrally shown. Subjects were requested to press two buttons at once with their left and right index fingers upon appearance of the pink boxes. Target trials were discarded from analysis. The inter trial interval (ITI) varied randomly between 6 s and 10 s and was defined as the time period between offset of the transient and onset of the next steady state stimulus train.

Before the experimental session, subjects were presented examples of one target and one non-target trial in order to ensure that they could discriminate the pink from the red boxes. During the experiment participants were allowed to take a break of one minute after 80 and 160 trials. After the experimental session subjects were detached from the electrodes and paid 10 $ for participation.

Electrophysiological recordings and preprocessing

EEG was recorded continuously from 257 electrodes using an Electrical Geodesics™ (EGI) high-density EEG system and digitized at a rate of 250 Hz, using Cz as a recording

reference. Impedances were kept below 50 kΩ. The EGI net-electrodes comprised a subset of electrodes placed at the outer canthi as well as below and above both eyes in order to record the vertical and horizontal electrooculogram (EOG). During data acquisition an online bandpass filter of 0.1 Hz to 100 Hz was applied.

EEG data was corrected for eyeblinks using an algorithm implemented in BESA™ software (Berg & Scherg, 1994). Further, movement artifacts were identified by visual inspection of the data and trials containing such artifacts were excluded from analysis. Electrodes located at the neck and cheeks of the subjects were excluded from analysis resulting in 216 electrode sites (figure 1, electrode locations without depicting any scalp potential). For each subject the same electrode set was discarded.

Before averaging the trials of the four conditions, data was average referenced and high pass filtered at a frequency of 1.0 Hz with a slope of 6 db per octave (zero phase). Additionally, a low pass filter at a frequency of 20 Hz with a slope of 48 db per octave (zero phase) was applied. For each condition (presentation of the transient stimulus at –240 ms, 240 ms, 480 ms and 720 ms after steady sate offset) epochs comprising a 1000 ms baseline before onset of steady state stimulation and a 3500 ms poststimulus time period yielded averages containing the SSVEP and the visual evoked responses (VEPs) of the transient stimuli for each subject. The whole 3500 ms data trace was baseline corrected using the 1000 ms prestimulus interval. In order to compare latencies and amplitudes of the VEPs of the various conditions, epochs with a 100 ms prestimulus and 400 ms poststimulus interval related to the onset of a transient stimulus (red boxes) were extracted from the baseline corrected 3500 ms epochs. This procedure ensured that the VEPs were baseline corrected using the 1000 ms prestimulus interval before steady state onset.

Spectral measures

Two parameters were estimated in order to assess the SSVEP. First, the amplitude of the SSVEP for each subject was determined by application of the Fast Fourier Transformation (FFT) over a poststimulus time interval (related to onset of steady state stimulation) of 500 ms to 1760 ms for each trial and electrode. This interval was chosen in order to exclude evoked responses of the steady sate onset and of the transient stimulus presented at 1760 ms after steady state onset (–240 ms condition). Then, the amplitude spectrum was averaged across each condition for each subject. Further, the scalp topography of the mean amplitude of the 12.5 Hz Fourier component across all subjects and conditions was determined in order to infer

an electrode site of maximal activation (see figure 1 and figure 3 of results) during steady state stimulation. Six neighboring electrodes were included in the electrode cluster. Thereafter, the mean amplitude spectrum across these electrodes was determined.

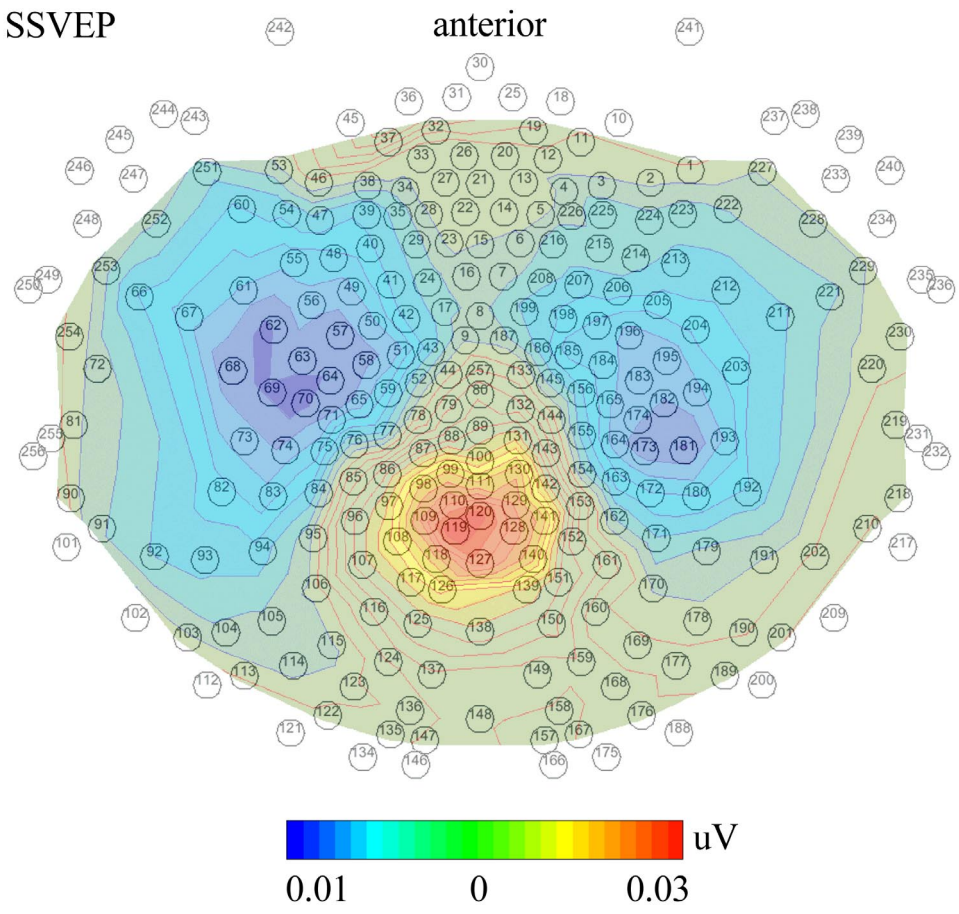

Figure 1: Sensor layout of the 257 channel EGI© system and the SSVEP topography of the grand mean across all subjects and conditions. The colorbar indicated the amplitude of the FFT amplitude spectrum. Electrodes for further analysis were chosen over sites of maximal activation (electrodes 110, 111, 119, 120, 129, 128 and 127).

Second, the phase stability of the SSVEP was estimated by complex demodulating the signal at 12.5 Hz over a time interval between 500 ms and 1760 ms after steady state onset at the electrode site of maximal 12.5 Hz amplitude (electrode 120). With a sampling rate of 250 Hz (sample interval of 4 ms) this resulted in 316 phase angles for each time point. The phase stability of the SSVEP was assessed by estimating the uniformity of phase angles (see below) and the mean length of the corresponding 316 vectors normalized for amplitudes.

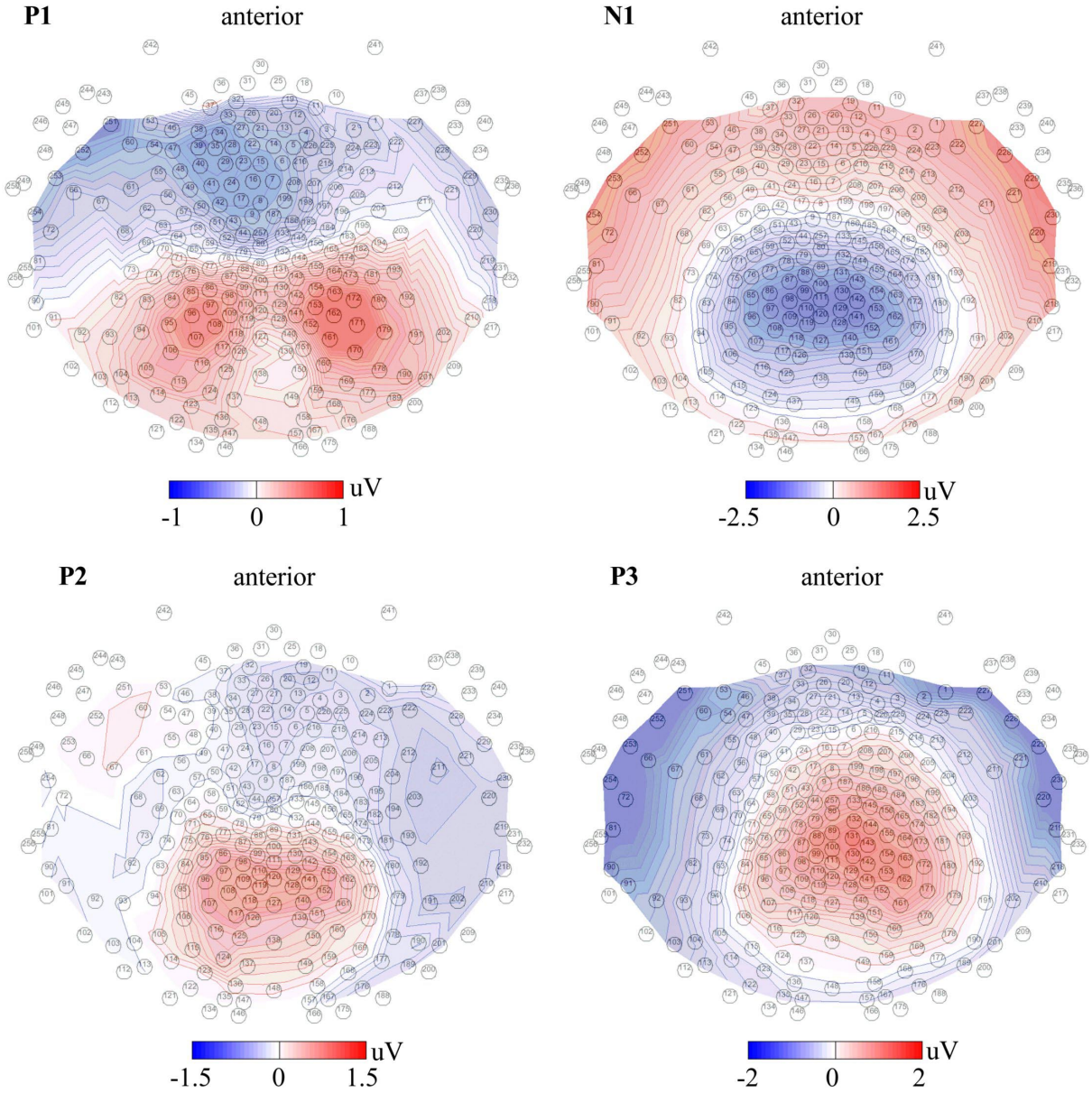

Figure 2: Sensor layout of the 257 channel EGI© system and the P1-N1-P2-P3 topography of the grand mean across all subjects and conditions. The colorbars indicate the amplitudes of the scalp potentials. Electrodes for further analysis were chosen over sites of maximal activation (see text). For better reading of electrode numbers see figure 1.

VEP measures

VEPs of the four conditions were derived by averaging the signal across electrode sites where the amplitude of the grand mean across all subjects and all conditions was greatest. Using this procedure two clusters for the P1 (left and right hemisphere), one cluster for the N1, P2 and P3 were obtained (see figure 2 and table 1).

Table 1: Electrodes chosen for analysis of the P1-N1-P2-P3 complex. For the P1 a left and right electrode cluster was determined.

component	*electrodes*						
P1 left	84	85	95	96	97	107	106
P1 right	152	153	161	162	163	171	172
N1	99	100	110	111	120	129	130
P2	99	100	110	111	120	129	130
P3	89	100	130	131	132	143	144

In order to identify the peaks and latencies of the various visual components four time segments were derived based on the grand averages and visual inspection of all conditions, containing P1 (73 ms – 125 ms), N1 (128 ms – 193 ms), P2 (197 ms – 285 ms) and P3 (289 ms – 397 ms) windows. Within each time window the amplitude of the maximal deflection and the latency with respect to the P1, N1, P2 and P3 component elicited by transient stimulus onset was measured across corresponding electrode sites (see above) for each condition and subject.

Statistical analysis

The 316 phase angles obtained by complex demodulation at stimulation frequency of 12.5 Hz were tested for uniformity for each subject using the Rayleigh test. The Rayleigh test is a circular statistic that assess if the corresponding 316 standardized (length of 1) vectors point to similar directions. The sum of all vectors divided by 316 represents the mean vector that has the ideal length of 1 if all vectors were equally directed in space. The shorter the mean vector, the less unimodal is the circular distribution of vector directions.

Amplitude and latencies of the P1, N1, P2 and P3 were submitted to repeated measures ANOVA with a repeated factor of condition (-240 ms, 240 ms, 480 ms and 720 ms condition) each. The degrees of freedom were corrected according to the procedure suggested by Greenhouse & Geisser (Greenhouse & Geisser, 1959). As left and right hemispheric electrode clusters were chosen for the P1, analysis of the P1 component contained an additional within-factor hemisphere (left, right). Whenever the repeated measures ANOVA indicated an overall difference between conditions, the dependent variables were evaluated using trend analysis testing for linear, quadratic and cubic trends over conditions as the factor condition was ordered (different increasing presentation times). In cases where the trend

analysis did not model an unambiguous trend, Fisher's LSD test was used in order to calculate post hoc tests. This stepwise procedure was applied, because no specific hypothesis were formulated (if this had been the case, trend tests would have been sufficient) as this is the first study to date that investigated an interaction between transient and steady state stimulation.

RESULTS

Assessment of the SSVEP

The topography of the mean amplitude of the 12.5 Hz Fourier component obtained by the FFT over 500 ms to 1760 ms poststimulus time (for the grand mean the last 240 ms of the 2000 ms steady state presentation time were discarded because of the –240 ms condition) across all subjects and conditions (-240 ms, 240 ms ,480 ms and 720 ms) is depicted in figure 3. The 12.5 Hz amplitude clustered at parietal electrode sites.

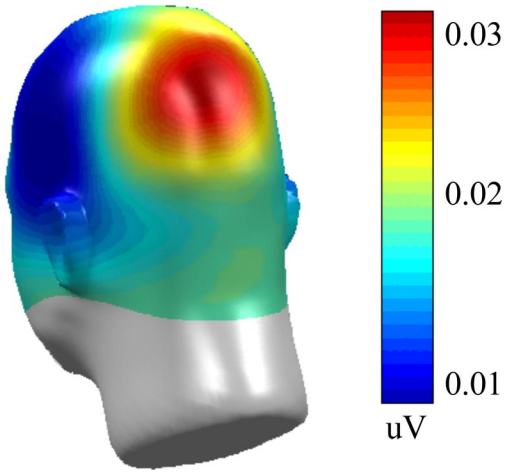

Figure 3: Topography of the mean amplitude of the 12.5 Hz Fourier component across all subjects and conditions estimated over a time period between 500 ms and 1760 ms after steady state onset. The 12.5 Hz amplitude clustered at parietal electrode sites. The colorbar indicates the amplitude of the 12.5 Hz Fourier component.

The mean amplitude spectrum over parietal electrode sites (see methods) across all subjects and conditions is shown in figure 4. As can be seen from figure 4, the amplitude peaked around 12.5 Hz in the frequency domain and paralleled the stimulation frequency.

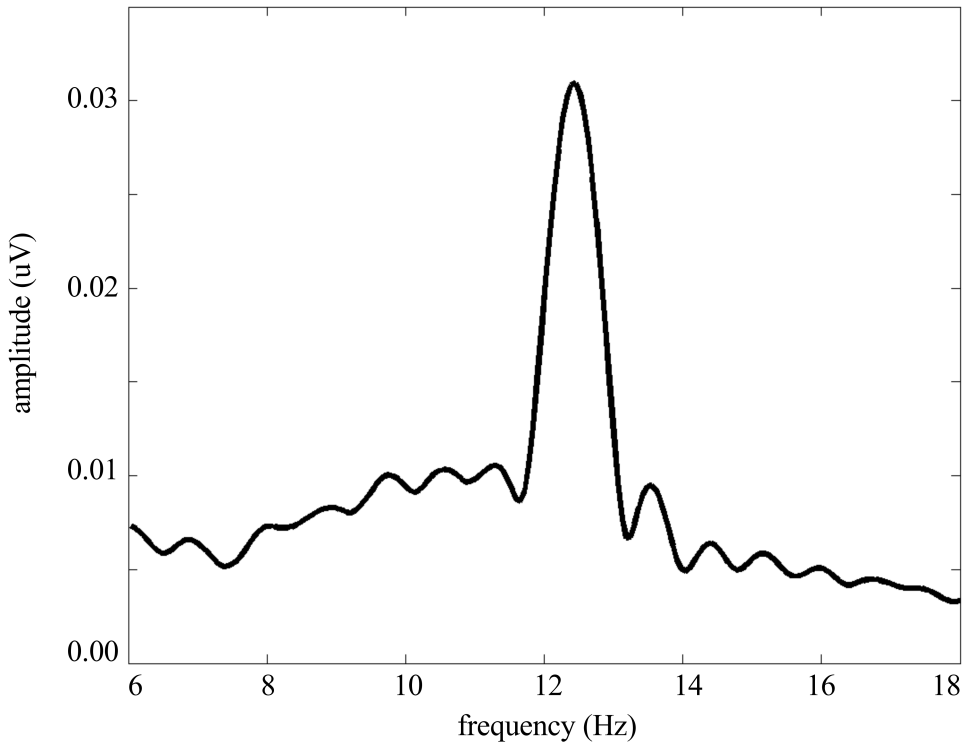

Figure 4: Mean amplitude spectrum across parietal electrode sites estimated during a time interval between 500 ms and 1760 ms after steady state onset. As can be seen, most of the amplitude is concentrated around 12.5 Hz paralleling the stimulation frequency.

Further, figure 5 shows the phaselocking vectors for all subjects determined at the center electrode of the parietal electrode cluster (see methods). Table 2 depicts the corresponding mean vector lengths and p values of the Rayleigh statistics.

Assessment of the amplitude and latency of evoked responses to the transient stimulus during and after the steady state stimulation

Altogether, the SSVEP showed a concentration of amplitude in the FFT spectrum in a narrow frequency band around 12.5 Hz and a stable phase of the signal. A further subject of investigation was the influence of the SSVEP on transient stimulation. For illustration, the grand mean waveform across all subjects (N=12) of electrode 120 (Pz) is shown in figure 6.

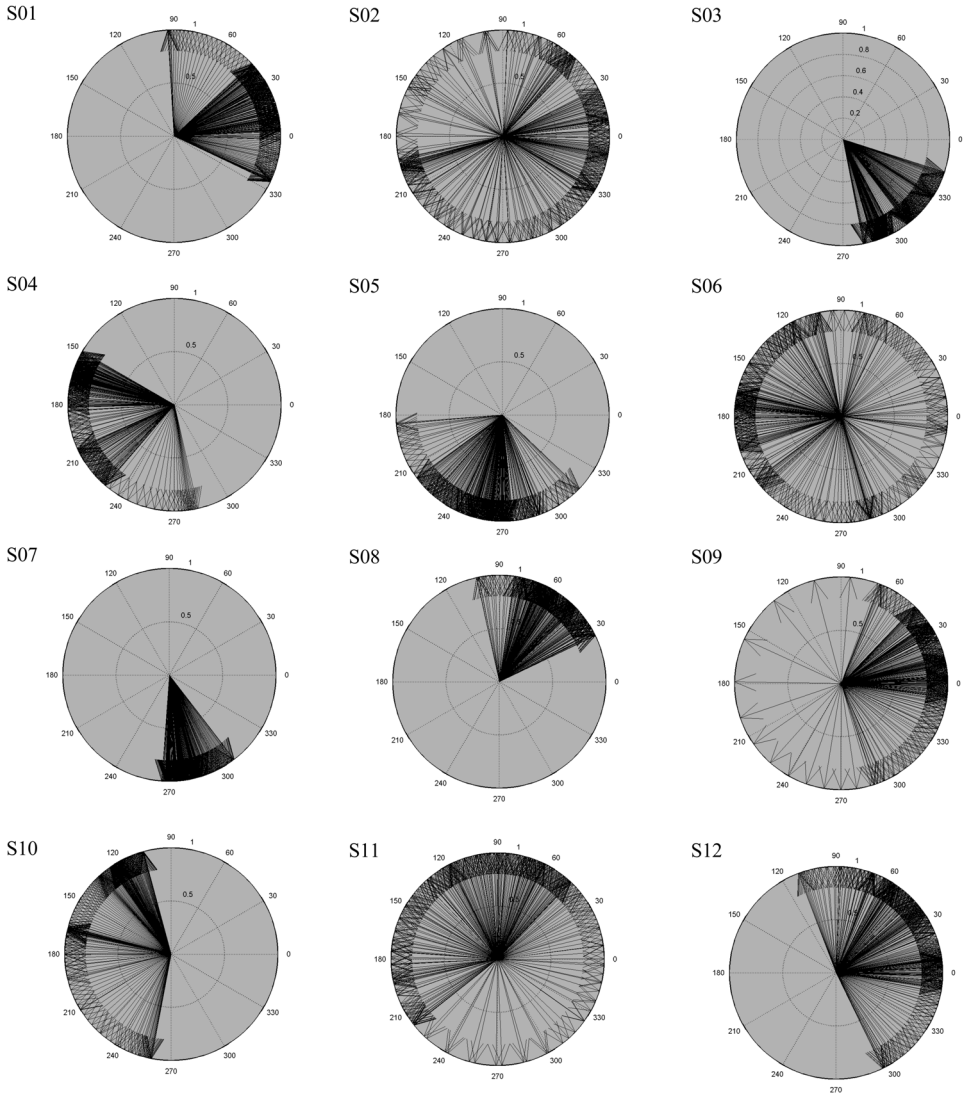

Figure 5: Normative phase vectors for each time point (N=316) during the steady state stimulation (500 ms to 1760 ms after steady state onset) and each subject (S01 – S11). During steady state stimulation the phase vectors are not uniformly distributed (see table 1). The clockwise numbers indicate angles in degree and the small numbers indicate the vector length.

Table 2: Mean length of phase vectors and corresponding p values of the Rayleigh statistics for each subject.

	S01	*S02*	*S03*	*S04*	*S05*	*S06*	*S07*	*S08*	*S09*	*S10*	*S11*	*S12*
Mean length	0.91	0.28	0.96	0.85	0.91	0.34	0.99	0.96	0.82	0.79	0.52	0.79
p value	< .0001	< .0001	< .0001	< .0001	< .0001	< .0001	< .0001	< .0001	< .0001	< .0001	< .0001	< .0001

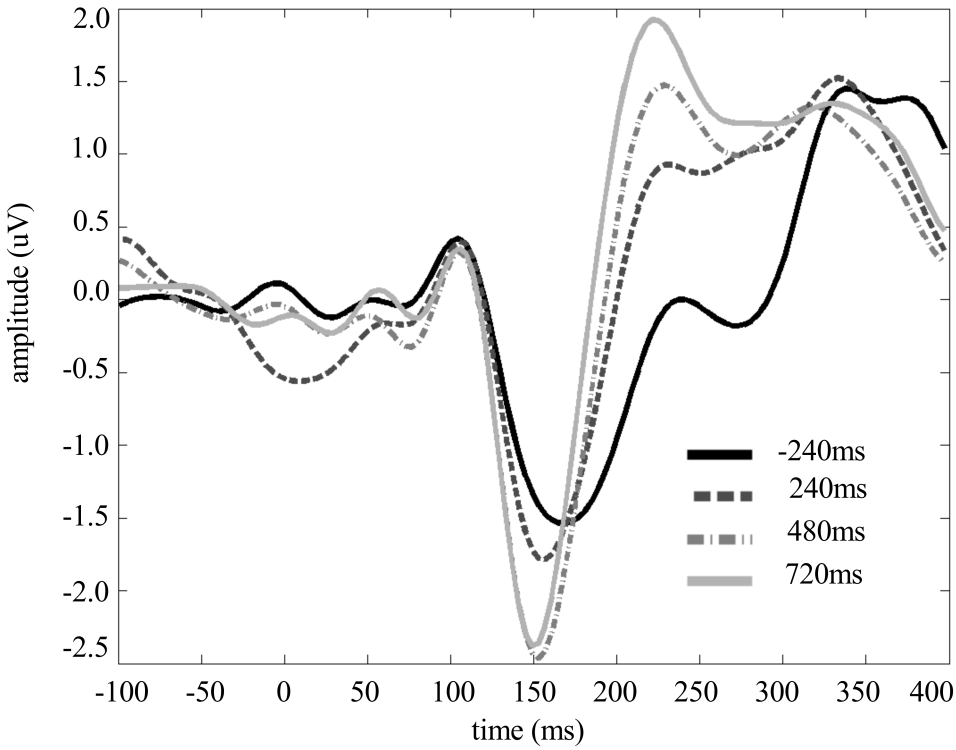

Figure 6: Grand mean waveforms (N=12) of electrode 120 (corresponding to Pz) for each condition. The legend indicates the time interval between steady state offset and presentation of the transient stimulus. Note, that the time scale at the x-axis was normalized to transient stimulus depiction in order to evaluate amplitude and latency differences. The labels indicate the P1-N1-P2-P3 complex.

The P1 amplitudes of left and right electrode sites did not differ ($F(1, 11) = 0.92$, $p > .10$) nor was an interaction between condition (-240 ms, 240 ms, 480 ms and 720 ms) and hemisphere (left and right) observed ($F(3, 33) = .07$, $p > .10$). The main effect condition was not significant ($F(3, 33) = 0.53$, $p > .10$). The same pattern was observed for P1 latencies (condition: $F(3, 33) = 2.8$, $p > .05$; hemi: $F(1, 11) = .46$, $p > .10$; hemi X condition: $F(3, 33) = 1.0$, $p > .10$).

The N1 amplitudes differed across conditions ($F(3, 33) = 4.8$, $p < .05$, $\varepsilon = .60$). A linear trend could be fitted across conditions ($F(1, 11) = 5.7$; $p < .05$). A cubic trend could not be fitted. However, a quadratic trend delivered a model fit of similar variance reduction ($F(1, 11) = 6.0$, $p < .05$) as the linear trend, indicating a deviation from a linear decline of N1 amplitudes across different presentation times of the transient stimulus (see figure 7). This was reflected by post hoc tests that indicated that the evoked N1 amplitude during steady state

stimulation was smaller than N1 deflections of conditions 480 ms and 720 ms (Fisher's LSD tests $p < .05$). All other single comparisons were not significant (see figure 7).

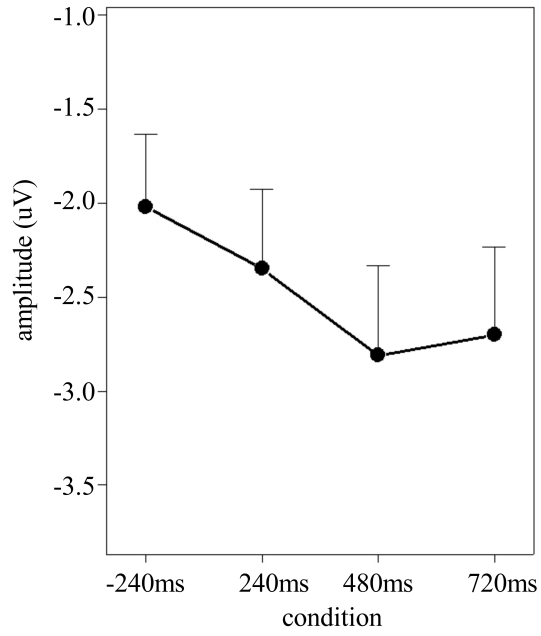

Figure 7: Mean N1 amplitudes and their corresponding standard errors for all conditions (-240 ms, 240 ms, 480 ms and 720 ms after steady state offset).

The N1 peaked at different latencies in each condition ($F(3, 33) = 3.5$, $p = .07$, $\varepsilon = .49$). A strong linear trend ($F(1, 11) = 11.7$, $p < .01$) indicated increasing latencies of the N1 component with decreasing time distances between steady state offset and transient stimulus depiction (see figure 8). No quadratic and cubic trend could be fitted. Figure 9 shows the N1 topography of the grand mean across all subjects ($N = 12$) for each condition.

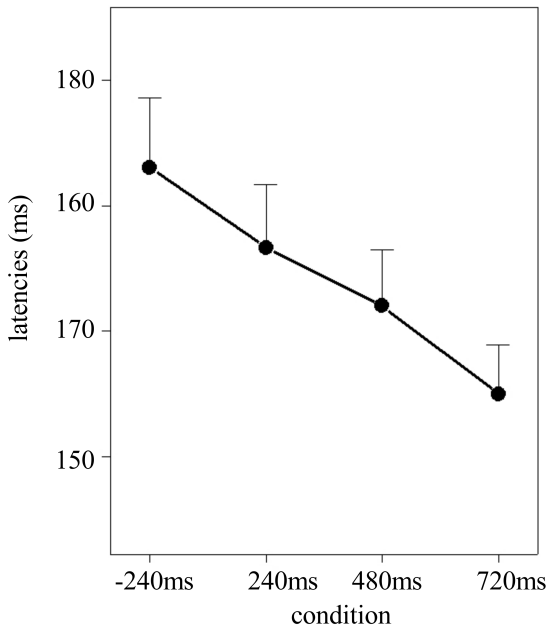

Figure 8: Mean N1 latencies and their corresponding standard errors for all conditions (-240 ms, 240 ms, 480 ms and 720 ms after steady state offset).

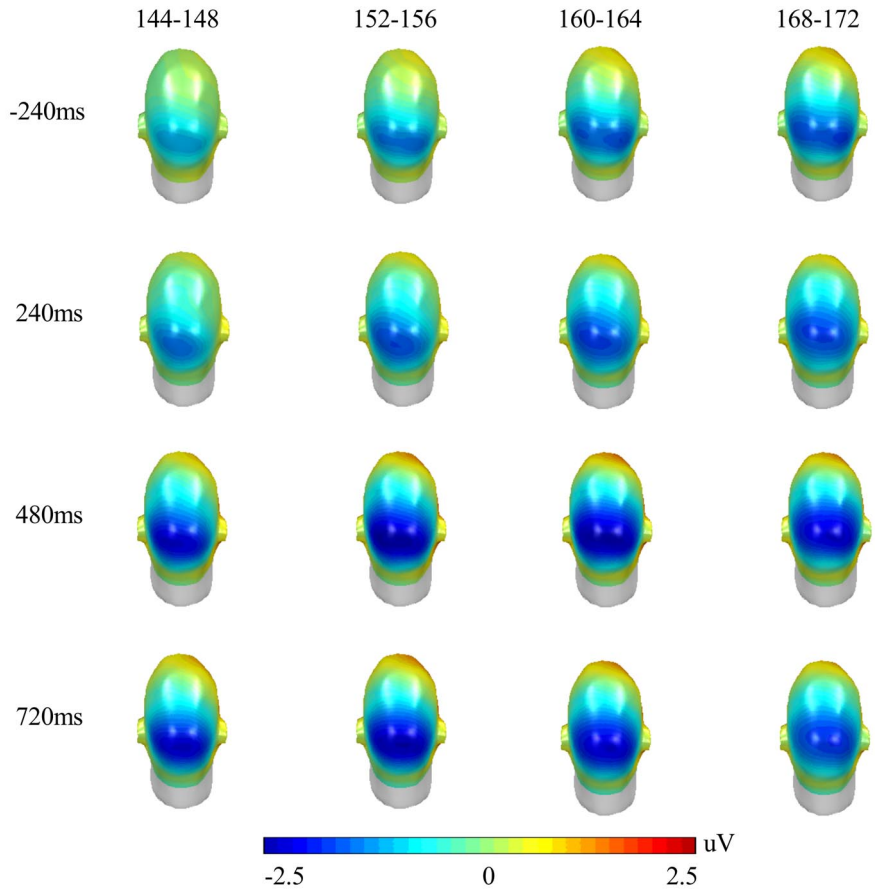

Figure 9: Topography of the grand mean of the N1 component across all subjects (N = 12) for each condition. The time values indexing the rows correspond to the various presentation times of the transient stimulus with respect to steady state offset. The numbers indexing the columns correspond to the latency with respect to transient stimulus depiction. The colorbar indicates the amplitude at an electrode site.

The P2 amplitude differed across conditions ($F(3, 33) = 13.9$, $p < .001$, $\varepsilon = .48$). A strong linear trend ($F(1, 11) = 17.1$, $p < .01$) indicated an increase of P2 amplitude with increasing time distance between steady state offset and transient stimulus onset (see figure 10). No quadratic and cubic trend could be fitted to the data.

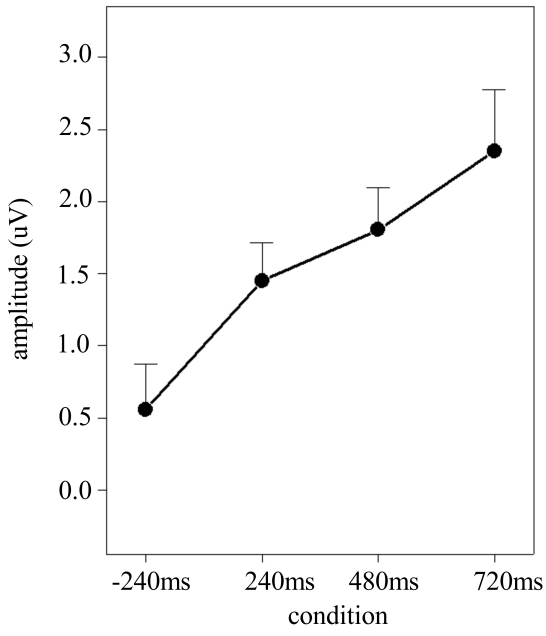

Figure 10: Mean P2 amplitudes and their corresponding standard errors for all conditions (-240 ms, 240 ms, 480 ms and 720 ms after steady state offset).

However, the P2 component did not peak at different latencies. Figure 11 depicts the P2 topography of the grand mean across all subjects (N = 12) for each condition. Neither the P3 amplitude or latency differed across conditions.

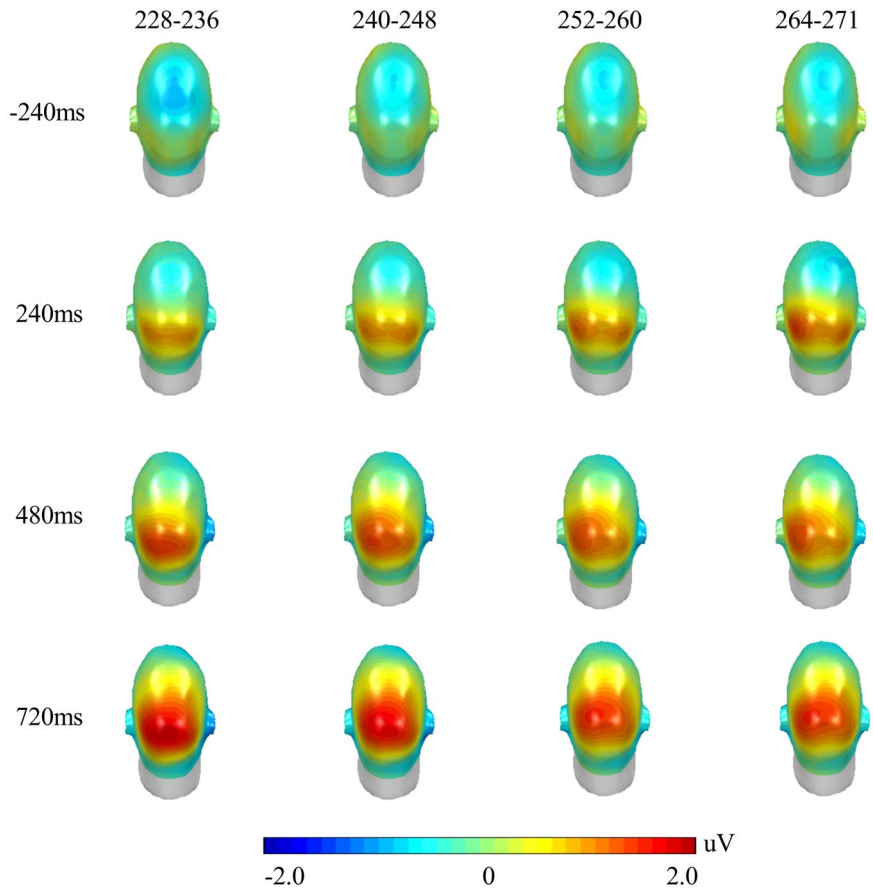

Figure 11: Topography of the grand mean of the P2 component across all subjects (N = 12) for each condition. The time values indexing the rows correspond to the various presentation times of the transient stimulus with respect to steady state offset. The numbers indexing the columns correspond to the latency with respect to transient stimulus depiction. The colorbar indicates the amplitude at an electrode site.

DISCUSSION

In the current chapter data of a steady state experiment was reported in order to familiarize the reader with the basic principles of steady state paradigms. First, it was demonstrated that steady state stimulation resulted in oscillatory brain activity that is dominated by the driving stimulus frequency. This is expressed by a narrow peak around the stimulation frequency in the amplitude spectrum determined by the FFT. Second, it was shown that steady state stimulation elicited cortical activity with a stable phase of the signal. This was demonstrated by evaluating the unimodality of phase vectors obtained by complex demodulation at the frequency of the driving stimulus. Both, amplitude concentration in a narrow bandpass around stimulation frequency and a stable phase have been regarded as important features of a SSVEP (Regan, 1989).

A further subject of investigation was the influence of the SSVEP on evoked responses to visual transient stimuli. Amplitude and latencies of the P1 component evoked during (-240 ms condition) and after (240 ms, 480 ms and 720 ms conditions) steady state stimulation did not differ. In contrast, the N1 component was influenced by presentation time of its corresponding transient stimulus. A quadratic trend indicated that the N1 amplitudes in the two earliest depiction conditions (-240 ms and 240 ms) were attenuated compared to N1 deflections during late transient stimulus presentation after steady state offset (480 ms and 720 ms). Latencies of the N1 component with respect to transient stimulus onset decreased with increasing time distance from steady state offset. Finally, the steady state stimulation had the strongest impact on P2 amplitude that increased over conditions (from the –240 ms to 720 ms condition). The variance reduction by the factor condition was greatest for the P2 amplitude (see big differences in figures 6, 10 and 11). Interestingly, this huge influence on P2 amplitude wasn't paralleled by a latency reduction over conditions of increasing time distance from steady state offset. For the P3 no effects could be observed neither for amplitude nor latency.

The partial reduction of N1 amplitude, increase of N1 latency and attenuation of P2 amplitude with increasing proximity to steady state offset is in line with a recent study of Clementz and collaborators (Clementz et al., 2004) that reported stimulus driven oscillating brain activity up to one second after steady state offset. However, as the steady state stimulation was presented to the left and right visual field, the centrally presented transient stimulus probably competed for spatial attentional resources. The N1 component has been reported to be sensitive to selective spatial attention (Hillyard & Anllo-Vento, 1998; Martinez et al., 1999; Martinez et al., 2001) and the observed effects in the present study could be due to attention effects rather than SSVEP activity per se. However, several arguments oppose this explanation.

First, the modulation of the N1 amplitude by selective spatial attention has been reported with no latency changes (Hillyard, Mangun, & Woldorff, 1995; Mangun, 1995). In the present study, the N1 latency increased with increasing proximity to steady state offset. This effect was even greater than the influence on the N1 amplitude. Second, the P1 amplitude has also been observed to be modulated by attention (Hillyard & Anllo-Vento, 1998; Martinez et al., 1999; Martinez et al., 2001). In the current work the P1 component was not affect by condition at all. In contrast, the SSVEP seemed to have the strongest impact on P2 amplitude that has not been associated with attentional processes. Altogether, the influence on VEPs by the steady state stimulation during and after its offset was different from

modulation patterns observed in spatial attention research. Therefore, attentional processes may only partly be associated with the current observations and ongoing stimulus driven oscillating brain activity is more likely to be responsible for the N1/ P2 changes. However, a direct test would be an experiment that presents the transient stimuli only after steady state offset at the same spatial location. As the original intention of the current study was to compare brain dynamics between schizophrenic and healthy controls, a transient stimulation during steady state stimulation was of special interest.

Traditionally, VEPs have been regarded as a product of neural activity within discrete, functionally defined visual cortical processing regions. Averaging the EEG was thought to cancel out background noise and sum up fixed latency brain events of distinct cortical origin. However, recently this view was challenged and 'background' activity is no longer considered as 'pure' noise. Moreover, some researchers suggested that phase resetting of background activity after stimulus onset results in VEPs (Makeig et al., 2002; Penny, Kiebel, Kilner, & Rugg, 2002). In a recent study Makeig et al. (2002) demonstrated that the visual N1 component could be a product of phase resetting of alpha activity after transient stimulus onset.

In several ways our data support this view. First, if the whole P1-N1-P2-P3 complex would be the product of distinct, latency fixed cortical events, latency effects should be observed for each component as a delay in the first component (P1) should add up. This was not the case in the present study and the P1 component was totally unaffected. Only the latency of the N1 component was affected by the SSVEP. Second, if a distinct cortical event is disrupted by SSVEP activity, changes in amplitude should be paralleled by latency changes. This was only the case for the N1 component but not for the P2. Further, the P2 amplitude decrease with increasing proximity to steady state offset was the strongest observed effect. As can seen from figure 6 and 11, the P2 peaked at almost exactly the same latency in each condition.

Thus, the latency and amplitude effects of the N1 and amplitude variations of the P2 that were uncoupled from all other components, could be the result of stimulus driven highly synchronous oscillatory SSVEP activity (see figure 5). The steady state stimulation with its repeating stimulus depictions induced a strong phase locked signal. Therefore, a transient stimulus trying to reset the phase of background activity (in this case the SSVEP or its remainder) to its own onset is exposed to massive competition as there are no degrees of freedom left in the neural system. The more distal to the steady state offset the transient stimulus is depicted, the less phase locked background activity is present and the phase

resetting can be initiated with more ease. Actually, Rodriguez et al. (Rodriguez et al., 1999) demonstrated that gamma synchronization by percept formation was followed by a period of desynchronization and further synchronization, coinciding with a motor response. The authors suggested that desynchronization allows the formation of new dynamic coupling of neuronal responses. A lack of desynchronization during and shortly after steady state stimulation could be a mechanism explaining the results of the current study. Single trial analysis of the current data with new techniques like independent component analysis (ICA) could elucidate such processes (Makeig et al., 2002).

In the context of the present thesis, it is important to note that this first study suggested that SSVEPs and SSVEFs appear to reflect oscillatory phenomena possibly indicative of complex, emergent large-scale brain processes. Importantly, coupling phenomena in macroscopic networks can be examined using the present approach. Investigating into these processes might provide powerful dependent variables with respect to the main topic of the present thesis, namely motivational/emotional stimulus processing. The following chapters will focus on effects of motivationally relevant stimuli on steady state visual evoked fields using the MEG technology.

SUMMARY

In Chapter 1 a steady state evoked potentials paradigm was reported that used visual stimuli in order to (i) elicit steady state visual evoked potentials (SSVEPs) and (ii) visual evoked potentials (VEPs) in response to transient stimulation. First, it was demonstrated that repetitive visual stimulation with a frequency of 12.5 Hz results in a peak in the amplitude spectrum within a narrow bandbass around stimulation frequency. Second, the elicited SSVEP was stable in phase as the phase vectors of the signal followed a unimodal circular distribution. VEPs of transient stimulation during steady state stimulation or at different time distances from steady state offset were modulated as a function of proximity to steady state offset. The N1 components of the VEPs evoked during and shortly after steady state stimulation were smaller than at later presentation times. The latency of the N1 decreased with more distal depiction times. The amplitude of the P2 followed a strong linear trend reflecting increasing amplitudes associated with increasing time intervals between steady state offset and transient stimulation. The P1 and P3 were not affected. The results do not support that VEPs are the product of discrete, latency fixed events originating in distinct brain areas. The findings of the present study were discussed in the framework of models assuming phase resetting of background activity as a possible mechanism generating VEPs.

REFERENCES

Berg, P., & Scherg, M. (1994). A multiple source approach to the correction of eye artifacts. *Electroencephalogr Clin Neurophysiol, 90*(3), 229-241.

Clementz, B. A., Keil, A., & Kissler, J. (2004). Aberrant brain dynamics in schizophrenia: delayed buildup and prolonged decay of the visual steady-state response. *Brain Res Cogn Brain Res, 18*(2), 121-129.

Diesch, E., Preissl, H., Haerle, M., Schaller, H. E., & Birbaumer, N. (2001). Multiple frequency steady-state evoked magnetic field mapping of digit representation in primary somatosensory cortex. *Somatosens Mot Res, 18*(1), 10-18.

Greenhouse, S. W., & Geisser, S. (1959). On methods in the analysis of profile data. *Psychometrika, 24*, 95-112.

Herrmann, C. S. (2001). Human EEG responses to 1-100 Hz flicker: resonance phenomena in visual cortex and their potential correlation to cognitive phenomena. *Exp Brain Res, 137*(3-4), 346-353.

Hillyard, S. A., & Anllo-Vento, L. (1998). Event-related brain potentials in the study of visual selective attention. *Proc Natl Acad Sci U S A, 95*(3), 781-787.

Hillyard, S. A., Mangun, G. R., & Woldorff, M. G. (1995). In M. S. Ganzzaniga (Ed.), *The Cognitve Neurosciences* (pp. 665-681). Cambridge, MA: MIT Press.

Keil, A., Moratti, S., Sabatinelli, D., Bradley, M. M., & Lang, P. J. (2004). Additive Effects of Emotional Content and Spatial Selective Attention on Electrocortical Facilitation. *Cereb Cortex*.

Makeig, S., Westerfield, M., Jung, T. P., Enghoff, S., Townsend, J., Courchesne, E., & Sejnowski, T. J. (2002). Dynamic brain sources of visual evoked responses. *Science, 295*(5555), 690-694.

Mangun, G. R. (1995). Neural mechanisms of visual selective attention. *Psychophysiology, 32*(1), 4-18.

Martinez, A., Anllo-Vento, L., Sereno, M. I., Frank, L. R., Buxton, R. B., Dubowitz, D. J., Wong, E. C., Hinrichs, H., Heinze, H. J., & Hillyard, S. A. (1999). Involvement of striate and extrastriate visual cortical areas in spatial attention. *Nat Neurosci, 2*(4), 364-369.

Martinez, A., DiRusso, F., Anllo-Vento, L., Sereno, M. I., Buxton, R. B., & Hillyard, S. A. (2001). Putting spatial attention on the map: timing and localization of stimulus selection processes in striate and extrastriate visual areas. *Vision Res, 41*(10-11), 1437-1457.

Morgan, S. T., Hansen, J. C., & Hillyard, S. A. (1996). Selective attention to stimulus location modulates the steady-state visual evoked potential. *Proc Natl Acad Sci U S A, 93*(10), 4770-4774.

Müller, M. M., & Hillyard, S. (2000). Concurrent recording of steady-state and transient event-related potentials as indices of visual-spatial selective attention. *Clin Neurophysiol, 111*(9), 1544-1552.

Muller, M. M., & Hubner, R. (2002). Can the spotlight of attention be shaped like a doughnut? Evidence from steady-state visual evoked potentials. *Psychol Sci, 13*(2), 119-124.

Müller, M. M., Picton, T. W., Valdes-Sosa, P., Riera, J., Teder-Salejarvi, W. A., & Hillyard, S. A. (1998). Effects of spatial selective attention on the steady-state visual evoked potential in the 20-28 Hz range. *Brain Res Cogn Brain Res, 6*(4), 249-261.

Müller, M. M., Teder, W., & Hillyard, S. A. (1997). Magnetoencephalographic recording of steady-state visual evoked cortical activity. *Brain Topogr, 9*(3), 163-168.

Oldfield, R. C. (1971). The assessment and analysis of handedness: The Edinbourgh Inventory. *Neuropsychologia, 9*, 97-113.

Penny, W. D., Kiebel, S. J., Kilner, J. M., & Rugg, M. D. (2002). Event-related brain dynamics. *Trends Neurosci, 25*(8), 387-389.

Perlstein, W. M., Cole, M. A., Larson, M., Kelly, K., Seignourel, P., & Keil, A. (2003). Steady-state visual evoked potentials reveal frontally-mediated working memory activity in humans. *Neurosci Lett, 342*(3), 191-195.

Picton, T. W., Vajsar, J., Rodriguez, R., & Campbell, K. B. (1987). Reliability estimates for steady-state evoked potentials. *Electroencephalogr Clin Neurophysiol, 68*(2), 119-131.

Plourde, G., & Picton, T. W. (1990). Human auditory steady-state response during general anesthesia. *Anesth Analg, 71*(5), 460-468.

Regan, D. (1989). *Human Brain Electrophysiology: Evoked Potentials and Evoked Magnetic Fields in Science and Medicine*. New York: Elsevier.

Rodriguez, E., George, N., Lachaux, J. P., Martinerie, J., Renault, B., & Varela, F. J. (1999). Perception's shadow: long-distance synchronization of human brain activity. *Nature, 397*(6718), 430-433.

Silberstein, R. B., Ciorciari, J., & Pipingas, A. (1995). Steady-state visually evoked potential topography during the Wisconsin card sorting test. *Electroencephalogr Clin Neurophysiol, 96*(1), 24-35.

Silberstein, R. B., Nunez, P. L., Pipingas, A., Harris, P., & Danieli, F. (2001). Steady state visually evoked potential (SSVEP) topography in a graded working memory task. *Int J Psychophysiol, 42*(2), 219-232.

Silberstein, R. B., Schier, M. A., Pipingas, A., Ciorciari, J., Wood, S. R., & Simpson, D. G. (1990). Steady-state visually evoked potential topography associated with a visual vigilance task. *Brain Topogr, 3*(2), 337-347.

Weisz, N., Keil, A., Wienbruch, C., Hoffmeister, S., & Elbert, T. (2004). One set of sounds, two tonotopic maps: exploring auditory cortex with amplitude-modulated tones. *Clin Neurophysiol, 115*(6), 1249-1258.

Chapter 2

Choosing the Right Relationship can make a Difference: A Linear Mixed Effects Model Approach to Heart Rate Time Series in Pavlovian Conditioning

INTRODUCTION

In recent years, linear mixed effects (LME) models have been increasingly used to model longitudinal and time series data. The advantage of such models is that the linear regression model is generalized by assuming certain correlation structures of the residuals modeling dependence of observations (Jennrich & Schluchter, 1986; Munoz, Carey, Schouten, Segal, & Rosner, 1992). Additionally, linear mixed models do not depend on balanced data, upon which classical statistical approaches such as repeated measures ANOVAs have been constructed (Schluchter, 1988). A further advantage is that utilizing a model of error variance increases the efficiency and power of tests. For example, multivariate analysis of variance (MANOVA) assumes a general variance structure leading to estimation of more parameters and consequently to loss of power. Rochon and Helms (Rochon & Helms, 1989) showed that with a first order autoregressive (AR(1)) covariance structure modeling one correlation parameter and an exponential decay, estimates of a general covariance pattern with ten correlation parameters could be reproduced. In that way the number of parameter estimates could be reduced.

Hence, LME models seem to be the appropriate choice for handling psychophysiological data. This approach has been already introduced by Bagiella et al. (Bagiella, Sloan, & Heitjan, 2000). LME models have not been used very often in psychophysiological research however. Therefore, the intention of the present work was to present an example of modeling heart rate (HR) data with LME models obtained from an aversive pavlovian conditioning experiment.

We have chosen HR data, because (i) it represents a typical psychophysiological time series, (ii) it has been a widely used measure of attentional, emotional and higher level cortical processes in psychophysiology (Bradley, Codispoti, Cuthbert, & Lang, 2001; Jennings, van der Molen, Somsen, Graham, & Gianaros, 2002; Moratti, Keil, & Stolarova, 2004; Somsen, Jennings, & Van Der Molen, 2002; Somsen, van der Molen, & Orlebeke,

1983; Thayer, Friedman, Borkovec, Johnsen, & Molina, 2000) and (iii) high variability between subjects in HR data has been usually observed (Hare, 1972; Hodes, Cook, & Lang, 1985), thus challenging the LME models applied here.

First, we will show that employing an AR(1) covariance estimate improved the model fit compared to a model assuming independent within subject errors as indicated by likelihood ratio tests and information criteria. Second in addition to the work of Bagiella et al. (Bagiella et al., 2000), we will demonstrate that modeling a proper correlation structure at the level of the individual subject will uncover HR waveform components not seen in the independent error model and in the grand average HR waveforms. Using cluster analysis similar to that proposed for instance by Hare (Hare, 1972) and Hodes et al. (Hodes et al., 1985) the detection of an interaction between condition (CS+ vs. CS- presentation) and an accelerative HR waveform component during acquisition trials of the conditioning procedure will be confirmed.

METHODS

Participants

Nineteen paid volunteers (10 females, 9 males , all right handed (Oldfield, 1971)) gave written consent to participate in the study. Their mean age was 27.8 years (range: 20-50 years). They had normal or corrected to normal vision and no family history of photic epilepsy. They did not report a recent critical live event or any history of psychotherapy. Due to equipment malfunction we lost HR data of one subject. Finally, data of eighteen (10 females, 8 males) subjects were submitted to further analysis.

Stimuli

Two gray shaded 45^{o} gratings perpendicular oriented to each other served as conditioned stimuli (CS). The CS were displayed in random order, subtending a visual angle of 8^{o} both horizontally and vertically. A red fixation cross was depicted in the middle of the screen and was present throughout the whole experiment. In each trial, a grating was shown in a flickering mode of 12.5 Hz for a period of 5000 ms resulting in 63 on/ off cycles, the grating being depicted for 40 ms, followed by 40 ms black screen during each cycle. During the inter-trial interval, which varied randomly between 6 and 8 seconds, a black screen was shown. The luminance modulation was done in order to elicit visual evoked steady state fields which can be recorded with MEG. The MEG data will be reported elsewhere.

One of the gratings was selected as CS+ or CS-, counterbalanced across subjects. During the last second of CS+ depiction, the unconditioned stimulus (US) consisting of a binaurally presented 110 dB white noise with instantaneous onset was presented for one second and terminated with the CS+. In 15% of the trials (see procedure section), the red fixation cross changed from red to blue for 500 ms either 1000, 2500 or 4000 ms after CS+ and CS- onset, each time lag equally probable.

Procedure

Upon arriving at the laboratory subjects were familiarized with the MEG chamber in which the recording took place. Thereafter, they were prepared for the MEG recording that will be described in more detail elsewhere. Subjects were instructed that in the first block of the experiment they will be shown different patterns and whenever the red cross during pattern depiction changes to blue, they will have to press a response button as fast as possible. They were also informed that during the first block no loud noise will be presented. Further, they were told that during the second block of the experiment they will have to do the same task as before, but from time to time they will hear a very loud noise which can startle them. After the instructions subjects gave written consent and the electrocardiogram (ECG) electrodes were attached at the left lower costal arch and the right collarbone.

The experimental session started with a written instruction on the screen in the MEG chamber explaining again the task and ensuring subjects that no loud noise will be delivered during the first block, which served as habituation phase. The habituation block consisted of twenty CS+, twenty CS- and six target trials (button press after the red cross turns blue during presentation of three CS+ and CS- stimuli) depicting the stimuli without pairing of the US with the CS+. Thereafter, a short break of one minute was taken and subjects were instructed via text depicted on the screen, that during the next block they will hear a loud noise from time to time. After the break the acquisition block began. The same number of trials for CS+, CS- and targets as in the habituation block were shown, except that the CS+ was always paired with the US. The CS- was never associated with the US. The extinction block started without a break after the acquisition trials, containing the same number of trials as the individual blocks before. The CS+ and CS- were never paired with the US during extinction. After the experiment, participants were paid 15 € (approximately 15 US dollars).

Recording

The ECG acquisition was done with a Synamps amplifier (NEUROSCAN™) using Ag/ Cl electrodes. As the ECG recording was coupled with an MEG measurement (MAGNES™, 2500 WH, 4D Neuroimage, San Diego, USA) data was sampled with 254.3 Hz and a band-pass filter of 0.1 to 50 Hz was applied on line.

Data preprocessing

Only the first four seconds of stimulus presentation were analyzed because during acquisition the last second overlapped with US presentation. Target trials were not submitted to analysis. HR change waveforms during presentations of the CS+ and CS- in acquisition and extinction trials were obtained using in-house-software written in MATLAB™. The algorithm of the software estimated the HR change over 4000 ms stimulus presentation in 500 ms steps using a 2000 ms pre-stimulus baseline. The frequency of the occurrence of an R-wave was derived from the interbeat-interval and weighted according to the distance from a 500 ms step within the time vector. The HR change was transformed in beats per minutes (bpm). The resulting HR waveforms consisted of changes in bpm compared to prestimulus baseline for nine consecutive time bins (0 ms to 4000 ms in 500 ms steps).

Statistical model formulation and analysis

The LME calculations for two proposed models were performed using R©, a free distributable statistical package (Team, 2004). Wilson (Wilson, 1974) suggested that analyzing differences in waveform components in order to illustrate varying HR response curves over time for different conditions is more meaningful than comparing differences in average mean HR change per time unit. Therefore, we selected *condition* (CS+ and CS-), *time* (0ms to 4000ms in 500ms steps, translated in 9 integer steps) for linear, $time^2$ for quadratic, $time^3$ for cubic and $time^4$ for quartic waveform components as fixed effects for the two models. As we were not interested in mean differences or drifts of the HR response curve per subject over all conditions and within conditions, we chose the intercept and the linear slope (*time*) to be random effects at both the *subject* and *condition within subject* level. The general form of that model is:

$$
\begin{aligned}
&y_{ij} = X_{ij}\beta + Z_{i,j}b_i + Z_{ij}b_{ij} + \varepsilon_{ij} \ , \\
&b_i \sim N(0, \Psi_1), \\
&b_{ij} \sim N(0, \sigma_2^2), \\
&\varepsilon_{ij} \sim N(0, \Sigma_{ij}),
\end{aligned}
\qquad (1)
$$

where $\mathbf{y}_{ij}$ is the response vector with 9 time steps for subject *i* in condition *j*. $\mathbf{X}_{ij}$ is the design matrix for the fixed effects and $\boldsymbol{\beta}$ is the vector containing the fixed effects. $\mathbf{Z}_{i,j}$ is the design matrix of the random effects for subject *i* on the measurements for condition *j* and $\mathbf{Z}_{ij}$ for the random effects for condition *j* within subject *i*. The vectors $\mathbf{b}_i$ and $\mathbf{b}_{ij}$ contain the random effects of their corresponding level, whereas $\boldsymbol{\varepsilon}_{ij}$ represents the vector of the residual errors. For model M1 we determined:

$$\Sigma_{ij} = \sigma^2 I \ , \qquad \text{model M1} \qquad (2)$$

where $\mathbf{I}$ is the identity matrix. Thus, $\boldsymbol{\Sigma}_{ij}$ is a diagonal matrix assuming no correlation between residual errors and implying that HR change observations over time are independent. Model M2 was identical to model M1, except that the residual errors $\boldsymbol{\varepsilon}_{ij}$ were assumed to follow a AR(1) serial correlation structure.

$$
\begin{aligned}
&\varepsilon_{ij} \sim N(0, \Lambda_{ij}), \\
&\Lambda_{ij} = \tau^2 H_{ij}
\end{aligned}
\qquad \text{model M2 (3)}
$$

$\boldsymbol{\Lambda}_{ij}$ is a variance-covariance matrix and $\mathbf{H}_{ij}$ is a covariance matrix modeled by an exponential serial correlation function of first order (AR(1)). The AR(1) model estimates one correlation parameter and assumes that the dependence between observations decays exponentially with increasing distance from each other. Such serial correlation structures have been introduced to model dependence in time-series data and are discussed for example in Pinheiro and Bates (Pinheiro & Bates, 2000) in more detail. Thus, model M1 represents an independent residual error model whereas model M2 assumes serial correlation between errors. For both models the parameters were estimated using restricted maximum likelihood estimation (REML). A description of the REML estimation method can be found in Searle et al. (Searle, Casella, & McCulloch, 1992).

The HR change data for CS+ and CS- presentation during acquisition and extinction trials (only non target trials) were submitted to model M1 and M2 each in order to asses interactions of condition (CS+, CS-) and waveform components (linear, quadratic, cubic, quartic). As model M1 and M2 are nested, likelihood ratio tests were applied to evaluate which of the two models was more appropriate. Additionally, information criteria AIC (Akaike, 1974) and BIC (Schwarz, 1978) were calculated. In order to locate the source of an interaction, separate analysis for conditions (CS+, CS-) were submitted to model M1 and M2 with fixed effect *condition* and random effect *condition within subject* removed.

HR data was further analyzed with cluster analysis similar as introduced by Hare et al. (Hare, 1972). Before, the HR waveforms were scored for each subject as follows: Within the first 2 seconds of stimulus presentation the fastest and the slowest HR were determined. If the fastest HR value followed the slowest, then the slowest was subtracted from the fastest yielding a more positive value indicating an accelerative slope. If the slowest HR value followed the fastest, the subtraction was done the other way round yielding a more negative value, describing a decelerative slope. The same procedure was applied for the subsequent two seconds of stimulus presentation. So, for every subject two waveform scores were obtained and submitted to cluster analysis using the Ward method. The HR waveforms of the emerging subject groups were only submitted to the LME model M2 as described above. In order to demonstrate the contribution of the different HR waveform components linear, quadratic, cubic and quartic polynomials were fitted to the grand mean of one cluster resulting from cluster analysis.

RESULTS

Comparison of the independent error and serial correlation models

Two models were fitted to the heart rate change data for the acquisition and extinction trials as described above. One model assumed independent errors (M1), the other model assumed within subject serial correlation of residuals (M2).

For the heart rate change during acquisition trials none of the waveform components (linear, quadratic, cubic and quartic) interacted with condition (CS+, CS-) when M1 was applied. By contrast, model M2 revealed an interaction between condition and the quartic waveform component (Table 1) although this was not visible in the mean HR change waveforms (see Fig. 1). A likelihood ratio test and smaller information criteria indicated that M2 was the more adequate model with respect to the data (Table 2).

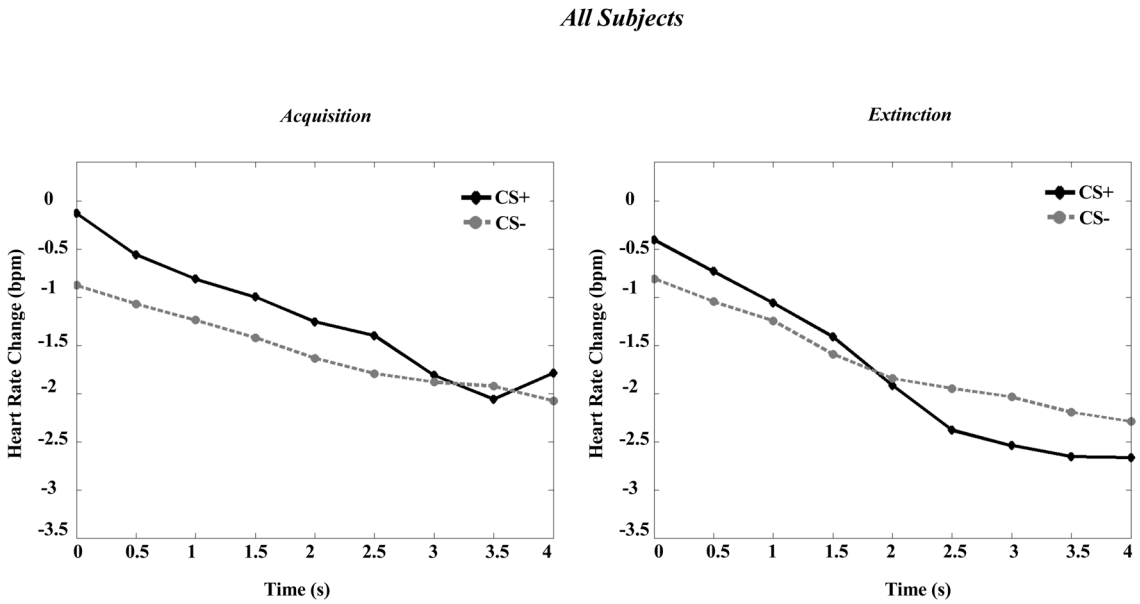

Figure 1. Mean heart rate change (HR) in beats per minute (bpm) over 4 s stimulus presentation for the CS+ and CS- averaged across all subjects (N=18). The left panel depicts HR changes during acquisition and the right panel during extinction trials.

Table 1. Interaction of waveform components and conditions (CS+, CS-) during acquisition for models M1 and M2. numDF = degrees of freedom numerator; denDF = degrees of freedom denominator.

			model M1		model M2	
interaction with condition	numDF	denDF	F value	p value	F value	p value
linear	1	280	1.5	n. s.	0.8	n. s.
quadratic	1	280	0.3	n. s.	2.0	n. s.
cubic	1	280	0.2	n. s.	1.0	n. s.
quatric	1	280	2.9	n. s.	*6.8*	*< .01*

Table 2. Comparison between models M1 and M2 for acquisition trials. numDF = degrees of freedom numerator; denDF = degrees of freedom denominator. DF = degrees of freedom; AIC = Akaike Information Criteria; BIC = Bayes Schwarz Information Criteria; logLik = log likelihood.

Model	DF	AIC	BIC	logLik	Test	L. Ratio	p value
M1	15	878.9	935.1	-424.4			
M2	16	649.7	709.7	-308.9	M1 vs. M2	*231.1*	*< .0001*

In order to locate the source of the observed interaction between a quartic component and condition, we fitted M1 and M2 to the data for condition CS+ and CS- separately. For CS+ model M1 revealed only a trend for the quartic waveform pattern ($F(1,140) = 3.6$, $p = 0.06$), whereas model M2 showed a significant pattern of that kind ($F(1,140) = 8.3$, $p < .01$). For CS- model M1 and model M2 did not reveal any significant quartic component. Again, as indicated by likelihood ratio tests and information criteria, model M2 delivered the better data fit (Tables 3 & 4).

Table 3. Comparison between model M1 and M2 for CS+ during acquisition. DF = degrees of freedom; AIC = Akaike Information Criteria; BIC = Bayes Schwarz Information Criteria; logLik = log likelihood.

Model	DF	AIC	BIC	logLik	Test	L. Ratio	p value
M1	8	463.6	488.1	-223.8			
M2	9	344.6	372.1	-163.3	M1 vs. M2	*121.0*	*< .0001*

Table 4. Comparison between model M1 and M2 for CS- during acquisition. DF = degrees of freedom; AIC = Akaike Information Criteria; BIC = Bayes Schwarz Information Criteria; logLik = log likelihood.

Model	DF	AIC	BIC	logLik	Test	L. Ratio	p value
M1	8	412.6	437.0	-198.3			
M2	9	305.0	332.5	-143.5	M1 vs. M2	*110.0*	*< .0001*

For the heart rate change during extinction trials the linear waveform component interacted with condition (Table 5) when M1 was applied as can be seen in the mean HR change waveforms for the extinction trials (see figure 1). In parallel, model M2 revealed the same interaction (Table 5). A likelihood ratio test and smaller information criteria indicated that M2 was the more adequate model with respect to the data (Table 6).

Table 5. Interaction of waveform components and conditions (CS+, CS-) during extinction for models M1 and M2. numDF = degrees of freedom numerator; denDF = degrees of freedom denominator.

			model M1		model M2	
interaction with condition	numDF	denDF	F value	p value	F value	p value
linear	1	280	*7.7*	*< .01*	*4.7*	*< .05*
quadratic	1	280	1.1	n. s.	1.2	n. s.
cubic	1	280	3.7	n. s.	3.7	n. s.
quatric	1	280	0.3	n. s.	0.3	n. s.

Table 6. Comparison between models M1 and M2 for extinction trials. DF = degrees of freedom; AIC = Akaike Information Criteria; BIC = Bayes Schwarz Information Criteria; logLik = log likelihood.

Model	DF	AIC	BIC	logLik	Test	L. Ratio	p value
M1	15	726.7	783.0	-348.3			
M2	16	496.8	556.8	-232.4	M1 vs. M2	*231.9*	*< .0001*

In order to locate the source of the observed interaction between a linear component and condition, we fitted M1 and M2 to the data for condition CS+ and CS- separately. For CS+ models M1 and M2 revealed a highly significant linear waveform component (M1: $F(1, 140) = 34.4$; $p < .0001$); M2: $F(1, 140) = 28.6$; $p < .0001$). For CS- models M1 and M2 revealed a significant linear waveform component (M1: $F(1, 140) = 8.9$; $p < .01$; M2: $F(1, 140) = 10.4$; $p < .01$), but the smaller F values and the interaction with condition in the higher order analysis (see above) indicated that the HR deceleration was more prominent during CS+ presentation in the extinction trials. Again, as indicated by likelihood ratio tests and information criteria, model M2 delivered the better data fit (Tables 7 & 8).

Table 7. Comparison between model M1 and M2 for CS+ during extinction. DF = degrees of freedom; AIC = Akaike Information Criteria; BIC = Bayes Schwarz Information Criteria; logLik = log likelihood.

Model	DF	AIC	BIC	logLik	Test	L. Ratio	p value
M1	8	373.0	397.4	-178.5			
M2	9	255.7	283.2	-118.9	M1 vs. M2	*119.3*	*< .0001*

Table 8. Comparison between model M1 and M2 for CS- during extinction. DF = degrees of freedom; AIC = Akaike Information Criteria; BIC = Bayes Schwarz Information Criteria; logLik = log likelihood.

Model	DF	AIC	BIC	logLik	Test	L. Ratio	p value
M1	8	374.1	398.5	-179.0			
M2	9	258.4	285.9	-120.2	M1 vs. M2	*117.7*	*< .0001*

M2 assuming serial correlation errors turned out to be the more adequate model for the HR change data. During acquisition trials a quartic waveform component for the CS+ condition possibly reflected an accelerative defensive reaction, whereas during extinction trials the CS+ seemed to elicit a stronger HR deceleration than the CS-. Thus, model M2 gave rise to further investigation of the HR data with respect to more individual HR change patterns in response to CS+ and CS-.

Delineation of different responders with cluster analysis and linear mixed models

As the application of model M2 indicated an interaction between a quartic waveform component and condition during acquisition not visible in the grand mean of HR change, we assumed great variability in the HR data. Therefore we performed a cluster analysis using the ward method on HR change during the first and subsequent two seconds of CS+ presentation for acquisition trials (see method section). We obtained three clusters reflecting subjects showing a defensive accelerative response (N=8) and two groups of subjects depicting a decelerative pattern (N=6 and N=4, respectively). In order to obtain samples of sufficient size for further analysis, the latter two groups were collapsed to one decelerative group (N=10). This grouping structure was applied to the extinction trials evaluating possible learning differences for accelerators and decelerators. The mean HR change waveforms resulting from the cluster analysis are shown in Figure 2. The waveform patterns suggested that only the accelerators showed a differentiated orientation response to the CS+ during extinction. To confirm that assumption we fitted model M2 to the HR change data for the acquisition and extinction trials for each group separately.

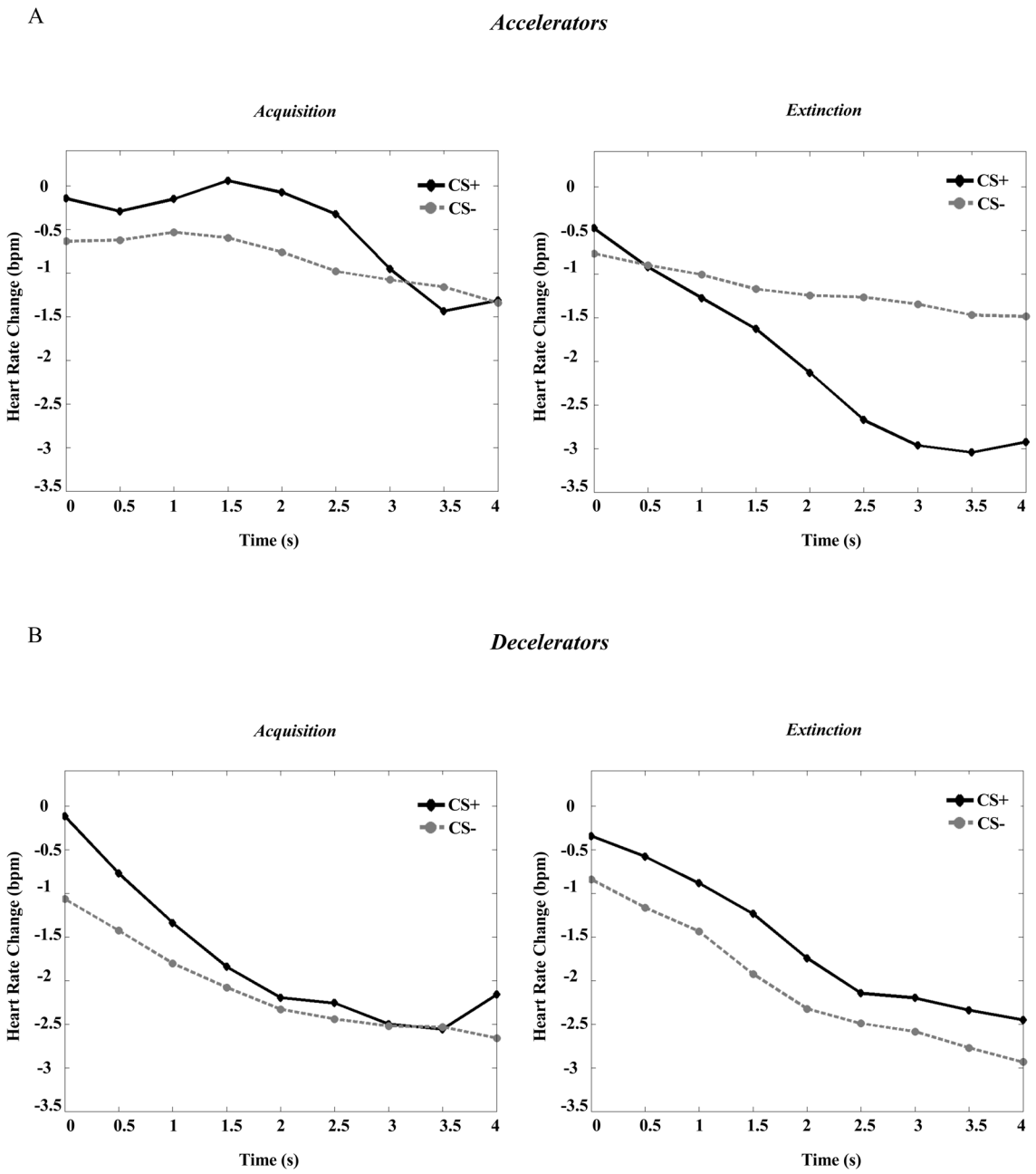

Figure 2. Mean heart rate (HR) change in beats per minute (bpm) over 4 s stimulus presentation for the CS+ and CS- averaged across the different groups obtained by cluster analysis. The upper panel (A) depicts HR change for accelerators (N=8) during acquisition (left) and extinction (right) trials. The lower panel (B) shows HR change for decelerators (N=10) during acquisition (left) and extinction (right) trials.

As suggested by the waveform patterns of figure 2, accelerators showed a clear defensive accelerative component as reflected by an interaction of a quartic component and condition (Table 9) during acquisition trials. This was confirmed by separate analysis of CS+ and CS- trials yielding only a quartic component waveform for CS+ ($F(1, 60) = 28.3$; $p < .0001$). During the extinction phase of the experiment accelerators showed a more pronounced

orientation response to CS+ than CS- as reflected by greater HR deceleration for CS+ presentation (Table 10 for interaction; linear component CS+: $F(1, 60) = 18.7$; $p < .0001$; linear component CS-: n.s.).

Table 9. Interaction of waveform components and conditions (CS+, CS-) during acquisition for accelerators. numDF = degrees of freedom numerator; denDF = degrees of freedom denominator.

			model M2	
interaction with condition	numDF	denDF	F value	p value
linear	1	120	1.1	n. s.
quadratic	1	120	0.5	n. s.
cubic	1	120	0.4	n. s.
quatric	1	120	*15.4*	*< .0001*

Table 10. Interaction of waveform components and conditions (CS+, CS-) during extinction for accelerators. numDF = degrees of freedom numerator; denDF = degrees of freedom denominator.

			model M2	
interaction with condition	numDF	denDF	F value	p value
linear	1	120	*9.4*	*< .01*
quadratic	1	120	3.6	n. s.
cubic	1	120	3.7	n. s.
quatric	1	120	0.5	n. s.

For decelerators an interaction between a quadratic waveform component and condition was obtained (Table 11). Separate analysis of acquisition trials during CS+ and CS- presentation showed that the quadratic component was more prominent for CS+ ($F(1, 76) = 20.6$; $p < .0001$) than for CS- ($F(1, 76) = 4.0$; $p < .05$). During the extinction phase of the experiment decelerators did not show any different HR change for CS+ and CS-.

Table 11. Interaction of waveform components and conditions (CS+, CS-) during acquisition for decelerators. numDF = degrees of freedom numerator; denDF = degrees of freedom denominator.

			model M2	
interaction with condition	numDF	denDF	F value	p value
linear	1	152	0.3	n. s.
quadratic	1	152	*4.4*	*< .05*
cubic	1	152	0.7	n. s.
quatric	1	152	1.0	n. s.

Altogether, applying model M2 to the different groups (accelerators and decelerators) revealed that only subjects showing an accelerative defense reaction to the CS+ during acquisition exhibited a greater orientation response to CS+ during extinction compared to CS- presentation.

For demonstration we show the results of a polynomial fit up to 4 degrees to the HR waveform of the accelerators elicited during CS+ presentation in the acquisition block (figure 3). As can be seen, the quartic waveform is superior to the other components as reflected by the lower residuals supporting the above LME analysis.

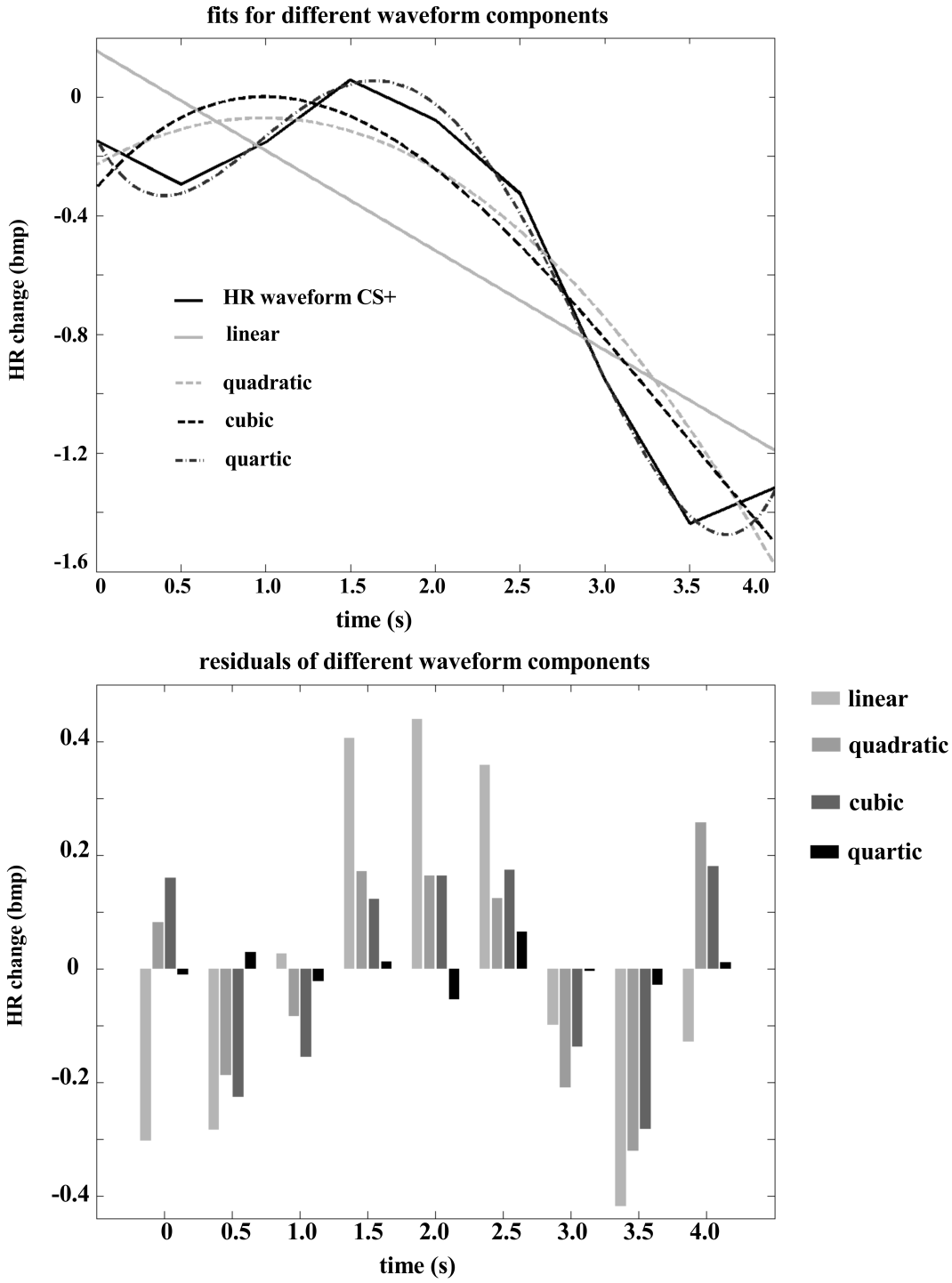

Figure 3. On the upper panel the mean heart rate (HR) change in beats per minute (bpm) over 4 s stimulus presentation for the CS+ averaged across accelerators (N=8) and the corresponding polynomial fits up to the 4th degree are shown. The lower panel of the figure depicts the residuals of the fits.

DISCUSSION

In the present work we applied two different LME models to HR data obtained from an aversive pavlovian conditioning experiment. Model M1 assumed independent residual errors implying that HR change observations over time are not correlated. In model M2 a first order autoregressive (AR(1)) covariance structure was incorporated assuming that HR changes between time bins follow a correlation structure with an exponential decay.

Likelihood ratio tests and information criteria indicated that model M2 resulted in a better data fit as can be expected from the work of Bagiella et al. (Bagiella et al., 2000). Further, we could demonstrate that modeling a proper correlation structure between observations (here HR change over time) at the individual subject level uncovered HR waveform components not revealed by model M1 and the grand average HR waveforms.

Indeed, further investigation by means of cluster analysis yielded two groups of subjects and confirmed the serial correlation LME model. Some subjects showed an accelerative HR response elicited by the CS+ during acquisition as reflected by a quartic waveform component. The other group of subjects mainly decelerated in response to the CS+ during acquisition with a slight acceleration at the end of the 4000 ms period as reflected by a quadratic waveform component. Thus, if we had not applied an LME model estimating an AR(1) covariance structure of residual errors we would not have initiated a cluster analysis and consequently not revealed the two different response patterns. The formulation of random effects in LME models and the application of correlation structures in order to model dependence in time series data at the individual subject level obviously considers variations between subjects more effectively.

The emergence of accelerators and mainly decelerators during acquisition trials is in concordance with results obtained by Hare (Hare, 1972) and Hodes et al. (Hodes et al., 1985). Interestingly, the two groups showed different learning sets as only accelerators showed an OR to CS+ in extinction trials. Decelerators did not depict any different response to CS+ and CS- during extinction. This observation will be discussed elsewhere in more detail together with the MEG data.

The present results demonstrated that LME models assuming a certain correlation structure between observations in time series data can lead to different results. Thus, it is important to compare different models in order to determine which model is more appropriate. If the models are nested a likelihood ratio test can be performed, if not information criteria can be called on (Akaike, 1974; Schwarz, 1978).

For the purpose of simplicity, we compared two models representing different approaches to the problem of psychophysiological time series data: one model was based on the assumption of independence between observations, whereas an AR(1)) model contained a typical correlation structure estimating the correlation of two subsequent observations and assuming an exponential decay of that dependence with increasing distance of observations. Of course, other correlation structures as the AR(1) model are possible (Pinheiro & Bates) and sophisticated approaches improving the covariance structure of LME models have been discussed (Verbeke, Lesaffre, & Brant, 1998). Our intention in the present work was to reintroduce the concept of LME models as has been done before (Bagiella et al., 2000) and to show that simple and available models can improve fitting psychophysiological data. We did not include a model with unstructured variance (MANOVA), as variances are usually structured in repeated measures designs. Therefore, MANOVA is generally inefficient if there are many repeated observations as in the case of HR change over some seconds.

In sum, LME models endow the researcher with a flexible way to model empirical data and to estimate parameters of interest more efficiently. In our example we were able to uncover effects based on individual differences between subjects using a more adequate model for time series. Additionally, we propose that besides effect parameters results of model comparisons should also be reported. This could improve the comparability of different studies. Finally, we agree with Bagiella et al. (Bagiella et al., 2000) that investigators in psychophysiology should consider LME models as a possible standard method for the analysis of repeated measures designs.

SUMMARY

The aim of the present work was to describe a methodological approach to handle psychophysiological data usually correlated in time. Here, we applied linear mixed models (LME) for the analysis of heart rate (HR) change over time obtained in an aversive pavlovian conditioning paradigm. The first model (M1) assumed independent residual errors whereas the second one (M2) contained a first order autoregressive (AR(1)) model estimating the covariance structure of the HR time series. Model M2 was more appropriate than model M1 as suggested by likelihood ratio tests. Additionally, model M2 revealed a quartic waveform component during acquisition for the CS+ suggesting an accelerative defense reaction not seen in the grand average HR waveforms. Cluster analysis confirmed model M2 as one group with accelerative and another group with decelerative response patterns to the CS+ during

acquisition emerged. Only the accelerators showed a discriminative orientation response (OR) to the CS+ during extinction. Using an LME model with an AR(1) corrleation structure revealed more distinct response patterns in HR data.

REFERENCES

Akaike, H. (1974). A new look at the statistical model identification. *IEEE Transactions on Automatic Control, 19*, 716-723.

Bagiella, E., Sloan, R. P., & Heitjan, D. F. (2000). Mixed-effects models in psychophysiology. *Psychophysiology, 37*(1), 13-20.

Bradley, M. M., Codispoti, M., Cuthbert, B. N., & Lang, P. J. (2001). Emotion and Motivation I: Defensive and Appetitive Reactions in Picture Processing. *Emotion, 1*(3), 276-298.

Hare, R. D. (1972). Cardiovascular components of orienting and defensive responses. *Psychophysiology, 9*(6), 606-614.

Hodes, R. L., Cook, E. W., 3rd, & Lang, P. J. (1985). Individual differences in autonomic response: conditioned association or conditioned fear? *Psychophysiology, 22*(5), 545-560.

Jennings, J. R., van der Molen, M. W., Somsen, R. J., Graham, R., & Gianaros, P. J. (2002). Vagal function in health and disease: studies in Pittsburgh. *Physiology & Behaviour, 77*(4-5), 693-698.

Jennrich, R. I., & Schluchter, M. D. (1986). Unbalanced repeated-measures models with structured covariance matrices. *Biometrics, 42*(4), 805-820.

Moratti, S., Keil, A., & Stolarova, M. (2004). Motivated attention in emotional picture processing is reflected by activity modulation in cortical attention networks. *Neuroimage, 21*(3), 954-964.

Munoz, A., Carey, V., Schouten, J. P., Segal, M., & Rosner, B. (1992). A parametric family of correlation structures for the analysis of longitudinal data. *Biometrics, 48*(3), 733-742.

Oldfield, R. C. (1971). The assessment and analysis of handedness: The Edinbourgh Inventory. *Neuropsychologia, 9*, 97-113.

Pinheiro, J. C., & Bates, D. M. (2000). *Mixed-Effects Models in S and S-PLUS* (1 ed.). New York, Berlin, Heidelberg: Springer.

Rochon, J., & Helms, R. W. (1989). Maximum likelihood estimation for incomplete repeated-measures experiments under an ARMA covariance structure. *Biometrics, 45*(1), 207-218.

Schluchter, M. D. (1988). Analysis of incomplete multivariate data using linear models with structured covariance matrices. *Statistics in Medicine, 7*(1-2), 317-324.

Schwarz, G. (1978). Estimating the dimension of a model. *The Annals of Statistics, 6*, 461-464.

Searle, S. R., Casella, G., & McCulloch, C. E. (1992). *Variance Components*. New York: Wiley.

Somsen, R., Jennings, J. R., & Van Der Molen, M. (2002). Human vagal heart rate responses in warned reaction time tasks: A cross-validation with simulated vagus-sino-atrial node interactions. *Journal of Electrocardiology, 35 Suppl*, 231-237.

Somsen, R. J., van der Molen, M. W., & Orlebeke, J. F. (1983). Phasic heart rate changes in reaction time, shock avoidance, and unavoidable shock tasks: are hypothetical generalizations about different S1-S2 tasks justified? *Psychophysiology, 20*(1), 88-94.

Team, R. D. C. (2004). R: A language and environment for statistical computing. R Foundation for Statistical Computing. Vienna, Austria: R Foundation for Statistical Computing.

Thayer, J. F., Friedman, B. H., Borkovec, T. D., Johnsen, B. H., & Molina, S. (2000). Phasic heart period reactions to cued threat and nonthreat stimuli in generalized anxiety disorder. *Psychophysiology, 37*(3), 361-368.

Verbeke, G., Lesaffre, E., & Brant, L. J. (1998). The detection of residual serial correlation in linear mixed models. *Statistics in Medicine, 17*(12), 1391-1402.

Wilson, R. S. (1974). CARDIVAR: the statistical analysis of heart rate data.

Psychophysiology, 11(1), 76-85.

Chapter 3

Motivated Attention in Emotional Picture Processing is Reflected by Activity Modulation in Cortical Attention Networks

INTRODUCTION

Recent developments in emotion theory have emphasized the importance of motivational systems and processes (Lang, Bradley, & Cuthbert, 1997). As one possible laboratory model of emotional processing, viewing of emotional pictures has been shown to co-vary with measures indicative of the motivational state of the organism. For instance, longer viewing time and higher skin conductance can be observed for stimuli rated as high in emotional arousal, compared to calm picture stimuli (Lang, Bradley, & Cuthbert, 1998). Likewise, measures of central nervous activity correlated with subjective arousal ratings of emotional pictures. Studies using Event-Related Potentials (ERPs) as a dependent variable demonstrated that high arousing stimuli (pleasant as well as unpleasant pictures) produce a sustained late positive wave which is attenuated for less arousing neutral images (Ito, Larsen, Smith, & Cacioppo, 1998; Mini, Palomba, Angrilli, & Bravi, 1996; Palomba, Angrilli, & Mini, 1997; Schupp et al., 2000). This late positive wave can be maintained for several seconds until picture presentation offset and is interpreted as reflecting greater activity in systems processing different aspects of the stimulus, including their motivational relevance (Cuthbert, Schupp, Bradley, Birbaumer, & Lang, 2000). Using dense array EEG and a source estimation technique Keil and collaborators (Keil et al., 2002) identified occipital and posterior parietal regions with a right hemispheric dominance as a possible origin of the arousal-modulated late positive wave.

In addition to these late ERP modulations by emotional intensity, several studies have reported ERP changes at earlier stages of visual processing. In a rapid serial picture presentation paradigm, Junghöfer and collaborators observed enhanced negativity at posterior recording sites in time ranges around 200 ms after onset of high arousing stimuli compared to neutral ones (Junghöfer, Bradley, Elbert, & Lan, 2001). Consistent with this finding, the

visual N1 component has been found to vary with affective arousal of visual stimuli (Keil et al., 2002; Pizzagalli, Regard, & Lehmann, 1999).

Taken together, this evidence suggests that the affective or motivational significance of a stimulus may amplify sensory processing at early stages of visual information processing reflecting fast discrimination. Thus, motivated attention (Lang et al., 1997) may represent automatic allocation of processing resources to visual features which are motivationally significant, paralleling a neural 'sensory gain' mechanism as hypothesized by authors in the field of selective attention (Hillyard & Anllo-Vento, 1998). In this framework, the late positive wave has been interpreted as a measure of cortical activity for allocating more attentional resources to arousing stimuli over time, whereas earlier amplification such as found in the range of the N1 component may indicate initial cortical facilitation for relevant features.

In addition to electrophysiological measures, hemodynamic/metabolic imaging studies have highlighted the role of cortical facilitation in attentional processes. For instance, recent imaging research in normal and pathological states has illuminated a fronto-parietal attention network which mediates orienting to external stimuli and maintaining the alert state (Fernandez-Duque & Posner, 2001). Imaging research with healthy participants not only revealed fronto-parietal networks in visuospatial orienting (Corbetta, 1998) but also identified the superior parietal cortex as being involved in attention shifts between non-spatial dimensions such as color and shape (Le, Pardo, & Hu, 1998; Rushworth, Paus, & Sipila, 2001). Pardo, Fox and Raichle (Pardo, Fox, & Raichle, 1991) investigated neural activity during a visual and somatosensory sustained attention task using Positron Emission Tomography (PET). Regardless of sensory modality, they found an increase in blood flow in right prefrontal and right superior parietal cortices. Thus, a general fronto-parietal network in the right hemisphere appears to be involved in orienting to a new stimulus as well as in maintaining attention to that stimulus. These brain areas project to subcortical structures e.g. the pulvinar of the thalamus linking ventral visual systems for object identification with the attention network (Fernandez-Duque & Posner, 2001).

In research on emotion, deep structures such as the amygdaloid complex have been discussed as central areas interacting with the ventral visual system (LeDoux, 1992; Shi & Davis, 2001) suggesting some degree of differentiation between 'cognitive' and 'emotional' attention systems. Nevertheless the location of activated brain areas reported during processing of emotional stimuli strikingly overlap with brain areas associated with orienting and sustained attention. In particular, the prefrontal cortex, the anterior cingulate and the

parietal cortex have been considered as crucial for emotional function (Davidson, Abercrombie, Nitschke, & Putnam, 1999).

In the light of the data reported above the question arises if high arousing visual stimuli increase the activity not only in sensory cortical areas but also in cortical networks mediating attentional processes over time. This would provide additional support for the concept of 'motivated attention' in emotion. The Steady State Visual Evoked Potential (SSVEP) has proved useful in electrocortical investigations of attentional processes over time (Müller & Hillyard, 2000). It can be recorded as a continuous brain response elicited by a repetitive stimulus that is periodically modulated in intensity at a fixed rate of 6-8 Hz or greater. The resulting waveform is oscillatory in nature, having the same fundamental frequency as the driving stimulus, often including higher harmonics (Regan, 1989). The SSVEP has been shown to be sensitive for tonic changes of the organism such as anaesthesia (Plourde & Picton, 1990), sleep (Picton, Vajsar, Rodriguez, & Campbell, 1987), or vigilance (Silberstein et al., 1990). But also phasic changes in central nervous activity have been observed using the SSVEP technique such as visual spatial selective attention whereby greater SSVEP amplitudes for attended vs. unattended stimuli were found (Morgan, Hansen, & Hillyard, 1996; Müller, Teder-Salejarvi, & Hillyard, 1998). Because of high correlation with the visual N1 component, the amplitude enhancement for attended stimuli was considered reflecting a greater signal to noise ratio in sensory systems as a result of a sensory gain mechanism facilitating feature discrimination (Muller & Hubner, 2002). The neuromagnetic counterpart of the SSVEP the Steady State Visual Evoked Field (SSVEF) measured with magnetoencephalography (MEG) also can be used to study higher-order attentional processes such as conscious perception (Srinivasan *et al.*, 1999). Advantages of this technique are related to the fact that they enable the researcher to collect a high number of trials in short periods of time, and to use frequency-domain analyses allowing for easy extraction of meaningful dependent variables that reflect the driving frequency (e.g. Fourier-based approaches). As a conceptual advantage, widely distributed functional networks oscillating coherently at the driving frequency can be examined at high temporal resolution and signal-to-noise ratios.

Few studies (Kemp *et al.*, 2002; Keil *et al*., in press) have used SSVEPs to investigate the effect of emotional pictures on electrocortical brain activity. Kemp and collaborators (Kemp, Gray, Eide, Silberstein, & Nathan, 2002) examined the influence of pictures from the International Affective Picture System (IAPS) on SSVEPs produced by a 13 Hz diffuse peripheral flicker. They manipulated the valence dimension (pleasantness) and kept the

arousal dimension low and constant for the valence categories (unpleasant, pleasant, neutral). These authors found a frontal latency reduction of the SSVEP for the unpleasant and pleasant picture categories compared to the neutral pictures as predicted by the model of Heller and collaborators (1997). Furthermore, unpleasant pictures decreased the amplitude of the flicker-induced SSVEP in frontal electrodes.

In a previous SSVEP study (Keil *et al*., in press) we examined the SSVEP produced by flickering (10 Hz) IAPS pictures themselves. We manipulated the arousal dimension of the picture content resulting in high (pleasant and unpleasant) and low (neutral) arousing pictures in order to direct motivated attention to high arousing stimuli. The SSVEP signal was most pronounced for high arousing compared to neutral pictures at occipital and parietal electrode sites. Phase information of the SSVEP suggested co-activation of frontal and temporal regions when viewing affectively arousing pictures. In general, EEG-based measures are limited with respect to spatial resolution. Neuromagnetic fields measured with MEG are not distorted by varying conductivities resulting from different tissues that affect electric field potentials. Consequently, in the case of MEG, using a homogenous sphere as a volume conductor model for source analysis introduces less spatial error. Therefore, the aim of the present study was to examine cortical sources of the SSVEF as modulated by emotional arousal, using MEG.

We hypothesized that pictures high in arousal should provoke greater SSVEF amplitudes reflecting an enhanced signal to noise ratio in sensory systems as a result of a sensory gain mechanism. Since the SSVEF response is a correlate of ongoing, continuous stimulation, it represents integrated stimulus driven neural activity over time. This should lead to oscillations in neuronal networks responsible for affective picture processing at the frequency of the driving stimulus. Therefore, we expect greater SSVEF amplitude for high arousing pictures not only in extrastriate cortex but also in higher attentional networks reflecting orienting and maintaining an alert state over a longer period. Applying the Minimum Norm Estimate (MNE; (Hauk, Berg, Wienbruch, Rockstroh, & Elbert, 1998; Hauk, Keil, Elbert, & Müller, 2002) to the SSVEF response in order to determine the sources of the neuromagnetic field we expected enhanced source activity in higher visual, parietal and frontal brain areas. Heart Rate (HR) was recorded to validate the effectiveness of picture presentation with respect to the observers' affective physiology. Evaluative judgments and viewing time were obtained as subjective measures of stimulus valence and intensity.

METHODS

Participants

15 paid volunteers (8 females, 7 males, 12 right handed, 1 left handed and 2 ambidextrous; (Oldfield, 1971)) gave written consent to participate in the study. Their mean age was 25.5 years (range: 20 to 32 years). They had normal or corrected-to-normal vision and no family history of photic epilepsy. They did not report a recent critical live event or any history of psychotherapy.

Stimuli

Sixty colored pictures from the IAPS were used as stimuli. According to the normative IAPS ratings (CSEA, 1999) 20 high arousing pleasant (erotic couples and happy families), 20 high arousing unpleasant (mutilated bodies and attack scenes) and 20 low arousing neutral pictures (household scenes and neutral persons) were chosen. Mean normative pleasure ratings on a 9 point scale for pleasant, neutral and unpleasant pictures were 7.33 (± 0.13), 4.87 (± 0.05) and 2.76 (± 0.19) , mean normative arousal ratings were 5.44 (± 0.24), 2.8 (± 0.13) and 6.9 (± 0.07) , respectively. Brightness, contrast and color spectra of the stimuli were adjusted such that there were no systematic differences between picture categories with respect to these parameters.

Using a video projector (JVC™, DLA-G11E) and a mirror system, the pictures were projected on a screen in the magnetically shielded MEG chamber. The pictures were displayed in a pseudo random order, subtending a visual angle of 10^{o} both horizontally and vertically. A fixation point was marked in the center of the display and was present throughout the whole experiment. In each trial, a picture was shown in a flickering mode of 10 Hz for a period of 6000 ms resulting in 60 on/ off cycles, the picture being depicted for 40 ms, followed by 60 ms black screen during each cycle. During the inter-trial interval, which varied randomly between 8 and 12 seconds, a black screen was shown.

Procedure

Upon arriving at the laboratory, participants were familiarized with the MEG chamber. Thereafter, they were prepared for the MEG recording. First, subjects were shown three pictures from the IAPS representing high arousing pleasant, unpleasant and low arousing neutral pictures which were not part of the stimuli presented during the MEG session. After giving informed consent participants were screened for family history of epilepsy, recent critical live events and history of psychotherapy. Handedness was determined using the

Edinburgh Inventory (Oldfield, 1971). For artifact control four electrodes for the electrooculogram (EOG) were attached, two at the left and right outer canthus and two above and below the right eye. Additionally, two electrodes for the electrocardiogram (ECG) were placed on the left and right medial forearms. Then, subjects were seated in the MEG chamber, their head-shapes were digitized, and index points (left and right periauricular points, nasion, a pseudo Cz and pseudo inion point at the forehead) were determined in order to calculate the relative head position within the MEG helmet for source analysis. Finally, subjects were placed under the MEG sensors.

The experimental session started with the presentation of 60 flickering (10 Hz) pictures in a pseudo-randomized order. Randomization was restricted such that a straight sequence of three pictures from the same affective category (unpleasant, pleasant, neutral) did not occur. After the first block subjects were offered a brief pause and a second block of the same 60 pictures in a different order was run. At the end of the MEG session subjects left the MEG chamber and electrodes were removed.

In a third block outside the MEG chamber participants were asked to rate the pictures regarding emotional valence and arousal using the Self-Assessment Manikin (SAM) self report scale (Lang, 1980). The same 60 pictures were presented on a computer screen in a 10 Hz flickering mode in a different order compared to both MEG blocks. Subjects were allowed to view the pictures as long as they wanted to, but had to press a key in order to stop the picture presentation before doing their rating. After finishing the evaluation of the current picture, the participant could start the presentation of the next picture by a second key press. The time interval between picture onset and offset was recorded as an index of viewing time. At the end of the experiment participants were paid 10 € (approximately 10 US dollar).

Data Acquisition and Preprocessing

The MEG was recorded continuously, and digitized at a rate of 678.17 Hz, using a 148 channel whole head system (MAGNES™ 2500 WH, 4D Neuroimage, San Diego, USA). A band-pass filter of 0.1 – 200 Hz was applied on line. The EOG and ECG acquisition was done with a Synamps amplifier (NEUROSCAN™) using Ag/Cl electrodes.

The MEG data were decimated by a factor of 2 and digitally band-pass filtered between 1 and 20 Hz (slopes: 6 dB/ octave, 24 dB/ octave, respectively) before averaging for picture category (pleasant, neutral, unpleasant) over 6000 ms subtracting a 200 ms baseline. Eye artifacts were corrected using the algorithm implemented in BESA™ software (Berg & Scherg, 1994). Additionally the MEG was visually inspected for movement artifacts. For each

category mean (baseline corrected 6000 ms) SSVEFs were derived using a moving window averaging procedure (time window 400 ms, time shift 100 ms) in order to extract 4 cycles of the 10 Hz brain response from the MEG signal (Perlstein *et al*., 2003). These 4 cycles per category were submitted to source analysis.

Heart rate changes were evaluated using in-house-software written in MATLAB™. The algorithm of the software estimated the HR change over 6000 ms picture presentation in 500 ms steps using a 2000 ms pre-stimulus baseline. Thereby, the frequency of the occurrence of an R-wave was derived from the inter-beat-interval and weighted according to the distance from a 500 ms step within the time vector. The HR change was transformed in beats per minutes (bpm).

For viewing time estimation the time between the key press starting the presentation of a new picture and the key press before picture evaluation was used as a measure of viewing time in order to exclude evaluation time. The viewing time was recorded with an IBM™ compatible personal computer.

Source Analysis

The average data resulting from the moving window averaging procedure was submitted to source analysis. Using a minimum norm estimate (MNE) (Hämäläinen & Ilmoniemi, 1984) cortical sources were estimated. This linear estimation technique assumes that the data vector **b**, which contains the recorded magnetic field distribution over the sensors, can be described as the product of the lead-field matrix **A**, which specifies the sensor's sensitivity to the sources located e.g. on a shell, and a current density vector **x** of these sources plus a noise component **ε** (Grave de Peralta Menendez, Hauk, Gonzalez Andino, Vogt, & Michel, 1997):

$$b = Ax + \varepsilon \qquad (1)$$

The MNE is characterized by minimizing the power of the estimated current density of the sources by multiplying the pseudo-inverse of **A** with the data **b**:

$$\hat{x}^T \hat{x} = \min, \qquad (2)$$

where $\hat{x}$ is the estimated solution, and $\hat{x}^T$ is the transpose of $\hat{x}$. The fit of $\hat{x}$ to the data is quantified using the residual variance:

$$(A\hat{x} - b)^T (A\hat{x} - b) = \hat{\varepsilon} > 0 \qquad (3)$$

Given the presence of noise and the high number of sensors a regularization is necessary in order to obtain a stable solution. A commonly applied regularization method is the Tikhonov-Phillips regularization during pseudo-inversion of **A**, leading to following solution for $\hat{x}$:

$$\hat{x} = A^T (AA^T + \lambda I)^{-1} b, \qquad (4)$$

where **I** is the identity matrix and **λ** the regularization parameter (Bertero, De Mol, & Pike, 1988). Regularization aims at suppressing the noise part of the solution. Therefore, increasing λ should enhance the stability of the solution. Larger λ values lead to increased residual variance $\hat{\varepsilon}$ and smoothing of the estimated solution (Bertero et al., 1988).

Plotting the norm of the solution estimate $\| \hat{x} \|^2$ versus the residual variance $\hat{\varepsilon}$, the regularization parameter λ at the turning point of this curve was considered as an optimal trade off between a stable solution estimate and a good data fit. For the determination of λ the solution was calculated for an average over all affective categories (unpleasant, pleasant and neutral) for each subject. This procedure should prevent that different regularization parameters per affective category could account for condition effects.

We used the algorithm suggested by Hauk and collaborators to calculate the MNE (Hauk et al., 2002). To this end, the lead-field matrix **A** was computed for each participant, based on information on the center of a fitted sphere to the digitized head-shape, and the positions of the MEG sensors relative to the head. A spheric shell with evenly distributed 197 dipole locations served as source space. In order to be able to average the obtained MNE solutions over different subjects, we employed a shell with a fixed radius of 6 cm (see Figure 6). Utilizing source spaces formed by a shell with a common radius in order to calculate grand average data led to solutions with adequate spatial resolution (Knosche, Praamstra, Stegeman, & Peters, 1996). The radius of 6 cm was chosen as a trade off between depth sensitivity and spatial resolution (Hauk et al., 2002).. Each of the 197 dipole locations consisted of two perpendicular dipoles oriented tangentially to the shell surface. This resulted in two MNEs for each dipole location. Computing the MNE (4) leads to an estimation of dipole strength for each of the two perpendicular oriented dipoles at each location resulting in an activity estimation distributed over the shell.

Using an FFT algorithm, the amplitude of the 10 Hz Fourier component of the brain response was estimated separately for each dipole orientation. The square root of the sum of squares of the amplitudes for the two orientations served as a measure of the total amplitude of the 10 Hz Fourier component at one location:

$$Amp_i = \sqrt{Amp_{i,1}{}^2 + Amp_{i,2}{}^2} \quad , i \in [1, \ldots., 197], \qquad (5)$$

where Amp_i is the total amplitude of the 10 Hz Fourier component at dipole location i and $Amp_{i,1}$ is the corresponding amplitude for the first and $Amp_{i,2}$ the amplitude for the second orientation.

Statistical Analysis

Statistical analyses was executed in multiple steps. First, to assess an overall affective arousal effect on the neuromagnetic response, we determined the mean amplitude of the 10 Hz Fourier component of the 4 cycles across all sensors for each subject. The mean amplitude for each affective category (pleasant, unpleasant and neutral) was submitted to a contrast analysis in order to test the hypothesis that high arousing stimuli generate a stronger neuromagnetic response than low arousing pictures. Second, to evaluate broadly distributed effects of affective arousal on SSVEF sources, the 197 dipoles on the shell were grouped into 6 regional means for each hemisphere, resulting in occipital inferior, occipital superior, lateral inferior, lateral superior, frontal inferior and frontal superior regions for the left and right hemisphere, respectively (see figure 1).

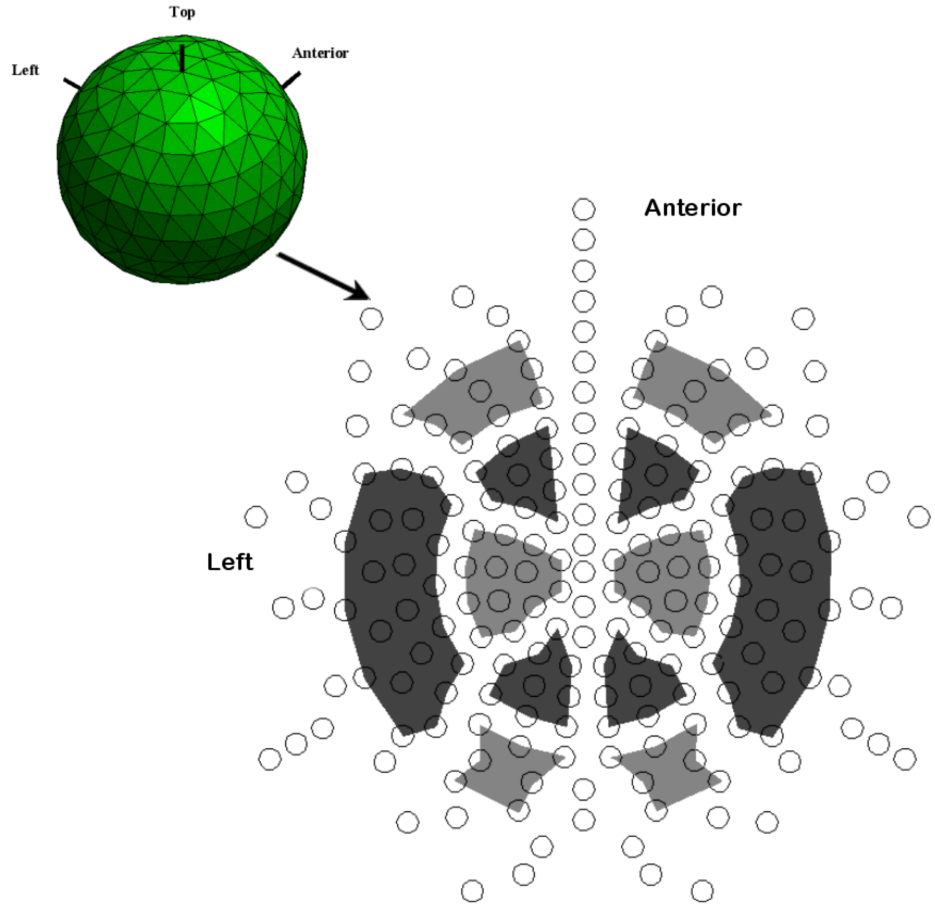

Figure 1: The upper left shell shows the triangulated MNE sphere, each node representing one of 197 dipole locations. On the bottom right, the 197 dipole sites are projected onto a plain. Gray shadings depict the 6 regions of interest for each hemisphere (occipital inferior, occipital superior, lateral inferior, lateral superior, frontal inferior and frontal superior).

The mean amplitudes of these 12 regions were submitted to a repeated-measures analysis of variance (ANOVA) with factors of picture content (3 levels: pleasant, neutral, unpleasant), hemisphere (2 levels: left, right), and region (6 levels: posterior inferior, posterior superior, lateral inferior, lateral superior, frontal inferior and frontal superior). Main effects were tested by means of contrast analyses for a quadratic trend to test the hypothesis that high arousing pleasant and unpleasant pictures produce a stronger brain response than low arousing neutral pictures.

Pooling dipoles of the minimum norm shell in order to form regions for statistical analysis considerably reduces the spatial information gained by using 197 dipoles. Therefore, in a second step, a contrast analysis for a quadratic trend was performed for each of the 197 dipoles and the F-values were mapped on the same shell as used by the MNE procedure. This visualization of the results provides higher spatial resolution and specificity and was intended to complement the repeated-measures ANOVA described above.

The HR data were scored according to a tri-phasic model of HR change over time (Hodes, Cook, & Lang, 1985). The minimum bpm value in the first 2 seconds after stimulus onset was scored as the initial deceleration, the maximum value in the following 2 seconds was scored as the following acceleration, and the minimum in the last 2 seconds were scored as the final deceleration.

Viewing times below or above two standard deviations of the mean within one affective category were rejected for each subject before calculating the average viewing time. For each subject viewing times for each condition were divided by the mean viewing time over all three affective categories (pleasant, neutral, unpleasant) for normalization. HR data and viewing times were evaluated by means of repeated-measures ANOVA with factor emotional content (3 levels: unpleasant, neutral, unpleasant). In the analysis of HR data a factor phase (3 levels: initial deceleration, following acceleration, final deceleration) was added. In all ANOVA analyses' the degrees of freedom were corrected where appropriate using the Greenhouse-Geisser procedure to account for possible violations of the sphericity assumption (Greenhouse & Geisser, 1959). Planned comparisons (contrast analyses) were used to examine the hypothesized differences related to affective valence and arousal. Where no planned comparisons were conducted, the Tukey Kramer procedure and the t-Test were utilized in order to evaluate main effects and interactions. SAM pleasure and arousal ratings were evaluated using repeated measures ANOVA with a single factor of picture content (pleasant, neutral, unpleasant).

RESULTS

SAM Ratings

As expected, SAM pleasure ratings differed as a function of affective category [$F(2,28) = 40.32$, $P < .0001$, $\varepsilon = .55$], with pleasant pictures rated as most pleasant followed by neutral pictures, and unpleasant pictures rated as least pleasant [mean pleasure ratings: $6.58 \pm .33$ (pleasant), $5.01 \pm .12$ (neutral), $2.64 \pm .30$ (unpleasant), Tukey-Kramer $P < .05$ for

all comparisons]. Arousal ratings also varied over affective categories [$F(2,28) = 48.67$, $P < .0001$, $\varepsilon = .85$], with pleasant and unpleasant pictures rated as more arousing than neutral pictures [mean arousal ratings: 4.80 ± .33 (pleasant), 2.59 ± .31 (neutral), 6.21 ± .32 (unpleasant), Tukey-Kramer $P < .05$ for all comparisons]. Unpleasant pictures were rated as more arousing than pleasant pictures [$t(14) = 4.9$, $P < .001$], which was consistent with the IAPS normative ratings.

Heart Rate

As hypothesized, the first, the following and the last two seconds of heart rate changes during 6 s picture presentation differed according to a triphasic model for all affective categories as detected by a main effect of phase [$F(2,28) = 13.37$, $P < .001$, $\varepsilon = .79$ (see figure 2)]. This difference was characterized by an initial deceleration, a following relative acceleration and a final deceleration [mean initial deceleration: -1.024 ± .17, mean following acceleration: -.477 ± .21, mean final deceleration: -1.53 ± .23, Tukey-Kramer $P < .05$ for all comparisons]. There was no interaction between affective category and phase of heart rate change.

However, a main effect of affective category [$F(2,28) = 9.03$, $P < .01$, $\varepsilon = .93$] revealed that the triphasic pattern of heart rate change elicited by unpleasant pictures was dominated by a stronger deceleration than the heart rate change elicited by neutral and pleasant pictures [mean deceleration: -1.61 ± .20 (unpleasant), -.60 ± .19 (neutral), -.84 ± .23 (pleasant), Tukey-Kramer $P < .05$ for comparisons between unpleasant, neutral and unpleasant, pleasant pictures]. There was no difference between neutral and pleasant pictures. The mean HR change pattern over subjects for each affective category is depicted in figure 2.

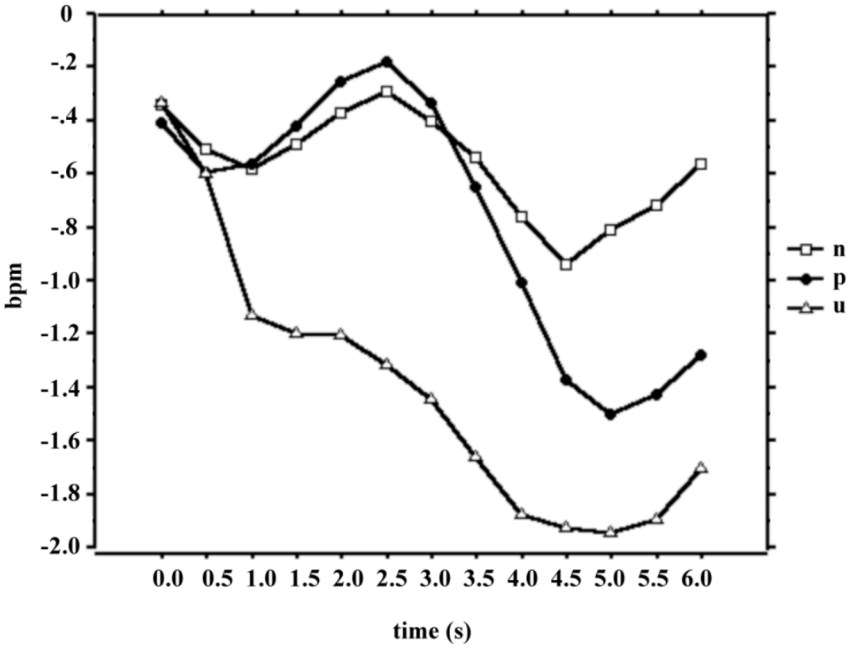

Figure 2: Mean heart rate (HR) change relative to pre-stimulus baseline (2s) across picture presentation time (6s) for each affective category: n = neutral, p = pleasant, u = unpleasant. The overall pattern for all categories followed a triphasic pattern ($F(2,28) = 13.37$, $P < .001$, $\varepsilon = .79$), whereas unpleasant pictures elicited the greatest HR deceleration ($F(2,28) = 9.03$, $P < .01$, $\varepsilon = .93$).

Viewing time

As expected, viewing times were longer for high arousing pleasant and unpleasant pictures than for low arousing neutral pictures, resulting in a significant main effect [$F(2,28) = 7.55$, $P < .005$, $\varepsilon = .94$] and a quadratic trend [$F(1,14) = 17.28$, $P < .005$].

SSVEF data

Four cycles of the SSVEF response measured from three representative subjects at one (A42, parietal location) of the 148 sensors are shown in figure 3.

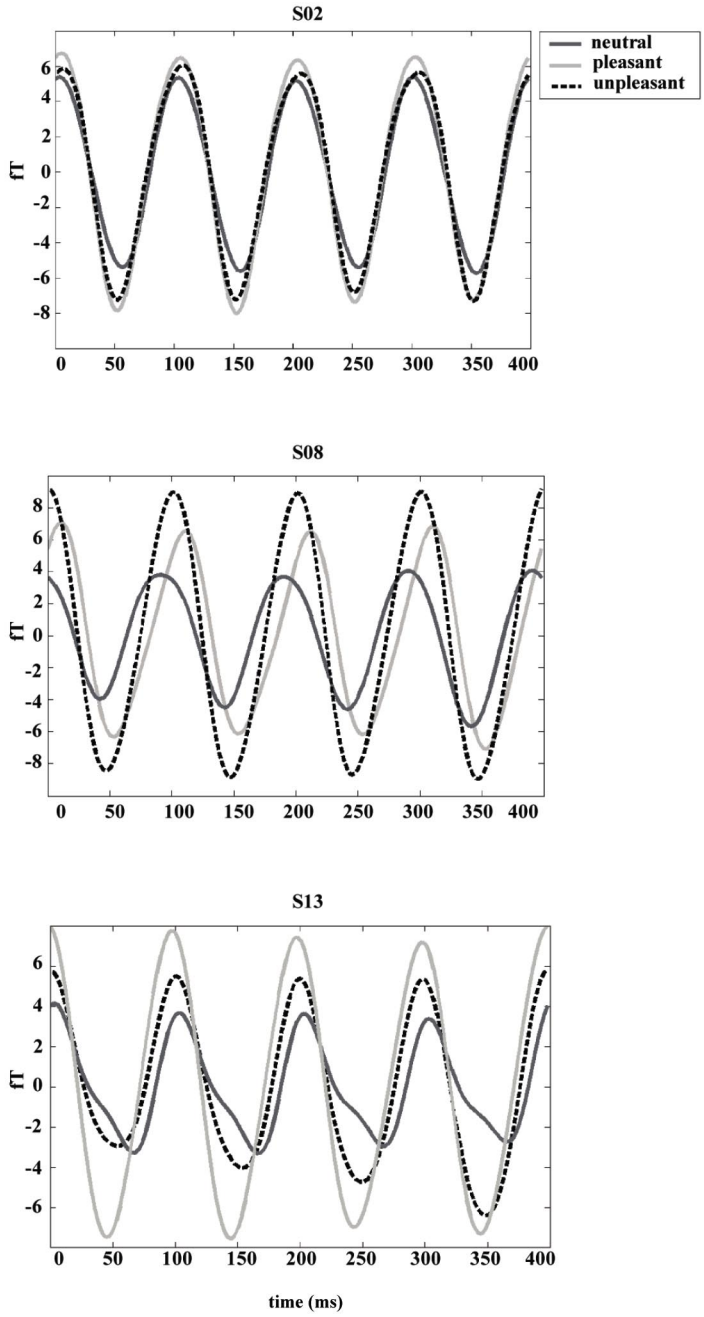

Figure 3: Four cycles of the 10 Hz SSVEF response of a MEG sensor for three representative subjects. Shadings of curves indicate the SSVEFs elicited by neutral, pleasant and unpleasant affective pictures.

The overall activation for each affective category as reflected by the mean amplitude estimate of the 10 Hz Fourier component of the 4 cycles over all sensors of the extracted SSVEF signal differed according to a quadratic trend [$F(1, 14) = 5.35$, $P < .05$]. The overall

neuromagnetic activity of the signal space was higher for high arousing pleasant and unpleasant stimuli than for calm neutral pictures (figure 4).

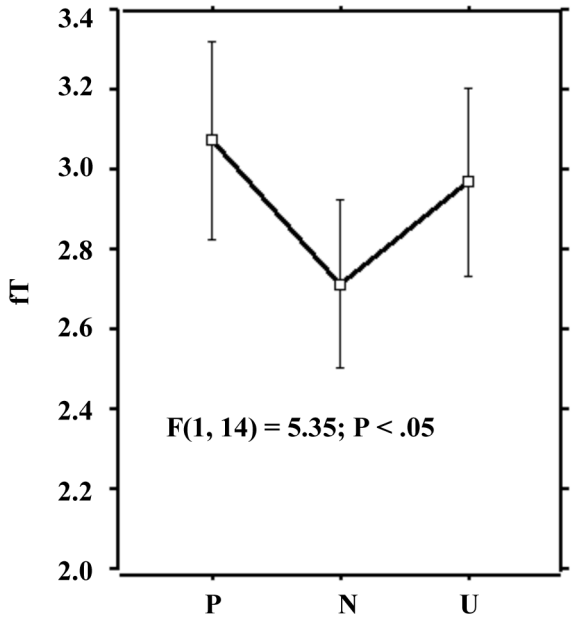

Figure 4: Mean amplitude estimate of the 10 Hz Fourier component of the SSVEF over all sensors and for each affective category: P = pleasant, N = neutral, U = unpleasant. High arousing unpleasant and pleasant pictures generated a higher SSVEF response than low arousing neutral pictures ($F(1, 14) = 5.35$, $P < .05$). Note that the high standard errors are due to the inter-subject variability of amplitude not affecting the significance of the within subject comparison.

Minimum Norm Estimate

In order to get information about the origin of this SSVEF modulation, the mean 10 Hz Fourier component amplitude estimates of 12 dipole clusters as shown in Figure 1 were submitted to statistical analysis. A main effect of region [$F(5, 70) = 35.15$; $P < .0001$; $\varepsilon = .32$] indicated that the visual stimulation elicited most activity over inferior and superior posterior regions as compared to all other areas [Tukey Kramer $P < .05$ for all comparisons between the two posterior and all other regions; the comparison between inferior and superior posterior regions did not reach significance]. A significant interaction of region and affective category [$F(10, 140) = 3.52$, $P < .05$, $\varepsilon = .30$] revealed that high arousing pictures (pleasant and unpleasant) also generated more activity than low arousing pictures (neutral) in frontal superior [$F(1, 14) = 5.37$, $P < .05$], lateral superior [$F(1, 14) = 7.45$, $P < .05$] and occiptal superior [$F(1, 14) = 5.59$, $P < .05$] regions (figure 5).

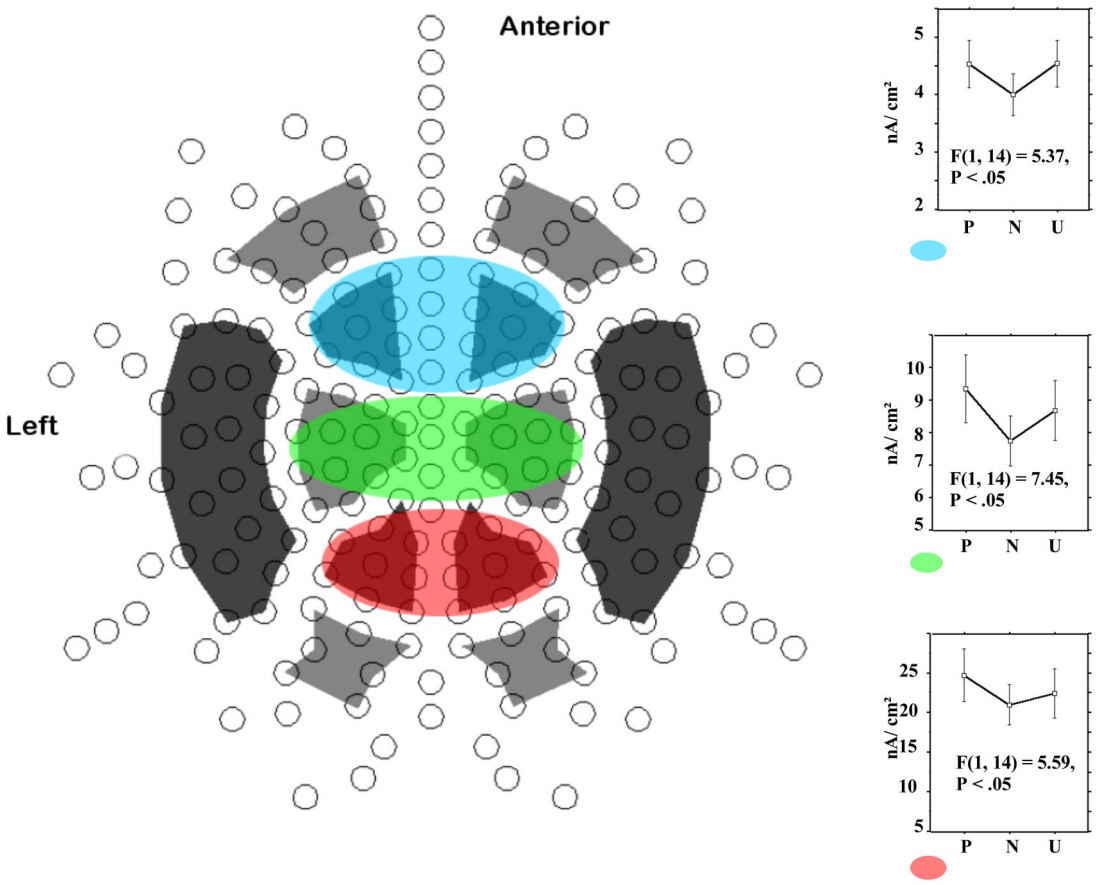

Figure 5: Regions of interest depicting a significant arousal modulation of dipole source strength are shown on the right. The blue area represents superior frontal regions (arousal modulation: $F(1, 14) = 5.37$, $P < .05$), the green area depicts superior lateral regions (arousal modulation: $F(1, 14) = 7.45$, $P < .05$) and the red area shows superior posterior regions (arousal modulation: $F(1, 14) = 5.59$, $P < .05$). Right panels: mean amplitude of dipole source strength of the 10 Hz SSVEF for each affective category and each region of interest which proved to be significant (color dot): P = pleasant, N = neutral, U = unpleasant. Note that the high standard errors are due to the high inter-subjects variability (different regularization parameters for each subject) not affecting the significance of the within-subject comparison.

Averaging activity clusters of dipoles reduces spatial resolution and leads to loss of information. A contrast analysis for a quadratic trend testing the hypothesis that high arousing pictures produce more activity than calm neutral pictures was therefore conducted for all 197 dipoles of the minimum norm shell. This resulted in a descriptive F map (figure 6).

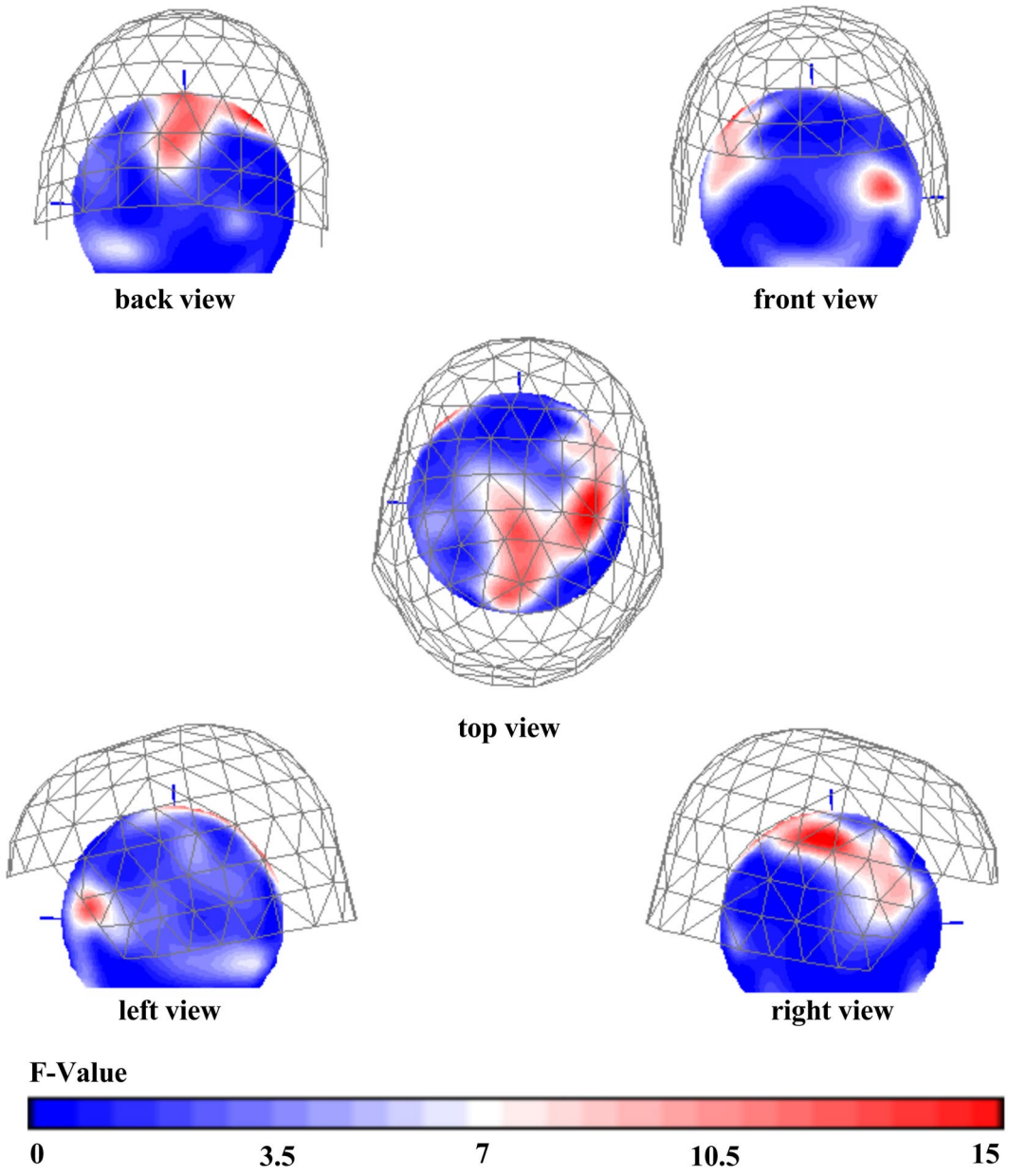

Figure 6: Mapping of statistical parameters testing the hypothesis that high arousing stimuli (pleasant and unpleasant vs. neutral) generate greater dipole strength. The colorbar indicates the F-value level. The different panels depict different views of the MNE shell containing the dipole locations the F-values are projected on. F-values lower than 7 are shown in blue and values greater than 7 are depicted in red (see text). The gray net represents the mean MEG sensor positions (each node represents one sensor) for the 15 subjects.

F values greater than 7 ($F(1, 14) = 7.0$; $P = .007$, uncorrected) are shown in red color and F values less than 7 are depicted in blue. As can be seen in figure 6, F values greater than 7 distribute across fronto-parietal regions with a predominance on the right hemisphere. The maximum F value is located at a right parietal dipole site ($F(1, 14) = 15.1$) as can be seen in

the middle panel of figure 6 (top view). An additional cluster of high F values is also found in left frontal regions (maximal F value in that cluster: F(1, 14) = 13.0). If the arbitrary threshold for the red color in Figure 6 is lowered to an F value of 5 (F(1, 14) = 5.0) in order to depict weaker modulations, high arousing affective pictures also show greater activity than neutral pictures in occipito-temporal regions (maximum of F value in right occipito-temporal cluster: F(1, 14) = 4.79; maximum of F value in left occipito-temporal cluster: F(1, 14) = 6.14; see figure 7) with a left-hemispheric predominance.

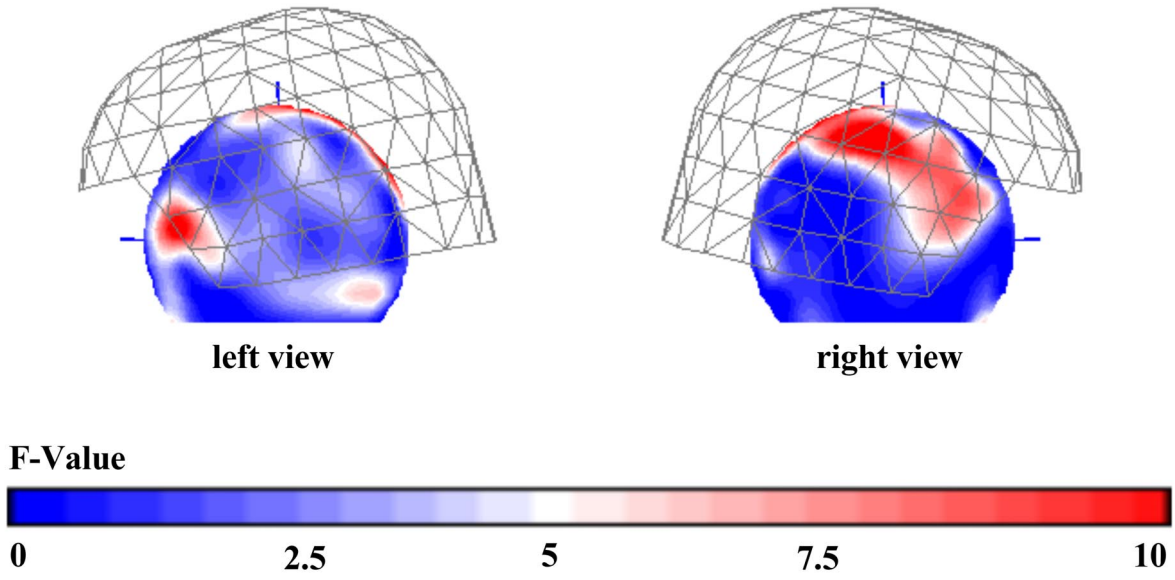

Figure 7: Left and right view of the statistical parameter map of figure 6. The scale of the F-map was downscaled in order to depict weaker activity modulations. As can be seen, arousal modulations also emerge in the ventral visual stream. The gray net represents the mean MEG sensor positions (each node represents one sensor) for the 15 subjects.

DISCUSSION

Examining MEG correlates of affective picture viewing by means of steady-state visual evoked fields, we studied the modulation of stimulus driven neural responses to visual stimuli differing as to their affective/motivational significance for the observer. The overall SSVEF response as reflected by the mean amplitude of the 10 Hz Fourier component over all MEG sensors suggested that high arousing pictures (pleasant and unpleasant) produced a greater SSVEF response than low arousing neutral pictures. This finding is consistent with studies using other central nervous measures of emotional picture processing reporting that

indices of higher-order processing of a stimulus varied as a function of emotional arousal (Cuthbert et al., 2000; Ito et al., 1998; Mini et al., 1996; Palomba et al., 1997; Schupp et al., 2000).

In attention research, investigating visual spatial selective attention over time by means of SSVEPs revealed that the SSVEP amplitude is greater for attended than for unattended visual stimuli (Morgan et al., 1996; Muller & Hubner, 2002). This effect is understood as an early sensory gain mechanism that enhances the signal to noise ratio in the underlying cortical networks and hence facilitates discrimination of the attended visual stimulus (Hillyard & Anllo-Vento, 1998). We suggest that the greater SSVEF amplitude while viewing arousing pictures may reflect a sensory gain mechanism interacting with a fronto-parietal attention mechanism regulating and maintaining the alert state (see below), reflecting 'automatic', motivated attention to biologically significant stimuli.

Assuming that steady state stimulation with emotional pictures leads to stimulus driven activity in cortical networks underlying affective picture processing, we conducted sources analysis. Estimating the sources of the SSVEF by means of a distributed source analysis technique, we observed that averaged dipole cluster strengths at superior occipital, superior lateral and superior frontal regions of interests were greater for high arousing than for low arousing pictures. This effect was greatest for superior lateral dipole clusters which were most sensitive to parietal cortical activity. Mapping of statistical parameters indicated that the modulation of source strength as a function of emotional arousal was greatest at fronto-parietal locations, with a predominance at right hemispheric dipole sites. The greatest F value was located at a right parietal dipole site, thus paralleling and confirming the dipole cluster analysis. Furthermore, a strong modulation by emotional arousal was observed at left frontal locations. Such a modulation was also evident at occipito-temporal dipole sites but to a much lesser extent. This pattern suggests that the SSVEF was greater for high arousing than for low arousing pictures in a fronto-parietal cortical network showing a right hemisphere preponderance, and maybe interacting with changes in occipito-temporal cortex. The spatio-temporal relationship between these two networks will be a target of future research using SSVEF together with measures of inter-dipole phase-locking.

While SSVEP studies of spatial selective attention have not employed source estimation techniques, event related potentials (ERP) studies in that field showed early modulations in extrastriate cortex (Hillyard & Anllo-Vento, 1998) and recurrent modulations in primary visual cortex (Di Russo, Martinez, & Hillyard, 2003). These results are paralleled by findings of early ERP modulations with affective arousal (Keil et al., 2002; Pizzagalli et

al., 1999) leading us to the assumption that a similar sensory gain mechanism as has been suggested for the field of spatial attention could mediate the allocation of motivated attention.

We observed arousal-related modulations in extrastriate regions (at occipito-temporal dipole sites) in addition to pronounced changes at fronto-parietal dipole locations. In our previous SSVEP study (Keil et al, in press) using the same picture material we found a corresponding pattern of enhanced amplitudes at occipital and parietal electrode sites and co-activation of frontal and temporal electrode sites during presentation of high arousing pictures. The topography of amplitude modulations of the present study at occipito-temporal and right parietal dipole sites is consistent with current source density maps reported by Junghöfer and collaborators (Junghöfer et al., 2001) who presented IAPS pictures in a rapid visual stream. Given that the SSVEF segment examined here reflects neuromagnetic activity over a 6000 ms window, it might be expected that structures related to allocation/regulation of attention show a more sustained pattern than do their target structures in visual cortex.

Compared to other measures of brain activity like fMRI and PET our source estimation results are in line with findings from attention research using metabolic imaging techniques. The modulation of activity at fronto-parietal dipole sites by the arousal dimension of emotional pictures observed here seems to involve cortical networks also discussed in attention research (Corbetta, 1998; Le et al., 1998; Pardo et al., 1991; Rushworth et al., 2001) and parallels results about orienting and maintaining the alert state (Fernandez-Duque & Posner, 2001). Taken together, the enhancement of the SSVEF and the spatial distribution of the arousal modulated dipole strengths in our study suggests that motivationally significant visual stimuli may engage a sensory gain mechanism facilitating sensory processing in extrastriate cortex interacting with the activation of a common cortical attention network mediating orienting and maintaining the alert state over picture presentation time, supporting the concept of ‘motivated attention’ in emotion (Lang et al., 1997).

Because of the experimental environment (MEG chamber) and the application of a SSVEF design with flickering pictures, it is important to ensure that we have triggered the same physiological and behavioral responses usually observed in an affective picture viewing context. Viewing emotional pictures usually elicits a classic triphasic pattern of heart rate change (Lang & Hnatiow, 1962) with an initial deceleration, a subsequent relative acceleration and a final deceleration. Aversive pictures generate a sustained heart rate deceleration over the whole picture presentation time with a less clear triphasic pattern compared to neutral and pleasant pictures (Lang et al., 1997). Pleasant pictures usually provoke a greater initial deceleration and a more pronounced accelerative component than

neutral pictures (Bradley, Codispoti, Cuthbert, & Lang, 2001). In our study we observed similar heart rate changes during affective picture viewing in the MEG chamber, although the pictures were presented in a flickering mode. High arousing unpleasant stimuli produced a sustained heart rate deceleration over the whole picture presentation time. However, in the present study we could not replicate a differentiation between pleasant and neutral pictures with respect to heart rate change. This could be due to the more aversive experimental environment of the MEG chamber. Another reason may lie in the high variability between subjects usually observed in heart rate data (Hodes et al., 1985). It is possible that with a small-sized sample (compared to sample sizes usually used in heart rate studies) only the most pronounced changes, related to aversive pictures lead to significant effects, whereas smaller differences such as the ones between neutral and pleasant pictures require bigger samples. This would especially hold in situations where motivational significance is highest for aversive pictures across subjects. Indeed, aversive pictures were rated as slightly more arousing than pleasant images in the present study. Further, the flickering mode of picture presentation did not influence subjective ratings and viewing time usually observed (Lang et al., 1998). As predicted, subjects' ratings validated that the categorization of the IAPS pictures according to the normative ratings indeed represented high (pleasant and unpleasant) and low (neutral) arousing affective pictures. Furthermore, subjects viewed high arousing pictures longer than neutral pictures during SAM rating sessions following the MEG recordings, possibly reflecting a higher motivational state to high arousing pictures. Thus, behavioral and physiological data suggest that we successfully manipulated the motivational significance of our stimuli in a SSVEF paradigm. Modulation of SSVEF amplitude therefore appears to reflect changes related to emotional arousal, as a function of picture category.

Several methodological constraints must be taken into account, however. First, we focused on amplitude data of the 10 Hz Fourier component and dismissed the phase information. This was done as our main goal was to use source space projection, allowing for conclusions about the origin of neuromagnetic activity. Magnetometer locations of maximum activity do not represent the origin of the sources. Additionally, subjects have different relative head positions in the MEG sensor helmet. Hence, we employed a MNE algorithm (Hauk et al., 1998) whereby two dipole orientations at each model dipole site must be taken into account (see above). While meaningful amplitude information can easily be obtained as described in the method section, pooling phase information across two perpendicular dipoles leads to distortions, which makes interpretation difficult. As a second constraint, the present study employed a homogenous sphere as a head model for the MNE. Thus, cortical areas

involved in generation of the signal were inferred from localizations on a shell. But we consider this approach more accurate than inferring activation of cortical areas from sensor/ electrode topographies because sensors/electrodes can be sensitive to distant cortical sources. In future studies, realistic head models derived from subjects' individual structural MRIs should be used in order to obtain more precise identification of brain regions.

The spatial distribution of the activity changes at the stimulus driven SSVEF response suggests that whenever visual emotional stimuli engage attentional resources extrastriate and higher order cortical attention networks also involved in orienting and maintaining the alert state (Fernandez-Duque & Posner, 2001) are active. We propose that an initial sensory gain mechanism as well as a general attention system mediating orienting and an alert state over time maintain an enhanced signal to noise ratio in these structures as reflected by the enhanced SSVEF neuromagnetic response. The higher-order attention network may interact with lower sensory systems processing stimulus features by top down processes. This view would be consistent with the theory of emotion proposed by Lang and collaborators (Lang, 1979) suggesting that affective information is integrated and represented in neuronal networks. The interplay of the above mentioned mechanisms in time should be investigated by future research.

SUMMARY

In the present study we presented high (pleasant and unpleasant) and low (neutral) arousing emotional pictures in a steady-state visual evoked field paradigm while recording the magnetoencephalogram. Applying a minimum norm estimation (MNE) technique we determined the origin and the strength of the evoked neuromagnetic field. In addition to magnetocortical data, we examined subjective ratings, heart rate change and viewing time to obtain a multi-variate data base of emotional experience related to the present paradigm. As evidenced by the MNE, pictures rated as high arousing elicited greater activity in fronto-parietal cortical networks than low arousing pictures, with a right hemispheric predominance. This effect was also observed in occipito-temporal regions but to a lesser extent. Longer viewing times for high arousing pictures and sustained heart rate deceleration for high arousing unpleasant pictures indicated that these stimuli were of high motivational relevance compared to neutral pictures. Taken together, we argue that activity in higher order fronto-parietal cortical attention networks is modulated by emotional arousal. In turn, this attention network influences activity in systems performing stimulus processing.

REFERENCES

Berg, P., & Scherg, M. (1994). A multiple source approach to the correction of eye artifacts. *Electroencephalogr Clin Neurophysiol, 90*(3), 229-241.

Bertero, M., De Mol, C., & Pike, E. R. (1988). Linear inverse problems with discrete data: II. Stability and regularization. *Inverse Problems, 4*, 573-594.

Bradley, M. M., Codispoti, M., Cuthbert, B. N., & Lang, P. J. (2001). Emotion and Motivation I: Defensive and Appetitive Reactions in Picture Processing. *Emotion, 1*(3), 276-298.

Corbetta, M. (1998). Frontoparietal cortical networks for directing attention and the eye to visual locations: identical, independent, or overlapping neural systems? *Proc Natl Acad Sci U S A, 95*(3), 831-838.

Cuthbert, B. N., Schupp, H. T., Bradley, M. M., Birbaumer, N., & Lang, P. J. (2000). Brain potentials in affective picture processing: covariation with autonomic arousal and affective report. *Biol Psychol, 52*(2), 95-111.

Davidson, R. J., Abercrombie, H., Nitschke, J. B., & Putnam, K. (1999). Regional brain function, emotion and disorders of emotion. *Curr Opin Neurobiol, 9*(2), 228-234.

Di Russo, F., Martinez, A., & Hillyard, S. A. (2003). Source analysis of event-related cortical activity during visuo-spatial attention. *Cereb Cortex, 13*(5), 486-499.

Fernandez-Duque, D., & Posner, M. I. (2001). Brain imaging of attentional networks in normal and pathological states. *J Clin Exp Neuropsychol, 23*(1), 74-93.

Grave de Peralta Menendez, R., Hauk, O., Gonzalez Andino, S., Vogt, H., & Michel, C. (1997). Linear inverse solutions with optimal resolution kernels applied to electomagnetic tomography. *Human Brain Mapping, 5*, 454-467.

Greenhouse, S. W., & Geisser, S. (1959). On methods in the analysis of profile data. *Psychometrika, 24*, 95-112.

Hämäläinen, M., & Ilmoniemi, R. (1984). *Interpreting measured magnetic fields of the brain: Estimates of current distributions.* (Technical Report TKK-F-A559). Helsinki: Helsinki University of Technology.

Hauk, O., Berg, P., Wienbruch, C., Rockstroh, B., & Elbert, T. (1998). *The minimum norm method as an effective mapping tool for MEG analysis.* Paper presented at the Biomag98, Sendai, Japan.

Hauk, O., Keil, A., Elbert, T., & Müller, M. M. (2002). Comparison of data transformation procedures to enhance topographical accuracy in time series analysis of the human EEG. *Journal of Neuroscience Methods, 113*(2), 111-122.

Hillyard, S. A., & Anllo-Vento, L. (1998). Event-related brain potentials in the study of visual selective attention. *Proc Natl Acad Sci U S A, 95*(3), 781-787.

Hodes, R. L., Cook, E. W., 3rd, & Lang, P. J. (1985). Individual differences in autonomic response: conditioned association or conditioned fear? *Psychophysiology, 22*(5), 545-560.

Ito, T. A., Larsen, J. T., Smith, N. K., & Cacioppo, J. T. (1998). Negative information weighs more heavily on the brain: the negativity bias in evaluative categorizations. *J Pers Soc Psychol, 75*(4), 887-900.

Junghöfer, M., Bradley, M. M., Elbert, T. R., & Lan, P. J. (2001). Fleeting images: a new look at early emotion discrimination. *Psychophysiology, 38*(2), 175-178.

Keil, A., Bradley, M. M., Hauk, O., Rockstroh, B., Elbert, T., & Lang, P. J. (2002). Large-scale neural correlates of affective picture processing. *Psychophysiology, 39*(5), 641-649.

Kemp, A. H., Gray, M. A., Eide, P., Silberstein, R. B., & Nathan, P. J. (2002). Steady-State Visually Evoked Potential Topography during Processing of Emotional Valence in Healthy Subjects. *Neuroimage, 17*(4), 1684-1692.

Knosche, T., Praamstra, P., Stegeman, D., & Peters, M. (1996). Linear estimation discriminates midline sources and a motor cortex contribution to the readiness potential. *Electroencephalogr Clin Neurophysiol, 99*(2), 183-190.

Lang, P. J. (1979). A bioinformational theory of emotional imagery. *Psychophysiology, 16*, 495-512.

Lang, P. J. (1980). Behavioral treatment and bio-behavioral assessment:

Computer applications. In J. B. Sidowski & J. H. Johnson & T. A. Williams (Eds.), *Technology in mental health care delivery systems* (pp. 119-137). Norwood, NJ: Ablex Publishing.

Lang, P. J., Bradley, M. M., & Cuthbert, B. N. (1997). Motivated Attention: Affect, Activation, and Action. In P. J. Lang & R. F. Simons & M. T. Balaban (Eds.), *Attention and Orienting: Sensory and Motivational Processes* (pp. 97-135). Hillsdale, N.J.: Lawrence Erlbaum Associates.

Lang, P. J., Bradley, M. M., & Cuthbert, B. N. (1998). Emotion, motivation, and anxiety: brain mechanisms and psychophysiology. *Biol Psychiatry, 44*(12), 1248-1263.

Lang, P. J., & Hnatiow, M. (1962). Stimulus repetition and the heart rate response. *Journal of Comparative and Physiological Psychology, 55*, 781-785.

Le, T. H., Pardo, J. V., & Hu, X. (1998). 4 T-fMRI study of nonspatial shifting of selective attention: cerebellar and parietal contributions. *J Neurophysiol, 79*(3), 1535-1548.

LeDoux, J. E. (1992). Emotion and the amygdala. In P. A. John (Ed.), *The amygdala: Neurobiological aspects of emotion, memory, and mental dysfunction.* (pp. 339-351): Wiley-Liss, New York, NY, US.

Mini, A., Palomba, D., Angrilli, A., & Bravi, S. (1996). Emotional information processing and visual evoked brain potentials. *Percept Mot Skills, 83*(1), 143-152.

Morgan, S. T., Hansen, J. C., & Hillyard, S. A. (1996). Selective attention to stimulus location modulates the steady-state visual evoked potential. *Proc Natl Acad Sci U S A, 93*(10), 4770-4774.

Müller, M. M., & Hillyard, S. (2000). Concurrent recording of steady-state and transient event-related potentials as indices of visual-spatial selective attention. *Clin Neurophysiol, 111*(9), 1544-1552.

Muller, M. M., & Hubner, R. (2002). Can the spotlight of attention be shaped like a doughnut? Evidence from steady-state visual evoked potentials. *Psychol Sci, 13*(2), 119-124.

Müller, M. M., Teder-Salejarvi, W., & Hillyard, S. A. (1998). The time course of cortical facilitation during cued shifts of spatial attention. *Nat Neurosci, 1*(7), 631-634.

Oldfield, R. C. (1971). The assessment and analysis of handedness: The Edinbourgh Inventory. *Neuropsychologia, 9*, 97-113.

Palomba, D., Angrilli, A., & Mini, A. (1997). Visual evoked potentials, heart rate responses and memory to emotional pictorial stimuli. *Int J Psychophysiol, 27*(1), 55-67.

Pardo, J. V., Fox, P. T., & Raichle, M. E. (1991). Localization of a human system for sustained attention by positron emission tomography. *Nature, 349*(6304), 61-64.

Picton, T. W., Vajsar, J., Rodriguez, R., & Campbell, K. B. (1987). Reliability estimates for steady-state evoked potentials. *Electroencephalogr Clin Neurophysiol, 68*(2), 119-131.

Pizzagalli, D., Regard, M., & Lehmann, D. (1999). Rapid emotional face processing in the human right and left brain hemispheres: an ERP study. *Neuroreport, 10*(13), 2691-2698.

Plourde, G., & Picton, T. W. (1990). Human auditory steady-state response during general anesthesia. *Anesth Analg, 71*(5), 460-468.

Regan, D. (1989). *Human Brain Electrophysiology: Evoked Potentials and Evoked Magnetic Fields in Science and Medicine*. New York: Elsevier.

Rushworth, M. F., Paus, T., & Sipila, P. K. (2001). Attention systems and the organization of the human parietal cortex. *J Neurosci, 21*(14), 5262-5271.

Schupp, H. T., Cuthbert, B. N., Bradley, M. M., Cacioppo, J. T., Ito, T., & Lang, P. J. (2000). Affective picture processing: the late positive potential is modulated by motivational relevance. *Psychophysiology, 37*(2), 257-261.

Shi, C., & Davis, M. (2001). Visual pathways involved in fear conditioning measured with fear-potentiated startle: behavioral and anatomic studies. *J Neurosci, 21*(24), 9844-9855.

Silberstein, R. B., Schier, M. A., Pipingas, A., Ciorciari, J., Wood, S. R., & Simpson, D. G. (1990). Steady-state visually evoked potential topography associated with a visual vigilance task. *Brain Topogr, 3*(2), 337-347.

Chapter 4

Cortical Activation during Pavlovian Fear Conditioning Depends on Heart Rate Response Patterns: An MEG Study

INTRODUCTION

Learning that certain events in an individual's environment signal potential threat or danger is an important ability in order to ensure survival of the organism. Pavlovian fear conditioning (Pavlov, 1927) as a laboratory model of the aforementioned ability represents a simple form of associative learning that is part of most mammalian defensive behavior systems (Fanselow, 1994).

The neural systems underlying fear conditioning have been elucidated by animal models as well as human imaging studies using functional magnetresonance imaging (fMRI) and positron emission tomography (PET) (Buchel & Dolan, 2000; Maren, 2001). The amygdala has been regarded as the key structure processing aversive stimuli via afferents from sensory thalamus (LeDoux, 1993; Shi & Davis, 2001) enabling fast evaluation of noxious stimuli without complex computations of the cortex. As the amygdaloid complex is highly interconnected with the temporal, orbito-frontal and insular cortices (Aggleton, Burton, & Passingham, 1980; Amaral, 1986; Mufson, Mesulam, & Pandya, 1981; Porrino, Crane, & Goldman-Rakic, 1981) the amygdala is anatomically well placed for stimulus association learning in various sensory domains. Given its fast access to sensory information and its neuroanatomical location the amygdala has been assigned a central role in mediating synaptic changes at the cortical level (McGaugh, Cahill, & Roozendaal, 1996) necessary for the association between the conditioned (CS) and the unconditioned stimulus (US). For example Buchel and colleagues (Buchel, Morris, Dolan, & Friston, 1998) demonstrated in an fMRI study that the amygdala activation was most prominent during acquisition of the conditioned response (CR) and LaBar and collaborators (LaBar & Disterhoft, 1998) showed a decline of amygdala activation over trials possibly reflecting that amygdala activation is only necessary until associations between the CS and US have been formed.

In addition to amygdala circuitry and highly interconnected with it, a distributed network of cortical areas seems to be involved in classical fear conditioning as well. For example in the visual system of primates the amygdala projects back to various stages in the ventral visual path and receives itself highly processed sensory information (Amaral, Price, Pitkaenen, & Carmichael, 1992). This neural architecture may be the basis of a mechanism, which enhances stimulus processing in visual sensory systems. In line with this notion, imaging studies in humans have shown greater activations for the reinforced CS (CS+) as compared to the nonreinforced CS (CS-) in temporal and occipital cortices (Cheng, Knight, Smith, Stein, & Helmstetter, 2003; Hugdahl et al., 1995).

Additional support to the involvement of cortical areas in fear conditioning comes from cognitive theories of Pavlovian conditioning that emphasize anticipation or attentional processes (Pearce & Hall, 1980). For instance Rescorla (Rescorla, 1988) has emphasized that the CS+ in a Pavlovian conditioning paradigm gains predictive value that enables the organism to anticipate an aversive event. The ability to obtain such a predictive value has been associated with the salience of a stimulus (Mackintosh, 2003). Thus, at a neurophysiological level cortical systems mediating attentional processes and maintaining an alert state should come into play.

In attention research, fronto-parietal cortical networks have been identified in visuospatial orienting (Corbetta, 1998). Further, shifting attention between nonspatial cues such as color and shape has been associated with activity within the parietal cortex (Le, Pardo, & Hu, 1998; Rushworth, Paus, & Sipila, 2001). Pardo et al. (Pardo, Fox, & Raichle, 1991) observed activity in right prefrontal and right superior parietal cortices during a sustained attention task whether it was of visual or somatosensory modality. Thus, there is good evidence for the involvement of a wide-spread fronto-parietal cortical network in orienting to a new stimulus as well as maintaining attention to that stimulus. This network is linked e.g. via the thalamus to the ventral visual system of the neocortex (Fernandez-Duque & Posner, 2001) and could be an alternative or complementary route to the amygdalafugal pathway, enhancing stimulus processing in visual areas during fear conditioning.

Indeed, in human imaging studies amygdala activity was observed specifically during early trials of conditioning (Buchel et al., 1998; LaBar & Disterhoft, 1998) and was sometimes revealed only when correlated with physiological output systems as indicated e.g. by the skin conductance response (Cheng et al., 2003; Furmark, Fischer, Wik, Larsson, & Fredrikson, 1997). Consistent with these findings, cortical regions like the frontal-, temporal-, parietal cortices and the anterior cingulate have been observed being more active during

processing of the CS+ (Buchel et al., 1998; Fischer, Andersson, Furmark, Wik, & Fredrikson, 2002; Fredrikson, Wik, Fischer, & Andersson, 1995; Hugdahl et al., 1995; Knight, Cheng, Smith, Stein, & Helmstetter, 2004; LaBar & Disterhoft, 1998) possibly reflecting the involvement of a neural network mediating attention/emotion aspects of that stimulus.

Further support to the hypothesis assuming the participation of cortical networks that mediate attentional processes in fear conditioning comes from event related potentials (ERP) studies using slow potentials. In these studies a first stimulus (S1) signals a second imperative stimulus (S2) occurring after a certain time interval. During the time interval between S1 and S2 the so-called negative contingent variation (CNV) is recorded. The negative shift of the slow potential developing during the time gap between the two stimuli has been associated with expectancy and attentional processes for motor as well as cognitive responding (Rockstroh, Elbert, Canavan, Lutzenberger, & Birbaumer, 1989; Rohrbaugh et al., 1986). The S1 can act as either the CS+ or CS- predicting the occurrence of an aversive stimulus after S2 which can be terminated by a motor response. The CNV has been reported to be greater during the S1/ S2 interval when S1 consists of the CS+ as compared to the CS- (Flor et al., 1996; Regan & Howard, 1995; Rockstroh et al., 1989). The development of a CNV has been hypothesized to reflect facilitatory processes in excitability of the cortex and may be a electrophysiological indicator of enhanced stimulus processing during allocating attentional resources to stimulus contingency and preparation of an adequate response (Rockstroh, Muller, Wagner, Cohen, & Elbert, 1993).

In the present work, we investigated changes of cortical processes over time using the steady state visual evoked field (SSVEF). The SSVEF is the neuromagnetic counterpart of the steady state visual evoked potential (SSVEP) in EEG research. In this approach, a stimulus is presented repetitively, modulated in intensity at a fixed rate of 6-8 Hz or greater. The resulting waveform is oscillatory in nature, having the same fundamental frequency as the driving stimulus, often including higher harmonics (Regan, 1989). The SSVEP is sensitive to both tonic changes of central nervous activity such as anesthesia, sleep or vigilance (Picton, Vajsar, Rodriguez, & Campbell, 1987; Plourde & Picton, 1990; Silberstein et al., 1990) and phasic changes such as visual spatial selective attention whereby greater SSVEP amplitudes for attended vs. unattended stimuli were found (Morgan, Hansen, & Hillyard, 1996; Müller, Teder-Salejarvi, & Hillyard, 1998).

Advantages of the SSVEP/ SSVEF technique relate to the fact that they enable the experimenter to collect a high number of trials in short periods of time, and to use time-frequency domain analyses allowing the easy extraction of dependent variables that reflect the

driving stimulus frequency over time (e.g. complex demodulation). A conceptual advantage is that widely distributed functional networks oscillating coherently at the driving stimulus frequency can be examined at high temporal resolution and signal-to-noise ratios. These oscillating networks can also reflect more complex cognitive processes such as working memory (Perlstein et al., 2003; Silberstein, Nunez, Pipingas, Harris, & Danieli, 2001).

As expectancy and attentional processes may be involved in Pavlovian conditioning as outlined above, the SSVEP/ SSVEF paradigm seems to be an adequate tool in order to track ongoing neural activity associated with processes of aversive conditioning. A recent SSVEP study by Gray and coworkers (Gray, Kemp, Silberstein, & Nathan, 2003) investigated cortical oscillatory activity during the anticipation of an electric shock and revealed the involvement of frontal, temporal and occipital electrode sites during anticipatory anxiety. Recently, Moratti and collaborators (Moratti, Keil, & Stolarova, 2004) have identified a fronto-parietal affective and attentive network during affective stimulus processing using magnetencephalography (MEG) suggesting that a general cortical attention network is involved in affective picture viewing. Further, it has been demonstrated that cued spatial attention and motivated attention to affective stimuli possibly interact within the same neuronal networks of attention and stimulus processing (Keil, Moratti, Sabatinelli, Bradley, & Lang, 2004). There is no study to date using the SSVEP/ SSVEF technique in combination with a discriminative delayed aversive conditioning design which allows the direct comparison between the stimulus driven neuromagnetic response of the CS+ and CS- during acquisition and extinction blocks.

Therefore, the aim of the present study was to examine cortical sources of the SSVEF as modulated by the predictive value of a visual CS during acquisition and extinction, using MEG. Since the SSVEF response is a stimulus driven ongoing oscillatory response in cortical networks responsible for processing the visual CS+ and CS-, estimating the underlying sources should elucidate the involvement of relevant cortical structures in Pavlovian conditioning. Applying the minimum norm estimate (MNE) (Hauk, Berg, Wienbruch, Rockstroh, & Elbert, 1998; Hauk, Keil, Elbert, & Müller, 2002) to the SSVEF response to determine the cortical sources of the neuromagnetic field, we hypothesized that after an association between the CS+ and the US has been established, the motivationally relevant CS+ will generate greater amplitudes in fronto-parietal and extrastriate cortex responsible for allocating attention and feature extraction, respectively. Further, applying the MNE to complex demodulated data we wanted to determine differences in the time course of the activations within these networks during CS+/ CS- presentation.

As the strength of the neuromagnetic field decreases with the square of distance, it is unlikely that deep cortical sources contribute to the neuromagnetic field. Therefore, we did not attempt any source localizations of deep cortical structures such as the amygdala.

Heart rate (HR) was recorded to validate the effectiveness of the conditioning procedure. Further, we wanted to evaluate the brain responses of subjects who accelerated or decelerated in response to the CS+ during acquisition as has been observed by various authors (Hamm & Vaitl, 1996; Hare, 1972; Hodes, Cook, & Lang, 1985). Subjective judgments of the US were obtained in order to assess the aversiveness of the US. Further, we collected questionnaire data in order to evaluate state/ trait anxiety and depressiveness of the participants.

METHODS

Participants

Nineteen paid volunteers (10 females, 9 males, all right handed (Oldfield, 1971)) gave written consent to participate in the study. Their mean age was 27.1 years (range: 20-49 years). They had normal or corrected to normal vision and no family history of photic epilepsy. They did not report a recent critical live event or any history of psychotherapy. On the German version of the state-trait anxiety inventory (STAI) (Laux, Glanzmann, Schaffner, & Spielberger, 1981) subjects reported a mean state anxiety score of 31.1 (± 1.1) and a mean trait anxiety score of 34.2 (± 1.8). Their mean depression score measured by a German version of the Beck depression inventory (BDI) (Hautzinger, Bailer, Worall, & Keller, 1992) was 3.8 (± 0.8). Due to equipment malfunction we lost HR data of one subject. Another subject had to be excluded from the analysis because of noise contaminated MEG data. The MEG data of the participant with the missing HR data was excluded from further processing because the MEG data of groups associated with different HR responses were analyzed separately (see below). Finally, HR data of eighteen (10 females, 8 males, state anxiety: 31.1 (± 1.1), trait anxiety: 34.4 (± 1.9), BDI: 3.8 (± 0.8)) subjects and MEG data of seventeen subjects (9 females, 8 males, state anxiety: 31.3 (± 1.2), trait anxiety: 34.4 (± 2.0), BDI: 3.4 (± 0.7)) will be reported.

Stimuli

Two gray shaded 45° gratings perpendicular oriented to each other served as conditioned stimuli (CS). Using a video projector (JVC™, DLA-G11E) and a mirror system, the CSs were projected on a screen in the magnetically shielded room in random order,

subtending a visual angle of 8° both horizontally and vertically. A red fixation cross was shown in the middle of the screen and was present throughout the whole experiment. In each trial, a grating was shown in a luminance modulated mode of 12.5Hz for a time period of 5000ms resulting in 63 on/ off cycles, the grating being shown for 40ms, followed by 40ms black screen during each cycle. During the intertrial interval, which varied randomly between 6 and 8 seconds, a black screen was shown. The luminance modulation was done in order to elicit visual evoked steady state fields that can be recorded with MEG.

One of the two gratings was selected as the CS+ or CS-, counterbalanced across subjects. Using an air tube system attached to a sound amplifier (BTi ® ASG, 1996), the unconditioned stimulus (US) consisting of a 110dB white noise with instantaneous onset was presented binaurally for one second during the last second of CS+ depiction, and terminated together with CS+ offset. In 15% of the trials (see below), the red fixation cross turned from blue into red color for 500 ms either 1000, 2500 or 4000 ms after CS+ and CS- onset, each time lag occurring with the same probability.

Procedure

Upon arriving at the laboratory subjects were familiarized with the MEG chamber in which the recording took place. Subsequently, participants were instructed that in the first block of the experiment they would be shown different patterns and they were asked to press a response button as fast as possible whenever the red cross during pattern depiction changed to blue. They were also told that during the first block no loud noise will be presented. Further, participants knew that the second part of the experiment started after a short break and that during that part of the experiment the task would be repeated, while occasional very loud noises would be presented. After the instruction, subjects gave written consent and completed the STAI and the BDI. Thereafter, participants were prepared for the recordings.

For artifact control, four electrodes for the electrooculogram (EOG) were attached, two at the left and right outer canthi and two above and below the right eye. Additionally, two electrodes for the electrocardiogram (ECG) were placed at the left lower costal arch and the right collarbone. Participants were then seated in the MEG chamber, their head shapes were digitized, and index points (left and right periauricular points, nasion, a pseudo-vertex and a pseudo inion point at the forehead) were determined to calculate the relative head position within the MEG helmet for source analysis. Finally, they were positioned under the MEG sensors and a projection screen was placed in front of them.

The experimental session started with participants reading a written instruction on the screen in the MEG chamber explaining again the task and ensuring subjects that no loud noise will be delivered during the first block, which served as a habituation phase. The habituation block consisted of twenty CS+, twenty CS- and six target trials which requested a button press after the red cross had turned into blue. The stimuli were depicted without pairing of the CS+ with the US. Thereafter, a short break of one minute was allowed and subjects were instructed via text depicted on the screen, that during the next block they will hear a loud noise from time to time. After the break, the acquisition block began, which was identical to the habituation block, except that the CS+ was always paired with the US. The extinction phase started without a break after the acquisition trials, containing the same number of trials as the individual blocks before. The CS+ and CS- were never paired with the US during extinction. After the experiment, participants rated pleasantness/ unpleasantness and the level of arousal on a 10 cm analog scale each, whereas a greater distance from the left starting point of the analog scale represented a higher level of unpleasantness and arousal, respectively. Finally, participants were interviewed if they had detected a rule behind US presentation and were coded as aware or unaware of conditioning contingency depending on rule identification. Subjects were paid 15 € (approximately 15 US dollars) for participation.

Data acquisition and preprocessing

The MEG was recorded continuously, and digitized at a rate of 254.3Hz, using a 148-channel whole head system (MAGNES™ 2500 WH, 4D Neuroimage, San Diego, USA). A bandpass filter of 0.1 – 50Hz was applied on line. The EOG and ECG acquisition was performed by means of a Synamps amplifier (NEUROSCAN™) using Ag/ Cl electrodes. As the EOG and ECG recordings were coupled with the MEG acquisition, the same sampling rate and bandpass filter were applied to them.

SSVEFs were derived for each condition (CS+ and CS-) and every experimental block (habituation, acquisition, extinction) by averaging the MEG data over 4000 ms subtracting a 500 ms pre-stimulus baseline. The last 1000 ms of CS presentations were omitted because during CS+ trials in the acquisition block a loud noise as US was presented and startling of the subjects caused movement artifacts. The target trials (subjects were requested to press a button) were not submitted to further analysis. Eye artifacts were corrected using the algorithm implemented in BESA™ software (Berg & Scherg, 1994). Additionally, all data was inspected visually for movement artifacts.

A subspace projection (Uusitalo & Ilmoniemi, 1997) of the eye artifact topography was applied on the SSVEFs for each condition (CS+ and CS-) and each experimental block (habituation, acquisition and extinction) in order to account for topography distortions using the eye correction algorithm (see below). Thereafter, the SSVEFs were complex demodulated (Regan, 1989) at the stimulation frequency of 12.5Hz in order to obtain stimulus driven amplitudes for the sine and cosine parts of the demodulated SSVEFs over time.

As with the MEG data, only the first 4000 ms of HR change during stimulus presentation were analyzed. Target trials were not submitted to analysis. HR change waveforms during presentations of the CS+ and CS- in the acquisition and extinction block (habituation block was not analyzed) were obtained using in-house-software written in MATLAB™. The algorithm of the software estimated the HR change over 4000 ms stimulus presentation in 500 ms steps using a 2000 ms pre-stimulus baseline. The frequency of the occurrence of an R-wave was derived from the interbeat-interval and weighted according to the distance from a 500 ms step within the time vector. The HR change was transformed in beats per minutes (bpm). The resulting HR waveforms consisted of changes in bpm compared to pre-stimulus baseline for nine consecutive time bins (0ms to 4000 ms in 500 ms steps).

Source analysis

In order to estimate the cortical sources of the complex demodulated SSVEFs a minimum norm estimation (MNE) technique was applied (Hamalainen & Ilmoniemi, 1994). This linear estimation technique assumes that the data vector **b**, that contains the recorded magnetic field distribution over the sensors, can be described as the product of the lead-field matrix **A**, which specifies the sensor's sensitivity to the sources located, for example, on a shell, and a current density vector **x** of these sources plus a noise component **ε** (Grave de Peralta Menendez, Hauk, Gonzalez Andino, Vogt, & Michel, 1997). The MNE procedure utilized in the present study was described in more detail in chapter 3 and will be outlined only in brief, here.

The MNE is characterized by minimizing the power of the estimated current density of the sources. Given the presence of noise and a high number of sensors, a regularization is necessary to obtain a stable current density solution (Bertero, De Mol, & Pike, 1988). Here, a Tikhonov-Phillips regularization was applied in order to suppress the noise part of the solution. For the determination of the regularization parameter **λ**, the L-curve method was used. Higher **λ** values increase the stability of the solution as expressed by an increased norm of the solution estimate $|| \hat{x} ||^2$. This leads to an increased smoothing of the solution and a

worse data fit as reflected by an augmented residual norm of the solution $\| A\hat{x} - b \|^2$ (Bertero et al., 1988). Plotting the logarithm of $\| \hat{x} \|^2$ versus the logarithm of $\| A\hat{x} - b \|^2$ results in an L-curve shaped function (Hansen & O'Leary, 1993). The turning point of this curve is considered as an optimal tradeoff between a stable solution estimate and a good data fit.

For the computation of the lead-field matrix **A,** we used the algorithm suggested by Hauk et al. (Hauk et al., 2002). To this end, **A** was calculated for each participant, based on information on the center of a fitted sphere to the digitized head shape, and the positions of the MEG sensors relative to the head. A subspace projection (Uusitalo & Ilmoniemi, 1997) of the eye artifact topography was applied to the lead-field matrix **A** in order to account for topographical distortions caused by the eye artifact correction (see above). A spherical shell with evenly distributed 350 dipole locations served as source space. The radius of the shell was 80% of the radius of the fitted sphere. According to Hauk et al. (Hauk et al., 2002) this radius was considered as a good approximation of the location of cortical sources.

For the derivation of λ and computation of the MNE solution, we used an L-curve and Tikhonov-Phillips regularization algorithm implemented in MATLAB™ by Hansen and O'Leary (Hansen & O'Leary, 1993) available at http://www.imm.dtu.dk/~pch/. As the phase information of the measured MEG signal is crucial for the computation of the MNE and is lacking in a complex demodulated signal, the MNE was estimated for the sine and cosine parts of the 12.5Hz complex demodulated SSVEFs separately for every condition (CS+ and CS-), experimental block (habituation, acquisition and extinction) and for each subject. This procedure was derived from an algorithm calculating the MNE in the frequency domain suggested by Jensen and Vanni (Jensen & Vanni, 2002). The square root of the sum of squares of the MNE amplitudes for the sine and cosine parts served as a measure of the total 12.5Hz current source density over stimulus presentation time:

$$Amp_i(t) = \sqrt{Amp^2_{i,\sin e}(t) + Amp^2_{i,\cos ine}(t)}\ ,\ i \in [1,...,350], t \in [0ms,...,4000ms] \qquad (1)$$

where $Amp_i(t)$ is the total amplitude of the 12.5Hz demodulated SSVEF at dipole location i and time t, and $Amp_{i,sine}(t)$ and $Amp_{i,cosine}(t)$ are the corresponding amplitudes of the sine and cosine parts for time t.

L-curves were calculated for the averaged baseline topography over the 500 ms pre-stimulus interval for each condition (CS+, CS-), experimental block (habituation, acquisition, extinction) and sine/ cosine parts within one subject. The highest λ value determined from the

resulting L-curves was used as regularization parameter. This procedure was chosen in order to prevent that different regularizations could account for condition effects. Finally, the MNE solutions were projected on a standard brain implemented in the EMEGS© analyzing software (Junghöfer & Peyk, 2004) freely available at http://www.uni-konstanz.de/win/emegs and submitted to a statistical mapping procedure (see below).

Statistical Analysis

In order to evaluate differences between processing of the CS+ and CS- over stimulus presentation time, the MNE amplitudes were averaged across three time windows (t1: 0-1.3 s; t2: 1.3-2.6 s and t3: 2.6-3.9 s) for each condition (CS+, CS-), each experimental block (habituation, acquisition and extinction) and each subject. Within every experimental block the interaction between *condition* (CS+, CS-) and *time* (t1, t2, t3) was modeled at 273 of the 350 sources of the MNE shell in order to identify source clusters of differential activations for the CS+ and CS-. Sources located at the bottom of the shell were not considered as meaningful and were omitted in order to enhance statistical power (reducing the number of dipoles from 350 to 273). The p values for the interaction terms were corrected for 273 multiple tests by the false discovery rate procedure (Benjamini & Hochberg, 1995; Keselman, Cribbie, & Holland, 2002) and mapped on a standard brain implemented in the EMEGS© analyzing software. The interactions were modeled using a linear mixed effects model (LME) applying restricted maximum likelihood estimators (REML) for parameter estimation. A detailed introduction of LME models in psychophysiological research is given by Bagiella et al. (Bagiella, Sloan, & Heitjan, 2000). A description of the REML estimation method can be found in Searle et al. (Searle, Casella, & McCulloch, 1992). As the factor *time* implies dependence of observations a first order autoregressive (AR(1)) covariance structure was applied that estimates one correlation parameter between observations and assumes that the interdependence of observations decays exponentially. Such serial correlation structures have been introduced to model dependence in time-series data and are discussed for example in Pinheiro and Bates (Pinheiro & Bates, 2000) in more detail. In the LME model we chose *condition* and *time* as fixed effects. As we were not interested in mean differences in MNE amplitudes between subjects over all conditions and within conditions we selected the intercept to be a random effect at the *subject* and *condition within subject* level. The statistical modeling was done using R© (Team, 2004), a freely available statistical package.

Source clusters were considered as meaningful whenever at three or more neighboring source locations the interaction terms survived the false discovery rate procedure for 273 tests

and thus consisted of sources with associated corrected p values less than .05. The mean amplitude across dipoles of an identified source cluster was submitted to LME analysis identical to the one described above, except that we added the fixed effect $time^2$ to the fixed effect *time* and considered them as ordered factors in order to assess different time courses of cortical activations for the CS+ and CS- (linear and quadratic time courses). Whenever the kind of time course (linear and/ or quadratic) interacted with condition, the time courses were modeled for the CS+ and CS- condition, separately. Additionally, we conducted paired t-tests in order to asses at which time slots (t1, t2, t3) the CS+ and CS- generated different cortical source activations.

The HR change time series data was also analyzed using an LME model. The model was identical to the LME model presented above, except that *time,* $time^2$*,* $time^3$ *and* $time^4$served as ordered fixed effects in order to asses a linear, quadratic, cubic and quartic time course of the HR data. This was implemented on the basis of earlier notions (Wilson, 1974) suggesting that analyzing differences in HR waveform components is more meaningful than comparing means. The *time* factors consisted of nine time bins containing 500 ms each (see above). As we were not interested in mean differences or drifts of the HR response curve per subject over all conditions and within conditions, we chose the intercept and the linear slope (*time*) to be random effects at both the *subject* and *condition within subject* level.

Finally, following the procedure described by Hodes et al. (Hodes et al., 1985), a cluster analysis was performed on heart rate data obtained in acquisition trials during CS+ presentation. This approach was chosen because we wanted to identify subjects who accelerated or decelerated in their HR response to the CS+ during acquisition as observed by previous studies (Hamm & Vaitl, 1996; Hare, 1972; Hodes et al., 1985).

The difference between HR accelerators and decelerators with respect to the sum scores of the questionnaires and to the distance from the left starting point of the analog scales were analyzed using t-tests. The frequency distributions of females and males and of subjects aware or unaware of conditioning contingency were assessed by χ^2-tests.

RESULTS

Delineation of different HR change responders by cluster analysis

The cluster analysis on HR change in acquisition trials during CS+ presentation revealed three groups. One group of subjects showed a defensive accelerative response to the CS+ (N=8) and the other two subgroups depicted a decelerative pattern (N=6 and N=4, respectively). In order to obtain samples of sufficient size for further analysis, the latter two

subgroups were collapsed into one decelerative group (N=10). The obtained grouping structure was applied to the extinction trials in order to evaluate possible learning differences between accelerators and decelerators.

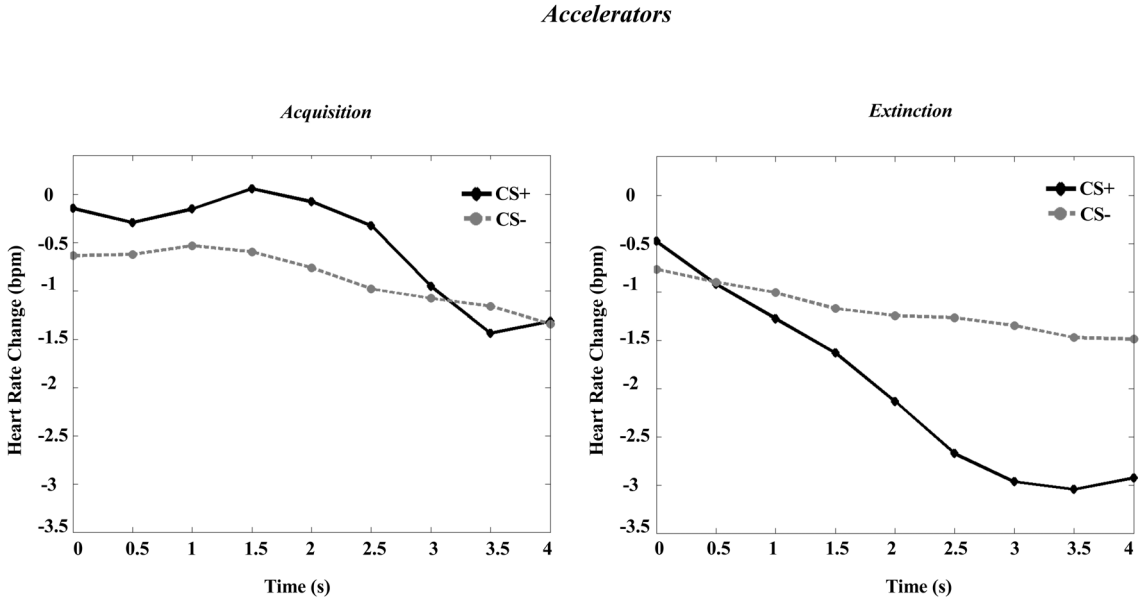

Figure 1: Heart rate change in acquisition (left panel) and extinction (right panel) blocks during CS+ and CS- depiction for accelerators (N=8). During acquisition the CS+ depiction elicited an accelerative response compared to the CS- presentation (quartic trend CS+: $F(1, 60) = 28.3$, $p < .0001$; quartic trend CS-: n. s.). During extinction accelerators showed a decelerative orientation response to the CS+ but not the CS- (linear trend CS+: $F(1, 60) = 18.7$, $p < .0001$; linear trend CS-: not significant (n. s.)).

As suggested by figure 1 accelerators showed a pronounced defense response to the CS+ (see table 1). This was confirmed by separate analysis of the CS+ and CS- trials yielding only a quartic waveform component for the CS+ ($F(1, 60) = 28.3$, $p < .0001$). During the extinction block of the experiment, accelerators reacted with an orientation response to the CS+ but not to the CS- (see figure 1 and table 2 for interaction; linear component CS+: $F(1, 60)=18.7$, $p < .0001$; CS-: not significant (n. s.)).

Table 1: Interaction between waveform components (linear, quadratic, cubic and quartic trends) and condition (CS+, CS-) during acquisition for accelerators. n. s. = not significant, numDF = degrees of freedom numerator, denDF = degrees of freedom denominator.

interaction with condition	numDF	denDF	F value	p value
linear	1	120	1.1	n. s.
quadratic	1	120	0.5	n. s.
cubic	1	120	0.4	n. s.
quatric	1	120	*15.4*	*< .0001*

Table 2: Interaction between waveform components (linear, quadratic, cubic and quartic trends) and condition (CS+, CS-) during extinction for accelerators. n. s. = not significant, numDF = degrees of freedom numerator, denDF = degrees of freedom denominator.

interaction with condition	numDF	denDF	F value	p value
linear	1	120	*9.4*	*< .01*
quadratic	1	120	3.6	n. s.
cubic	1	120	3.7	n. s.
quatric	1	120	0.5	n. s.

For decelerators, an interaction between a quadratic waveform component and condition was obtained in the acquisition block (see table 3 and figure 2). Separate analyses of the acquisition trials during CS+ and CS- presentation showed that the quadratic component was more prominent for the CS+ ($F(1, 76)=20.6$, $p < .0001$) than for the CS- ($F(1, 76)=4.0$, $p < .05$). During extinction decelerators did not show any different HR changes for the CS+ and CS- (see figure 2).

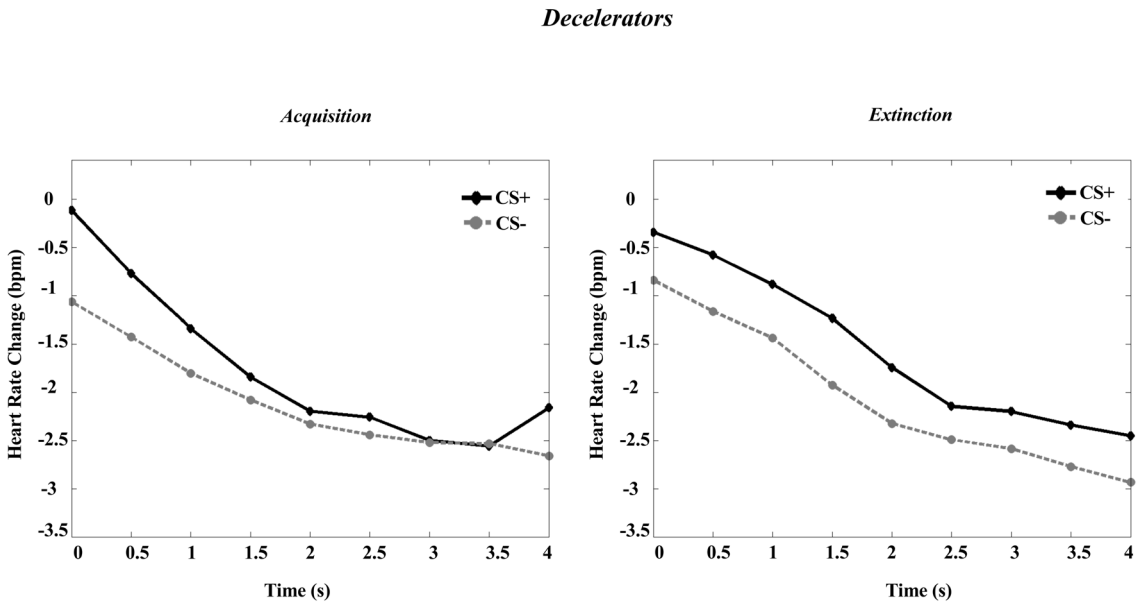

Figure 2: Heart rate change in acquisition (left panel) and extinction (right panel) blocks during CS+ and CS- depiction for decelerators (N=10). During acquisition a quadratic waveform component that was more prominent for the CS+ than for the CS- (quadratic trend CS+: $F(1, 76) = 20.6$, $p < .0001$; quadratic trend CS-: $F(1, 76) = 4.0$, $p < .05$) was elicited. During extinction decelerators did not show any differential HR response patterns to the CS+ and CS-.

Table 3: Interaction between waveform components (linear, quadratic, cubic and quartic trends) and condition (CS+, CS-) during acquisition for decelerators. n. s. = not significant, numDF = degrees of freedom numerator, denDF = degrees of freedom denominator.

interaction with condition	numDF	denDF	F value	p value
linear	1	152	0.3	n. s.
quadratic	1	152	*4.4*	*< .05*
cubic	1	152	0.7	n. s.
quatric	1	152	1.0	n. s.

Thus, the HR data indicated that specifically the accelerators showed a differential defense – and orientation response to the CS+ during acquisition and extinction, respectively. During acquisition the decelerators first showed an orientation response followed by an acceleration of their HR response to the CS+. This was also the case for the CS- but to a much lesser extent. Within extinction trials decelerators did not differentiate between the CS+ and CS- with respect to HR change.

MNE data for all subjects

Figure 3 shows the grand mean of the MNE solutions over all subjects for the CS+ and CS- during habituation, acquisition and extinction trials. The processing of the gratings was left lateralized as depicted in figure 3. Activity in visual areas declined over stimulus presentation time, but note the increase in the late time segment (2.6-3.9s) for the CS+ during extinction.

The p values of the interaction terms of *condition* (CS+, CS-) and *time* (t1, t2, t3) obtained by the LME model that survived the false discovery rate correction and the spatial distribution criterion (see Methods) were mapped on a standard brain. No source locations meeting the above mentioned criteria emerged during habituation. During acquisition trials left orbito-frontal sources (figure 4) showed different time courses of activations (quadratic trend x condition: $F(1, 64)=9.3$, $p < .005$) in as much that the stimulus driven SSVEF response to the CS- decreased linearly over time (linear trend CS-: $F(1, 32)=10.7$, $p < .005$; quadratic trend CS-: n. s.) whereas the linear decrease of the CS+ generated amplitude was followed by an increase during the last time period of CS+ presentation (linear trend CS+: $F(1, 32)=17.4$, $p < .001$; quadratic trend CS+: $F(1, 32)=10.1$, $p < .005$). The condition comparisons for the three time blocks revealed that during the first 1.3 seconds of CS presentation the CS+ produced a stronger SSVEF in left orbito-frontal brain regions (t1: $t = 3.5$, $df = 16$, $p < .005$; t2 and t3: n. s.).

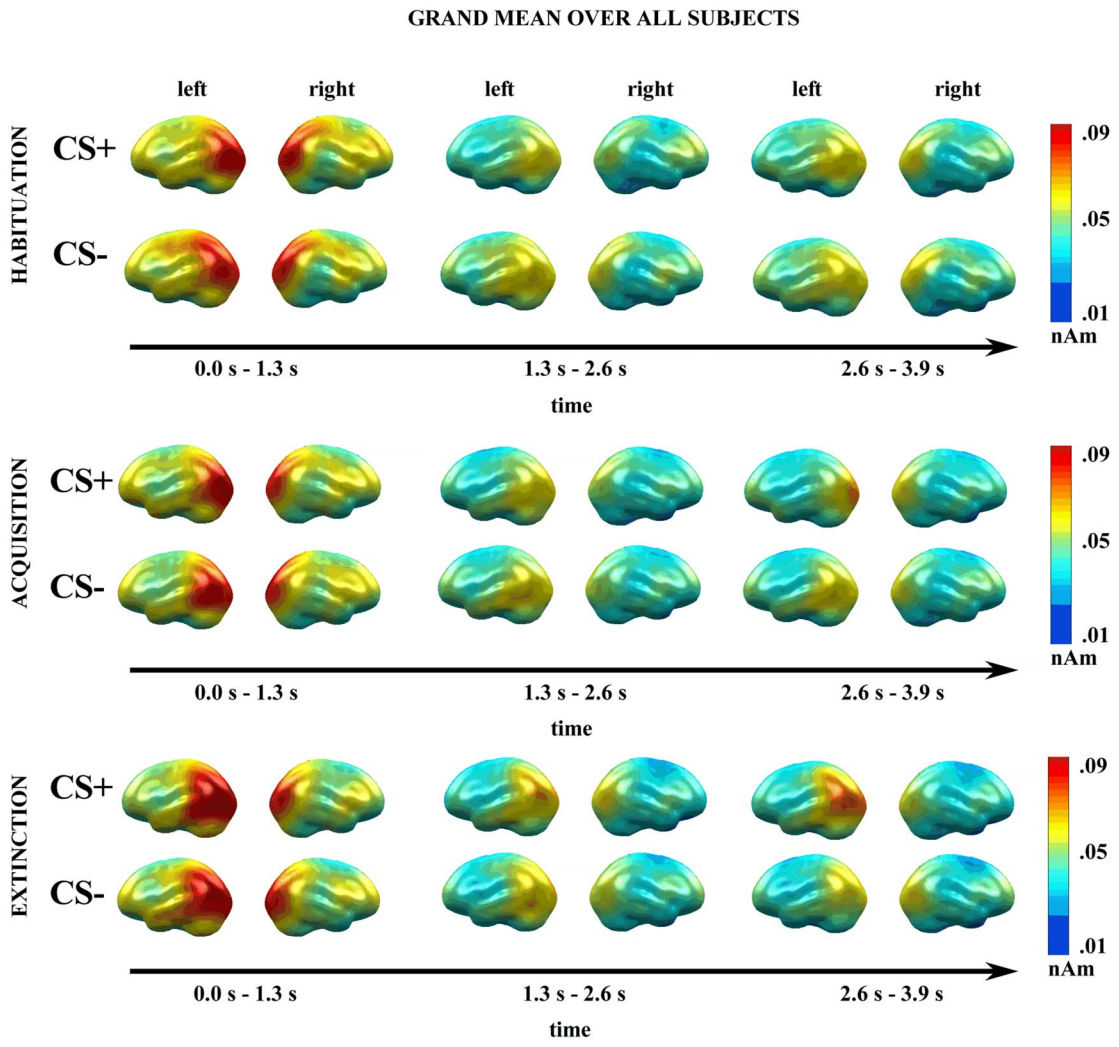

Figure 3: Grand mean of the minimum norm estimates (MNE) over all subjects (N=17) for CS+ and CS- trials during the habituation, acquisition and extinction phase of the experiment. Left and right hemispheres are shown. The arrows indicate the time of CS presentation. Below the arrows the time interval of the depicted MNE topographies is indicated. The colorbars on the right show the activation strength in nAm.

Altogether, left orbito-frontal brain regions responded stronger to the CS+ than to the CS- during early stimulus presentation time. Thereafter, the amplitude generated by the CS+ decreased strongly and then increased again, whereas the SSVEF response to the CS- decreased gradually over time (figure 4).

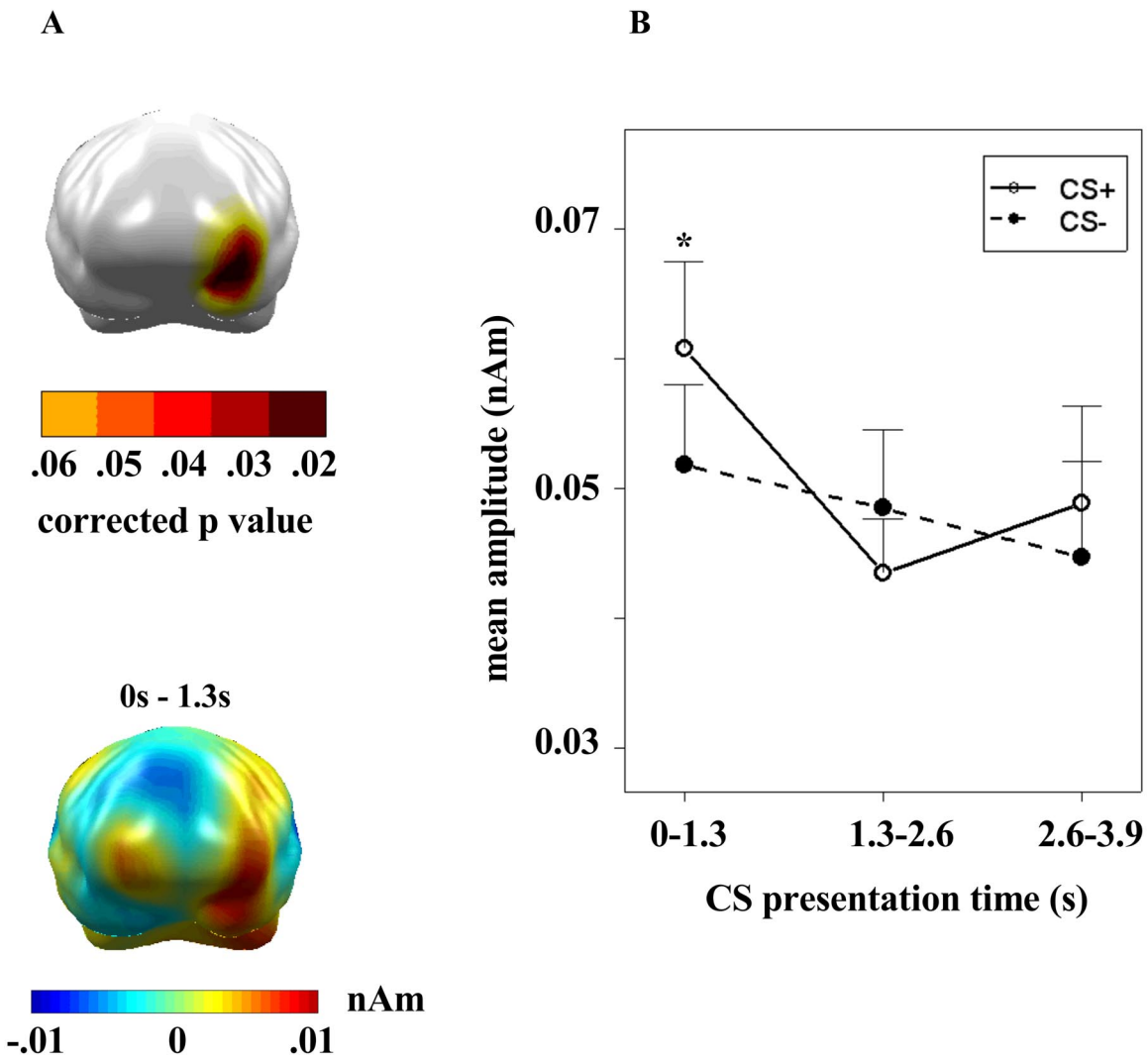

Figure 4: Left orbito-frontal sources showed a differential time course of activation during acquisition. The upper part of panel A depicts sources of significant interaction of stimulus presentation time and condition (CS+, CS-). The lower part of panel A shows the difference map of the minimum norm estimates (CS+ minus CS- condition) during early stimulus presentation time (0s-1.3s). Panel B depicts the mean amplitudes and standard errors of the means over significant source clusters as identified by the linear mixed effects procedure. * $p < .05$ paired comparisons.

During extinction trials activity of midline cortical sources (figure 5) were characterized by a stronger linear decrease of amplitude for the CS+ than for the CS- condition (linear trend x condition: $F(1, 64) = 9.1$, $p < .005$; linear trend CS+: $F(1, 32) = 47.2$, $p < .0001$; linear trend CS-: $F(1, 32) = 20.0$, $p < .0001$). The stronger decrease for the CS+ in midline cortical brain regions was due to a greater activation for the CS+ compared to the CS-

condition during early time segments and a subsequent drop off to the same activation level of the CS- during later stimulus presentation times (t1: t = 2.1, df = 16, p < .05; t1 and t2: n. s.).

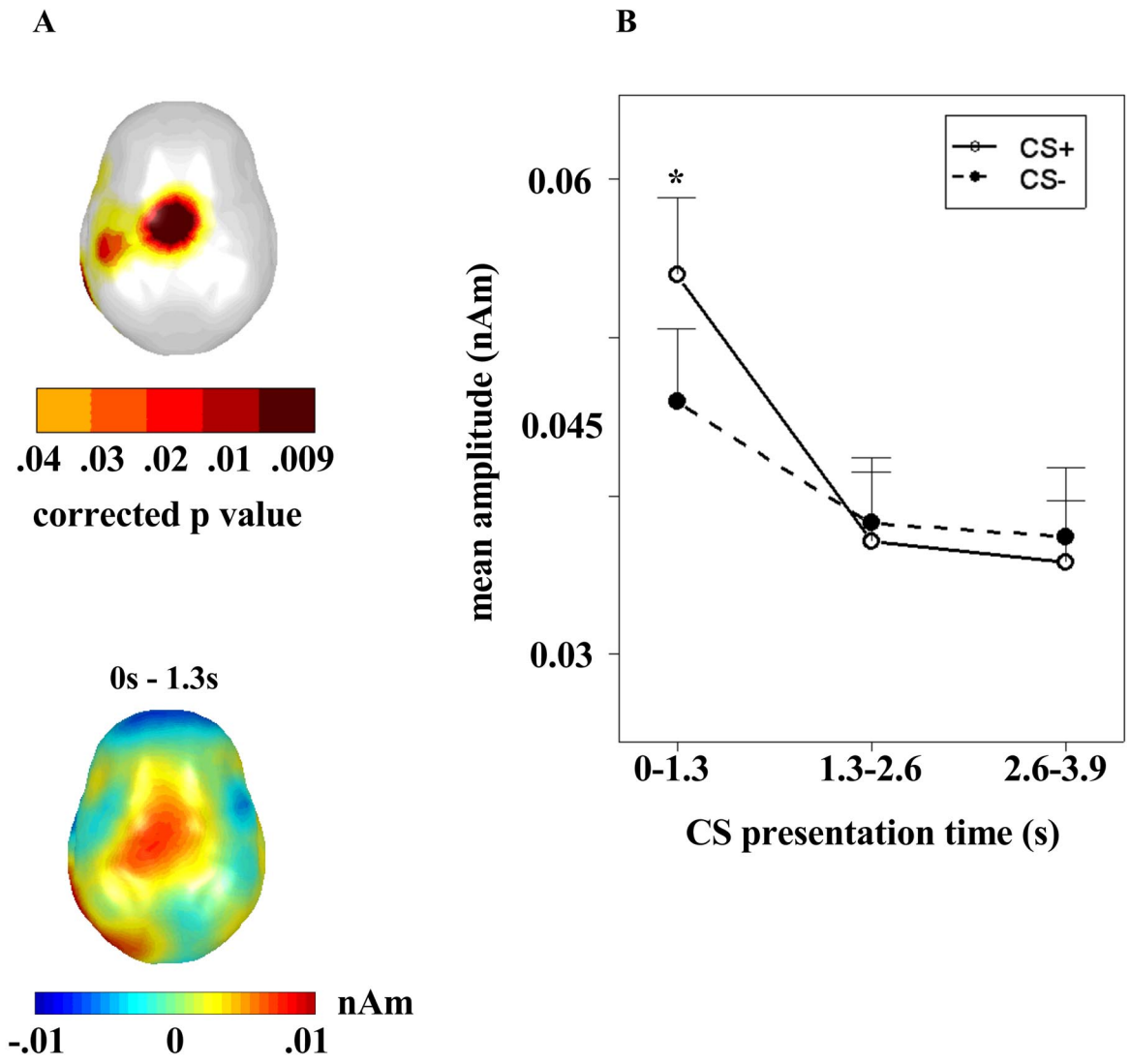

Figure 5: Midline cortical sources showed a differential time course of activation during extinction. The upper part of panel A depicts sources of significant interaction of stimulus presentation time and condition (CS+, CS-). The lower part of panel A shows the difference map of the minimum norm estimates (CS+ minus CS- condition) during early stimulus presentation time (0s-1.3s). Panel B depicts the mean amplitudes and standard errors of the means over significant source clusters as identified by the linear mixed effects procedure. * p < .05 paired comparisons.

Activity of left parietal cortical sources (figure 6) declined over time for both conditions (linear trend CS+: F(1, 32) = 7.1, p < .05; linear trend CS-: F(1, 32) = 20.8, p < .001), but a quadratic trend only for the CS+ trials (quadratic trend x condition: F(1, 64) =

4.03, p < .05; quadratic trend CS+: F(1, 32) = 25.1, p < .0001; quadratic trend CS-: n. s.) indicated that during the last 1.3 seconds (t3) of the analyzing window the activity increased again in comparison to the CS- condition (t1 and t2: n. s.; t3: t = 2.4, df = 16, p < .05).

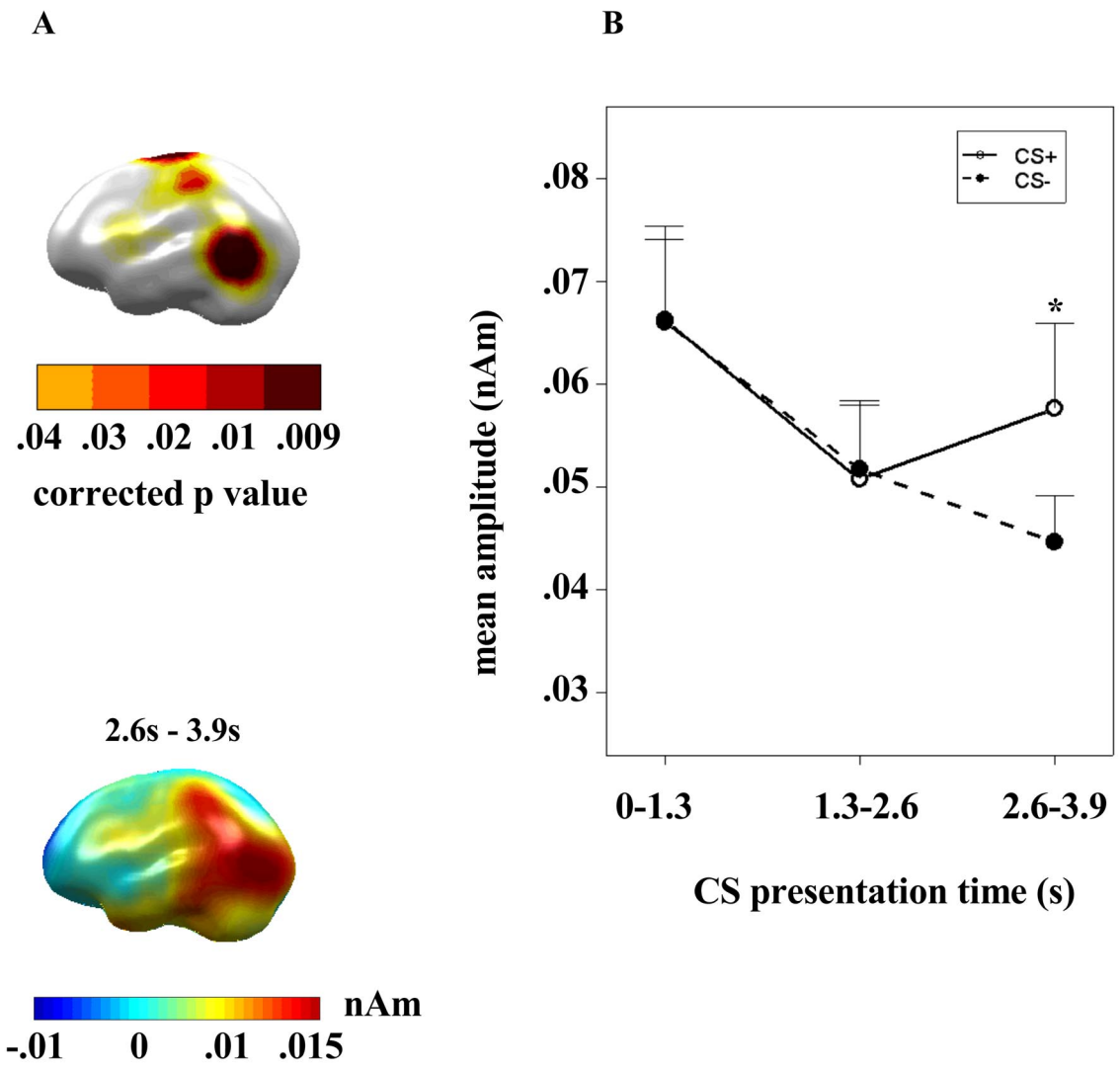

Figure 6: Left parietal sources showed a differential time course of activation during extinction. The upper part of panel A depicts sources of significant interaction of stimulus presentation time and condition (CS+, CS-). The lower part of panel A shows the difference map of the minimum norm estimates (CS+ minus CS- condition) during last stimulus presentation time before US presentation (2.6s-3.9s). Panel B depicts the mean amplitudes and standard errors of the means over significant parietal source clusters (small cluster above the occipito-temporal cluster described figure 7) as identified by the linear mixed effects procedure. * p < .05 paired comparisons.

In left occipito-temporal brain regions (see figure 7) the time course of SSVEF amplitude reflected the one observed for the parietal cortical sources.

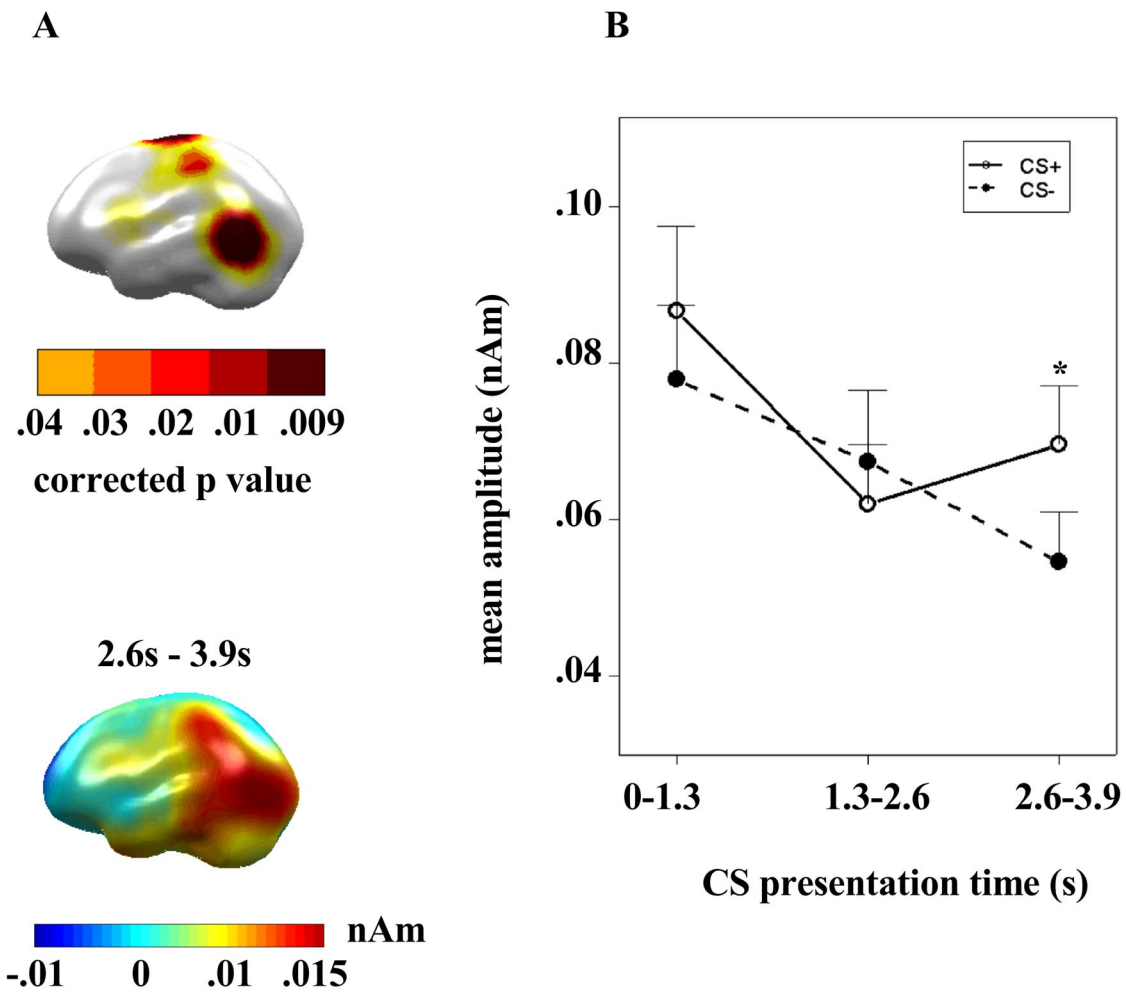

Figure 7: Left occipito-temporal sources showed a differential time course of activation during extinction. The upper part of panel A depicts sources of significant interaction of stimulus presentation time and condition (CS+, CS-). The lower part of panel A shows the difference map of the minimum norm estimates (CS+ minus CS- condition) during last stimulus presentation time before US presentation (2.6s-3.9s). Panel B depicts the mean amplitudes and standard errors of the means over significant occipito-temporal source clusters (cluster below the parietal cluster described in figure 6) as identified by the linear mixed effects procedure. * $p < .05$ paired comparisons.

Activation during CS+ presentation increased again towards the late CS+ presentation time period compared to CS- depiction (quadratic trend x condition: $F(1, 64) = 10.9$, $p < .01$;

quadratic trend CS+: $F(1, 32) = 19.0$, $p < .001$; quadratic trend CS-: n. s.). Mean amplitude of the last time segment (t3) was greater for the CS+ than for the CS- (t1 and t2: n. s.; t3: $t = 3.3$, $df = 16$, $p < .005$) in left occipito-temporal brain regions during extinction.

MNE data for subgroups HR Accelerators and HR Decelerators

As shown above subjects differed in respect to their HR responses to the CS+ during acquisition trials. One group reacted with an HR acceleration to the CS+ relative to the CS-. The other group responded with an HR deceleration during CS+ presentation and an HR acceleration towards the occurrence of the US. This U-shaped HR pattern was more pronounced for the CS+ than the CS- trials. During extinction only the accelerators showed a differential OR response to the CS+. Decelerators slowed down their HR in both conditions during extinction. Because of these different physiological response patterns we analyzed the MNE data for both subgroups (accelerators and decelerators), separately.

Accelerators: During acquisition no interaction between condition (CS+, CS-) and time (t1, t2, t3) could be observed in any brain region. However, in extinction trials accelerators showed a decline of SSVEF activity in right temporal brain regions for the CS+ whereas during CS- presentation SSVEF amplitude remained the same for all time blocks (linear trend x condition: $F(1, 28) = 9.8$, $p < .005$; linear trend CS+: $F(1, 14) = 16.7$, $p < .005$; linear trend CS-: n. s.). The decline of right temporal source activation for the CS+ was due to activity amplification relative to the CS- during the first two time segments (t1: $t = 2.8$, $df = 7$, $p < .05$; t2: $t = 2.1$, $df = 7$, $p = 0.06$; t3: n. s.).

In the left hemisphere, parietal cortical sources showed a quadratic activation time course only during CS+ presentation (quadratic trend x condition: $F(1, 28) = 6.4$, $p < .05$; quadratic trend CS+: $F(1, 14) = 20.7$, $p < .001$; quadratic trend CS-: n. s.) indicating an increase in SSVEF amplitude in the late time segment of CS+ depiction compared to CS- presentation (t1 and t2: n. s.; t3: $t = 2.1$, $df = 7$, $p = 0.07$). For left occipito-temporal brain regions a similar difference in the time course of activation emerged (quadratic trend x condition: $F(1, 28) = 13.7$, $p < .001$; quadratic trend CS+: $F(1, 14) = 12.8$, $p < .005$; quadratic trend CS-: n. s.). This effect was not only driven by an increase of CS+ activation towards the time the US could be expected, but was also due to a decline of CS+ amplitude beneath the activity level of the CS- during the second time segment (t1: n. s.; t2: $t = -2.4$, $df = 7$, $p < .05$; t3: $t = 3.3$, $df = 7$, $p < .05$). The results for the accelerators are summarized in figure 8.

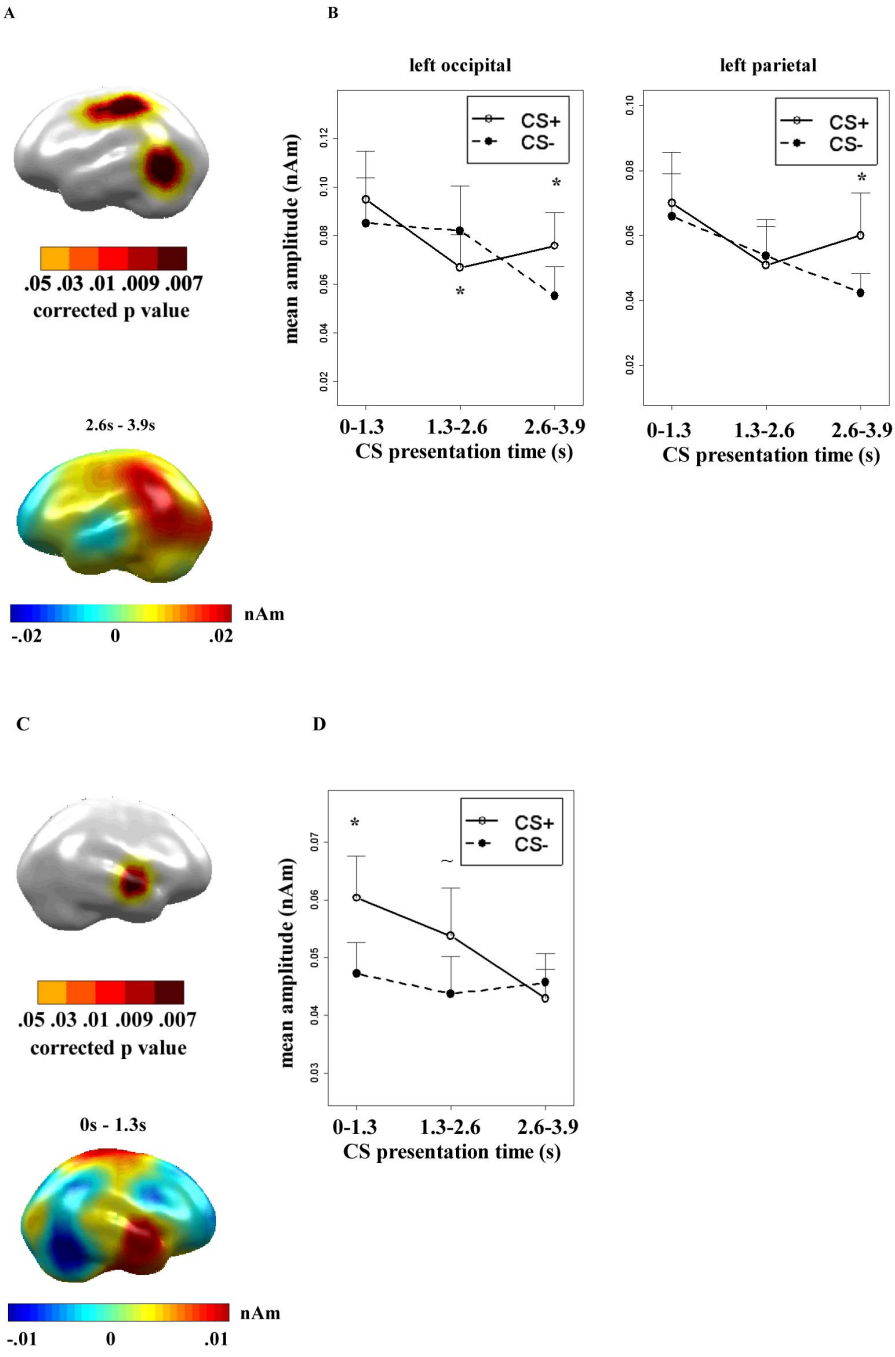

Figure 8: Left occipital and parietal significant (interaction CS presentation time and condition) source clusters for accelerators during extinction are depicted in the upper part of panel A. The lower part of panel A shows the difference map of the minimum norm estimates (CS+ minus CS- condition) during last stimulus presentation time before US presentation (2.6s-3.9s). Panel B depicts the mean amplitudes and standard errors of the means over significant occipito-temporal and parietal source clusters as identified by the linear mixed effects procedure. Right temporal significant source clusters are depicted in the upper part of panel C. The lower part of panel C shows the difference map of the minimum norm estimates (CS+ minus CS- condition) during early stimulus presentation time (0s-1.3s). Panel D depicts the mean amplitudes and standard errors of the means over significant right temporal source clusters as identified by the linear mixed effects procedure. * $p < .05$; ~ $p < .10$ paired comparisons.

Decelerators: During acquisition decelerators showed a strong quadratic time course of cortical source activation in left orbito-frontal brain regions only for the CS+ and not for the CS- (quadratic trend x condition: $F(1, 32) = 10.7$, $p < .005$; quadratic trend CS+: $F(1, 16) = 9.4$, $p < .01$; quadratic trend CS-: n. s.). The CS- activation remained at the same level over all time segments (linear trend CS-: n. s.). The mean SSVEF amplitude in left orbito-frontal brain areas elicited by the CS+ was greater than the activation generated by the CS- during the initial (t1) and final (t3) stimulus presentation times (t1: $t = 3.4$, $df = 8$, $p < .01$; t2: n. s.; t3: $t = 2.3$, $df = 8$, $p < .05$). The SSVEF amplitude of left inferior temporal brain regions generated by the CS+ was characterized by a decline over time whereas the amplitude elicited by the CS- remained at the same level (linear trend x condition: $F(1, 32) = 10.4$, $p < .005$; linear trend CS+: $F(1, 16) = 43.2$, $p < .0001$; linear trend CS-: n. s.). However, single comparisons of the amplitude means of the CS+ and CS- for each time segments did not reveal any differences (t1, t2 and t3: n. s.).

During extinction no interaction between condition (CS+, CS-) and time (t1, t2, t3) could be observed in any brain region for the decelerators. The results for the decelerators are summarized in figure 9.

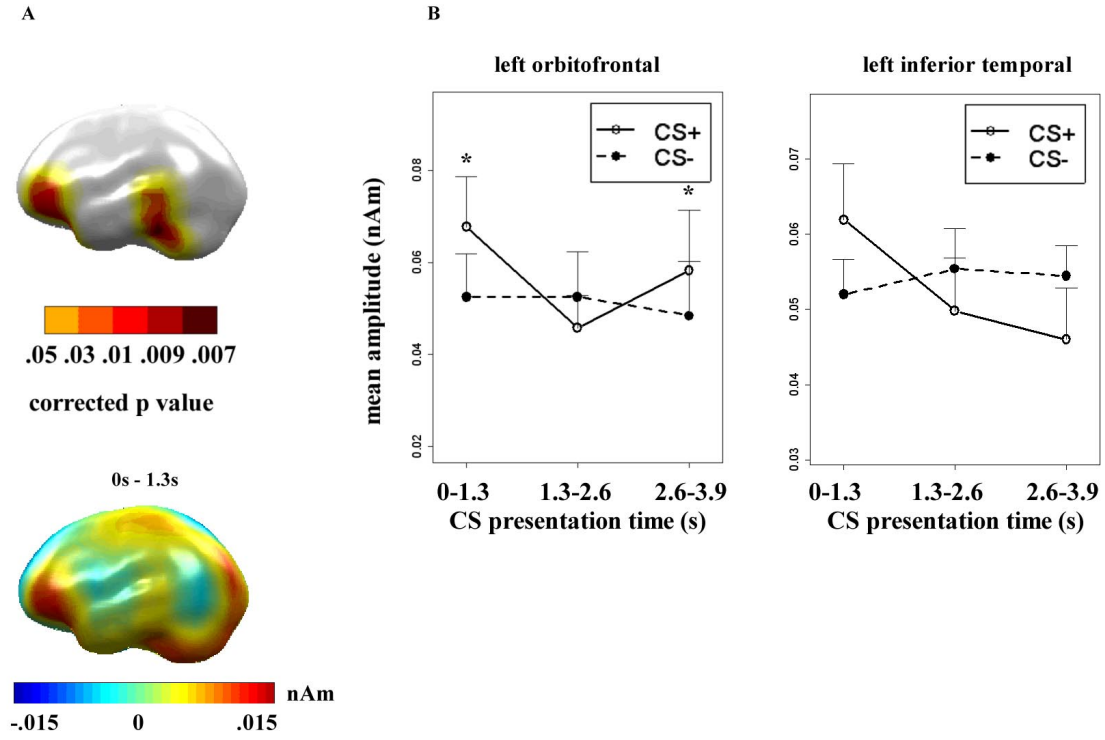

Figure 9: Left orbito-frontal and inferior temporal significant (interaction CS presentation time and condition) source clusters for decelerators during acquisition are depicted in the upper part of panel A. The lower part of panel A shows the difference map of the minimum norm estimates (CS+ minus CS- condition) during early stimulus presentation time (0s-1.3s). Panel B depicts the mean amplitudes and standard errors of the means over significant source clusters as identified by the linear mixed effects procedure. * $p < .05$ paired comparisons.

Questionnaires and demographic data

As two groups emerged with respect to a physiological response such as HR and accelerators and decelerators showed differences in the MNE data, we also analyzed if accelerators and decelerators differed in state-trait anxiety, BDI scores, awareness of reinforcement contingency, age, gender, valence and arousal ratings of the US.

As expected, the state and trait scores of the STAI over all subjects correlated ($r = 0.56$, $p < .05$). Considering accelerators and decelerators separately, the both groups did not show any differences in state or trait scores of the STAI (state STAI: accelerators mean: 29.9 (± 2.0); decelerators mean: 32.1 (± 1.3); trait STAI: accelerators mean: 32.4 (± 3.1); decelerators mean: 36.0 (± 2.5)). The two groups also did not differ in depression scores as measured by the BDI (accelerators: 2.5 (± 1.0); decelerators: 4.9 (± 1.2)). Accelerators and decelerators rated the white noise that served as US equally unpleasant and high arousing (valence: accelerators: 9.1 (± 0.3); decelerators: 8.4 (± 0.4); arousal: accelerators: 8.1 (± 0.6); decelerators: 7.8 (± 0.6)). Accelerators and decelerators were of about the same age (accelerators: 27.6 (± 1.7); decelerators: 27.1 (± 2.6)) and females and males were similarly represented in the accelerator and decelerator groups (accelerators: 4 females, 4 males; decelerators: 6 females, 4 males). Altogether, only 3 out of 18 subjects could report a contingency awareness. Two aware subjects were accelerators and one aware subject was a decelerator. The corresponding t-tests and χ^2 - tests were not significant.

DISCUSSION

Examining MEG correlates of Pavlovian fear conditioning by means of steady state visual evoked fields (SSVEF), we studied the modulation of stimulus-driven magnetocortical responses to visual stimuli differing in their motivational significance (reinforced CS+ vs. nonreinforced CS-) after one stimulus had been paired with an aversive event. Using the techniques of complex demodulation and minimum norm estimation, we aimed to investigate the changes in cortical processing over stimulus presentation time related to the experimental manipulation that one previous biologically irrelevant stimulus such as a grating gains predictive value of an aversive event.

In the present study, CS+ processing was facilitated in left orbito-frontal cortical regions during acquisition trials as indexed by amplitude enhancement relative to the CS-. The amplification of CS+ processing in that brain region emerged during early (first 1.3 s) stimulus presentation time. Similarly, early increased SSVEF amplitudes in response to the

CS+ were observed at central midline cortical sources during extinction. Activity modulations due to the motivational relevance of the stimuli during late stimulus depiction were observed in left parietal and occipito-temporal brain regions during extinction trials.

In general, the modulations of the SSVEFs observed across various cortical areas are in line with previous imaging (Buchel et al., 1998; Fischer et al., 2002; Fredrikson et al., 1995; Hugdahl et al., 1995; Knight et al., 2004; LaBar & Disterhoft, 1998) and CNV studies (Flor et al., 1996; Regan & Howard, 1995; Rockstroh et al., 1989) in that cortical networks involved in attentive stimulus processing were differentially modulated during Pavlovian fear conditioning. For visual stimuli, it has been shown that the aversively reinforced CS generated higher activations in temporal and occipital cortices (Cheng et al., 2003; Hugdahl et al., 1995) paralleling our results of enhanced CS+ processing in occipito-temporal regions during extinction.

The cortical areas displaying differential CS+ and CS- processing were selectively contributed by two subgroups of subjects as identified by cluster analysis of the HR data. With respect to heart rate (HR) data, we replicated earlier findings, reported e.g. by Hare (Hare, 1972) or by Hodes and collaborators (Hodes et al., 1985). We separated subjects that responded with HR acceleration to the CS+ (accelerators) and another subset of subjects that reacted with HR slowing and a subsequent acceleration during late CS+ presentation (decelerators) in acquisition trials. During extinction, accelerators depicted a marked OR response to the CS+ and not to the CS- as indexed by a HR deceleration solely to the CS+. Decelerators slowed down their HR to both the CS+ and the CS- during extinction. Most remarkably, accelerators and decelerators differed in their brain responses while processing the CS+ and CS- in acquisition and extinction trials.

Accelerators did not show any differences in the time course of SSVEF activations with respect to the CS+ and CS- in the acquisition block. In contrast, they showed marked differences during extinction. In right anterior temporal brain regions accelerators showed stimulus-driven oscillatory activity that remained at about the same level for the CS- over stimulus presentation time. The CS+ generated greater activity than the CS- in the first two time segments of stimulus presentation (0-1.3 s and 1.3-2.6 s) and subsequently fell to the activation level of the CS-. This activity modulation by motivational relevance over a long period of stimulus presentation possibly originated from TE regions within the ventral visual path, since that region is reported to have heavy interconnections with the amygdala (Amaral et al., 1992). The amygdala has been regarded as a key structure for Pavlovian fear conditioning (LeDoux, 1993; Shi & Davis, 2001) and has been given a central role in

mediating synaptic changes at the cortical level (McGaugh et al., 1996). It has been hypothesized that the TE region as a visual unimodal area (Pandya & Yeterian, 1985) not only receives input from the amygdala but is a source of highly processed visual input to the amygdala (Amaral et al., 1992). An enhanced stimulus processing of the CS+ within longer time windows (2.6 s) during CS+ depiction in the highly amygdaloid interconnected TE area could reflect the reciprocal information transfer between the two structures reflecting ongoing stimulus evaluation. Interestingly, stimulus driven activity amplification for the CS+ in right anterior temporal brain regions was observed only in subjects that decelerated their HR response selectively to the CS+ during extinction. As a highly speculative explanation one might argue that the visual amygdala-TE system of the subjects who showed a defense HR acceleration during learning trials selectively classified the CS+ as aversive during extinction. As a consequence, HR bradycardia could be maintained by the amygdala via permanent input from TE. In line with this notion, several studies have reliably shown that viewing aversive pictures triggers HR slowing (Bradley, Codispoti, Cuthbert, & Lang, 2001; Lang, Bradley, & Cuthbert, 1997; Moratti et al., 2004).

Long lasting right anterior temporal involvement in Pavlovian fear conditioning only emerged in subjects showing a pronounced HR deceleration to the CS+. Interestingly, Kuniecki et al. (Kuniecki, Coenen, & Kaiser, 2002) observed a correlation between HR deceleration and amygdala activity during extinction in an animal model. Although the time course of differential CS+/ CS- processing in right anterior temporal cortical sources fits the above mentioned explanation, the contribution of the amygdala and an interaction between anterior temporal activity and the amygdaloid complex cannot be proven since MEG recordings as used here most likely reflect the activation of cortical sources.

As seen in the whole group data, the amplitude enhancement in left parietal and left occipito-temporal brain regions during extinction was driven by the accelerators and did not emerge in the decelerator group. These effects could be caused by attentional processes reflected by the OR response to the CS+ and the amplitude amplification in left occipito-temporal and parietal regions towards the end of CS+ presentation when the US could be expected. There are several lines of argumentation that support this view.

First, the grand average of MNE solutions clearly showed a left lateralized topography of stimulus processing for both, the CS+ and CS-. The statistical map depicting activity modulation with respect to condition (CS+, CS-) and time (t1, t2, t3) in left occipito-temporal regions demonstrated that the motivational significant stimulus generated a greater amplitude in areas where the stimulus was processed. This observation is in line with results in the field

of attention research showing that attended visual stimuli produce greater SSVEPs than unattended (Morgan et al., 1996; Müller, Picton et al., 1998). Further, ERP studies have elucidated that attention can modulate activity in extrastriate and primary visual cortex (Di Russo, Martinez, & Hillyard, 2003; Hillyard & Anllo-Vento, 1998). Finally, studies in the area of emotion research showed that high arousing biologically significant stimuli generate greater neural responses in posterior areas (Junghöfer, Bradley, Elbert, & Lan, 2001; Keil et al., 2002). Thus, increased CS+ amplitude in left occipto-temporal regions may reflect attention modulated sensory processing of the CS+ in extrastriate cortex.

Second, parietal brain areas often have been associated with attentional processes (Corbetta, 1998; Le et al., 1998; Pardo et al., 1991; Rushworth et al., 2001). Although these processes have been linked to the right hemisphere, the left dominant processing of the stimuli could have caused the involvement of the left parietal cortex in the present study. An alternative explanation of left parietal involvement could be that this brain region has been associated with orientating attention to specific time moments (Coull, 2004). As the stimuli were presented for five seconds and the US was presented always at the end of stimulus presentation time, orienting in time could be of special relevance.

Third, the observed facilitated SSVEF for the CS+ in left parietal areas were observed towards the end of CS+ depiction when the US could be expected further supporting the involvement of attentional processes. As the time courses of activations in left occipto-temporal and left parietal areas were quite parallel, it can be assumed that attentional processes may tune feature processing in sensory areas reflecting a sensory gain mechanism as hypothesized by authors in the field of selective attention (Hillyard & Anllo-Vento, 1998).

Taken together, as the OR as indexed by HR deceleration reached its maximum towards the end of CS+ depiction, left parietal brain regions possibly mediating attentional processes come into play and may influence the sensory cortex by top down processes in order to facilitate stimulus analysis in extrastriate cortex. However, only three out of 17 subjects were aware of the contingency between the CS+ and the US, challenging the argumentation in favor of attentional processes as long as consciousness is regarded a necessary prerequisite to attention. However, Hamm and Vaitl (Hamm & Vaitl, 1996) argued that the fear network can be activated automatically and that overt knowledge of past stimulus relations is not necessary for the expression of fear responses to the CS+.

Contrary, the subgroup of HR decelerators did not show any differences in the time course of the stimulus driven SSVEF amplitude between the CS+ and CS- presentations paralleling the lack of a differential HR response during the extinction trials. However, the

greater amplitude during CS+ as compared to CS- depiction in left orbito-frontal regions observed in the whole group data in acquisition trials, originated from the decelerators. The amplification of the CS+ generated amplitude in left orbito-frontal cortical sources was present in the first time segment (0-1.3s) of stimulus depiction.

Orbito-frontal brain regions have recently been associated with emotion regulation in general (Davidson, Putnam, & Larson, 2000) and with reversal learning in particular that has been characterized as changing emotional behavior in response to a previously punished (or rewarded) stimulus (Rolls, 1999; Rolls, Hornak, Wade, & McGrath, 1994). Humans with higher left frontal baseline activity have been reported to be more successful in suppressing negative emotional states (Davidson et al., 2000). Recently, Ghashghaei and Barbas (Ghashghaei & Barbas, 2002) showed that the orbito-frontal cortex exercises inhibitory control onto the central nucleus of the amygdala. The subjects of our study who did not show an accelerative defense HR reaction generated more SSVEF activity in response to the CS+ than to the CS- at orbito-frontal cortical sources possibly reflecting a suppression of an autonomic fear response such as HR acceleration. Hamm and Vaitl (Hamm & Vaitl, 1996) demonstrated in a Pavlovian fear conditioning experiment that conditioned startle potentiation was stronger for cardiac accelerators than for decelerators further supporting that HR acceleration indicates learned fear and that HR decelerators do not acquire a fear/ defense response. Unfortunately, we have not recorded a startle response in our subjects since we have used a white noise as an US. But only the HR accelerators and not the decelerators showed a differential HR response during extinction partly paralleling the results of Hamm and Vaitl (Hamm & Vaitl, 1996). Altogether, increased activity in the orbito-frontal cortex may have suppressed the acquisition of a fear response as indexed by HR acceleration in the cardiac decelerator group.

Decelerators and accelerators did not differ in the pleasantness and aversiveness ratings of the US. Thus, differences in the subjective evaluation of the US could not account for the discriminative brain and HR responses of the two groups. Further, accelerators did not report higher levels of state/ trait anxiety and BDI depression scores than decelerators nor were there any gender differences between the two groups. The distribution of aware and unaware subjects was equal within the accelerators and decelerators, but there were only three subjects reporting a contingency awareness making it difficult to draw conclusions about the aware/ unaware issue on that aspect. Currently, the effects of awareness on the ratings of the US, HR and brain responses are tested in a follow-up study in our laboratory.

With respect of laterality, we observed significant changes in both cerebral hemispheres. In the literature no consistent findings with respect to lateralization of effects during conditioning have been reported (Cheng et al., 2003; Fischer et al., 2002; Fredrikson et al., 1995; Hugdahl, 1998; Hugdahl et al., 1995; Knight et al., 2004; LaBar, Gatenby, Gore, LeDoux, & Phelps, 1998). In the present study, accelerators showed a right anterior temporal activity modulation due to the CS+ during extinction. All other observed effects were rather left sided. As already mentioned above, there are several possibilities contributing to the lateralization effects. First, as illustrated in the topographical maps of the grand mean MNE solutions, condition effects were strong in areas with high signal. Thus, the left lateralization in left parietal and left occipto-temporal regions may be due to the grating perception per se. A similar relationship between topographical activity distributions and lateralization was observed in a study by Keil et al. (Keil et al., 2002), who suggested that motivated attention acts to amplify activity in cortical areas that are engaged in processing of specific features. These might be located on the left or right, depending on the channel and kind of information presented (i.e. verbal, pictorial etc.). Interestingly, LaBar and collaborators found left prefrontal activity modulations in favor of the CS+ during conditioning using geometrical patterns as CS (LaBar & Disterhoft, 1998). Possibly, the left orbito-frontal involvement in cardiac decelerators of the present study was also due to the utilization of geometrical patterns such as gratings. Contrary, Fisher et al. (Fischer et al., 2002) found right sided frontal activation during fear learning using pictures of snakes as CS. Fisher and collaborators explained the laterality difference to the LaBar et al. study with valence differences in stimulus material (snakes vs. geometric patterns). Taken together, laterality effects could be due to varying preferences of the hemispheres for various stimulus material rather than emotion specific functions. As we used gratings, left sided effects of enhanced CS+ processing may reflect facilitation in cortical networks analyzing the stimulus per se. Alternatively, left parietal differential activation during a delayed conditioning paradigm could also be attributed to attentional processes in time as the left parietal cortex has been associated with orientation in time (Coull, 2004). However, the observed amplitude amplification to the CS+ in anterior right temporal areas actually may be due to emotion specific functioning.

There are several limitations to our study. First, we modeled the origin of the SSVEF using a spherical head model and projected the solutions on a standard brain. This approach is less accurate than using a realistic head model instead of a shell. However, for the present

purpose of studying cortical regions on a macroscopic level, using a MNE technique that smoothes the solution, we considered a spherical head model as sufficient.

Second, as brain imaging studies involve high computational power our sample size was relatively small as compared to HR studies. We tried to circumvent the problem of a low number of subjects with respect to the HR data by utilizing linear mixed models that can more adequately model time series data such as HR change. Separating two responder groups also reduces sample size and power of the brain data. For instance, we did not observe the midcentral activation differences with respect to the CS+ and CS- in accelerators and decelerators as reported for the whole sample. This illustrates the problem that we might have missed brain areas of discriminative CS+/ CS- activations due to relatively small sample size and loss of statistical power.

Finally, we found support for our original hypothesis that motivationally relevant stimuli engage cortical networks that are involved in attentional processes such as the parietal cortex (Fernandez-Duque & Posner, 2001). We did not observe an engagement of a right fronto-parietal network as we would have predicted from previous work using affective pictures (Moratti et al., 2004). Instead, left parietal cortex was more active during CS+ than CS- depiction. Amplification of SSVEF amplitude in left extrastriate cortex by the CS+ and the parallel time course of that difference with the one observed for parietal sources indicated that top-down processes facilitated the processing of a motivationally significant stimulus in sensory areas reflecting a sensory gating mechanism (Hillyard & Anllo-Vento, 1998). These results were restricted to subjects that showed a fear response in acquisition trials and were paralleled by an OR response during extinction. Subjects that did not accelerate their HR to the CS+ during acquisition responded with greater orbito-frontal brain activity during learning possibly reflecting a fear reaction suppression process. Future experiments may try to further elucidate the underlying mechanism that separates cardiac accelerators and decelerators at several response levels such as verbal evaluation and startle potentiation (Hamm & Vaitl, 1996; Hodes et al., 1985). Our work added evidence of different response patterns at the cortical level with respect to cardiac accelerators and decelerators.

SUMMARY

In the present study we examined stimulus driven neuromagnetic activity in a delayed Pavlovian aversive conditioning paradigm using steady state visual evoked fields (SSVEF). For the whole sample left orbito-frontal cortical sources responded stronger to the reinforced than to the nonreinforced conditioned stimulus (CS+ and CS-, respectively) during early stimulus presentation time in acquisition blocks. In extinction trials midcentral sources generated a greater SSVEF during CS+ as compared to CS- depiction. In late time intervals the CS+ elicited a stronger neuromagnetic response than the CS- in extrastriate and parietal cortex during extinction. However, only subjects showing an accelerative heart rate (HR) response to the CS+ during learning trials exhibited an increased activation in sensory and parietal cortex due to CS+ depiction in the extinction block. Additionally, HR accelerators generated an enhanced neuromagnetic response in right temporal brain regions during CS+ presentation. However, they did not show any differential cortical activation patterns during acquisition. In contrast, subjects slowing their HR in response to the CS+ during learning showed greater activity in left orbito-frontal brain regions in the acquisition block but did not show differential SSVEF patterns during extinction. The results suggests that HR accelerators and decelerators differ in their cortical responses and provide evidence for a role of the neocortex in delayed Pavlovian conditioning.

REFERENCES

Aggleton, J. P., Burton, M. J., & Passingham, R. E. (1980). Cortical and subcortical afferents to the amygdala of the rhesus monkey (Macaca mulatta). *Brain Res, 190*(2), 347-368.

Amaral, D. G. (1986). Amygdalohippocampal and amygdalocortical projections in the primate brain. *Adv Exp Med Biol, 203*, 3-17.

Amaral, D. G., Price, J. L., Pitkaenen, A., & Carmichael, S. T. (1992). Anatomical organization of the primate amygdaloid complex. In J. P. Aggleton (Ed.), *The amygdala: Neurobiological aspects of emotion, memory, and mental dysfunction.* (pp. 1-66). New York: Wiley-Liss.

Bagiella, E., Sloan, R. P., & Heitjan, D. F. (2000). Mixed-effects models in psychophysiology. *Psychophysiology, 37*(1), 13-20.

Benjamini, Y., & Hochberg, Y. (1995). Controlling the false discovery rate: a practical and powerful approach to multiple testing. *J Roy Stat Soc B STA, 57*, 289-300.

Berg, P., & Scherg, M. (1994). A multiple source approach to the correction of eye artifacts. *Electroencephalogr Clin Neurophysiol, 90*(3), 229-241.

Bertero, M., De Mol, C., & Pike, E. R. (1988). Linear inverse problems with discrete data: II. Stability and regularization. *Inverse Problems, 4*, 573-594.

Bradley, M. M., Codispoti, M., Cuthbert, B. N., & Lang, P. J. (2001). Emotion and Motivation I: Defensive and Appetitive Reactions in Picture Processing. *Emotion, 1*(3), 276-298.

Buchel, C., & Dolan, R. J. (2000). Classical fear conditioning in functional neuroimaging. *Curr Opin Neurobiol, 10*(2), 219-223.

Buchel, C., Morris, J., Dolan, R. J., & Friston, K. J. (1998). Brain systems mediating aversive conditioning: an event-related fMRI study. *Neuron, 20*(5), 947-957.

Cheng, D. T., Knight, D. C., Smith, C. N., Stein, E. A., & Helmstetter, F. J. (2003). Functional MRI of human amygdala activity during Pavlovian fear conditioning: stimulus processing versus response expression. *Behav Neurosci, 117*(1), 3-10.

Corbetta, M. (1998). Frontoparietal cortical networks for directing attention and the eye to visual locations: identical, independent, or overlapping neural systems? *Proc Natl Acad Sci U S A, 95*(3), 831-838.

Coull, J. T. (2004). fMRI studies of temporal attention: allocating attention within, or towards, time. *Brain Res Cogn Brain Res, 21*(2), 216-226.

Davidson, R. J., Putnam, K. M., & Larson, C. L. (2000). Dysfunction in the neural circuitry of emotion regulation--a possible prelude to violence. *Science, 289*(5479), 591-594.

Di Russo, F., Martinez, A., & Hillyard, S. A. (2003). Source analysis of event-related cortical activity during visuo-spatial attention. *Cereb Cortex, 13*(5), 486-499.

Fanselow, M. S. (1994). Neural organization of the defensive behavior system responsible for fear. *Psychon Bull Rev, 1*, 429-438.

Fernandez-Duque, D., & Posner, M. I. (2001). Brain imaging of attentional networks in normal and pathological states. *J Clin Exp Neuropsychol, 23*(1), 74-93.

Fischer, H., Andersson, J. L., Furmark, T., Wik, G., & Fredrikson, M. (2002). Right-sided human prefrontal brain activation during acquisition of conditioned fear. *Emotion, 2*(3), 233-241.

Flor, H., Birbaumer, N., Roberts, L. E., Feige, B., Lutzenberger, W., Hermann, C., & Kopp, B. (1996). Slow potentials, event-related potentials, "gamma-band" activity, and motor responses during aversive conditioning in humans. *Exp Brain Res, 112*(2), 298-312.

Fredrikson, M., Wik, G., Fischer, H., & Andersson, J. (1995). Affective and attentive neural networks in humans: a PET study of Pavlovian conditioning. *Neuroreport, 7*(1), 97-101.

Furmark, T., Fischer, H., Wik, G., Larsson, M., & Fredrikson, M. (1997). The amygdala and individual differences in human fear conditioning. *Neuroreport, 8*(18), 3957-3960.

Ghashghaei, H. T., & Barbas, H. (2002). Pathways for emotion: interactions of prefrontal and anterior temporal pathways in the amygdala of the rhesus monkey. *Neuroscience, 115*(4), 1261-1279.

Grave de Peralta Menendez, R., Hauk, O., Gonzalez Andino, S., Vogt, H., & Michel, C. (1997). Linear inverse solutions with optimal resolution kernels applied to electomagnetic tomography. *Hum Brain Mapp, 5*, 454-467.

Gray, M., Kemp, A. H., Silberstein, R. B., & Nathan, P. J. (2003). Cortical neurophysiology of anticipatory anxiety: an investigation utilizing steady state probe topography (SSPT). *Neuroimage, 20*(2), 975-986.

Hamalainen, M. S., & Ilmoniemi, R. J. (1994). Interpreting magnetic fields of the brain: minimum norm estimates. *Med Biol Eng Comput, 32*(1), 35-42.

Hamm, A. O., & Vaitl, D. (1996). Affective learning: awareness and aversion. *Psychophysiology, 33*(6), 698-710.

Hansen, P. C., & O'Leary, D. P. (1993). The use of the L-curve in the regularization of discrete ill-posed problems. *SIAM J. Sci. Comput., 14*, 1487-1503.

Hare, R. D. (1972). Cardiovascular components of orienting and defensive responses. *Psychophysiology, 9*(6), 606-614.

Hauk, O., Berg, P., Wienbruch, C., Rockstroh, B., & Elbert, T. (1998). *The minimum norm method as an effective mapping tool for MEG analysis.* Paper presented at the Biomag98, Sendai, Japan.

Hauk, O., Keil, A., Elbert, T., & Müller, M. M. (2002). Comparison of data transformation procedures to enhance topographical accuracy in time series analysis of the human EEG. *J Neurosci Meth, 113*(2), 111-122.

Hautzinger, M., Bailer, M., Worall, H., & Keller, F. (1992). *Beck - Depressions-Inventar*. Bern: Huber.

Hillyard, S. A., & Anllo-Vento, L. (1998). Event-related brain potentials in the study of visual selective attention. *Proc Natl Acad Sci U S A, 95*(3), 781-787.

Hodes, R. L., Cook, E. W., 3rd, & Lang, P. J. (1985). Individual differences in autonomic response: conditioned association or conditioned fear? *Psychophysiology, 22*(5), 545-560.

Hugdahl, K. (1998). Cortical control of human classical conditioning: autonomic and positron emission tomography data. *Psychophysiology, 35*(2), 170-178.

Hugdahl, K., Berardi, A., Thompson, W. L., Kosslyn, S. M., Macy, R., Baker, D. P., Alpert, N. M., & LeDoux, J. E. (1995). Brain mechanisms in human classical conditioning: a PET blood flow study. *Neuroreport, 6*(13), 1723-1728.

Jensen, O., & Vanni, S. (2002). A new method to identify multiple sources of oscillatory activity from magnetoencephalographic data. *Neuroimage, 15*(3), 568-574.

Junghöfer, M., Bradley, M. M., Elbert, T. R., & Lan, P. J. (2001). Fleeting images: a new look at early emotion discrimination. *Psychophysiology, 38*(2), 175-178.

Junghöfer, M., & Peyk, P. (2004). Analyse und Visualisierung von Hirnstrom- und Hirnmagnetfeld-Messungen. *MATLAB select, 2*, 24-28.

Keil, A., Bradley, M. M., Hauk, O., Rockstroh, B., Elbert, T., & Lang, P. J. (2002). Large-scale neural correlates of affective picture processing. *Psychophysiology, 39*(5), 641-649.

Keil, A., Moratti, S., Sabatinelli, D., Bradley, M. M., & Lang, P. J. (2004). Additive Effects of Emotional Content and Spatial Selective Attention on Electrocortical Facilitation. *Cereb Cortex*.

Keselman, H. J., Cribbie, R., & Holland, B. (2002). Controlling the rate of Type I error over a large set of statistical tests. *Br J Math Stat Psychol, 55*(Pt 1), 27-39.

Knight, D. C., Cheng, D. T., Smith, C. N., Stein, E. A., & Helmstetter, F. J. (2004). Neural substrates mediating human delay and trace fear conditioning. *J Neurosci, 24*(1), 218-228.

Kuniecki, M., Coenen, A. M., & Kaiser, J. (2002). Correlation between long latency evoked potentials from amygdala and evoked cardiac response to fear conditioned stimulus in rats. *Acta Neurobiol Exp (Wars), 62*(2), 85-92.

LaBar, K. S., & Disterhoft, J. F. (1998). Conditioning, awareness, and the hippocampus. *Hippocampus, 8*(6), 620-626.

LaBar, K. S., Gatenby, J. C., Gore, J. C., LeDoux, J. E., & Phelps, E. A. (1998). Human amygdala activation during conditioned fear acquisition and extinction: a mixed-trial fMRI study. *Neuron, 20*(5), 937-945.

Lang, P. J., Bradley, M. M., & Cuthbert, B. N. (1997). Motivated Attention: Affect, Activation, and Action. In P. J. Lang & R. F. Simons & M. T. Balaban (Eds.), *Attention and Orienting: Sensory and Motivational Processes* (pp. 97-135). Hillsdale, N.J.: Lawrence Erlbaum Associates.

Laux, L., Glanzmann, P., Schaffner, P., & Spielberger, C. D. (1981). *Das State-Trait-Angstinventar*. Weinheim: Beltz.

Le, T. H., Pardo, J. V., & Hu, X. (1998). 4 T-fMRI study of nonspatial shifting of selective attention: cerebellar and parietal contributions. *J Neurophysiol, 79*(3), 1535-1548.

LeDoux, J. E. (1993). Emotional networks in the brain. In J. M. H. Michael Lewis (Ed.), *Handbook of emotions.* (pp. 109-118): Guilford Press, New York, NY, US.

Mackintosh, N. J. (2003). Pavlov and associationism. *Span J Psychol, 6*(2), 177-184.

Maren, S. (2001). Neurobiology of Pavlovian fear conditioning. *Annu Rev Neurosci, 24*, 897-931.

McGaugh, J. L., Cahill, L., & Roozendaal, B. (1996). Involvement of the amygdala in memory storage: interaction with other brain systems. *Proc Natl Acad Sci U S A, 93*(24), 13508-13514.

Moratti, S., Keil, A., & Stolarova, M. (2004). Motivated attention in emotional picture processing is reflected by activity modulation in cortical attention networks. *Neuroimage, 21*(3), 954-964.

Morgan, S. T., Hansen, J. C., & Hillyard, S. A. (1996). Selective attention to stimulus location modulates the steady-state visual evoked potential. *Proc Natl Acad Sci U S A, 93*(10), 4770-4774.

Mufson, E. J., Mesulam, M. M., & Pandya, D. N. (1981). Insular interconnections with the amygdala in the rhesus monkey. *Neuroscience, 6*(7), 1231-1248.

Müller, M. M., Picton, T. W., Valdes-Sosa, P., Riera, J., Teder-Salejarvi, W. A., & Hillyard, S. A. (1998). Effects of spatial selective attention on the steady-state visual evoked potential in the 20-28 Hz range. *Brain Res Cogn Brain Res, 6*(4), 249-261.

Müller, M. M., Teder-Salejarvi, W., & Hillyard, S. A. (1998). The time course of cortical facilitation during cued shifts of spatial attention. *Nat Neurosci, 1*(7), 631-634.

Oldfield, R. C. (1971). The assessment and analysis of handedness: The Edinbourgh Inventory. *Neuropsychologia, 9*, 97-113.

Pandya, D. N., & Yeterian, E. H. (1985). Architecture and connections of cortical association areas. In A. Peters & E. G. Jones (Eds.), *Cerebral Cortex* (Vol. 4, pp. 3-55). New York: Plenum Press.

Pardo, J. V., Fox, P. T., & Raichle, M. E. (1991). Localization of a human system for sustained attention by positron emission tomography. *Nature, 349*(6304), 61-64.

Pavlov, I. P. (1927). *Conditioned Reflexes: An Investigation of the Physiological Activity of the Cerebral Cortex*. London: Oxford University Press.

Pearce, J. M., & Hall, G. (1980). A model for Pavlovian learning: variations in the effectiveness of conditioned but not of unconditioned stimuli. *Psychol Rev, 87*(6), 532-552.

Perlstein, W. M., Cole, M. A., Larson, M., Kelly, K., Seignourel, P., & Keil, A. (2003). Steady-state visual evoked potentials reveal frontally-mediated working memory activity in humans. *Neurosci Lett, 342*(3), 191-195.

Picton, T. W., Vajsar, J., Rodriguez, R., & Campbell, K. B. (1987). Reliability estimates for steady-state evoked potentials. *Electroencephalogr Clin Neurophysiol, 68*(2), 119-131.

Pinheiro, J. C., & Bates, D. M. (2000). *Mixed-Effects Models in S and S-PLUS* (1 ed.). New York, Berlin, Heidelberg: Springer.

Plourde, G., & Picton, T. W. (1990). Human auditory steady-state response during general anesthesia. *Anesth Analg, 71*(5), 460-468.

Porrino, L. J., Crane, A. M., & Goldman-Rakic, P. S. (1981). Direct and indirect pathways from the amygdala to the frontal lobe in rhesus monkeys. *J Comp Neurol, 198*(1), 121-136.

R Developer Core Team. (2004). R: A language and environment for statistical computing. R Foundation for Statistical Computing. Vienna, Austria: R Foundation for Statistical Computing. http://www.r-project.org/.

Regan, D. (1989). *Human Brain Electrophysiology: Evoked Potentials and Evoked Magnetic Fields in Science and Medicine*. New York: Elsevier.

Regan, M., & Howard, R. (1995). Fear conditioning, preparedness, and the contingent negative variation. *Psychophysiology, 32*(3), 208-214.

Rescorla, R. A. (1988). Pavlovian conditioning. It's not what you think it is. *Am Psychol, 43*(3), 151-160.

Rockstroh, B., Elbert, T., Canavan, A., Lutzenberger, W., & Birbaumer, N. (1989). *Slow Cortical Potentials and Behavior* (2nd ed.). Baltimore, Munich, Vienna: Urban & Schwarzenberg.

Rockstroh, B., Muller, M., Wagner, M., Cohen, R., & Elbert, T. (1993). "Probing" the nature of the CNV. *Electroencephalogr Clin Neurophysiol, 87*(4), 235-241.

Rohrbaugh, J. W., McCallum, W. C., Gaillard, A. W., Simons, R. F., Birbaumer, N., & Papakostopoulos, D. (1986). ERPs associated with preparatory and movement-related processes. A review. *Electroencephalogr Clin Neurophysiol Suppl, 38*, 189-229.

Rolls, E. T. (1999). *The Brain and Emotion*. Oxford: Oxford University Press.

Rolls, E. T., Hornak, J., Wade, D., & McGrath, J. (1994). Emotion-related learning in patients with social and emotional changes associated with frontal lobe damage. *J Neurol Neurosurg Psychiatry, 57*(12), 1518-1524.

Rushworth, M. F., Paus, T., & Sipila, P. K. (2001). Attention systems and the organization of the human parietal cortex. *J Neurosci, 21*(14), 5262-5271.

Searle, S. R., Casella, G., & McCulloch, C. E. (1992). *Variance Components*. New York: Wiley.

Shi, C., & Davis, M. (2001). Visual pathways involved in fear conditioning measured with fear-potentiated startle: behavioral and anatomic studies. *J Neurosci, 21*(24), 9844-9855.

Silberstein, R. B., Nunez, P. L., Pipingas, A., Harris, P., & Danieli, F. (2001). Steady state visually evoked potential (SSVEP) topography in a graded working memory task. *Int J Psychophysiol, 42*(2), 219-232.

Silberstein, R. B., Schier, M. A., Pipingas, A., Ciorciari, J., Wood, S. R., & Simpson, D. G. (1990). Steady-state visually evoked potential topography associated with a visual vigilance task. *Brain Topogr, 3*(2), 337-347.

Uusitalo, M. A., & Ilmoniemi, R. J. (1997). Signal-space projection method for separating MEG or EEG into components. *Med Biol Eng Comput, 35*(2), 135-140.

Wilson, R. S. (1974). CARDIVAR: the statistical analysis of heart rate data. *Psychophysiology, 11*(1), 76-85.

Chapter 5

Cortical Activation during Pavlovian Fear Conditioning in fully Aware Subjects depends on Heart Rate Response Patterns: An MEG Study.

INTRODUCTION

Pavlovian conditioning as a laboratory model of the ability to predict aversive events in order to ensure the survival of the organism represents a simple form of associative learning. Two forms of conditioning have been investigated intensively, eye blink conditioning and autonomic fear conditioning (Fanselow & Poulos, 2004). As both conditioning paradigms are considered to establish associative processes, there has been an ongoing debate if these processes depend on declarative or implicit memory systems and consequently if awareness of stimulus contingencies is necessary for Pavlovian conditioning (Lovibond & Shanks, 2002; Manns, Clark, & Squire, 2002; Shanks & Lovibond, 2002; Wiens & Ohman, 2002).

Basically, two forms of Pavlovian conditioning paradigms with respect to the timing of the stimulus contingencies have been investigated. In both, delay and trace conditioning the conditioned stimulus (CS) precedes the unconditioned stimulus (US). However, in delay conditioning procedures the US overlaps and coterminates with the US, whereas in trace conditioning paradigms the US is delivered after some time interval between CS offset and US onset (usually more than 500 ms). In eye blink conditioning differences between these two kind of contingencies have been investigated with respect of the role of awareness of the stimulus contingencies for the expression of a conditioned response (CR).

Findings in animal models of delay eye blink conditioning demonstrated that an intact cerebellum and brainstem is necessary and sufficient for normal retention of eye blink conditioning. Decerebrated animals without forebrain structures (including the hippocampus) were not impaired in delayed eye blink conditioning (Mauk & Thompson, 1987). Like delay conditioning, trace conditioning also requires an intact cerebellum (Woodruff-Pak, Lavond, & Thompson, 1985) but was heavily disturbed by the removal of forebrain structures and the hippocampus (Kim, Clark, & Thompson, 1995; Kronforst-Collins & Disterhoft, 1998). Findings in humans have been consistent in as much that delay conditioning was disturbed in

patients with cerebellar and brainstem lesions. Contrary, patients with hippocampal lesions but intact cerebellum performed normally in delay eye blink conditioning but were disturbed in trace conditioning (Gabrieli et al., 1995; McGlinchey-Berroth, Carrillo, Gabrieli, Brawn, & Disterhoft, 1997).

Research in healthy normal subjects investigated the role of declarative and implicit memory systems in delay and trace eye blink conditioning using the logic that if declarative memory is necessary for the formation of an association between the CS and US, the expression of a CR is dependent of awareness of the stimulus contingencies. In delay conditioning it has been reported that CR expression is independent of contingency awareness, whereas in trace conditioning expression of the CR was closely related to awareness (Clark, Manns, & Squire, 2001; Manns, Clark, & Squire, 2001; Manns, Clark, & Squire, 2000; Manns et al., 2002). Thus, Clark, Manns and Squire (Clark, Manns, & Squire, 2002) concluded that delay conditioning solely depends on implicit memory systems, whereas trace conditioning also requires declarative memory systems paralleling findings in animal work and results of patient studies. However, Lovibond and Shanks (Lovibond & Shanks, 2002) opposed this view, citing negative reports (Knuttinen, Power, Preston, & Disterhoft, 2001) and claiming that awareness measures used by the above mentioned studies possibly underestimated the level of awareness of the subjects.

A similar debate has been fought about autonomic Pavlovian fear conditioning. In autonomic fear conditioning fear relevant CSs like spiders, snakes or angry faces have been used to study the role of conscious knowledge of the stimulus contingencies for the expression of the CR. For example, Esteves and collaborators (Esteves, Parra, Dimberg, & Ohman, 1994) used the technique of backward masking angry faces that represented the reinforced CS (CS+) by an electric shock during acquisition. This method prevented the conscious perception of the CS+ and the relationship with the US. Nevertheless, subjects exhibited an increased skin conductance response (SCR) to the CS+ during unmasked presentation of the CS+ in extinction trials. Thus, the authors concluded that unconscious Pavlovian fear conditioning is possible. Morris, Öhman and Dolan (Morris, Ohman, & Dolan, 1998) demonstrated that masked conditioned angry faces can activate the amygdala, a structure known to be important for emotional responding (Adolphs, Tranel, Damasio, & Damasio, 1995; Calder et al., 1996) and especially for fear conditioning (LeDoux, 2000). As the amygdala receives afferents from sensory thalamus, fast evaluation of aversive stimuli without complex computations of the cortex is possible (LeDoux, 1993; Shi & Davis, 2001).

Thus, subcortical pathways may be the neuroanatomical basis of Pavlovian fear conditioning in the absence of awareness.

Lovibond and Shanks (Lovibond & Shanks, 2002) criticized the technique of backward masking by assuming that subjects may have used some features of the complex visual stimuli for discrimination of the CS+ and CS-. However, in a recent study a bilaterally cortical blind patient showed substantially startle potentiation to a CS+ although primary sensory cortex was structurally and functionally absent ruling out the possibility that some features could have been used for discrimination (Hamm et al., 2003). Knight and collaborators (Knight, Nguyen, & Bandettini, 2003) circumvented the technique of backward masking by presenting tones below and above the perceptual threshold as CS+ and observed differential SCRs in perceived and unperceived trials. Finally, Wiens, Katkin and Öhman (Wiens, Katkin, & Ohman, 2003) demonstrated that unconscious differential SCRs to the CS+ and CS- are rather an effect of trial order than residual feature perception in masked Pavlovian fear conditioning experiments since they observed conditioning only if trials were presented pseudo- and not completely randomly. Thus, it is possible that in prior studies using masked stimuli trial order could have resulted in conditioning. Nevertheless, subjects reporting unawareness of the trial order contingency in the pseudo random condition of the Wiens et al. study (Wiens et al., 2003) expressed differential SCRs.

In sum, subcortical pathways potentially may mediate unconscious autonomic fear conditioning relating it to implicit memory processes. In a previous study of our laboratory (see chapter 4), we investigated the steady state visual evoked field (SSVEF) measured by magnetencephalography in a discriminative delayed Pavlovian fear conditioning paradigm. The SSVEF is elicited by visual stimuli that are luminance modulated at a certain frequency. The resulting brain response is oscillatory in nature, having the same fundamental frequency as the driving stimulus (Regan, 1989). A conceptual advantage is that widely distributed functional networks oscillating coherently at the driving stimulus frequency can be examined at high temporal resolution and signal-to-noise ratios. (Perlstein et al., 2003; Silberstein, Nunez, Pipingas, Harris, & Danieli, 2001).

In our previous study (see chapter 4) we found increased SSVEF amplitude during presentation of the CS+ in sensory and parietal areas responsible for stimulus processing in extinction trials. This effect was driven by subjects showing an accelerative heart rate (HR) response during acquisition and a differential orientation response (OR) indexed by HR deceleration to the CS+ during extinction. Participants who decelerated their HR to the CS+ during acquisition did not depict any differential HR and stimulus driven brain response

during extinction. Accelerators and decelerators possibly learned different things during aversive conditioning. Hodes et al. (Hodes, Cook, & Lang, 1985) hypothesized that accelerators acquire a fear response (fear character of the CS+) whereas decelerators just learn that two events are related in time (signal character of the CS+). Indeed, Hamm and Vaitl (Hamm & Vaitl, 1996) completed this picture by reporting that only HR accelerators exhibited a potentiated startle response to the CS+ whereas decelerators did not.

Interestingly, only three out of 18 subjects in our previous study could report the CS-US contingency after the experiment implying that most participants were unaware. Thus, we concluded that the CS+ can trigger a defense response during acquisition and an OR during extinction involving sensory and attentional brain circuits as observed in experiments using emotional pictures (Junghöfer, Bradley, Elbert, & Lan, 2001; Keil et al., 2002; Moratti, Keil, & Stolarova, 2004). Obviously, these processes can be elicited in subjects without the ability to report the stimulus contingency.

In the present study, we wanted to investigate the neuromagnetic response using exactly the same experimental paradigm as in our previous study except that we manipulated the instruction. Subjects were told that during acquisition one of two gratings will be paired with an aversive noise in order to establish full awareness of stimulus contingencies in all participants (in the previous study subjects were not informed about stimulus contingencies).

As prior steady state visual evoked potentials (SSVEP, the counterpart of the SSVEF in EEG research) studies in the field of attention research showed that attended stimuli produce a greater SSVEP amplitude compared with unattended stimuli (Morgan, Hansen, & Hillyard, 1996; Müller, Gruber, & Keil, 2000; Muller & Hubner, 2002) we hypothesized that this time the neuromagnetic cortical response in sensory and attentional brain circuits should be increased for the CS+ during acquisition rather extinction trials. Further, we expected that the proportion of HR decelerators exhibiting an OR to the CS+ is greater than that of HR accelerators showing a fear response during acquisition as for fully aware subjects the conditioning procedure should gain a signal rather than a fear character. Hamm and Vaitl (Hamm & Vaitl, 1996) pointed out the importance of distinguishing between orienting and fear processes during conditioning procedures (see also above). In the present study we expected that in subjects fully aware of the CS-US association orienting responses should dominate over fear reactions as indexed by HR patterns representing ORs and enhanced SSVEF amplitude in sensory and attentive brain networks during and not after acquisition.

METHODS

Participants

Twenty one subjects (10 females, 11 males) took part in the study after having given written consent. Two of the 21 participants were left handed, whereas the remaining subjects were right handed (Oldfield, 1971). The mean age of the sample was 25.6 years (range: 19-55 years). They had normal or corrected to normal vision and no family history of photic epilepsy. All subjects except one did not report any history of psychotherapy and none of the participants did report a recent critical live event. The subject that had consulted a psychotherapist did score within in the normal range in both the German version of the state-trait anxiety inventory (STAI) (Laux, Glanzmann, Schaffner, & Spielberger, 1981) and the German version of the Beck depression inventory (BDI) (Hautzinger, Bailer, Worall, & Keller, 1992) (state anxiety: 32; trait anxiety: 27; BDI: 0). Further, this subject did not claim about any symptoms at the time of recording.

Overall, the whole sample reported a mean state anxiety score of 33 (± 1.8), a mean trait anxiety score of 35 (± 1.7) and a mean BDI score of 3.5 (± 1.0) whereas state STAI, trait STAI and BDI of one subject was missing because of language problems (one subject was of Egypt nationality, the remaining participants were Germans). The BDI score of one additional participant was missing because of data loss. Due to equipment malfunction we lost HR data of one subject. Therefore, HR data of 20 subjects will be reported. The MEG data of all 21 participants will be presented but MEG data separated according to different HR response patterns (see below) will only contain the 20 subjects the HR data was available for.

Stimuli

The stimuli were exactly the same as in the previous conditioning study (see chapter 4) but in order to give a complete picture about the experimental setting we will report the stimuli of the current study, again. Two gray shaded 45° gratings perpendicular oriented to each other served as conditioned stimuli (CS). Utilizing a video projector (JVC™, DLA-G11E) and a mirror system, the CS were projected on a screen in the magnetically shielded room in random order, subtending a visual angle of 8° both horizontally and vertically. A red fixation cross was shown in the middle of the screen and was present throughout the whole experiment. In each trial, a grating was shown in a luminance modulated mode of 12.5Hz for a time period of 5000ms resulting in 63 on/ off cycles, the grating being shown for 40ms, followed by 40ms black screen during each cycle. During the intertrial interval, which varied randomly between 6 and 8 seconds, a black screen was shown. The luminance modulation

was done in order to generate visual evoked steady state fields that can be recorded with MEG.

One of the two gratings served as the CS+ or CS-, counterbalanced across subjects. Using an air tube system attached to a sound amplifier (BTi ® ASG, 1996), the unconditioned stimulus (US) consisting of a 110dB white noise with instantaneous onset was presented binaurally for one second during the last second of CS+ depiction, and terminated together with CS+ offset. In 15% of the trials (see below), the red fixation cross turned from blue into red color for 500 ms either 1000, 2500 or 4000 ms after CS+ and CS- onset, each time lag being equally probable.

Procedure

The procedure of the current experiment was exactly the same as in the prior conditioning study (see chapter 4) except that the introduction was changed in order to induce awareness of CS-US contingency. After having been familiarized with the MEG chamber in which the recording took place, subjects were instructed that in the first block of the experiment they will be shown different patterns and they were asked to press a response button as fast as possible whenever the red cross during pattern depiction changed to blue. Further, they were told that during the first block no loud noise will be delivered. Finally, participants knew that the second part of the experiment started after a short break and that during that part of the experiment the task would be repeated, while a certain pattern would *predict* the presentation of a very loud noise. Subjects were requested to identify that pattern and they were told that after the experiment they would have to recognize it for the experimentator. After the instruction, participants gave written consent and completed the handedness questionnaire, the screening questions, the STAI and the BDI. Thereafter, subjects were prepared for the recordings.

For artifact control, four electrodes for the electrooculogram (EOG) were attached, two at the left and right outer canthi and two above and below the right eye. Additionally, two electrodes for the electrocardiogram (ECG) were placed at the left lower costal arch and the right collarbone. Participants were then seated in the MEG chamber, their head shapes were digitized, and index points (left and right periauricular points, nasion, a pseudo-vertex and a pseudo inion point at the forehead) were determined to calculate the relative head position within the MEG helmet for source analysis. Finally, they were positioned under the MEG sensors and a projection screen was placed in front of them.

The experimental session started with a written instruction on the screen in the MEG chamber explaining again the task and ensuring subjects that no loud noise will be delivered during the first block, which served as a habituation phase. The habituation block consisted of twenty CS+, twenty CS- and six target trials which requested a button press after the red cross had turned into blue. The stimuli were depicted without pairing of the CS+ with the US. Thereafter, a short break of one minute was taken and subjects were instructed via text depicted on the screen, that during the next block a *certain* pattern will predict a loud noise. In the prior conditioning study (see chapter 4) they had been informed solely that a loud noise will be presented from time to time. After the break, the acquisition block began, that was identical to the habituation block, except that the CS+ was always paired with the US. The extinction phase started without a break after the acquisition trials, containing the same number of trials as the individual blocks before. The CS+ and CS- were never paired with the US during extinction. After the experiment, participants were shown the patterns that served as CS+ and CS- and had to identify the pattern that predicted the loud noise. If subjects correctly recognized the stimulus associated with the US during acquisition they were scored as aware, otherwise as unaware. Finally, participants rated pleasantness/ unpleasantness and the level of arousal on a 10 cm analog scale each, whereas a greater distance from the left starting point of the analog scale represented a higher level of unpleasantness and arousal, respectively . Subjects were paid 15 € (approximately 15 US dollars) for participation.

Data acquisition and preprocessing

The MEG was recorded continuously, and digitized at a rate of 254.3Hz, using a 148-channel whole head system (MAGNES™ 2500 WH, 4D Neuroimage, San Diego, USA). A bandpass filter of 0.1 – 50Hz was applied on line. The EOG and ECG acquisition was done with a Synamps amplifier (NEUROSCAN™) using Ag/ Cl electrodes. As the EOG and ECG recordings were coupled with the MEG acquisition, the same sampling rate and bandpass filter were applied to them.

SSVEFs were derived for each condition (CS+ and CS-) and every experimental block (habituation, acquisition, extinction) by averaging the MEG data over 4000 ms subtracting a 500 ms pre-stimulus baseline. The last 1000 ms of CS presentations were omitted because during CS+ trials in the acquisition block a loud noise as US was presented and startling of the subjects caused movement artifacts. The target trials (subjects were requested to press a button) were not submitted to further analysis. Eye artifacts were corrected using the

algorithm implemented in BESA™ software (Berg & Scherg, 1994). Additionally, all data was inspected visually for movement artifacts.

A subspace projection (Uusitalo & Ilmoniemi, 1997) of the eye artifact topography was applied on the SSVEFs for each condition (CS+ and CS-) and each experimental block (habituation, acquisition and extinction) in order to account for topography distortions using the eye correction algorithm (see below). Thereafter, the SSVEFs were complex demodulated (Regan, 1989) at the stimulation frequency of 12.5Hz in order to obtain stimulus driven amplitudes for the sine and cosine parts of the demodulated SSVEFs over time.

As with the MEG data, only the first 4000 ms of HR change during stimulus presentation were analyzed. Target trials were not submitted to analysis. HR change waveforms during presentations of the CS+ and CS- in the acquisition and extinction block (habituation block was not analyzed) were obtained using in-house-software written in MATLAB™. The algorithm of the software estimated the HR change over 4000 ms stimulus presentation in 500 ms steps using a 2000 ms pre-stimulus baseline. The frequency of the occurrence of an R-wave was derived from the interbeat-interval and weighted according to the distance from a 500 ms step within the time vector. The HR change was transformed in beats per minutes (bpm). The resulting HR waveforms consisted of changes in bpm compared to pre-stimulus baseline for nine consecutive time bins (0ms to 4000 ms in 500 ms steps).

Source analysis

In order to estimate the cortical sources of the complex demodulated SSVEFs a minimum norm estimation (MNE) technique was applied (Hamalainen & Ilmoniemi, 1994). The MNE procedure utilized in the present study was described in more detail in a recent study by Moratti and collaborators (Moratti et al., 2004) and in the prior conditioning study (see chapter 4).Therefore, only essential specifications of this widely used source estimation approach will be reported here.

For the computation of the lead-field matrix **A,** we used the algorithm suggested by Hauk et al. (Hauk, Keil, Elbert, & Müller, 2002). To this end, **A** was calculated for each participant, based on information on the center of a fitted sphere to the digitized head shape, and the positions of the MEG sensors relative to the head. A subspace projection (Uusitalo & Ilmoniemi, 1997) of the eye artifact topography was applied to the lead-field matrix **A** in order to account for topographical distortions caused by the eye artifact correction (see above). A spherical shell with evenly distributed 350 dipole locations served as source space. The radius of the shell was 80% of the radius of the fitted sphere. According to Hauk et al.

(Hauk et al., 2002) this radius was considered as a good approximation of the location of cortical sources.

As the MNE estimation technique is a over parameterized linear system, we used the Tikhonov-Phillips regularization in order to obtain stable solutions (Bertero, De Mol, & Pike, 1988). For the derivation of the regularization parameter λ, the L-curve method was used (Hansen & O'Leary, 1993). As the phase information of the measured MEG signal is crucial for the computation of the MNE and is lacking in a complex demodulated signal, the MNE was estimated for the sine and cosine parts of the 12.5Hz complex demodulated SSVEFs separately for every condition (CS+ and CS-), experimental block (habituation, acquisition and extinction) and for each subject. This procedure was derived from an algorithm calculating the MNE in the frequency domain suggested by Jensen and Vanni (Jensen & Vanni, 2002). The square root of the sum of squares of the MNE amplitudes for the sine and cosine parts served as a measure of the total 12.5Hz current source density over stimulus presentation time:

$$Amp_i(t) = \sqrt{Amp^2_{i,\sin e}(t) + Amp^2_{i,\cos ine}(t)}\ ,\ i \in [1,...,350], t \in [0ms,...,4000ms] \qquad (1)$$

where $Amp_i(t)$ is the total amplitude of the 12.5Hz demodulated SSVEF at dipole location i and time t, and $Amp_{i,sine}(t)$ and $Amp_{i,cosine}(t)$ are the corresponding amplitudes of the sine and cosine parts for time t.

L-curves were calculated for the averaged baseline topography over the 500 ms pre-stimulus interval for each condition (CS+, CS-), experimental block (habituation, acquisition, extinction) and sine/ cosine parts within one subject. The highest λ value determined from the resulting L-curves was used as regularization parameter. This procedure was chosen in order to prevent that different regularizations could account for condition effects. Finally, the MNE solutions were projected on a schematic brain implemented in the MATLAB™ package EMEGS (see also: www.uni-konstanz.de/win/emegs; (Junghöfer & Peyk, 2004) and submitted to a statistical mapping procedure (see below).

Statistical Analysis

In the present study we used exactly the same statistical analysis methods as in our previous work (see chapter 4) in order to locate regions of significant interactions between time course of stimulus driven cortical source activation and condition (CS+ and CS-) on a spherical shell. Before, the MNE amplitudes were averaged across three time windows (t1: 0-

1.3 s; t2: 1.3-2.6 s and t3: 2.6-3.9 s) for each condition (CS+, CS-), each experimental block (habituation, acquisition and extinction) and each subject. Within every experimental block the interaction between *condition* (CS+, CS-) and *time* (t1, t2, t3) was modeled at 273 of the 350 sources of the MNE shell in order to identify source clusters of differentiated activations for the CS+ and CS-. Sources located at the bottom of the shell were not considered as meaningful and were omitted in order to enhance statistical power (reducing the number of dipoles from 350 to 273). The p values for the interaction terms were corrected for 273 multiple tests by the false discovery rate procedure (Benjamini & Hochberg, 1995; Keselman, Cribbie, & Holland, 2002) and mapped on a schematic brain implemented in the MATLAB™ package EMEGS (see also: www.uni-konstanz.de/win/emegs; (Junghöfer & Peyk, 2004).

The interactions between *time* and *condition* were modeled using a linear mixed effects model (LME) applying restricted maximum likelihood estimators (REML) for parameter estimation. The factors *time* and *condition* were chosen as fixed effects, whereas the mean differences in MNE amplitudes between subjects over all conditions and within conditions were selected as random effects (levels *subject* and *condition within subject*). As the factor *time* implies dependence of observations, a first order autoregressive (AR(1)) covariance structure was applied to the LME model (Bagiella, Sloan, & Heitjan, 2000).

Source clusters were considered as meaningful whenever at three or more neighboring source locations the interaction terms survived the false discovery rate procedure for 273 tests and thus consisted of sources with associated corrected p values less than .05. The mean amplitude across dipoles of an identified source cluster was submitted to LME analysis identical to the one described above, except that we added the fixed effect $time^2$ to the fixed effect *time* and considered them as ordered factors in order to assess different time courses of cortical activations for the CS+ and CS- (linear and quadratic time courses). Whenever the kind of time course (linear and/ or quadratic) interacted with condition, the time courses were modeled for the CS+ and CS- condition, separately. Additionally, we conducted paired t-tests in order to asses at which time slots (t1, t2, t3) the CS+ and CS- generated different cortical source activations.

The HR change time series data was also analyzed using an LME model. This model is described in detail in chapter 2 and will be outlined in brief, here. The model was nearly identical to the LME model presented above, except that *time, $time^2$, $time^3$ and $time^4$* served as ordered fixed effects in order to asses a linear, quadratic, cubic and quartic time course of the HR data. This was implemented on the basis of earlier notions (Wilson, 1974) suggesting that analyzing differences in HR waveform components is more meaningful than comparing

means. The *time* factors consisted of nine time bins containing 500 ms each (see above). As we were not interested in mean differences or drifts of the HR response curve per subject over all conditions and within conditions, we chose the intercept and the linear slope (*time*) to be random effects at both the *subject* and *condition within subject* level. The AR(1) covariance structure was applied in order to account for dependence between time bins of the HR time series data. Whenever *time, time², time³ or time⁴* interacted with *condition*, separate analysis for the CS+ and CS- concerning the time course of HR pattern were conducted.

Finally, the slopes of the first and last two seconds of the HR response curves of the second block of acquisition trials (N=10) were submitted to cluster analysis following the procedure described by Hodes et al. (Hodes et al., 1985). This approach was chosen because we wanted to identify subjects who accelerated or decelerated in their HR response to the CS+ during acquisition as observed by previous studies (Hamm & Vaitl, 1996; Hare, 1972; Hodes et al., 1985) and as described in chapter 4.

In order to evaluate if subjects rated the US as unpleasant and high arousing, a one sample t-test was used that assessed if the scores deviated significantly from the midline of the analog scales (5 cm). The differences between HR accelerators and decelerators with respect to the sum scores of the questionnaires, age and to the distance from the left starting point of the analog scales were analyzed using two sample t-tests. The frequency distributions of females and males and of subjects aware or unaware of conditioning contingency within the HR accelerator and decelerator groups were assessed by χ^2-tests. Finally, we tested the Null hypothesis of equal proportions of HR accelerators and decelerators in the present study and in our previous work (see chapter 4) using the χ^2 procedure.

RESULTS

Heart Rate Data

We obtained two groups of subjects that had different HR response patterns to the CS+ during acquisition trials. The accelerator group (N=9) reacted with an HR increase to the CS+ and no HR change to the CS- in the acquisition block as indicated by a quartic trend for the CS+ only (quartic trend x condition: $F(1, 136) = 13.6$, $p < .001$; quartic trend CS+: $F(1, 68) = 25.2$, $p < .0001$; quartic trend CS-: not significant (n.s.)). During extinction accelerators showed a HR deceleration to the CS+ with a subsequent saturation of HR slowing during the last second of stimulus presentation. The HR response to the CS- remained about the same level during stimulus depiction (cubic trend x condition: $F(1, 136) = 3.3$, $p = .07$; cubic trend

CS+: F(1, 68) = 7.4, p < .01; cubic trend CS-: n. s.). The HR patterns of the accelerators during acquisition and extinction are summarized in figure 1.

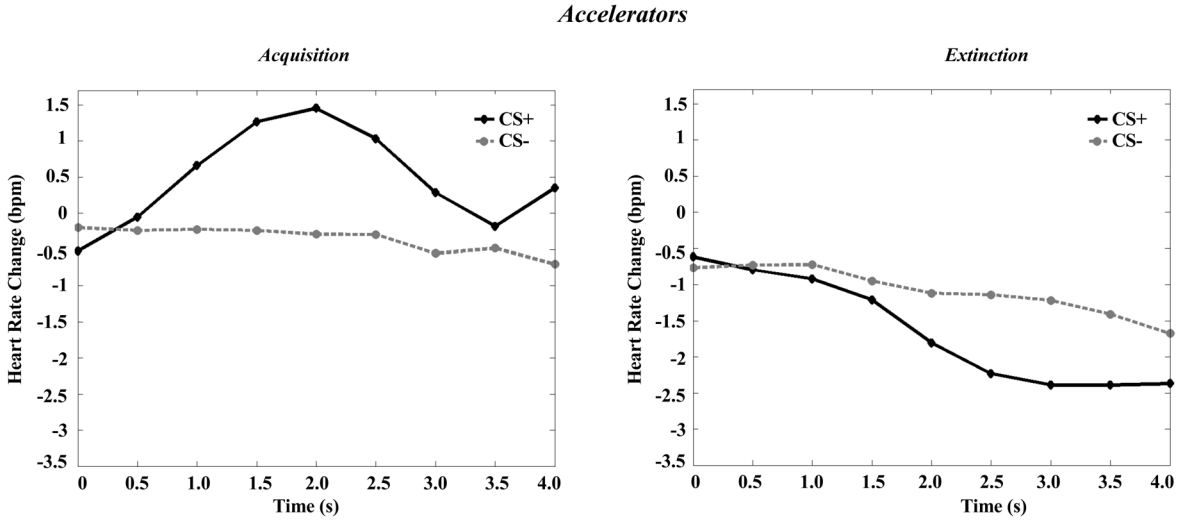

Figure 1: Cardiac waveforms (hear rate change in beats per minutes) for heart rate accelerators (N=9) during acquisition (left) and extinction (right).

The decelerator group (N=11) responded with a more pronounced HR slowing to the CS+ than to the CS- during acquisition trials (linear trend x condition: F(1, 168) = 3.3, p = .07; linear trend CS+: F(1, 84) = 15.2, p < .0005; linear trend CS-: F(1, 84) = 10.3; p < .005). In the extinction block, decelerators reacted the same way as during acquisition except that the difference in HR slowing between CS+ and CS was more distinctive (linear trend x condition: F(1, 168) = 4.7, p < .05; linear trend CS+: F(1, 84) = 20.2, p < .0001; linear trend CS-: F(1, 84) = 4.3, p < .05). The HR patterns of the decelerators during acquisition and extinction are summarized in figure 2.

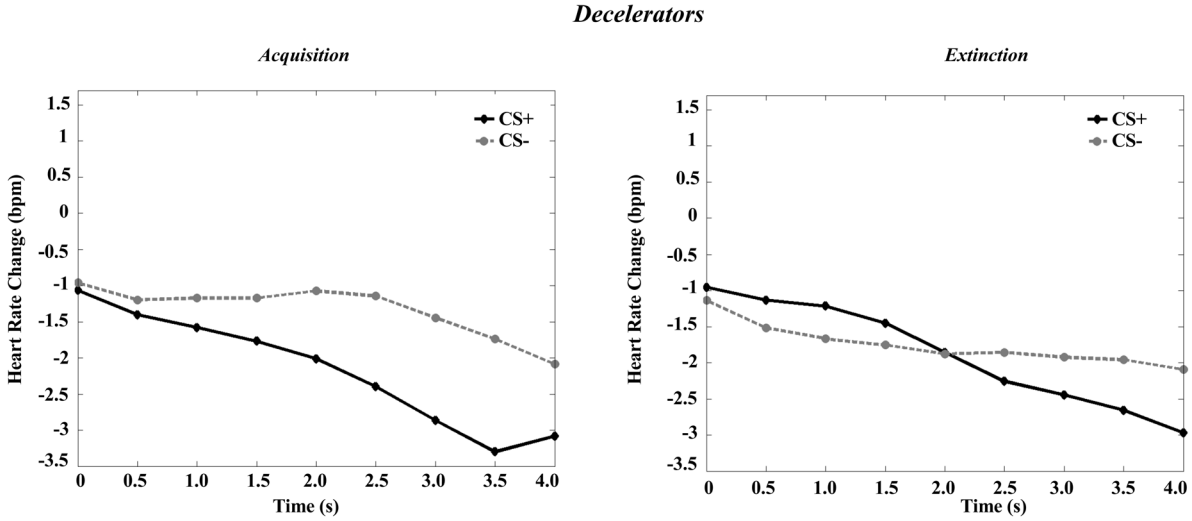

Figure 2: : Cardiac waveforms (hear rate change in beats per minutes) for heart rate decelerators (N=11) during acquisition (left) and extinction (right).

MNE data for all subjects

The grand mean of the MNE data over all subjects for the CS+ and the CS- depicted during habituation, acquisition and extinction is shown in figure 3. The processing of the CSs seemed to be left lateralized as can be seen from figure 3.

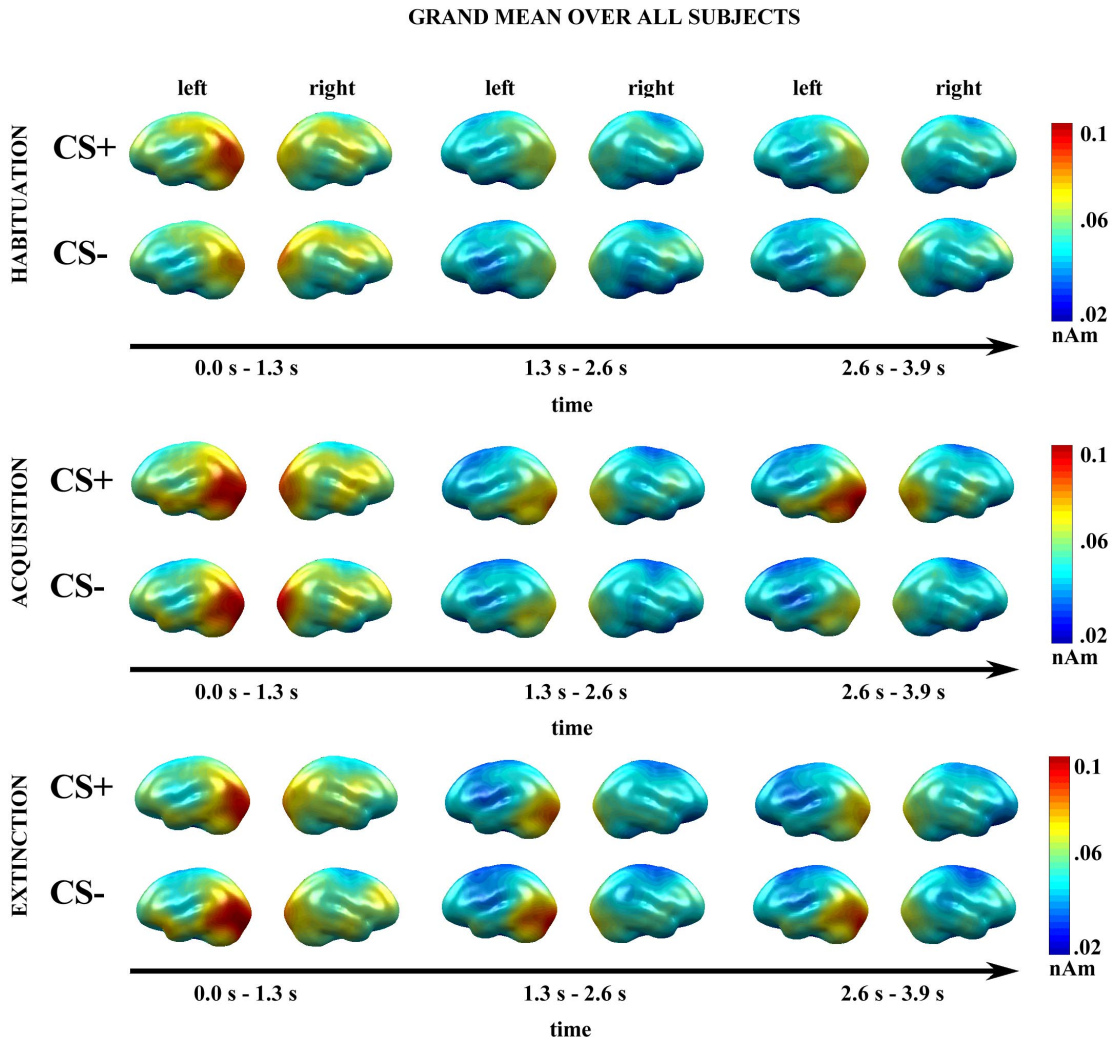

Figure 3: Grand mean of the minimum norm estimates (MNE) over all subjects (N=21) for CS+ and CS- trials during the habituation, acquisition and extinction phase of the experiment. Left and right hemispheres are shown. The arrows indicate the time of CS presentation. Below the arrows the time interval of the depicted MNE topographies is indicated. The colorbars on the right show the activation strength in nAm.

Figure 4 depicts the p values obtained from the LME model estimating the interaction terms between *time* (t1: 0-1.3s, t2: 1.3-2.6s and t3: 2.6-3.9s) and *condition* (CS+, CS-) that survived the false discovery rate correction for multiple comparisons (273 dipole locations) and the spatial distribution criterion. Only during the acquisition phase of the experiment such a source cluster emerged and was localized to the visual cortex and to some extent to parietal cortex (see figure 4). No source clusters meeting the above mentioned criteria were found during the habituation and extinction trials.

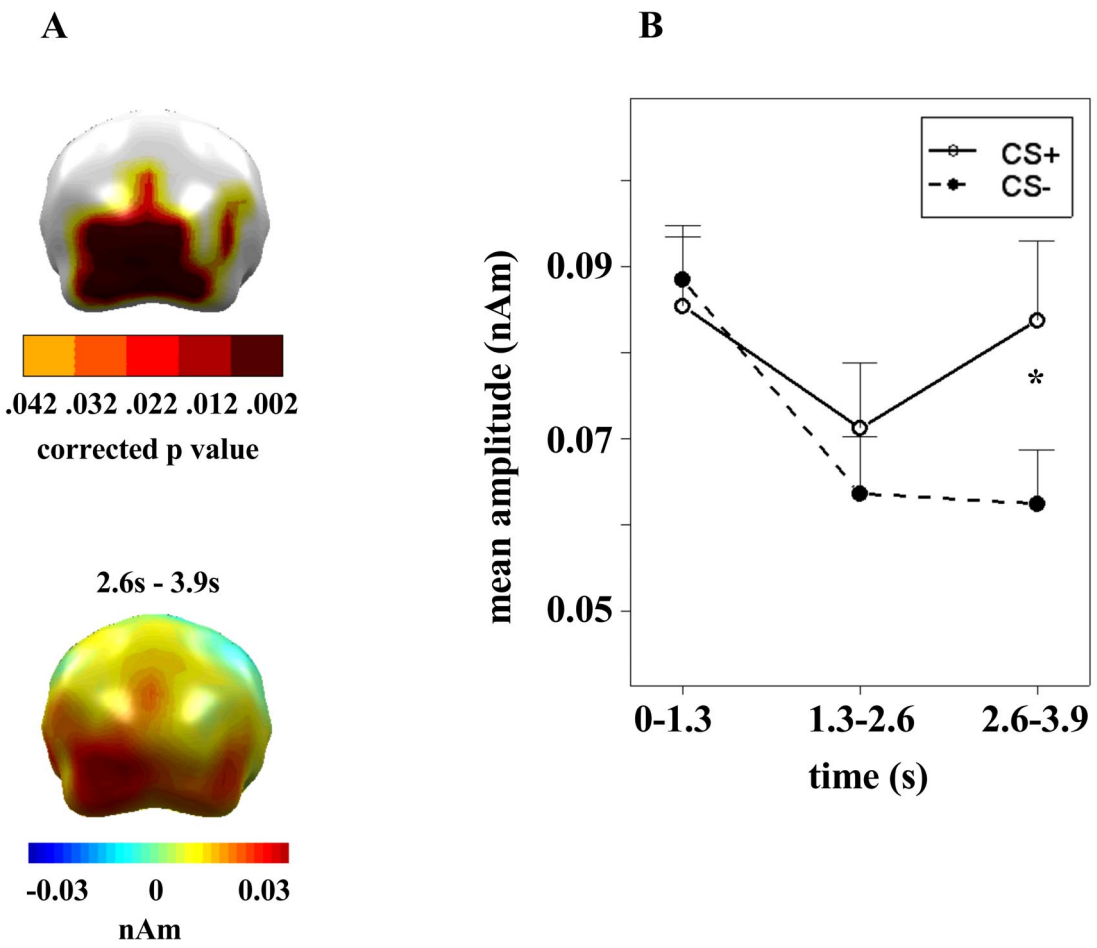

Figure 4: Sources in visual and parietal brain areas showed a differentiated time course of activation during acquisition. The upper part of panel A depicts sources of significant interaction of stimulus presentation time and condition (CS+, CS-). The lower part of panel A shows the difference map of the minimum norm estimates (CS+ minus CS- condition) during late stimulus presentation time (2.6s-3.9s). Panel B depicts the mean amplitudes and standard errors of the means over significant source clusters as identified by the linear mixed effects procedure. * $p < .05$ paired comparisons.

The mean amplitude across the source cluster in visual cortex during acquisition declined over stimulus presentation time only for the CS- as indicated by a significant interaction of a linear trend and condition (linear trend x condition: $F(1, 80) = 16.6$, $p < .0005$; linear trend CS+: n. s.; linear trend CS-: $F(1, 40) = 93.9$, $p < .0001$). During the last time period of before US presentation (2.6-3.9s) the SSVEF generated in visual cortex increased for the CS+ relative to the CS- condition (t1: n. s.; t2: n. s.; t3: $t = 2.6$, $df = 20$, $p < .05$, see also figure 4). However, this activation pattern did not show up in an interaction of a quadratic trend and condition, because such a trend could be fitted to both, the CS+ and CS-

(CS+: $F(1, 40) = 11.0$, $p < .0001$; CS-: $F(1, 40) = 16.0$, $p < .0001$). In sum, cortical activation in visual cortex elicited by the grating that gained predictive value (CS+) for the occurrence of the US was not subject of a general decline of amplitude over time as was the case for the CS-, that had never been paired with the US. Contrary, in the last time segment before US application, the activity generated by the CS+ in visual cortex increased again.

MNE data for subgroups HR accelerators and decelerators

As we had compared the time course of SSVEF activations for subjects that accelerated and decelerated to the CS+ during acquisition in our previous work (see chapter 4), we conducted the statistical mapping as done before for HR accelerators and decelerators of the present study, separately.

Accelerators: During acquisition HR accelerators showed a marked differentiated cortical activation pattern for CS+ and CS- trials in visual and parietal cortex. The SSVEF amplitude generated in visual cortex by CS- depiction declined over stimulus presentation time, whereas the neuromagnetic response to the CS+ did not follow that pattern (linear trend x condition: $F(1, 32) = 30.9$, $p < .0001$; linear trend CS+: n. s.; linear trend CS-: $F(1, 16) = 144$, $p < .0001$). The interaction of condition and a quadratic trend did not reach significance but only the CS+ activation time course could be fitted by a quadratic trend (CS+: $F(1, 16) = 6.8$, $p < .05$; CS-: n. s.). In the second and third time interval of stimulus depiction (1.3-2.6s and 2.6-3.9s), the CS+ generated amplitude in visual cortex was greater than that of the CS- (t1: n. s.; t2: $t = 2.7$, $df = 8$, $p < .05$; t3: $t = 3.4$, $df = 8$, $p < .01$).

In left frontal regions a small dipole cluster (N=3) emerged from the statistical mapping procedure. An interaction between condition and a quadratic trend for the mean amplitudes of that source cluster indicated a somewhat different time course of activation during CS+ and CS- depiction in acquisition trials (quadratic trend x condition: $F(1, 32) = 6.8$, $p < .05$). However, modeling a quadratic trend for the CS+ and CS- condition did not reveal any difference between the activation patterns (CS+: $F(1, 16) = 3.2$, $p = .09$; CS-: $F(1, 16) = 3.9$, $p = .07$). Further, single comparisons did not show any differences in amplitude for the CS+ and CS- in any of the three time intervals. The results for the accelerators during acquisition are summarized in figure 5.

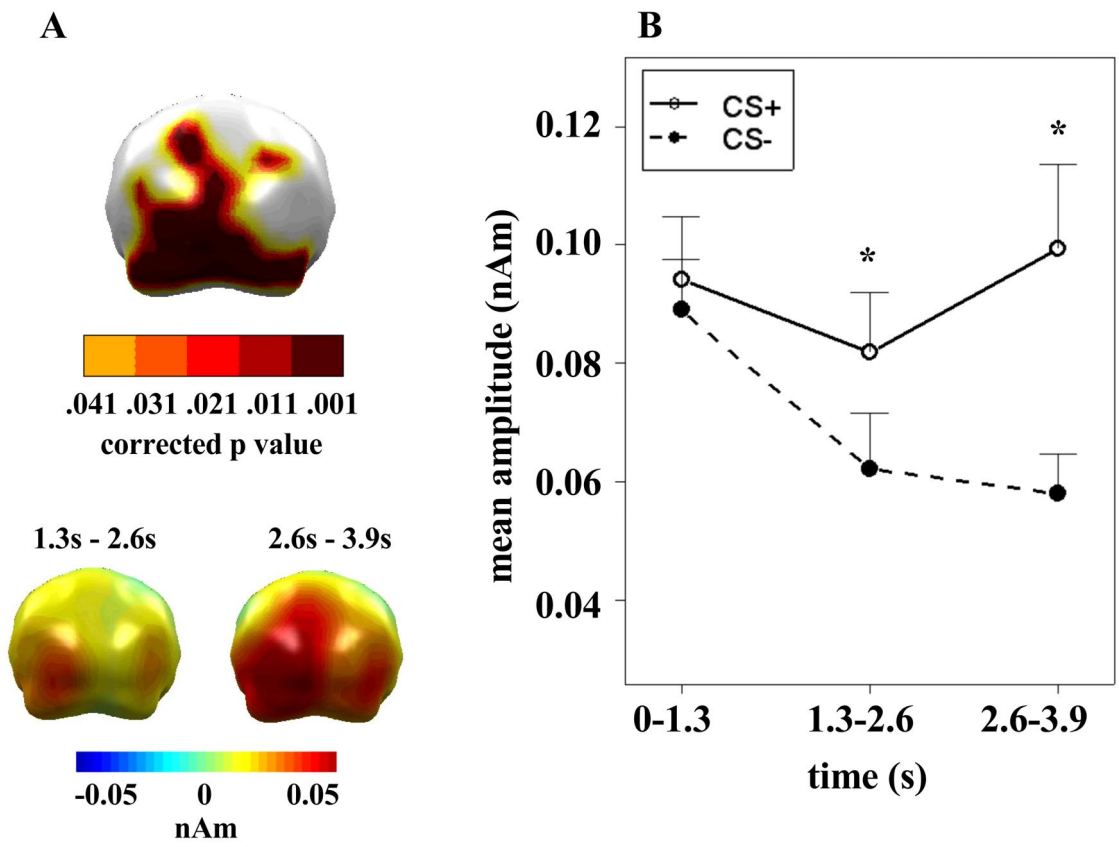

Figure 5: Sources in visual and parietal brain areas showed a differentiated time course of activation during acquisition for HR accelerators. The upper part of panel A depicts sources of significant interaction of stimulus presentation time and condition (CS+, CS-). The lower part of panel A shows the difference map of the minimum norm estimates (CS+ minus CS- condition) during stimulus middle and late presentation times (left: 1.3s-2.6s; right: 2.6s-3.9s). Panel B depicts the mean amplitudes and standard errors of the means over significant source clusters as identified by the linear mixed effects procedure. * $p < .05$ paired comparisons.

During extinction HR accelerators showed a differentiated cortical activation pattern for CS+ and CS- trials in right central brain regions (number of significant sources N=3). The SSVEF amplitude generated in that region by CS- depiction declined over stimulus presentation time as both, the CS- and the CS+ could be fitted with a linear trend (CS-: $F(1, 16) = 10.0$, $p < 0.01$; CS+: $F(1, 16) = 7.2$, $p < .05$), whereas the neuromagnetic response to the CS+ additionally followed a quadratic trend (quadratic trend x condition: $F(1, 32) = 13.2$, $p < .005$; quadratic trend CS+: $F(1, 16) = 17.7$, $p < .001$; quadratic trend CS-: n. s.). However, the amplitudes elicited by the CS+ and the CS- were about the same level as no single comparison within the time intervals (t1, t2, t3) reached significance, although the time course within this activation level seemed to differ between conditions (CS+, CS-).

Decelerators: During acquisition trials no differentiated stimulus driven cortical source activations were found for HR decelerators. However, in the extinction block of the experiment a frontal source cluster emerged from statistical mapping and indicated a different time course of activation during CS+ and CS- depiction in that brain region. Both, the CS+ and CS- driven amplitudes dropped over stimulus presentation time as indicated by a linear trend for both conditions (CS+: $F(1, 20) = 15.7$, $p <. 001$, CS-: $F(1, 20) = 19.7$, $p < .001$). However, the CS+ elicited SSVEF fell below the cortical activation level generated by the CS- during the second time interval (1.3-2.6s) of stimulus presentation as indicated by an interaction between condition and a quadratic trend (condition x quadratic trend: $F(1, 40) = 18.1$, $p < .001$; quadratic trend CS+: $F(1, 20) = 22.8$, $p < .0001$; quadratic trend CS-: n. s.). However, single comparison of the CS+ and CS- driven activity during the second time interval revealed only a difference at the 10% level (t2: $t = -1.9$, $df = 10$, $p = 0.08$) in left frontal brain regions.

Left parietal brain regions identified by the statistical mapping procedure (number of neighboring sources N=3) showed a stronger linear decline for the CS+ activation over time than for the CS- (condition x linear trend: $F(1, 40) = 13.6$, $p < .001$; linear trend CS+: $F(1, 20) = 61.0$, $p < .0001$; linear trend CS-: $F(1, 20) = 7.4$, $p < .05$). Whereas the CS+ driven activity continued to drop after the second time interval, the SSVEF generated in left parietal sources increased again as reflected in a quadratic fit for the CS- ($F(1, 20) = 49.8$, $p <.0001$), although the interaction between condition and quadratic trend did not reach significance. Single comparisons revealed that during the last time period of stimulus depiction (2.6-3.9s) the CS+ activation was reduced compared to the neuromagnetic response to the CS- (t1: n. s.; t2: n. s.; t3: $t = -2.4$, $df = 10$, $p < .05$) in left parietal brain regions. The results for the decelerators during extinction are summarized in figure 6.

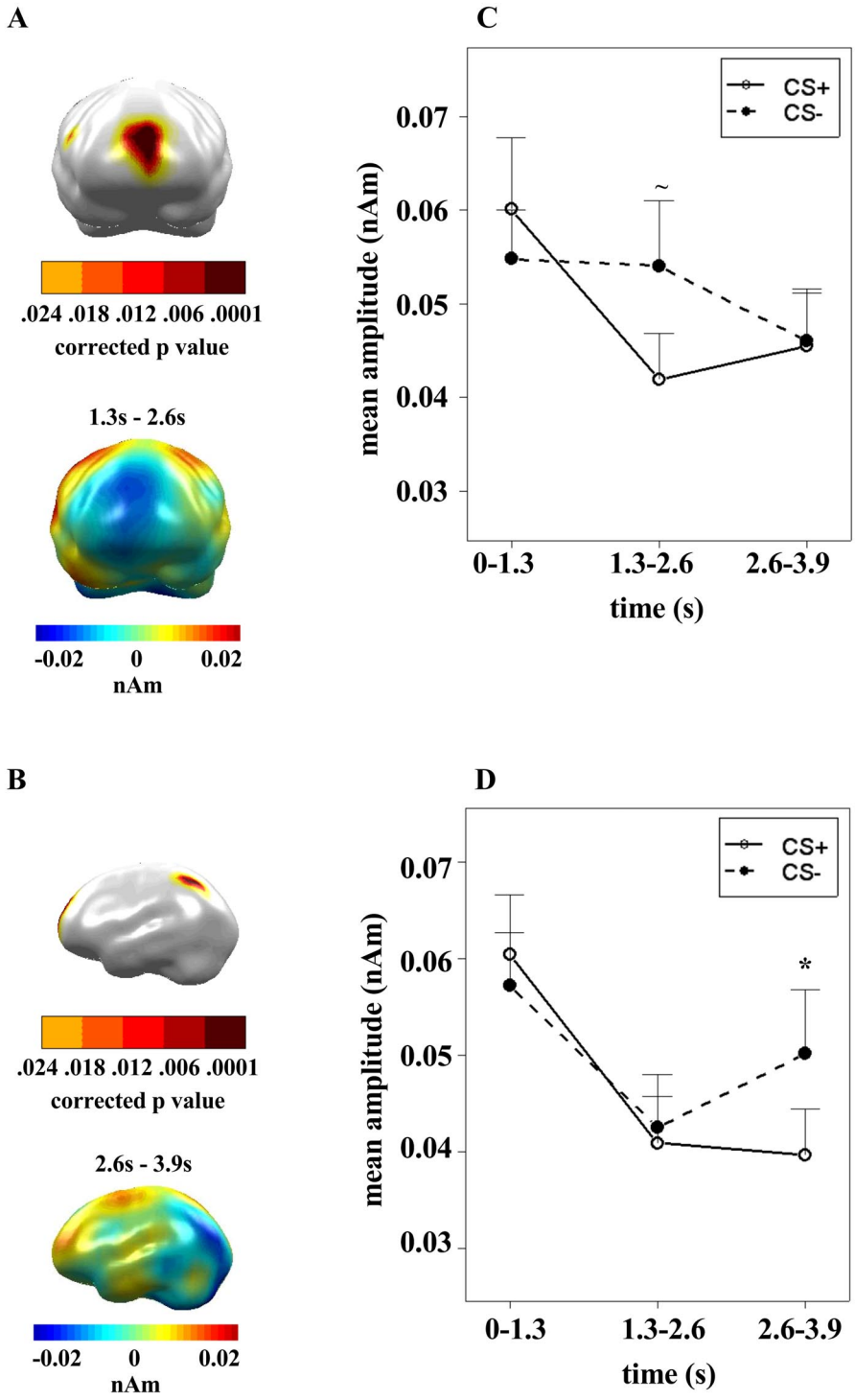

Figure 6: Significant sources of decelerators during extinction. Frontal significant (interaction CS presentation time and condition) source clusters for decelerators are depicted in the upper part of panel A. The lower part of panel A shows the difference map of the minimum norm estimates (CS+ minus CS- condition) during middle stimulus presentation time before US presentation (1.3s-2.6s). Panel C (upper right) depicts the mean amplitudes and standard errors of the means over significant frontal source clusters as identified by the linear mixed effects procedure. Left parietal significant source clusters are depicted in the upper part of panel B. The lower part of panel B shows the difference map of the minimum norm estimates (CS+ minus CS- condition) during late stimulus presentation time (2.6s-3.9s). Panel D depicts the mean amplitudes and standard errors of the means over significant left parietal source clusters as identified by the linear mixed effects procedure. * $p < .05$; ~ $p < .10$ paired comparisons.

Questionnaires, demographic data and proportion of HR accelerators and decelerators

At the end of the experiment all subjects but one recognized the grating that served as CS+ during acquisition properly (aware subjects N=20, one unaware subject). The mean valence rating for the US over all subjects was 8.66cm (±0.3) and the mean arousal rating was 7.1cm (±0.6) on the analog scales. Both, the valence rating ($t = 12.3$, $df = 19$, $p < .0001$) and the arousal rating ($t = 3.6$, $df = 19$, $p < 0.005$) differed significantly from the midline of the analog scale (5 cm).

Heart rate accelerators and decelerators were about the same age (accelerators: 27.3 years (±3.6); decelerators: 24.4 years (±0.9); two sample t-test n. s.) and did not differ in their valence (mean accelerators: 8.7cm (±0.5); mean decelerators: 8.6cm (±0.4); two sample t-test n. s.) and arousal (mean accelerators: 7.2cm (±0.9); mean decelerators: 7.0 (±0.9); two sample t-test n. s.) ratings of the US. Accelerators and decelerators did score equally on the state STAI, trait STAI and BDI (see table 1). The proportion of females and males within HR accelerator and decelerator groups were somewhat different but the χ^2-test did not turn out to be significant (accelerators: 3 females and 6 males; decelerators: 7 females and 4 males; χ^2-test n. s.).

- table 1 about here

One of hour hypothesis was that if participants were told the contingency of the CS+ and the US, the experiment would gain more signal character and therefore, the proportion of subjects decelerating their HR response to the CS+ during acquisition to HR accelerators should be higher in the present than in our prior study. In our previous work, we identified 8 accelerators and 10 decelerators, whereas in the present study 9 accelerators and 11 decelerators emerged from cluster analysis. Thus, the proportions of subjects accelerating and slowing down their HR response to the CS+ during acquisition were about the same across the two studies (χ^2-test n. s).

DISCUSSION

In the present study, we investigated cortical sources of SSVEFs elicited by luminance modulated gratings that served as conditioned stimuli in an aversive delayed Pavlovian conditioning paradigm whereby participants had been fully informed about the CS-US contingency before acquisition. Analogue scale ratings of unpleasantness and arousal of the

white noise that served as the US revealed that subjects experienced the US as an aversive event. In acquisition trials, we observed stronger visual and to some extent parietal cortex activation generated by the CS+ during the last time period (2.6s – 3.9s) before US administration than by the CS- during equivalent time segments. This is in line with our hypothesis that in subjects fully aware of the CS-US contingency the processing of the CS+ will be facilitated in sensory and attentive brain networks compared to the CS-. Imaging studies in the field of Pavlovian conditioning reported that stimuli associated with an aversive event, have generated more activity in brain areas of the visual system (Cheng, Knight, Smith, Stein, & Helmstetter, 2003; Hugdahl et al., 1995) paralleling our results.

In the area of spatial attention research, SSVEP studies have shown that attended stimuli generate greater SSVEPs than unattended stimuli (Morgan et al., 1996; Müller et al., 1998). Further, ERP studies have demonstrated that attention can modulate activity in extra striate and striate cortex (Di Russo, Martinez, & Hillyard, 2003; Hillyard & Anllo-Vento, 1998). Recently, Keil and collaborators (Keil, Moratti, Sabatinelli, Bradley, & Lang, 2004) reported additive effects of emotional stimulus content and spatial selective attention on SSVEP responses and speculated that a common neural mechanism mediates motivated attention of emotion and spatial attention (Keil et al., 2004). Studies using affective pictures consistently showed increased electrocortical activity for aversive stimuli in occipital and parietal brain regions (Junghöfer et al., 2001; Keil et al., 2002). Recently, Moratti et al. (chapter 3) observed the involvement of fronto-parietal attention networks in the processing of affective pictures. Taken together, general attentive cortical networks that facilitate feature extraction in visual cortex by top down processes may underlie spatial and motivated attention in emotion. These mechanisms may also have been responsible for enhanced CS+ processing in visual and parietal cortex in the present study.

However, it is unclear to what extent the current findings with respect of the whole sample reflect attentional processes associated with directed attention due to the expectation of an aversive event or represents affective facets of motivated attention as discussed in the emotion literature (Bradley, Codispoti, Cuthbert, & Lang, 2001). This issue will be addressed when the cortical activation patterns of the HR accelerators and decelerators are discussed (see below). Indeed, our original hypothesis was that instructing subjects about the CS-US relationship in order to induce full awareness of contingency will dye the CS+ into a signal rather into a fear character. Therefore, we hypothesized that the majority of subjects will show an OR as indicated by an HR deceleration during CS+ depiction in acquisition trials. Under these circumstances a defense response indexed by HR acceleration was supposed to occur

only in a few subjects. Therefore, we predicted that enhanced CS+ processing should be a consequence of such an OR response. However, the proportion of HR accelerators and decelerators was about 9 to 11 and did not differ to the one observed in our previous conditioning study (see chapter 4) in that only 3 out of 17 subjects could report a CS-US contingency. Thus, with respect to our HR data we did not observe any difference between the current and our previous conditioning study. Approximately the same proportion of subjects showed a fear response during acquisition as indexed by HR acceleration regardless if they were aware or unaware of stimulus contingencies. This is in line with previous findings reporting that a fear network can be triggered automatically without conscious processing of the CS-US relationship (Esteves et al., 1994; Hamm & Vaitl, 1996; Hamm et al., 2003; Ohman & Soares, 1998). However, it is possible that we underestimated the number of aware subjects in our prior study because we asked subjects after the extinction trials and this may have distorted the memory of stimulus contingencies (Lovibond & Shanks, 2002).

As sample sizes of HR accelerators and decelerators were big enough, we conducted a separate analysis of the MNE data as in our previous study (see chapter 4). Accelerators were characterized by HR acceleration during CS+ depiction in acquisition trials. Decelerators slowed down their HR to the CS+ presentation during that experimental phase. During extinction accelerators and decelerators showed a stronger OR to the CS+ compared to the CS- as indicated by a greater HR deceleration to the CS+. The emergence of HR accelerators and decelerators is consistent with previous findings in the fear conditioning literature (Hamm & Vaitl, 1996; Hare, 1972; Hodes et al., 1985). In our prior study described in chapter 4 we observed a distinct OR to the CS+ during extinction only in HR accelerators. In the present study we could not replicate this finding as decelerators also showed a stronger decelerative response pattern to the CS+ in extinction trials. However, the difference between the two studies could reflect that aware subjects orient to the CS+ during extinction regardless of their HR response pattern in acquisition trials. Eventually, in unaware subjects a fear response has to be learned in acquisition trials in order to be able to express an OR during extinction.

The reported facilitated neuromagnetic response to the CS+ compared to the CS- during acquisition in the whole sample (see above) was driven by the accelerator group. Decelerators did not show any differentiated processing in any brain region during acquisition. Moreover, the distinct CS+/ CS- processing towards the time period just before US presentation was not only generated in visual areas. Parietal cortical sources were far more engaged in accelerators than in the whole sample. Obviously, a greater stimulus driven SSVEF response to the CS+ in attentive and sensory cortical areas is not only a pure

expectation effect caused by instructed CS-US contingency. Otherwise, accelerators as well as decelerators should have shown greater occipito-parietal activation by CS+ depiction. Further, a simple 'to-be-attended' effect caused by the instruction would have led to an enhancement of CS+ processing over the whole stimulus presentation time and not to a fine tuned facilitation just before US presentation.

The expression of a fear response to the CS+ seemed to be necessary in order to engage an attentive sensory cortical network as only HR accelerators showed this effect and accelerative HR response patterns have been associated with fear responses (Hare & Blevings, 1975). This result did clearly contradict our original hypothesis that enhanced CS+ processing will be related to an OR indexed by HR deceleration. Hamm and collaborators (Hamm & Vaitl, 1996) reported that only accelerators did show enhanced startle potentiation to the CS+ paralleling our results although on a different response level. It would be interesting to replicate the findings at cortical and reflexive response systems within one sample. Interestingly, conditioning of skin conductance was not affected by the HR response pattern in the above cited study (Hamm & Vaitl, 1996). It is very unlikely that the lack of a differentiated neuromagnetic CS+/ CS- response in HR decelerators during acquisition is an artifact of reduced statistical power due to splitting the whole sample into two groups as the effects observed in accelerators are stronger and evident in a greater cortical network. Indeed, dividing the whole sample into HR accelerators and decelerators seemed to reduce variance.

As the proportions of HR accelerators and decelerators were the same in the present and our previous study (see chapter 4), we argue (see above) that the fear character of the conditioning procedure remained the same whether subjects are aware of CS-US contingency or not contradicting our initial hypothesis (see above). In the prior study (see chapter 4) we also demonstrated that only HR accelerators showed a facilitation of CS+ processing in sensory and attentive cortical networks paralleling the results of the present study.

However, there are some marked differences about that aspect in our prior work (see chapter 4). First, the enhanced neuromagnetic response in favor of the CS+ in sensory and attentive cortical networks was spatially more focused to left extrastriate and left parietal cortex. As in the older study the MNE topography over all subjects indicated that the stimulus driven SSVEFs for both, the CS+ and the CS-, were generated in more left sided occipital areas, we concluded that the CS+ elicited activity was simply amplified in areas were the stimulus is processed per se. A similar relationship between topographical activity distributions and lateralization was discussed by Keil et al. (Keil et al., 2002). This notion is in line with the concept of a sensory gain mechanism that facilitates processing of attended

stimuli as hypothesized in attention research (Hillyard & Anllo-Vento, 1998). In the present study we also observed a rather left sided topographical distribution of the MNE solution. However, the statistical mapping of stimulus presentation time (0-1.3s; 1.3-2.6s, 2.6-3.9s) and condition (CS+, CS-) revealed the involvement of widespread cortical sources in the visual system possibly including primary visual areas and central parietal cortex. Therefore, it can be supposed that awareness of stimulus contingency or expectation of the occurrence of the US engages a sensory attentive network more extensively. Nevertheless, the involvement of a sensory attentive cortical network in Pavlovian conditioning seems to be closely linked to the acquisition of a fear response indexed by HR acceleration. This points to the view that emotional processing engages general attention systems in the brain and supports the concept of motivated attention in emotion. However, an alternative explanation of the difference in the extent of the involvement of sensory and attentional brain areas between our two studies could be that in the experiment investigating unaware subjects only a few participants acquired a conditioned response at all and therefore, statistical mapping revealed smaller parts of that network. This issue has to be tackled by future research and should be investigated with within-designs.

Second, in the previous conditioning study (see chapter 4) the above mentioned effects in sensory and attentive brain areas were observed during extinction and not acquisition trials as in the present study. During extinction no effects were observed in the accelerator group in the current work. Originally, we suggested that fully informed subjects will show different cortical activation patterns during acquisition due to a more pronounced cuing character of the conditioning procedure eliciting an OR indexed by HR deceleration. But as the amount of HR accelerators showing a fear response was about the same as in our older study (see chapter 4), we cannot support this view. Now, we hypothesize that learning and extinction of the CS-US association within the cortical visual and attention system occurred faster in fully aware than in unaware subjects and therefore the observed effects could be observed in earlier phases of the experiment. But this hypothesis has to be tested in a further experiment.

Accelerators did not only show a greater SSVEF response in posterior brain regions. Statistical mapping also revealed the involvement of left frontal cortical sources during acquisition. Imaging studies using PET (Fischer, Andersson, Furmark, Wik, & Fredrikson, 2002; Hugdahl et al., 1995) and fMRI (LaBar, Gatenby, Gore, LeDoux, & Phelps, 1998) have demonstrated that the frontal cortex seems to be engaged in the acquisition of a conditioned response. Perlstein and collaborators (Perlstein et al., 2003) have shown that during a memory task the activation of the frontal cortex can be imaged by using SSVEPs. However, analyzing

the mean amplitude of the left frontal cortical sources in the HR accelerator group did not support an amplitude facilitation during any CS+ presentation time period before the presentation of the US. Although the three left frontal neighboring dipoles survived the false discovery rate procedure, the mapped statistical effect did not seem to be reliable. Maybe the spatial distribution criterion of three adjacent dipoles is not strict enough to suppress false positive findings. Therefore, the left frontal activation pattern has to be considered with caution. A similar interpretation has to be done for right central cortical brain areas that encompassed also only three statistically significant cortical sources for accelerators during extinction. The analysis of the time course of the activation of these three sources reliably demonstrated a quadratic trend for the CS+ only, but single comparisons at any of the three time slots (0-1.3s; 1.3-2.6s; 2.6-3.9s) did not reveal any differences. Therefore, we do not interpret these effects.

As contrasted above, HR decelerators did not show any differentiated CS+/ CS- stimulus driven cortical source activations during acquisition trials. The lack of a fear response (HR acceleration) in this subgroup of subjects possibly did not impart motivational relevance to the CS+. Hence, a CS+ elicited increased neuromagnetic stimulus driven response in sensory and attentive brain networks could not be observed in HR decelerators because the CS+ did engage systems involved in motivated attention.

In the accelerator group, however, no reliable effects were found in the extinction block of the experiment. HR decelerators showed some distinct SSVEF generation for the CS+ and CS- in this experimental phase. In frontal areas the amplitude generated by the CS+ dropped below the level of the CS- during the second analyzing window (1.3-2.6s). An activity drop of the CS+ compared to the CS- elicited neuromagnetic response in thelate presentation time period was observed in a left parietal source cluster during extinction. Although these results may be seen in the light of some inhibition processes during extinction (Pavlov, 1927), we did not expect such activation patterns and our hypothesis's were not designed in order to be verified or to be discarded by such observations. Therefore, we keep the interpretation of the activation time courses in HR decelerators during extinction trials open.

The differences between HR accelerators and decelerators described in the previous paragraphs could not be explained by personality variables. Accelerators and decelerators did not differ with respect to gender, age, state/ trait anxiety- or depression scores. Both groups rated the US equally unpleasant and arousing.

In sum, subjects that were fully informed about the CS-US contingency and therefore were aware of the CS-US relationship could be separated into two subgroups with respect of HR response patterns as in our previous study (see chapter 4). Our original hypothesis that in participants fully aware of the CS-US contingency an OR prevails as indexed by a majority of HR decelerators in the sample, had to be refuted. The proportion of HR accelerators and decelerators were about the same as in our previous study in that most of the subjects could not verbalize the CS-US relationship.

In our initial hypothesis, we argued that enhanced processing of the CS+ during acquisition in aware participants should be a consequence of an OR indexed by HR deceleration. Contrary, we observed that enhanced neuromagnetic responses originating in visual and parietal cortex due to the association between the CS+ and the US were only observed in HR accelerators. Accelerative responses have been associated with fear responses (Hare & Blevings, 1975). This points to the importance of the aspect of motivated attention in affective stimulus processing (Lang, Bradley, & Cuthbert, 1997) during Pavlovian conditioning procedures.

In general, our previous (see chapter 4) and current study have demonstrated that visual stimuli that gain motivational relevance in a delayed aversive Pavlovian conditioning paradigm generate greater neuromagnetic responses in sensory and attentive cortical networks. This is in line with network theories of motivated attention in emotion (Lang, 1979; Lang et al., 1997). Further, our results parallel findings of studies using affective picture material (Junghöfer et al., 2001; Keil, 2000; Keil et al., 2002; Moratti et al., 2004; Palomba, Angrilli, & Mini, 1997; Schupp, Junghöfer, Weike, & Hamm, 2002) and exclude the possibility that varying complexities of stimulus material could have accounted for the enhanced electro-/ magnetocortical responses of the visual system as we have used simple gratings. Moreover, the co-registration of HR responses and SSVEF revealed the importance of fear responses in Pavlovian conditioning in order to elicit facilitated CS+ processing in cortical sensory and attentive networks.

SUMMARY

In the present study we investigated steady state visual evoked fields in a discriminative Pavlovian delayed fear conditioning paradigm using magnetencephalography. As in our previous conditioning study almost no subjects had been aware of the contingency of the conditioned (CS) and unconditioned stimulus (US), we instructed participants that a certain stimulus will predict the US in order to induce full awareness. As in our prior study,

only subjects showing a fear response as indexed by heart rate acceleration exhibited facilitated processing of the reinforced CS (CS+) in visual and parietal cortex. Heart rate decelerators did not show an enhancement of stimulus driven cortical activation for the CS+. The results are discussed in the context of motivated attention in emotion .

REFERENCES

Adolphs, R., Tranel, D., Damasio, H., & Damasio, A. R. (1995). Fear and the human amygdala. *J Neurosci, 15*(9), 5879-5891.

Bagiella, E., Sloan, R. P., & Heitjan, D. F. (2000). Mixed-effects models in psychophysiology. *Psychophysiology, 37*(1), 13-20.

Benjamini, Y., & Hochberg, Y. (1995). Controlling the false discovery rate: a practical and powerful approach to multiple testing. *J Roy Stat Soc B STA, 57*, 289-300.

Berg, P., & Scherg, M. (1994). A multiple source approach to the correction of eye artifacts. *Electroencephalogr Clin Neurophysiol, 90*(3), 229-241.

Bertero, M., De Mol, C., & Pike, E. R. (1988). Linear inverse problems with discrete data: II. Stability and regularization. *Inverse Problems, 4*, 573-594.

Bradley, M. M., Codispoti, M., Cuthbert, B. N., & Lang, P. J. (2001). Emotion and Motivation I: Defensive and Appetitive Reactions in Picture Processing. *Emotion, 1*(3), 276-298.

Calder, A. J., Young, A. W., Rowland, D., Perrett, D. I., Hodges, J. R., & Etcoff, N. L. (1996). Facial emotion recognition after bilateral amygdala damage: Differentially severe impairment of fear. *Cognitive Neuropsychology, 13*, 699-745.

Cheng, D. T., Knight, D. C., Smith, C. N., Stein, E. A., & Helmstetter, F. J. (2003). Functional MRI of human amygdala activity during Pavlovian fear conditioning: stimulus processing versus response expression. *Behav Neurosci, 117*(1), 3-10.

Clark, R. E., Manns, J. R., & Squire, L. R. (2001). Trace and delay eyeblink conditioning: contrasting phenomena of declarative and nondeclarative memory. *Psychol Sci, 12*(4), 304-308.

Clark, R. E., Manns, J. R., & Squire, L. R. (2002). Classical conditioning, awareness, and brain systems. *Trends Cogn Sci, 6*(12), 524-531.

Di Russo, F., Martinez, A., & Hillyard, S. A. (2003). Source analysis of event-related cortical activity during visuo-spatial attention. *Cereb Cortex, 13*(5), 486-499.

Esteves, F., Parra, C., Dimberg, U., & Ohman, A. (1994). Nonconscious associative learning: Pavlovian conditioning of skin conductance responses to masked fear-relevant facial stimuli. *Psychophysiology, 31*(4), 375-385.

Fanselow, M. S., & Poulos, A. M. (2004). The Neuroscience of Mammalian Associative Learning. *Annu Rev Psychol*.

Fischer, H., Andersson, J. L., Furmark, T., Wik, G., & Fredrikson, M. (2002). Right-sided human prefrontal brain activation during acquisition of conditioned fear. *Emotion, 2*(3), 233-241.

Gabrieli, J. D., McGlinchey-Berroth, R., Carrillo, M. C., Gluck, M. A., Cermak, L. S., & Disterhoft, J. F. (1995). Intact delay-eyeblink classical conditioning in amnesia. *Behav Neurosci, 109*(5), 819-827.

Hamalainen, M. S., & Ilmoniemi, R. J. (1994). Interpreting magnetic fields of the brain: minimum norm estimates. *Med Biol Eng Comput, 32*(1), 35-42.

Hamm, A. O., & Vaitl, D. (1996). Affective learning: awareness and aversion. *Psychophysiology, 33*(6), 698-710.

Hamm, A. O., Weike, A. I., Schupp, H. T., Treig, T., Dressel, A., & Kessler, C. (2003). Affective blindsight: intact fear conditioning to a visual cue in a cortically blind patient. *Brain, 126*(Pt 2), 267-275.

Hansen, P. C., & O'Leary, D. P. (1993). The use of the L-curve in the regularization of discrete ill-posed problems. *SIAM J. Sci. Comput., 14*, 1487-1503.

Hare, R. D. (1972). Cardiovascular components of orienting and defensive responses. *Psychophysiology, 9*(6), 606-614.

Hare, R. D., & Blevings, G. (1975). Defensive responses to phobic stimuli. *Biol Psychol, 3*(1), 1-13.

Hauk, O., Keil, A., Elbert, T., & Müller, M. M. (2002). Comparison of data transformation procedures to enhance topographical accuracy in time series analysis of the human EEG. *Journal of Neuroscience Methods, 113*(2), 111-122.

Hautzinger, M., Bailer, M., Worall, H., & Keller, F. (1992). *Beck - Depressions-Inventar*. Bern: Huber.

Hillyard, S. A., & Anllo-Vento, L. (1998). Event-related brain potentials in the study of visual selective attention. *Proc Natl Acad Sci U S A, 95*(3), 781-787.

Hodes, R. L., Cook, E. W., 3rd, & Lang, P. J. (1985). Individual differences in autonomic response: conditioned association or conditioned fear? *Psychophysiology, 22*(5), 545-560.

Hugdahl, K., Berardi, A., Thompson, W. L., Kosslyn, S. M., Macy, R., Baker, D. P., Alpert, N. M., & LeDoux, J. E. (1995). Brain mechanisms in human classical conditioning: a PET blood flow study. *Neuroreport, 6*(13), 1723-1728.

Jensen, O., & Vanni, S. (2002). A new method to identify multiple sources of oscillatory activity from magnetoencephalographic data. *Neuroimage, 15*(3), 568-574.

Junghöfer, M., Bradley, M. M., Elbert, T. R., & Lan, P. J. (2001). Fleeting images: a new look at early emotion discrimination. *Psychophysiology, 38*(2), 175-178.

Junghöfer, M., & Peyk, P. (2004). Analyse und Visualisierung von Hirnstrom- und Hirnmagnetfeld-Messungen. *MATLAB select, 2*, 24-28.

Keil, A. (2000). *Oscillatory brain activity in human affective stimulus processing.* University of Konstanz, Konstanz.

Keil, A., Bradley, M. M., Hauk, O., Rockstroh, B., Elbert, T., & Lang, P. J. (2002). Large-scale neural correlates of affective picture processing. *Psychophysiology, 39*(5), 641-649.

Keil, A., Moratti, S., Sabatinelli, D., Bradley, M. M., & Lang, P. J. (2004). Additive Effects of Emotional Content and Spatial Selective Attention on Electrocortical Facilitation. *Cereb Cortex*.

Keselman, H. J., Cribbie, R., & Holland, B. (2002). Controlling the rate of Type I error over a large set of statistical tests. *Br J Math Stat Psychol, 55*(Pt 1), 27-39.

Kim, J. J., Clark, R. E., & Thompson, R. F. (1995). Hippocampectomy impairs the memory of recently, but not remotely, acquired trace eyeblink conditioned responses. *Behav Neurosci, 109*(2), 195-203.

Knight, D. C., Nguyen, H. T., & Bandettini, P. A. (2003). Expression of conditional fear with and without awareness. *Proc Natl Acad Sci U S A, 100*(25), 15280-15283.

Knuttinen, M. G., Power, J. M., Preston, A. R., & Disterhoft, J. F. (2001). Awareness in classical differential eyeblink conditioning in young and aging humans. *Behav Neurosci, 115*(4), 747-757.

Kronforst-Collins, M. A., & Disterhoft, J. F. (1998). Lesions of the caudal area of rabbit medial prefrontal cortex impair trace eyeblink conditioning. *Neurobiol Learn Mem, 69*(2), 147-162.

LaBar, K. S., Gatenby, J. C., Gore, J. C., LeDoux, J. E., & Phelps, E. A. (1998). Human amygdala activation during conditioned fear acquisition and extinction: a mixed-trial fMRI study. *Neuron, 20*(5), 937-945.

Lang, P. J. (1979). A bioinformational theory of emotional imagery. *Psychophysiology, 16*, 495-512.

Lang, P. J., Bradley, M. M., & Cuthbert, B. N. (1997). Motivated Attention: Affect, Activation, and Action. In P. J. Lang & R. F. Simons & M. T. Balaban (Eds.), *Attention and Orienting: Sensory and Motivational Processes* (pp. 97-135). Hillsdale, N.J.: Lawrence Erlbaum Associates.

Laux, L., Glanzmann, P., Schaffner, P., & Spielberger, C. D. (1981). *Das State-Trait-Angstinventar*. Weinheim: Beltz.

LeDoux, J. E. (1993). Emotional networks in the brain. In J. M. H. Michael Lewis (Ed.), *Handbook of emotions.* (pp. 109-118): Guilford Press, New York, NY, US.

LeDoux, J. E. (2000). Emotion circuits in the brain. *Annu Rev Neurosci, 23*, 155-184.

Lovibond, P. F., & Shanks, D. R. (2002). The role of awareness in Pavlovian conditioning: empirical evidence and theoretical implications. *J Exp Psychol Anim Behav Process, 28*(1), 3-26.

Manns, J. R., Clark, R. E., & Squire, L. (2001). Single-cue delay eyeblink conditioning is unrelated to awareness. *Cogn Affect Behav Neurosci, 1*(2), 192-198.

Manns, J. R., Clark, R. E., & Squire, L. R. (2000). Parallel acquisition of awareness and trace eyeblink classical conditioning. *Learn Mem, 7*(5), 267-272.

Manns, J. R., Clark, R. E., & Squire, L. R. (2002). Standard delay eyeblink classical conditioning is independent of awareness. *J Exp Psychol Anim Behav Process, 28*(1), 32-37.

Mauk, M. D., & Thompson, R. F. (1987). Retention of classically conditioned eyelid responses following acute decerebration. *Brain Res, 403*(1), 89-95.

McGlinchey-Berroth, R., Carrillo, M. C., Gabrieli, J. D., Brawn, C. M., & Disterhoft, J. F. (1997). Impaired trace eyeblink conditioning in bilateral, medial-temporal lobe amnesia. *Behav Neurosci, 111*(5), 873-882.

Moratti, S., Keil, A., & Stolarova, M. (2004). Motivated attention in emotional picture processing is reflected by activity modulation in cortical attention networks. *Neuroimage, 21*(3), 954-964.

Morgan, S. T., Hansen, J. C., & Hillyard, S. A. (1996). Selective attention to stimulus location modulates the steady-state visual evoked potential. *Proc Natl Acad Sci U S A, 93*(10), 4770-4774.

Morris, J. S., Ohman, A., & Dolan, R. J. (1998). Conscious and unconscious emotional learning in the human amygdala. *Nature, 393*(6684), 467-470.

Müller, M. M., Gruber, T., & Keil, A. (2000). Modulation of induced gamma band activity in the human EEG by attention and visual information processing. *Int J Psychophysiol, 38*(3), 283-299.

Muller, M. M., & Hubner, R. (2002). Can the spotlight of attention be shaped like a doughnut? Evidence from steady-state visual evoked potentials. *Psychol Sci, 13*(2), 119-124.

Müller, M. M., Picton, T. W., Valdes-Sosa, P., Riera, J., Teder-Salejarvi, W. A., & Hillyard, S. A. (1998). Effects of spatial selective attention on the steady-state visual evoked potential in the 20-28 Hz range. *Brain Res Cogn Brain Res, 6*(4), 249-261.

Ohman, A., & Soares, J. J. (1998). Emotional conditioning to masked stimuli: expectancies for aversive outcomes following nonrecognized fear-relevant stimuli. *J Exp Psychol Gen, 127*(1), 69-82.

Oldfield, R. C. (1971). The assessment and analysis of handedness: The Edinbourgh Inventory. *Neuropsychologia, 9*, 97-113.

Palomba, D., Angrilli, A., & Mini, A. (1997). Visual evoked potentials, heart rate responses and memory to emotional pictorial stimuli. *Int J Psychophysiol, 27*(1), 55-67.

Pavlov, I. P. (1927). *Conditioned Reflexes: An Investigation of the Physiological Activity of the Cerebral Cortex*. London: Oxford University Press.

Perlstein, W. M., Cole, M. A., Larson, M., Kelly, K., Seignourel, P., & Keil, A. (2003). Steady-state visual evoked potentials reveal frontally-mediated working memory activity in humans. *Neurosci Lett, 342*(3), 191-195.

Regan, D. (1989). *Human Brain Electrophysiology: Evoked Potentials and Evoked Magnetic Fields in Science and Medicine*. New York: Elsevier.

Schupp, H. T., Junghöfer, M., Weike, A. I., & Hamm, A. O. (2002). Emotional facilitation of sensory processing in the visual cortex. *Psychological Science*, in press.

Shanks, D. R., & Lovibond, P. F. (2002). Autonomic and eyeblink conditioning are closely related to contingency awareness: reply to Wiens and Ohman (2002) and Manns et al. (2002). *J Exp Psychol Anim Behav Process, 28*(1), 38-42.

Shi, C., & Davis, M. (2001). Visual pathways involved in fear conditioning measured with fear-potentiated startle: behavioral and anatomic studies. *J Neurosci, 21*(24), 9844-9855.

Silberstein, R. B., Nunez, P. L., Pipingas, A., Harris, P., & Danieli, F. (2001). Steady state visually evoked potential (SSVEP) topography in a graded working memory task. *Int J Psychophysiol, 42*(2), 219-232.

Uusitalo, M. A., & Ilmoniemi, R. J. (1997). Signal-space projection method for separating MEG or EEG into components. *Med Biol Eng Comput, 35*(2), 135-140.

Wiens, S., Katkin, E. S., & Ohman, A. (2003). Effects of trial order and differential conditioning on acquisition of differential shock expectancy and skin conductance conditioning to masked stimuli. *Psychophysiology, 40*(6), 989-997.

Wiens, S., & Ohman, A. (2002). Unawareness is more than a chance event: comment on Lovibond and Shanks (2002). *J Exp Psychol Anim Behav Process, 28*(1), 27-31.

Wilson, R. S. (1974). CARDIVAR: the statistical analysis of heart rate data. *Psychophysiology, 11*(1), 76-85.

Woodruff-Pak, D. S., Lavond, D. G., & Thompson, R. F. (1985). Trace conditioning: abolished by cerebellar nuclear lesions but not lateral cerebellar cortex aspirations. *Brain Res, 348*(2), 249-260.

CONCLUSION

The aim of the present thesis was to investigate oscillatory cortical activity evoked by repetitive visual stimulation using stimuli with varying emotional content. It was not subject of the current work to infer feelings, thoughts or moods individuals had during affective stimulus depiction from neuromagnetic responses measured with magnetencephalography. As emotions were understood as *phasic reactions of motivational systems to distinct biologically significant stimuli in the environment of an individual preparing it for action*, the main question was rather how visual stimuli of high motivational significance for the organism were processed in sensory and association cortex. One of the main hypothesis was that stimuli with high motivational impact for the individual should lead to a facilitated processing in visual sensory brain regions such as extrastriate cortex in order to extract relevant information more effectively from the environment and to promote preparing for proper action.

In order to introduce the main method of steady state stimulation a steady state visual evoked potentials study was presented in chapter 1, demonstrating two important features of the such signals; amplitude peak around the repetition frequency of the stimuli and a stable phase of the elicited waveforms over a longer time period. In chapter 2 basic principles of linear mixed models were described that were intensively used in chapters 4 and 5.

The main finding of chapter 3 was that high arousing visual stimuli generate greater neuromagnetic responses in visual and parietal cortex. Using pictures from the International Affective Picture System (IAPS), it was demonstrated that arousing pleasant and unpleasant pictures engage fronto-parietal cortical networks and extrastriate cortex to a greater extent than neutral low arousing pictures. Concurrent measurement of heart rate change during picture depiction and recorded viewing times of the subjects assessed after the experimental session, indicated that the affective stimuli were actually of high motivational relevance. As fronto-parietal cortex is discussed as part of a general attention network, it is possible that such a network is engaged during affective picture viewing.

In chapters 4 and 5, it was demonstrated that not only complex stimuli like pictures of the IAPS set can mediate high motivational relevance. Using delayed aversive Pavlovian conditioning paradigms, it was shown that simple gratings paired with an aversive noise generated more activity in visual sensory and parietal cortex than gratings never paired with the unconditioned stimulus. Interestingly, only subjects reacting with an heart rate increase in response to the reinforced conditioned stimulus during acquisition trials demonstrated the facilitated cortical neuromagnetic response. Heart rate increase to aversive stimuli have been considered as fear responses in the conditioning literature.

To date, many researchers in the field of affective neuroscience have considered the amygdala as a neuronal core substrate for emotional evaluation of stimuli and autonomic reaction in response to them. Direct projections from the thalamus to the amygdala have been discussed as a fast route for fear relevant information circumventing slow detailed cortical processing. Efferents from the amygdala to various stages of visual and temporal cortex in turn, could be one possible way to facilitate visual processing of motivational relevant stimuli at early stages of visual stimulus processing. However, the present data also suggests that cortical attention mechanism possibly sharing the same neuronal substrate as attention systems discussed in spatial selective attention could enhance feature processing in visual cortex. A network comprising parietal and frontal cortex could be a candidate for a general attention system also engaged in motivated attention in emotion. The studies presented in the current thesis have shown the involvement of parietal cortex in processing of affective pictures as well as of aversively reinforced simple gratings coinciding with enhanced activity in visual cortex. Therefore, attentional processes during processing of affective stimuli should be investigated in future research more intensively in order to further elucidate brain mechanism of affective processing.

ZUSAMMENFASSUNG

Das Ziel der vorliegenden Arbeit war die Untersuchung oszillatorischer, neuronaler Aktivität, die durch repetetive Darbietung von Reizen mit unterschiedlichen affektiven Gehalts evoziert wurde. Es sei betont, dass aus den neuromagnetischen Daten nicht auf die Gefühle, Gedanken oder Gemütslagen der Versuchsteilnehmer während der Betrachtung affektiven Bildmaterials geschlossen werden kann. Die vorliegende Arbeit versteht Emotionen als *phasische Reaktionen des motivaitonalen Systems eines Organismus, welches die Handlungen eines Individuums bezüglich distinkter, biologisch signifikanter Reize in der Umgebung disponiert.* Somit ergab sich die Frage, wie motivational relevante, visuelle Reize im sensorischen- und Assoziationskortex verarbeitet werden. Eine der Haupthypothesen bestand aus der Annahme, dass Stimuli, welche für das Individuum eine hohe motivationale Relevanz besitzen, effektiver in sensorischen Hirnregionen wie dem extrastriatalen Kortex verarbeitet werden, damit wichtige Informationen aus der Umwelt extrahiert werden können und diese als Grundlage für eine angemessene Handlungsvorbereitung dienen.

Um den Leser mit der Hauptmethode der Steady State Stimulation vertraut zu machen, eröffnete das erste Kapitel mit einer Studie zu Steady State evozierten Potentialen, um zwei Hauptmerkmale solcher Signale zu demonstrieren: Amplitudenmaxima an der Stimulationsfrequenz und eine stabile Phase der Wellenformen über einen längeren Zeitraum hinweg. Im zweiten Kapitel wurden Basiskonzepte von „linear mixed models“ (LME) dargestellt, welche intensiv in den Kapiteln 4 und 5 Anwendung fanden.

Das Hauptergebnis aus Kapitel 3 bestand darin, dass hoch erregende Bilder eine größere neuromagnetische Antwort im visuellen und parietalen Kortex generierten. Durch die Verwendung von Bildern aus dem Internationalen affektiven Bilder System (IAPS) konnte gezeigt werden, dass erregende, angenehme und unangenehme Bilder fronto-parietale kortikale Netzwerke sowie den extrastriären Kortex stärker involvieren als niedrig erregendes Bildmaterial. Die gleichzeitige Messung der Herzratenveränderung während der Bildpräsentation und die Aufzeichnung der Bildbetrachtungszeiten nach dem Experiment, konnte zeigen, dass die hocherregenden Bilder tatsächlich von hoher motivationaler Relevanz waren. Da der fronto-parietale Kortex auch als Grundlage eines generellen Aufmerksamkeitsnetzwerkes gesehen wird, könnte es möglich sein, dass ein solches Netzwerk bei der Betrachtung affektiver Bilder eingeschaltet wird.

In den Kapiteln 4 und 5 wurde demonstriert, dass nicht nur komplexe Reize wie IAPS Bilder hohe motivationale Relevanz vermitteln können. Indem ein aversives Pavlovsches Konditionierungsparadigma verwendet wurde, konnte gezeigt werden, dass einfache

Strichmuster, welche mit einem aversiven, lauten, akustischen Rauschen gepaart wurden, mehr Aktivität in visuellen und parietalen Hirnregionen als der unkonditionierte Stimulus generierten. Interessanterweise wurde nur bei Versuchsteilnehmern, welche mit einer Herzratenbeschleunigung auf den konditionierten Stimulus reagierten, die fazilitierte kortikale neuromagnetische Reaktion beobachtet. Eine Hertzratenbeschleunigung auf aversive Reize hin wird in der Konditionierungsliteratur als Furchtreaktion bewertet.

Zur Zeit betrachten viele Forscher im Feld der affektiven Neurowissenschaften die Amygdala als eine Zentralstruktur für die emotionale Bewertung von Reizen und für die Expression autonomer Reaktionen. Direkte Projektionen vom Thalamus zur Amygdala werden als „schnelle Bahn“ für furchtrelevante Informationen gesehen, welche die Umgehung einer langsamen, detaillierten, kortikalen Analyse ermöglicht. Efferenzen von der Amygdala zu verschiedenen Verarbeitungsstationen im visuellen und temporalen Kortex hingegen könnten die Basis für die Amplifizierung der Verarbeitung von motivational relevanten Stimuli auf frühen, visuellen Verarbeitungsstufen darstellen. Dennoch weisen die vorliegenden Daten darauf hin, dass kortikale Aufmerksamkeitsmechanismen, welche möglicherweise auf den selben neuronalen Substrat wie Mechanismen der räumlichen Aufmerksamkeit beruhen, die Merkmalsverarbeitung im visuellen Kortex verstärken. Ein generelles fronto-parietales Aufmerksamkeitsnetzwerk könnte ebenfalls in den Prozess der motivierten Aufmerksamkeit gegenüber emotionalen Reizen involviert sein. Die Studien der vorliegenden Arbeit haben zumindest die Beteiligung des Parietalkortex bei der Verarbeitung von affektiven Bildern und aversiv verstärkten Mustern gezeigt. Dies ging mit einer erhöhten Aktivierung im visuellen Kortex einher. Deshalb sollten zukünftige Studien die Rolle von Aufmerksamkeitsprozessen während affektiver Reizverarbeitung stärker berücksichtigen.

OVERALL REFERENCES

Adolphs, R., Tranel, D., Damasio, H., & Damasio, A. R. (1995). Fear and the human amygdala. *J Neurosci, 15*(9), 5879-5891.

Aggleton, J. P., Burton, M. J., & Passingham, R. E. (1980). Cortical and subcortical afferents to the amygdala of the rhesus monkey (Macaca mulatta). *Brain Res, 190*(2), 347-368.

Akaike, H. (1974). A new look at the statistical model identification. *IEEE Transactions on Automatic Control, 19*, 716-723.

Amaral, D. G. (1986). Amygdalohippocampal and amygdalocortical projections in the primate brain. *Adv Exp Med Biol, 203*, 3-17.

Amaral, D. G., Price, J. L., Pitkaenen, A., & Carmichael, S. T. (1992). Anatomical organization of the primate amygdaloid complex. In J. P. Aggleton (Ed.), *The amygdala: Neurobiological aspects of emotion, memory, and mental dysfunction.* (pp. 1-66). New York: Wiley-Liss.

Bagiella, E., Sloan, R. P., & Heitjan, D. F. (2000). Mixed-effects models in psychophysiology. *Psychophysiology, 37*(1), 13-20.

Benjamini, Y., & Hochberg, Y. (1995). Controlling the false discovery rate: a practical and powerful approach to multiple testing. *Journal of the Royal Statistical Society Series B, 57*, 289-300.

Berg, P., & Scherg, M. (1994). A multiple source approach to the correction of eye artifacts. *Electroencephalogr Clin Neurophysiol, 90*(3), 229-241.

Bertero, M., De Mol, C., & Pike, E. R. (1988). Linear inverse problems with discrete data: II. Stability and regularization. *Inverse Problems, 4*, 573-594.

Bradley, M. M., Codispoti, M., Cuthbert, B. N., & Lang, P. J. (2001). Emotion and Motivation I: Defensive and Appetitive Reactions in Picture Processing. *Emotion, 1*(3), 276-298.

Buchel, C., & Dolan, R. J. (2000). Classical fear conditioning in functional neuroimaging. *Curr Opin Neurobiol, 10*(2), 219-223.

Buchel, C., Morris, J., Dolan, R. J., & Friston, K. J. (1998). Brain systems mediating aversive conditioning: an event-related fMRI study. *Neuron, 20*(5), 947-957.

Burton, M. J., Mora, F., & Rolls, E. T. (1975). Proceedings: Visual and taste neurones in the lateral hypothalamus and substantia innominata: modulation of responsiveness by hunger. *J Physiol, 252*(2), 50P-51P.

Burton, M. J., Rolls, E. T., & Mora, F. (1976). Effects of hunger on the responses of neurons in the lateral hypothalamus to the sight and taste of food. *Exp Neurol, 51*(3), 668-677.

Cador, M., Robbins, T. W., & Everitt, B. J. (1989). Involvement of the amygdala in stimulus-reward associations: interaction with the ventral striatum. *Neuroscience, 30*(1), 77-86.

Calder, A. J., Young, A. W., Rowland, D., Perrett, D. I., Hodges, J. R., & Etcoff, N. L. (1996). Facial emotion recognition after bilateral amygdala damage: Differentially severe impairment of fear. *Cognitive Neuropsychology, 13*, 699-745.

Cheng, D. T., Knight, D. C., Smith, C. N., Stein, E. A., & Helmstetter, F. J. (2003). Functional MRI of human amygdala activity during Pavlovian fear conditioning: stimulus processing versus response expression. *Behav Neurosci, 117*(1), 3-10.

Clark, R. E., Manns, J. R., & Squire, L. R. (2001). Trace and delay eyeblink conditioning: contrasting phenomena of declarative and nondeclarative memory. *Psychol Sci, 12*(4), 304-308.

Clark, R. E., Manns, J. R., & Squire, L. R. (2002). Classical conditioning, awareness, and brain systems. *Trends Cogn Sci, 6*(12), 524-531.

Clementz, B. A., Keil, A., & Kissler, J. (2004). Aberrant brain dynamics in schizophrenia: delayed buildup and prolonged decay of the visual steady-state response. *Brain Res Cogn Brain Res, 18*(2), 121-129.

Corbetta, M. (1998). Frontoparietal cortical networks for directing attention and the eye to visual locations: identical, independent, or overlapping neural systems? *Proc Natl Acad Sci U S A, 95*(3), 831-838.

Coull, J. T. (2004). fMRI studies of temporal attention: allocating attention within, or towards, time. *Brain Res Cogn Brain Res, 21*(2), 216-226.

CSEA. (1999). *International affective picture system (IAPS): Technical manual and affective ratings.* Gainesville, FL: NIMH-Center for the study of emotion and attention, University of Florida.

Cuthbert, B. N., Bradley, M. M., & Lang, P. J. (1996). Probing picture perception: activation and emotion. *Psychophysiology, 33*(2), 103-111.

Cuthbert, B. N., Schupp, H. T., Bradley, M. M., Birbaumer, N., & Lang, P. J. (2000). Brain potentials in affective picture processing: covariation with autonomic arousal and affective report. *Biol Psychol, 52*(2), 95-111.

Davidson, R. J., Abercrombie, H., Nitschke, J. B., & Putnam, K. (1999). Regional brain function, emotion and disorders of emotion. *Curr Opin Neurobiol, 9*(2), 228-234.

Davidson, R. J., Putnam, K. M., & Larson, C. L. (2000). Dysfunction in the neural circuitry of emotion regulation--a possible prelude to violence. *Science, 289*(5479), 591-594.

Di Russo, F., Martinez, A., & Hillyard, S. A. (2003). Source analysis of event-related cortical activity during visuo-spatial attention. *Cereb Cortex, 13*(5), 486-499.

Diesch, E., Preissl, H., Haerle, M., Schaller, H. E., & Birbaumer, N. (2001). Multiple frequency steady-state evoked magnetic field mapping of digit representation in primary somatosensory cortex. *Somatosens Mot Res, 18*(1), 10-18.

Esteves, F., Parra, C., Dimberg, U., & Ohman, A. (1994). Nonconscious associative learning: Pavlovian conditioning of skin conductance responses to masked fear-relevant facial stimuli. *Psychophysiology, 31*(4), 375-385.

Fanselow, M. S. (1994). Neural organization of the defensive behavior system responsible for fear. *Psychon Bull Rev, 1*, 429-438.

Fanselow, M. S., & Poulos, A. M. (2004). The Neuroscience of Mammalian Associative Learning. *Annu Rev Psychol*.

Fernandez-Duque, D., & Posner, M. I. (2001). Brain imaging of attentional networks in normal and pathological states. *J Clin Exp Neuropsychol, 23*(1), 74-93.

Fischer, H., Andersson, J. L., Furmark, T., Wik, G., & Fredrikson, M. (2002). Right-sided human prefrontal brain activation during acquisition of conditioned fear. *Emotion, 2*(3), 233-241.

Flor, H., Birbaumer, N., Roberts, L. E., Feige, B., Lutzenberger, W., Hermann, C., & Kopp, B. (1996). Slow potentials, event-related potentials, "gamma-band" activity, and motor responses during aversive conditioning in humans. *Exp Brain Res, 112*(2), 298-312.

Foa, E. B., & Kozak, M. J. (1998). Clinical Applications of Bioinformational Theory: Understanding Anxiety and Its Treatment. *Behavior Therapy, 29*, 675-690.

Fredrikson, M., Wik, G., Fischer, H., & Andersson, J. (1995). Affective and attentive neural networks in humans: a PET study of Pavlovian conditioning. *Neuroreport, 7*(1), 97-101.

Furmark, T., Fischer, H., Wik, G., Larsson, M., & Fredrikson, M. (1997). The amygdala and individual differences in human fear conditioning. *Neuroreport, 8*(18), 3957-3960.

Gabrieli, J. D., McGlinchey-Berroth, R., Carrillo, M. C., Gluck, M. A., Cermak, L. S., & Disterhoft, J. F. (1995). Intact delay-eyeblink classical conditioning in amnesia. *Behav Neurosci, 109*(5), 819-827.

Ghashghaei, H. T., & Barbas, H. (2002). Pathways for emotion: interactions of prefrontal and anterior temporal pathways in the amygdala of the rhesus monkey. *Neuroscience, 115*(4), 1261-1279.

Grave de Peralta Menendez, R., Hauk, O., Gonzalez Andino, S., Vogt, H., & Michel, C. (1997). Linear inverse solutions with optimal resolution kernels applied to electomagnetic tomography. *Human Brain Mapping, 5*, 454-467.

Gray, M., Kemp, A. H., Silberstein, R. B., & Nathan, P. J. (2003). Cortical neurophysiology of anticipatory anxiety: an investigation utilizing steady state probe topography (SSPT). *Neuroimage, 20*(2), 975-986.

Greenhouse, S. W., & Geisser, S. (1959). On methods in the analysis of profile data. *Psychometrika, 24*, 95-112.

Hämäläinen, M., & Ilmoniemi, R. (1984). *Interpreting measured magnetic fields of the brain: Estimates of current distributions.* (Technical Report TKK-F-A559). Helsinki: Helsinki University of Technology.

Hamalainen, M. S., & Ilmoniemi, R. J. (1994). Interpreting magnetic fields of the brain: minimum norm estimates. *Med Biol Eng Comput, 32*(1), 35-42.

Hamm, A. O., & Vaitl, D. (1996). Affective learning: awareness and aversion. *Psychophysiology, 33*(6), 698-710.

Hamm, A. O., Weike, A. I., Schupp, H. T., Treig, T., Dressel, A., & Kessler, C. (2003). Affective blindsight: intact fear conditioning to a visual cue in a cortically blind patient. *Brain, 126*(Pt 2), 267-275.

Hansen, P. C., & O'Leary, D. P. (1993). The use of the L-curve in the regularization of discrete ill-posed problems. *SIAM J. Sci. Comput., 14*, 1487-1503.

Hare, R. D. (1972). Cardiovascular components of orienting and defensive responses. *Psychophysiology, 9*(6), 606-614.

Hare, R. D., & Blevings, G. (1975). Defensive responses to phobic stimuli. *Biol Psychol, 3*(1), 1-13.

Hauk, O., Berg, P., Wienbruch, C., Rockstroh, B., & Elbert, T. (1998). *The minimum norm method as an effective mapping tool for MEG analysis.* Paper presented at the Biomag98, Sendai, Japan.

Hauk, O., Keil, A., Elbert, T., & Müller, M. M. (2002). Comparison of data transformation procedures to enhance topographical accuracy in time series analysis of the human EEG. *Journal of Neuroscience Methods, 113*(2), 111-122.

Hautzinger, M., Bailer, M., Worall, H., & Keller, F. (1992). *Beck - Depressions-Inventar*. Bern: Huber.

Herrmann, C. S. (2001). Human EEG responses to 1-100 Hz flicker: resonance phenomena in visual cortex and their potential correlation to cognitive phenomena. *Exp Brain Res, 137*(3-4), 346-353.

Hillyard, S. A., & Anllo-Vento, L. (1998). Event-related brain potentials in the study of visual selective attention. *Proc Natl Acad Sci U S A, 95*(3), 781-787.

Hillyard, S. A., Mangun, G. R., & Woldorff, M. G. (1995). In M. S. Ganzzaniga (Ed.), *The Cognitve Neurosciences* (pp. 665-681). Cambridge, MA: MIT Press.

Hodes, R. L., Cook, E. W., 3rd, & Lang, P. J. (1985). Individual differences in autonomic response: conditioned association or conditioned fear? *Psychophysiology, 22*(5), 545-560.

Hugdahl, K. (1998). Cortical control of human classical conditioning: autonomic and positron emission tomography data. *Psychophysiology, 35*(2), 170-178.

Hugdahl, K., Berardi, A., Thompson, W. L., Kosslyn, S. M., Macy, R., Baker, D. P., Alpert, N. M., & LeDoux, J. E. (1995). Brain mechanisms in human classical conditioning: a PET blood flow study. *Neuroreport, 6*(13), 1723-1728.

Ito, T. A., Larsen, J. T., Smith, N. K., & Cacioppo, J. T. (1998). Negative information weighs more heavily on the brain: the negativity bias in evaluative categorizations. *J Pers Soc Psychol, 75*(4), 887-900.

Jennings, J. R., van der Molen, M. W., Somsen, R. J., Graham, R., & Gianaros, P. J. (2002). Vagal function in health and disease: studies in Pittsburgh. *Physiology & Behaviour, 77*(4-5), 693-698.

Jennrich, R. I., & Schluchter, M. D. (1986). Unbalanced repeated-measures models with structured covariance matrices. *Biometrics, 42*(4), 805-820.

Jensen, O., & Vanni, S. (2002). A new method to identify multiple sources of oscillatory activity from magnetoencephalographic data. *Neuroimage, 15*(3), 568-574.

Junghöfer, M., Bradley, M. M., Elbert, T. R., & Lan, P. J. (2001). Fleeting images: a new look at early emotion discrimination. *Psychophysiology, 38*(2), 175-178.

Junghöfer, M., & Peyk, P. (2004). Analyse und Visualisierung von Hirnstrom- und Hirnmagnetfeld-Messungen. *MATLAB select, 2*, 24-28.

Keil, A. (2000). *Oscillatory brain activity in human affective stimulus processing.* University of Konstanz, Konstanz.

Keil, A., Bradley, M. M., Hauk, O., Rockstroh, B., Elbert, T., & Lang, P. J. (2002). Large-scale neural correlates of affective picture processing. *Psychophysiology, 39*(5), 641-649.

Keil, A., Moratti, S., Sabatinelli, D., Bradley, M. M., & Lang, P. J. (2004). Additive Effects of Emotional Content and Spatial Selective Attention on Electrocortical Facilitation. *Cereb Cortex*.

Keil, A., Muller, M. M., Gruber, T., Wienbruch, C., Stolarova, M., & Elbert, T. (2001). Effects of emotional arousal in the cerebral hemispheres: a study of oscillatory brain activity and event-related potentials. *Clin Neurophysiol, 112*(11), 2057-2068.

Kemp, A. H., Gray, M. A., Eide, P., Silberstein, R. B., & Nathan, P. J. (2002). Steady-State Visually Evoked Potential Topography during Processing of Emotional Valence in Healthy Subjects. *Neuroimage, 17*(4), 1684-1692.

Keselman, H. J., Cribbie, R., & Holland, B. (2002). Controlling the rate of Type I error over a large set of statistical tests. *Br J Math Stat Psychol, 55*(Pt 1), 27-39.

Kim, J. J., Clark, R. E., & Thompson, R. F. (1995). Hippocampectomy impairs the memory of recently, but not remotely, acquired trace eyeblink conditioned responses. *Behav Neurosci, 109*(2), 195-203.

Klüver, H., & Bucy, J. P. (1937). Psychich blindness and other symptoms following bilateral temporal lobectomy in rhesus monkeys. *Am Jn Physiol, 119*, 352-353.

Knight, D. C., Cheng, D. T., Smith, C. N., Stein, E. A., & Helmstetter, F. J. (2004). Neural substrates mediating human delay and trace fear conditioning. *J Neurosci, 24*(1), 218-228.

Knight, D. C., Nguyen, H. T., & Bandettini, P. A. (2003). Expression of conditional fear with and without awareness. *Proc Natl Acad Sci U S A, 100*(25), 15280-15283.

Knosche, T., Praamstra, P., Stegeman, D., & Peters, M. (1996). Linear estimation discriminates midline sources and a motor cortex contribution to the readiness potential. *Electroencephalogr Clin Neurophysiol, 99*(2), 183-190.

Knuttinen, M. G., Power, J. M., Preston, A. R., & Disterhoft, J. F. (2001). Awareness in classical differential eyeblink conditioning in young and aging humans. *Behav Neurosci, 115*(4), 747-757.

Kronforst-Collins, M. A., & Disterhoft, J. F. (1998). Lesions of the caudal area of rabbit medial prefrontal cortex impair trace eyeblink conditioning. *Neurobiol Learn Mem, 69*(2), 147-162.

Kuniecki, M., Coenen, A. M., & Kaiser, J. (2002). Correlation between long latency evoked potentials from amygdala and evoked cardiac response to fear conditioned stimulus in rats. *Acta Neurobiol Exp (Wars), 62*(2), 85-92.

LaBar, K. S., & Disterhoft, J. F. (1998). Conditioning, awareness, and the hippocampus. *Hippocampus, 8*(6), 620-626.

LaBar, K. S., Gatenby, J. C., Gore, J. C., LeDoux, J. E., & Phelps, E. A. (1998). Human amygdala activation during conditioned fear acquisition and extinction: a mixed-trial fMRI study. *Neuron, 20*(5), 937-945.

Lang, P. J. (1968). Fear reduction and fear behavior: Problems in treating a construct, *Research in psychotherapy III*. Washington: American Psychiatric Association.

Lang, P. J. (1979). A bioinformational theory of emotional imagery. *Psychophysiology, 16*, 495-512.

Lang, P. J. (1980). Behavioral treatment and bio-behavioral assessment:

Computer applications. In J. B. Sidowski & J. H. Johnson & T. A. Williams (Eds.), *Technology in mental health care delivery systems* (pp. 119-137). Norwood, NJ: Ablex Publishing.

Lang, P. J. (1995). The emotion probe: Studies of motivation and attention. 102nd Annual Convention of the American Psychological Association Distinguished Scientific Contributions Award Address (1994, Los Angeles, California). *American Psychologist, 50*(5), 372-385.

Lang, P. J., Bradley, M. M., & Cuthbert, B. N. (1997). Motivated Attention: Affect, Activation, and Action. In P. J. Lang & R. F. Simons & M. T. Balaban (Eds.), *Attention and Orienting: Sensory and Motivational Processes* (pp. 97-135). Hillsdale, N.J.: Lawrence Erlbaum Associates.

Lang, P. J., Bradley, M. M., & Cuthbert, B. N. (1998). Emotion, motivation, and anxiety: brain mechanisms and psychophysiology. *Biol Psychiatry, 44*(12), 1248-1263.

Lang, P. J., Greenwald, M. K., Bradley, M. M., & Hamm, A. O. (1993). Looking at pictures: affective, facial, visceral, and behavioral reactions. *Psychophysiology, 30*(3), 261-273.

Lang, P. J., & Hnatiow, M. (1962). Stimulus repetition and the heart rate response. *Journal of Comparative and Physiological Psychology, 55*, 781-785.

Lang, P. J., Melamed, B. G., & Hart, J. (1970). A psychophysiological analysis of fear modification using an automated desensitization procedure. *J Abnorm Psychol, 76*(2), 220-234.

Laux, L., Glanzmann, P., Schaffner, P., & Spielberger, C. D. (1981). *Das State-Trait-Angstinventar*. Weinheim: Beltz.

Le, T. H., Pardo, J. V., & Hu, X. (1998). 4 T-fMRI study of nonspatial shifting of selective attention: cerebellar and parietal contributions. *J Neurophysiol, 79*(3), 1535-1548.

LeDoux, J. (1992). Emotional memories in the brain. In e. nd (Ed.), *Neuropsychology of memory* (pp. 463-469): Guilford Press, New York, NY, US.

LeDoux, J. E. (1990). Fear pathways in the brain: Implications for a theory of the emotional brain. In P. F. Brain & S. Parmigiani & R. J. Blanchard & D. Mainardi (Eds.), *Fear and defence. Ettore Majorana international life sciences series, Vol. 8.* (pp. 163-177): Harwood Academic Publishers, London, England.

LeDoux, J. E. (1992). Emotion and the amygdala. In P. A. John (Ed.), *The amygdala: Neurobiological aspects of emotion, memory, and mental dysfunction.* (pp. 339-351): Wiley-Liss, New York, NY, US.

LeDoux, J. E. (1993). Emotional networks in the brain. In J. M. H. Michael Lewis (Ed.), *Handbook of emotions.* (pp. 109-118): Guilford Press, New York, NY, US.

LeDoux, J. E. (1994). Emotion, memory and the brain. *Sci Am, 270*(6), 50-57.

LeDoux, J. E. (2000). Emotion circuits in the brain. *Annu Rev Neurosci, 23*, 155-184.

Lovibond, P. F., & Shanks, D. R. (2002). The role of awareness in Pavlovian conditioning: empirical evidence and theoretical implications. *J Exp Psychol Anim Behav Process, 28*(1), 3-26.

Mackintosh, N. J. (2003). Pavlov and associationism. *Span J Psychol, 6*(2), 177-184.

Makeig, S., Westerfield, M., Jung, T. P., Enghoff, S., Townsend, J., Courchesne, E., & Sejnowski, T. J. (2002). Dynamic brain sources of visual evoked responses. *Science, 295*(5555), 690-694.

Mangun, G. R. (1995). Neural mechanisms of visual selective attention. *Psychophysiology, 32*(1), 4-18.

Manns, J. R., Clark, R. E., & Squire, L. (2001). Single-cue delay eyeblink conditioning is unrelated to awareness. *Cogn Affect Behav Neurosci, 1*(2), 192-198.

Manns, J. R., Clark, R. E., & Squire, L. R. (2000). Parallel acquisition of awareness and trace eyeblink classical conditioning. *Learn Mem, 7*(5), 267-272.

Manns, J. R., Clark, R. E., & Squire, L. R. (2002). Standard delay eyeblink classical conditioning is independent of awareness. *J Exp Psychol Anim Behav Process, 28*(1), 32-37.

Maren, S. (2001). Neurobiology of Pavlovian fear conditioning. *Annu Rev Neurosci, 24*, 897-931.

Martinez, A., Anllo-Vento, L., Sereno, M. I., Frank, L. R., Buxton, R. B., Dubowitz, D. J., Wong, E. C., Hinrichs, H., Heinze, H. J., & Hillyard, S. A. (1999). Involvement of striate and extrastriate visual cortical areas in spatial attention. *Nat Neurosci, 2*(4), 364-369.

Martinez, A., DiRusso, F., Anllo-Vento, L., Sereno, M. I., Buxton, R. B., & Hillyard, S. A. (2001). Putting spatial attention on the map: timing and localization of stimulus selection processes in striate and extrastriate visual areas. *Vision Res, 41*(10-11), 1437-1457.

Mauk, M. D., & Thompson, R. F. (1987). Retention of classically conditioned eyelid responses following acute decerebration. *Brain Res, 403*(1), 89-95.

McGaugh, J. L., Cahill, L., & Roozendaal, B. (1996). Involvement of the amygdala in memory storage: interaction with other brain systems. *Proc Natl Acad Sci U S A, 93*(24), 13508-13514.

McGlinchey-Berroth, R., Carrillo, M. C., Gabrieli, J. D., Brawn, C. M., & Disterhoft, J. F. (1997). Impaired trace eyeblink conditioning in bilateral, medial-temporal lobe amnesia. *Behav Neurosci, 111*(5), 873-882.

Miller, W. R., & Seligman, M. E. (1975). Depression and learned helplessness in man. *J Abnorm Psychol, 84*(3), 228-238.

Mini, A., Palomba, D., Angrilli, A., & Bravi, S. (1996). Emotional information processing and visual evoked brain potentials. *Percept Mot Skills, 83*(1), 143-152.

Moratti, S., Keil, A., & Stolarova, M. (2004). Motivated attention in emotional picture processing is reflected by activity modulation in cortical attention networks. *Neuroimage, 21*(3), 954-964.

Morgan, S. T., Hansen, J. C., & Hillyard, S. A. (1996). Selective attention to stimulus location modulates the steady-state visual evoked potential. *Proc Natl Acad Sci U S A, 93*(10), 4770-4774.

Morris, J. S., Ohman, A., & Dolan, R. J. (1998). Conscious and unconscious emotional learning in the human amygdala. *Nature, 393*(6684), 467-470.

Morris, J. S., Ohman, A., & Dolan, R. J. (1999). A subcortical pathway to the right amygdala mediating "unseen" fear. *Proc Natl Acad Sci U S A, 96*(4), 1680-1685.

Mufson, E. J., Mesulam, M. M., & Pandya, D. N. (1981). Insular interconnections with the amygdala in the rhesus monkey. *Neuroscience, 6*(7), 1231-1248.

Müller, M. M., Gruber, T., & Keil, A. (2000). Modulation of induced gamma band activity in the human EEG by attention and visual information processing. *Int J Psychophysiol, 38*(3), 283-299.

Müller, M. M., & Hillyard, S. (2000). Concurrent recording of steady-state and transient event-related potentials as indices of visual-spatial selective attention. *Clin Neurophysiol, 111*(9), 1544-1552.

Muller, M. M., & Hubner, R. (2002). Can the spotlight of attention be shaped like a doughnut? Evidence from steady-state visual evoked potentials. *Psychol Sci, 13*(2), 119-124.

Müller, M. M., Picton, T. W., Valdes-Sosa, P., Riera, J., Teder-Salejarvi, W. A., & Hillyard, S. A. (1998). Effects of spatial selective attention on the steady-state visual evoked potential in the 20-28 Hz range. *Brain Res Cogn Brain Res, 6*(4), 249-261.

Müller, M. M., Teder, W., & Hillyard, S. A. (1997). Magnetoencephalographic recording of steady-state visual evoked cortical activity. *Brain Topogr, 9*(3), 163-168.

Müller, M. M., Teder-Salejarvi, W., & Hillyard, S. A. (1998). The time course of cortical facilitation during cued shifts of spatial attention. *Nat Neurosci, 1*(7), 631-634.

Munoz, A., Carey, V., Schouten, J. P., Segal, M., & Rosner, B. (1992). A parametric family of correlation structures for the analysis of longitudinal data. *Biometrics, 48*(3), 733-742.

Ohman, A., & Soares, J. J. (1998). Emotional conditioning to masked stimuli: expectancies for aversive outcomes following nonrecognized fear-relevant stimuli. *J Exp Psychol Gen, 127*(1), 69-82.

Oldfield, R. C. (1971). The assessment and analysis of handedness: The Edinbourgh Inventory. *Neuropsychologia, 9*, 97-113.

Osgood, C., Suci, G., & Tannenbaum, P. (1957). *The measurement of meaning*: Urbana, Univeristy of Illinois.

Palomba, D., Angrilli, A., & Mini, A. (1997). Visual evoked potentials, heart rate responses and memory to emotional pictorial stimuli. *Int J Psychophysiol, 27*(1), 55-67.

Pandya, D. N., & Yeterian, E. H. (1985). Architecture and connections of cortical association areas. In A. Peters & E. G. Jones (Eds.), *Cerebral Cortex* (Vol. 4, pp. 3-55). New York: Plenum Press.

Pardo, J. V., Fox, P. T., & Raichle, M. E. (1991). Localization of a human system for sustained attention by positron emission tomography. *Nature, 349*(6304), 61-64.

Pavlov, I. P. (1927). *Conditioned Reflexes: An Investigation of the Physiological Activity of the Cerebral Cortex*. London: Oxford University Press.

Pearce, J. M., & Hall, G. (1980). A model for Pavlovian learning: variations in the effectiveness of conditioned but not of unconditioned stimuli. *Psychol Rev, 87*(6), 532-552.

Penny, W. D., Kiebel, S. J., Kilner, J. M., & Rugg, M. D. (2002). Event-related brain dynamics. *Trends Neurosci, 25*(8), 387-389.

Perlstein, W. M., Cole, M. A., Larson, M., Kelly, K., Seignourel, P., & Keil, A. (2003). Steady-state visual evoked potentials reveal frontally-mediated working memory activity in humans. *Neurosci Lett, 342*(3), 191-195.

Picton, T. W., Vajsar, J., Rodriguez, R., & Campbell, K. B. (1987). Reliability estimates for steady-state evoked potentials. *Electroencephalogr Clin Neurophysiol, 68*(2), 119-131.

Pinheiro, J. C., & Bates, D. M. (2000). *Mixed-Effects Models in S and S-PLUS* (1 ed.). New York, Berlin, Heidelberg: Springer.

Pizzagalli, D., Regard, M., & Lehmann, D. (1999). Rapid emotional face processing in the human right and left brain hemispheres: an ERP study. *Neuroreport, 10*(13), 2691-2698.

Plourde, G., & Picton, T. W. (1990). Human auditory steady-state response during general anesthesia. *Anesth Analg, 71*(5), 460-468.

Porrino, L. J., Crane, A. M., & Goldman-Rakic, P. S. (1981). Direct and indirect pathways from the amygdala to the frontal lobe in rhesus monkeys. *J Comp Neurol, 198*(1), 121-136.

Regan, D. (1989). *Human Brain Electrophysiology: Evoked Potentials and Evoked Magnetic Fields in Science and Medicine*. New York: Elsevier.

Regan, M., & Howard, R. (1995). Fear conditioning, preparedness, and the contingent negative variation. *Psychophysiology, 32*(3), 208-214.

Rescorla, R. A. (1988). Pavlovian conditioning. It's not what you think it is. *Am Psychol, 43*(3), 151-160.

Rochon, J., & Helms, R. W. (1989). Maximum likelihood estimation for incomplete repeated-measures experiments under an ARMA covariance structure. *Biometrics, 45*(1), 207-218.

Rockstroh, B., Elbert, T., Canavan, A., Lutzenberger, W., & Birbaumer, N. (1989). *Slow Cortical Potentials and Behavior* (2nd ed.). Baltimore, Munich, Vienna: Urban & Schwarzenberg.

Rockstroh, B., Muller, M., Wagner, M., Cohen, R., & Elbert, T. (1993). "Probing" the nature of the CNV. *Electroencephalogr Clin Neurophysiol, 87*(4), 235-241.

Rodriguez, E., George, N., Lachaux, J. P., Martinerie, J., Renault, B., & Varela, F. J. (1999). Perception's shadow: long-distance synchronization of human brain activity. *Nature, 397*(6718), 430-433.

Rohrbaugh, J. W., McCallum, W. C., Gaillard, A. W., Simons, R. F., Birbaumer, N., & Papakostopoulos, D. (1986). ERPs associated with preparatory and movement-related processes. A review. *Electroencephalogr Clin Neurophysiol Suppl, 38*, 189-229.

Rolls, E. T. (1990). A theory of emotion, and its application to understanding the neural basis of emotion. *Cognition and Emotion, 4*, 161-190.

Rolls, E. T. (1995). A theory of emotion and consciousness, and its application to understanding the neural basis of emotion. In M. S. Gazzaniga (Ed.), *The cognitive neurosciences.* (pp. 1091-1106). Cambridge, MA, US: MIT Press.

Rolls, E. T. (1999). *The Brain and Emotion*. Oxford: Oxford University Press.

Rolls, E. T., Burton, M. J., & Mora, F. (1976). Hypothalamic neuronal responses associated with the sight of food. *Brain Res, 111*(1), 53-66.

Rolls, E. T., Burton, M. J., & Mora, F. (1980). Neurophysiological analysis of brain-stimulation reward in the monkey. *Brain Res, 194*(2), 339-357.

Rolls, E. T., Hornak, J., Wade, D., & McGrath, J. (1994). Emotion-related learning in patients with social and emotional changes associated with frontal lobe damage. *J Neurol Neurosurg Psychiatry, 57*(12), 1518-1524.

Rolls, E. T., Sanghera, M. K., & Roper-Hall, A. (1979). The latency of activation of neurones in the lateral hypothalamus and substantia innominata during feeding in the monkey. *Brain Res, 164*, 121-135.

Rushworth, M. F., Paus, T., & Sipila, P. K. (2001). Attention systems and the organization of the human parietal cortex. *J Neurosci, 21*(14), 5262-5271.

Schluchter, M. D. (1988). Analysis of incomplete multivariate data using linear models with structured covariance matrices. *Statistics in Medicine, 7*(1-2), 317-324.

Schupp, H. T., Cuthbert, B. N., Bradley, M. M., Cacioppo, J. T., Ito, T., & Lang, P. J. (2000). Affective picture processing: the late positive potential is modulated by motivational relevance. *Psychophysiology, 37*(2), 257-261.

Schupp, H. T., Junghöfer, M., Weike, A. I., & Hamm, A. O. (2002). Emotional facilitation of sensory processing in the visual cortex. *Psychological Science*, in press.

Schwarz, G. (1978). Estimating the dimension of a model. *The Annals of Statistics, 6*, 461-464.

Searle, S. R., Casella, G., & McCulloch, C. E. (1992). *Variance Components*. New York: Wiley.

Seligman, M. E. (1972). Learned helplessness. *Annu Rev Med, 23*, 407-412.

Shanks, D. R., & Lovibond, P. F. (2002). Autonomic and eyeblink conditioning are closely related to contingency awareness: reply to Wiens and Ohman (2002) and Manns et al. (2002). *J Exp Psychol Anim Behav Process, 28*(1), 38-42.

Shi, C., & Davis, M. (2001). Visual pathways involved in fear conditioning measured with fear-potentiated startle: behavioral and anatomic studies. *J Neurosci, 21*(24), 9844-9855.

Silberstein, R. B., Ciorciari, J., & Pipingas, A. (1995). Steady-state visually evoked potential topography during the Wisconsin card sorting test. *Electroencephalogr Clin Neurophysiol, 96*(1), 24-35.

Silberstein, R. B., Nunez, P. L., Pipingas, A., Harris, P., & Danieli, F. (2001). Steady state visually evoked potential (SSVEP) topography in a graded working memory task. *Int J Psychophysiol, 42*(2), 219-232.

Silberstein, R. B., Schier, M. A., Pipingas, A., Ciorciari, J., Wood, S. R., & Simpson, D. G. (1990). Steady-state visually evoked potential topography associated with a visual vigilance task. *Brain Topogr, 3*(2), 337-347.

Somsen, R., Jennings, J. R., & Van Der Molen, M. (2002). Human vagal heart rate responses in warned reaction time tasks: A cross-validation with simulated vagus-sino-atrial node interactions. *Journal of Electrocardiology, 35 Suppl*, 231-237.

Somsen, R. J., van der Molen, M. W., & Orlebeke, J. F. (1983). Phasic heart rate changes in reaction time, shock avoidance, and unavoidable shock tasks: are hypothetical generalizations about different S1-S2 tasks justified? *Psychophysiology, 20*(1), 88-94.

Team, R. D. C. (2004). R: A language and environment for statistical computing. R Foundation for Statistical Computing. Vienna, Austria: R Foundation for Statistical Computing.

Thayer, J. F., Friedman, B. H., Borkovec, T. D., Johnsen, B. H., & Molina, S. (2000). Phasic heart period reactions to cued threat and nonthreat stimuli in generalized anxiety disorder. *Psychophysiology, 37*(3), 361-368.

Treisman, A. M., & Kanwisher, N. G. (1998). Perceiving visually presented objects: recognition, awareness, and modularity. *Curr Opin Neurobiol, 8*(2), 218-226.

Uusitalo, M. A., & Ilmoniemi, R. J. (1997). Signal-space projection method for separating MEG or EEG into components. *Med Biol Eng Comput, 35*(2), 135-140.

Verbeke, G., Lesaffre, E., & Brant, L. J. (1998). The detection of residual serial correlation in linear mixed models. *Statistics in Medicine, 17*(12), 1391-1402.

Weiskrantz, L. (1956). Behavioral changes associated with ablation of the amygdaloid complex in monkeys. *Journal of Comparative and Physiological Psychology, 49*, 381-391.

Weisz, N., Keil, A., Wienbruch, C., Hoffmeister, S., & Elbert, T. (2004). One set of sounds, two tonotopic maps: exploring auditory cortex with amplitude-modulated tones. *Clin Neurophysiol, 115*(6), 1249-1258.

Wiens, S., Katkin, E. S., & Ohman, A. (2003). Effects of trial order and differential conditioning on acquisition of differential shock expectancy and skin conductance conditioning to masked stimuli. *Psychophysiology, 40*(6), 989-997.

Wiens, S., & Ohman, A. (2002). Unawareness is more than a chance event: comment on Lovibond and Shanks (2002). *J Exp Psychol Anim Behav Process, 28*(1), 27-31.

Wilson, R. S. (1974). CARDIVAR: the statistical analysis of heart rate data. *Psychophysiology, 11*(1), 76-85.

Woodruff-Pak, D. S., Lavond, D. G., & Thompson, R. F. (1985). Trace conditioning: abolished by cerebellar nuclear lesions but not lateral cerebellar cortex aspirations. *Brain Res, 348*(2), 249-260.